UNIVERSITÉ DE TOURS

ÉCOLE DOCTORALE : SSBCV

UMR CNRS 7261, Institut de Recherche sur la Biologie de l'Insecte

THÈSE présentée par :

Florent FIGON

soutenue le : **02 septembre 2020**

pour obtenir le grade de : **Docteur de l'université de Tours**

Discipline / Spécialité : Sciences de la vie et de la santé

PHOTOBIOCHIMIE ET BIOLOGIE CELLULAIRE DES OMMOCHROMES : Implications dans le changement de couleur

THÈSE dirigée par :

M. CASAS Jérôme	Professeur, université de Tours

RAPPORTEURS :

Mme DERAVI Leila	Professeure, université Northeastern de Boston
M. KHILA Abderrahman	Directeur de recherche CNRS, école normale supérieure de Lyon

---

JURY :

M. CASAS Jérôme	Professeur, université de Tours
Mme DERAVI Leila	Professeure, université Northeastern de Boston
Mme GUIVARC'H Nathalie	Professeure, université de Tours, **présidente du jury**
M. JACQUEMIN Denis	Professeur, université de Nantes
M. KHILA Abderrahman	Directeur de recherche CNRS, école normale supérieure de Lyon
Mme RAPOSO Graça	Directrice de recherche CNRS, institut Curie

Of all remarkable substances of our experience —rain, leaves, baby toes—
light is perhaps the most miraculous.

Sönke Johnsen, *The Optics of Life* (2012)

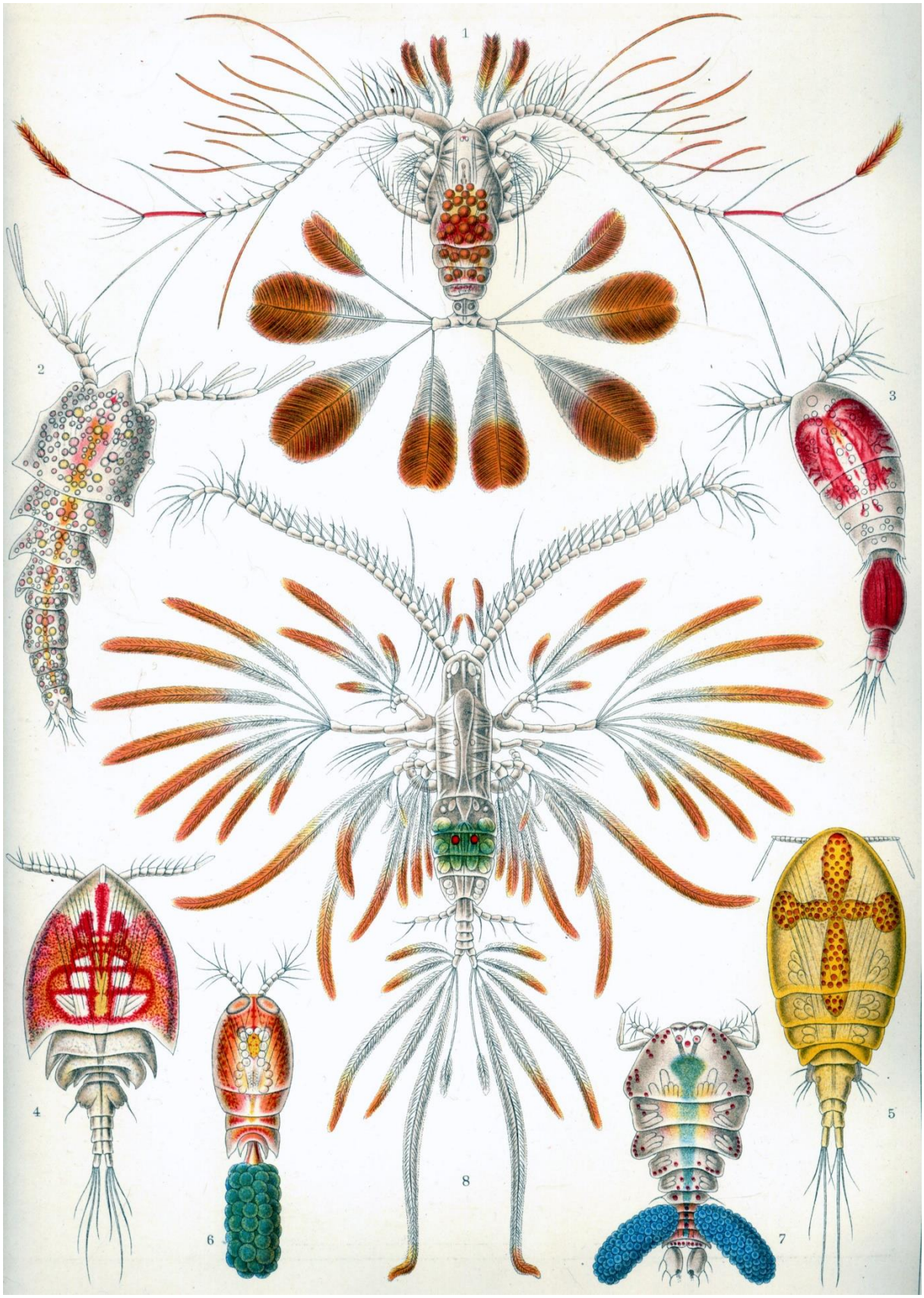

Les copépodes, des crustacés à la variété de couleurs.
Lithographie d'Ernst Haeckel (1904), *Formes artistiques de la nature* (retouches : Wikimedia)

Table des matières

TABLE DES MATIERES **3**

REMERCIEMENTS **5**

CURRICULUM VITAE **8**

RESUME **12**

ABSTRACT **13**

LISTE DES FIGURES **14**

FIGURES PRINCIPALES 14

FIGURES SUPPLEMENTAIRES 16

LISTE DES TABLES **18**

TABLES PRINCIPALES 18

TABLES SUPPLEMENTAIRES 18

CHAPITRE 1 – INTRODUCTION GENERALE **19**

1.0 SOMMAIRE 20

1.1 UNE VIE HAUTE EN COULEUR 21

1.2 APERÇU DE L'HISTOIRE DE LA BIOLOGIE DE LA COULEUR 22

1.3 LA CHIMIE DES COULEURS 26

1.4 L'IMPORTANCE BIOLOGIQUE DES PIGMENTS CHEZ LES ANIMAUX 31

1.5 OBJECTIFS DE LA THESE 38

CHAPITRE 2 – LES CHANGEMENTS DE COULEUR MORPHOLOGIQUE ET PHYSIOLOGIQUE DES ANIMAUX **41**

2.0 SOMMAIRE 42

2.1 OBJECTIFS 43

2.2 REVUE DE LA LITTERATURE 44

2.3 CONCLUSION 66

CHAPITRE 3 – LES OMMOCHROMES CHEZ LES INVERTEBRES : BIOCHIMIE ET BIOLOGIE CELLULAIRE **67**

3.0 SOMMAIRE 68

3.1 OBJECTIFS 69

3.2 Revue de la litterature 70
3.3 Conclusion 119

CHAPITRE 4 – LA XANTHOMMATINE NON-CYCLISEE EST UN INTERMEDIAIRE CLE DANS LA COLORATION DES INVERTEBRES 121

4.0 Sommaire 122
4.1 Objectifs et methodologies 124
4.2 Travail experimental 125
4.3 Conclusion 171

CHAPITRE 5 – LE CHANGEMENT DE COULEUR DES OMMOCHROMES REPOSE SUR LES COUPLAGES ELECTRONIQUES DE LA FORME REDUITE 173

5.0 Sommaire 174
5.1 Objectifs et methodologies 175
5.2 Travail experimental 177
5.3 Conclusion 215

CHAPITRE 6 – LES ORGANITES PIGMENTES APPARENTES AUX ENDOLYSOSOMES A L'ORIGINE DES CHANGEMENTS DE COULEUR DES ARAIGNEES CRABES 217

6.0 Sommaire 218
6.1 Objectifs et methodologies 219
6.2 Travail expérimental 220
6.3 Conclusion 254

CHAPITRE 7 – DISCUSSION GENERALE : LA BIOLOGIE INTEGRATIVE DES OMMOCHROMES 257

7.0 Sommaire 258
7.1 Introduction 259
7.2 Le role cle des ommochromes en tant que pigments changeant de couleur 260
7.3 Les fonctions biochimiques et physiologiques des ommochromes en-dehors de l'aspect visuel 266
7.4 Des contextes ecologiques de l'utilisation des ommochromes 276
7.5 Les ommochromes dans le contexte d'une origine commune des organites pigmentes 282
7.6 Conclusion : « Le caractere multi-texture » de la couleur 285

BIBLIOGRAPHIE 286

Remerciements

Cette thèse est avant tout le résultat d'une interaction entre un étudiant et un directeur de thèse. Je souhaite donc te remercier tout particulièrement, **Jérôme,** pour ton aide, tes conseils et ton soutien. J'ai eu la chance de pouvoir travailler avec toi avant cette thèse – huit ans déjà ! – et la relation que nous avons construite au fil du temps a joué un rôle clé. Merci donc de m'avoir dirigé vers les meilleurs endroits où réaliser mes stages, merci de m'avoir suivi pendant les trois ans où je passais les concours de l'enseignement et découvrais le monde de l'entreprise, merci de m'avoir laissé tant de liberté dans la construction et la mise en œuvre de cette thèse. Et merci d'encore me conseiller sur le présent et le futur de ma recherche.

Je souhaite remercier l'ensemble des membres de mon jury de thèse, **Leila Deravi**, **Nathalie Guivarc'h**, **Denis Jacquemin**, **Abderrahman Khila** et **Graça Raposo**, qui ont accepté de participer à ma soutenance de thèse et d'évaluer mes travaux. Je remercie tout particulièrement **Leila Deravi** et **Abderrahman Khila** qui me font l'honneur de prendre de leur temps en étant les rapporteuse et rapporteur de ce manuscrit de thèse.

Je remercie **Cédric Delevoye**, **Emmanuel Gaquerel** et **Arnaud Lanoue** d'avoir fait partie de mon comité de thèse. Vos conseils et vos remarques ont été d'une grande aide pour envisager, à mi-parcours, la suite de la thèse.

Je remercie l'**ENS de Lyon** de m'avoir accordé un financement doctoral et la liberté de construire mon sujet de thèse.

Un grand merci à l'ensemble de l'**IRBI**, et plus particulièrement aux membres de la direction, **David**, **Christelle** et **Simon**. L'excellente ambiance de ce laboratoire est une de ses marques de fabrique – pas étonnant que j'y sois retourné à trois reprises au cours de ces huit dernières années ! – et c'est en grande partie grâce à vous. Je remercie aussi tous les membres du secrétariat, tout particulièrement **Nathalie** qui a le don de communiquer sa joie de vivre.

Je remercie l'ensemble des membres de l'équipe **INOV** pour les nombreuses discussions scientifiques, et moins scientifiques. On apprécie d'autant plus la recherche quand on se retrouve avec des personnes comme vous ! Un grand merci donc, **Sylvain**, pour l'animation de l'équipe. Merci à toi et à **Claudio** pour votre aide et vos conseils sur de multiples aspects de ma thèse. Merci aussi, **Thomas**, pour toutes les fois où tu m'as dépanné.

Un travail de recherche n'aurait aucun sens s'il n'était pas réalisé en collaboration. Je souhaite donc vivement remercier le laboratoire **Biomolécules et Biotechnologies Végétales** à l'université de Tours pour avoir mis à disposition son savoir et son savoir-faire analytiques. Un merci tout particulier à **Arnaud** et **Thibaut**, l'idée de travailler sur des pigments de mouches et d'araignées au milieu de vos alcaloïdes de plantes ne vous a pas effrayé, bien au contraire ! Vu le nombre d'injections, je crois qu'on peut dire objectivement que notre collaboration a été fructueuse ; encore merci pour tout ce que vous m'avez appris, votre

confiance et surtout votre bonne humeur. Merci aussi à **Marianne** et **Kévin** pour votre aide et nos discussions.

Je remercie aussi le **Groupe Innovation et Ciblage Cellulaire** à l'université de Tours pour avoir mis à disposition ses outils de chimie de synthèse et de RMN. Merci **Marie-Claude** pour votre confiance. Un grand merci **Cécile** pour tout le temps que tu as passé à synthétiser de la xanthommatine, à essayer de la caractériser par RMN, … et pour les pauses café à discuter des façons d'attraper une araignée crabe !

Je crois que je ne pourrai jamais assez remercier l'ensemble de l'équipe **Structure et Compartiments Membranaires** de l'institut Curie. Si j'ai pu utiliser les plus belles techniques d'imagerie sur l'un des modèles les plus insolites – qui aurait cru que des araignées crabes se baladeraient au 6e étage du bâtiment Burg ? – c'est grâce à toi, **Graça**, et à tous les membres de ton labo. Votre enthousiasme, votre joie de vivre, votre bonne humeur, votre sens du travail en équipe et votre rigueur scientifique sont incroyables ; venir dans vos locaux était à chaque fois un vrai plaisir ! Un merci plus particulier à **Cédric** pour toutes nos discussions et les nombreuses capsules de café que tu m'as offertes. Merci aussi **Ilse**, **Xavier** et **Maryse** pour toute votre aide, qu'elle ait été scientifique, technique ou morale. Merci **Cécile**, **Fred**, **Gisela**, **Julia**, **Lia**, **Mathilde**, **Riddhi**, **Roberta** et **Silvia** pour les fous rires et les bonnes adresses de la rue Mouffetard. Enfin, merci **Léa** et **Cédric** de m'avoir initié à la biologie cellulaire, cette thèse n'aurait pas du tout été la même sans vous.

Toujours à l'institut Curie, mais à Orsay cette fois, un grand merci **Sylvain** d'avoir été aussi vite emballé à l'idée de passer des araignées crabes en STEM. Ce n'était pas gagné d'avance vu ce que tu as dû faire subir au porte-échantillon et vu la fragilité des supports Synchrotron, mais nous nous y sommes arrivés en un temps record. Merci surtout pour ton accueil chaleureux et ta bonne humeur.

Pas si loin d'Orsay, je souhaite maintenant remercier le **Synchrotron SOLEIL** et plus particulièrement les scientifiques et ingénieurs de la ligne de lumière Nanoscopium. Un grand merci, **Andrea** et **Kadda**, pour m'avoir fait découvrir le principe du Synchrotron, pour votre curiosité sans limite et nos nombreuses discussions. C'est aussi grâce à vous que les weekends, soirées et nuits blanches passés à analyser des échantillons sous un faisceau de rayons X ont été un réel plaisir. Merci, **Gilles**, pour ton aide technique et merci à **Igor Choupra** pour m'avoir fait mettre un pied dans le monde du Synchrotron.

Finalement, si ma thèse a acquis une saveur aussi « chimique » et interdisciplinaire, c'est grâce aux membres du groupe ***Chemical Theory and Modelling*** à Chimie ParisTech – PSL. Un grand merci, **Ilaria** et **Carlo**, pour l'intérêt que vous avez très rapidement porté à mon projet, pour toute votre aide, pour la mise à disposition de vos clusters de calculs, et surtout pour votre humour et votre bonne humeur. Confronter nos deux communautés a été très formateur ! Merci à **Bernardino**, **Dario**, **Francesco**, **Michele** et **Laure** pour m'avoir accueilli dans leurs bureaux. Merci **Allistar** pour toute ton aide côté informatique.

Parce que la thèse n'a pas uniquement été de la recherche, je remercie l'ensemble des membres du département de **Biologie Animale et Génétique** de l'université de Tours pour leur accueil et leur aide dans la préparation des TD et TP. Je remercie tout particulièrement

Corinne et **Géraldine** pour la gestion du département et pour m'avoir fait confiance pour leurs cours. Merci aussi **Stéphanie** pour ton aide au secrétariat.

Je souhaite aussi remercier celles et ceux qui m'ont aidé de manière plus ponctuelle tout au long de cette thèse : **Antoine Touzé** et **Marc Clastre** pour m'avoir laissé très librement utiliser leurs ultracentrifugeuses ; **Teresita** pour m'avoir appris les arcanes de l'histologie appliquée à l'araignée crabe ; **Rustem Uzbekov** et **Philippe Roingeard** pour la microscopie électronique des organites purifiés ; tous les membres, actuels et passés, du **plateau d'écologie chimique** qui m'ont conseillé et aidé dans mes expériences de chimie analytique ; **Leila** pour les discussions autour des ommochromes ; **Carole** pour ton aide avec « l'élevage » d'araignées crabes ; et **Ana** pour tous tes conseils sur les araignées crabes et pour m'avoir fait découvrir à quel point elles étaient étonnantes.

Bien sûr, je n'aurais pas passé trois ans de thèse aussi riches sans tou·te·s mes ami·e·s irbien·ne·s. Alors j'aimerais dire un grand merci à : la « best PhD team » **Sophie** et **Lucas**, on se sera soutenu·e·s, aidé·e·s et surtout bien marré·e·s jusqu'au bout ; **Mourad** pour ton flegme sans pareil, ta bonne humeur permanente et ta relecture ; **Caroline** pour avoir été la plus fun des marraines ; **Anthony** et **Julie** pour vos nombreuses invitations à venir bien manger ; **Antoine** pour les discussions entomologiques et la capture de papillons ; **Fanny** pour ton humour et le partage de ton amour des araignées ; **Aurélia** et **Bruno** pour les sorties naturalistes, mais aussi piscine ; **Nicolas**, **Ludovic** et **Miguel** pour l'ambiance dans le bureau. Enfin, merci à tous les doctorant·e·s, post-doctorant·e·s, ingénieur·e·s, ATER et stagiaires de master pour les déjeuners, les pauses, les sorties – bref, tous les « à côté » de la thèse.

Je remercie aussi tou·te·s mes ami·e·s en-dehors de la thèse, qui sont aussi parfois passé·e·s par là. Une pensée plus particulière pour **Adrien**, les **Antoine**, **Céline** et **Morgan**, **Édouard**, **Émilie** et **Raph** (sans oublier **Nono** !), **Florian**, **Lucas**, **Marion**, **Martin**, **Mathilde** et **Thibault**, **Perrine**, **Timothée** et **Jeanne**, et **Vincent** ; quand on se retrouve, c'est un peu comme si je n'avais jamais quitté Lyon !

Un grand merci à **Julien**, **Sylvie** et **Denise** pour m'avoir hébergé sur Paris et à Savigny. Bien des expériences n'auraient pas pu être faites sans ça – au moins pas aussi facilement et confortablement. Merci aussi pour votre curiosité ; communiquer sur sa thèse aide à la penser.

Un énorme merci à toute ma famille, plus particulièrement à mes **parents**, mon **frère** et ma **sœur**. Vous avez toujours été d'un soutien sans faille, et mes retours à Lyon ont été des grands bols d'air frais indispensables. Enfin, merci **Suzie** – pour tout. Pour avoir accepté et enduré les allers-retours à Paris. Pour ton aide, ta relecture et ton enthousiasme lorsqu'il fallait capturer des araignées. Pour ta curiosité et pour ton soutien. Merci de m'avoir supporté et compris pendant cette dernière ligne droite de la « thèse confinée ».

Curriculum vitae

Florent Figon

florent.figon@univ-tours.fr Université de Tours
Tel. +33 (0)2 47 36 69 81 Institut de Recherche sur la Biologie de l'Insecte,
ORCID : 0000-0002-6172-3865 UMR CNRS 7261, université de Tours

Thèse de doctorat

Photobiochimie et biologie cellulaire des ommochromes : implications dans le changement de couleur (soutenue le 02 septembre 2020). Directeur : Prof. Jérôme Casas.

Parcours universitaire

Sept. 2016 – août 2017 **Master 2**, Biologie
École normale supérieure de Lyon, Lyon, France

Sept. 2013 – juil. 2014 **Agrégation de SV-STU**, Biologie et géologie
École normale supérieure de Lyon, Lyon, France

Sept. 2012 – août 2013 **Master 1**, Biologie
École normale supérieure de Lyon, Lyon, France

Sept. 2011 – août 2012 **Licence 3**, Biologie
École normale supérieure de Lyon, Lyon, France

Sept. 2009 – juin 2011 **Classe préparatoire BCPST**, Biologie, Géologie, Maths et Phys.-Chim.
Lycée du Parc, Lyon, France

Parcours de recherche

Sept. 2017 – août 2020 **Doctorant** (Directeur : Prof. J. Casas)
Université de Tours, Institut de Recherche sur la Biologie de l'Insecte, Tours, France

Janv. 2020 – juin 2020 **Co-encadrant** (avec Prof. J. Casas)
Laurène Chevallier – Stage de M2 : Etude du polyphénisme de couleur chez un papillon, la Carte géographique, université de Tours, Institut de Recherche sur la Biologie de l'Insecte, Tours, France

Janv. 2017 – juil. 2017 **Stagiaire de M2** (Encadrants : Dr. C. Delevoye et Dr. L. Ripoll)
Institut Curie, UMR 144 Biologie Cellulaire et Cancer, Paris, France

Avr. 2016 – juil. 2016 **Stagiaire** (Encadrant : Prof. J. Casas)
Université de Tours, Institut de Recherche sur la Biologie de l'Insecte, Tours, France

Janv. 2013 – août 2013	**Stagiaire de M1** (Encadrant : Prof. E. Gaquerel) Institut Max Planck Institute de Chimie Ecologique, Département d'Ecologie Moléculaire, Jena, Allemagne
Juin 2012 – août 2012	**Stagiaire de L3** (Encadrants : Prof. J. Casas et Dr. A. L. Llandres) Université de Tours, Institut de Recherche sur la Biologie de l'Insecte, Tours, France

Parcours d'enseignement

Sept. 2017 – présent	**Vacataire à l'université** Université de Tours, Département de Biologie Animale et Génétique, Tours, France
Mai 2017 – juin 2017	**Colleur en SVT** Lycée du Parc, Classe préparatoire BCPST, Lyon, France
Sept. 2014 – juin 2015	**Colleur en SVT** Lycée du Parc, Classe préparatoire BCPST, Lyon, France

Parcours non-académique

Août 2015 – mars 2016	**Directeur éditorial** Collection Cycles 3 et 4 des manuels d'Histoire-Géographie pour le collège, édition 2016 – Lelivrescolaire.fr (éditeur scolaire), Lyon France
Juin 2015 – juil. 2015	**Eco-volontaire** Projects Abroad, Iles Galapgos, Equateur
Sept. 2014 – juin 2015	**Assistant éditorial** Lelivrescolaire.fr, Lyon France

Bourses

Mai 2019	Projet 20190205 : Ligne de lumière Nanoscopium au Synchrotron SOLEIL
Mai 2018	Projet 20180104 : Ligne de lumière Nanoscopium au Synchrotron SOLEIL
Sept. 2017	Contrat doctoral spécifique normalien (3 ans), école normale supérieure de Lyon
Sept. 2011	Contrat Normalien (4 ans), école normale supérieure de Lyon

Langues et activités

Langues	Français, anglais, espagnol
Passions	Guitare, Photographie, Education, Management, Natation

Publications dans des journaux internationaux à comité de lecture

Florent Figon, Jérôme Casas, Ilaria Ciofini, Carlo Adamo (2021). *Electronic Coupling in the Reduced State Lies at the Origin of Color Changes of Ommochromes*. Dyes and Pigments; **185**:108661. DOI: 10.1016/j.dyepig.2020.108661

Florent Figon, Thibaut Munsch, Cécile Croix, Marie-Claude Viaud-Massuard, Arnaud Lanoue, Jérôme Casas (2020). *Uncyclized xanthommatin is a key ommochrome intermediate in invertebrate coloration.* Insect Biochemistry and Molecular Biology; **124**:103403. DOI: 10.1016/j.ibmb.2020.103403

Florent Figon, Jérôme Casas (2019). *Ommochromes in invertebrates: Biochemistry and cell biology*. Biological Reviews; **94**(1):156-183. DOI:10.1111/brv.12441

Léa Ripoll, Xavier Heiligenstein, Ilse Hurbain, Lia Domingues, **Florent Figon**, Karl J. Petersen, Megan K. Dennis, Anne Houdusse, Michael S. Marks, Graça Raposo, Cédric Delevoye (2018). *Myosin VI and branched actin filaments mediate membrane constriction and fission of melanosomal tubule carriers*. The Journal of Cell Biology; **217**(8):2709-2726. DOI:10.1083/jcb.201709055

Ana L Llandres, **Florent Figon**, Jean-Philippe Christidès, Nicole Mandon, Jérôme Casas (2013). *Environmental and hormonal factors controlling reversible color change in crab spiders*. Journal of Experimental Biology; **216**(20):3886-95. DOI:10.1242/jeb.086470

Chapitres de livre

Florent Figon, Jérôme Casas (2018). *Morphological and Physiological Colour Changes in the Animal Kingdom*. eLS (eds: John Wiley & Sons, Ltd); Pages 1-11, ISBN: 9780470016176, DOI:10.1002/9780470015902.a0028065

Léa Ripoll, **Florent Figon**, Cédric Delevoye (2018). *Mécanismes inter- et intracellulaires contrôlant la pigmentation des mélanocytes de la peau*. Biologie cutanée CoBIP: fonctions normales et pathologiques de la barrière cutanée (ed: M Haftek) ; Lyon, France : Matrix; Pages 4-28.

Prépublication

Florent Figon, Ian T. Baldwin, Emmanuel Gaquerel (2020). *Ethylene is a local modulator of jasmonate-dependent phenolamide accumulation during* Manduca sexta *herbivory* in Nicotiana attenuata. bioRxiv. DOI: 10.1101/2020.07.21.213371

Peer Review

Biomolecules (1) et **Evolutionary Ecology** (1)

Communications scientifiques

Florent Figon*, Thibaut Munsch, Cécile Croix, Marie-Claude Viaud-Massuard, Arnaud Lanoue et Jérôme Casas (2019). *Identification de la xanthommatine non cyclisée, un intermédiaire clé de la biosynthèse pigmentaire des ommochromes chez les invertébrés*. 32nd Biotechnocentre symposium, Seillac, France. **Prix de la meilleure présentation orale**.

Florent Figon*, Jérôme Casas (2019). *Color-changing Crab Spiders: Classical Ecological Model, New Cell Biology Tools*. UMR 144 Seminar, Institut Curie, Paris, France. **Présentation orale**.

Florent Figon*, Teresita Insausti, Jérôme Casas (2018). *How the Ommochromasome Life Cycle of Colour-Changing Crab Spiders Can Enlighten Melanosome Catabolism*. 21st annual meeting of the European Society for Pigment Cell Research, Rennes, France. ***Flash-talk* et poster**.

Articles et chapitres de vulgarisation et d'enseignement scientifique

Thibault Lorin, **Florent Figon** (2020). *Fonctions adaptatives et évolution des couleurs des Animaux*. https://planet-vie.ens.fr/thematiques/ecologie/relations-interspecifiques/fonctions-adaptatives-et-evolution-des-couleurs-des. Planet-Vie (ENS).

Florent Figon, Thibault Lorin (2019). *La coloration des Animaux : éléments de physique et de chimie*. https://planet-vie.ens.fr/thematiques/cellules-et-molecules/biophysique/la-coloration-des-animaux-elements-de-physique-et-de. Planet-Vie (ENS).

Florent Figon (2019). *L'érosion, processus et conséquences*. Sciences de la vie et de la Terre 2nde, collection 2019 (eds: Lelivrescolaire.fr); Pages 163-178. https://www.lelivrescolaire.fr/page/7184122

Florent Figon (2019). *Erosion et activités humaines.* Sciences de la vie et de la Terre, lycée 2nde, collection 2019 (eds: Lelivrescolaire.fr); Pages 193-205. https://www.lelivrescolaire.fr/page/7255496

Florent Figon (2017). *L'évolution de la biodiversité.* Sciences de la vie et de la Terre, collège 3e, collection 2017 (eds: Lelivrescolaire.fr); Pages 131-145. https://www.lelivrescolaire.fr/manuel/1339497/svt-3e-2017/chapitre/1339647/l-evolution-de-la-biodiversite/page/1341398/l-evolution-de-la-biodiversite/lecon

Florent Figon, Thibault Lorin (2017). *D'où viennent les iguanes des Galapagos ?* Espèces; **24**:12-19. Repris sur Planet-Terre et Planet-Vie.

Réseaux

ORCID : 0000-0002-6172-3865

HAL : florent-figon

ResearcherID/Publons : U-6880-2019

Laboratoire - Google Scholar – ResearchGate

Résumé

La capacité qu'ont les animaux à changer de couleur en réponse à un environnement variable est remarquable. Les raisons pour lesquelles les animaux ont acquis une telle palette de couleurs ont toujours eu une place prépondérante en biologie. Encore aujourd'hui, la recherche sur la couleur des animaux est très active ; la difficile question de la valeur adaptative de la couleur et des changements de couleur nécessite des approches multidisciplinaires. Cela est encore plus vrai pour les pigments, dont les propriétés et les fonctions se situent à l'interface entre la chimie et la biologie. En effet, la structure électronique et l'état intracellulaire des pigments sont des paramètres clés influençant aussi bien leurs propriétés optiques que leur réactivité chimique. Ainsi, la biochimie et la biologie cellulaire des pigments peuvent informer sur leurs fonctions et leurs propriétés de changement de couleur.

Dans cette thèse, je m'intéresse aux couleurs chimiques des insectes, araignées et céphalopodes qui sont dues aux pigments appelés ommochromes. Les ommochromes contribuent efficacement aux changements de couleur pour plusieurs raisons. Premièrement, ils possèdent la capacité unique parmi les pigments d'animaux à pouvoir changer rapidement vers le rouge une fois réduits. Deuxièmement, leur diversité structurale est à l'origine d'une palette de couleurs, allant du jaune au rouge et violet. Enfin, ils sont produits à l'intérieur d'organites intracellulaires qui peuvent alterner dynamiquement entre production et dégradation. Cependant, malgré leur importance, ces mécanismes sont encore mal compris. Les fonctions biologiques de ces changements de couleur, si elles existent, sont rarement connues malgré des décennies de recherche particulièrement chez les araignées crabes. Dans ces travaux, je postule que le lien structure–propriété à plusieurs échelles des ommochromes représente un aspect important de leur biologie. Ainsi, l'étude des mécanismes de changement de couleur aux échelles moléculaires, biochimiques et subcellulaires devrait fournir des informations sur les potentielles fonctions et utilisations des ommochromes.

Dans cette perspective, je fais premièrement une revue des changements de couleur chez les animaux en comparant leurs mécanismes, leurs régulations et leurs fonctions. Je fais ensuite une synthèse de la biochimie et de la biologie cellulaire des ommochromes, fournissant ainsi une mise à jour depuis la dernière revue exhaustive sur le sujet il y a plus de 40 ans. Je procède enfin à une étude expérimentale de trois systèmes biologiques en lien avec les propriétés de changement de couleur des ommochromes, c'est-à-dire leur biosynthèse chez la mouche domestique, la couleur nuptiale chez les libellules et le changement de couleur réversible des araignées crabes. Les résultats renforcent l'idée que la couleur des ommochromes est associée à d'autres fonctions biologiques, dont la capacité antiradicalaire et le stockage des métaux. Ainsi, les ommochromes ne devraient pas être étudiés uniquement à travers le prisme de la couleur, mais aussi à la lumière de leur dynamique chimique et cellulaire intrinsèque, ce qui est en accord avec d'autres systèmes pigmentaires.

En somme, cette étude est une première étape vers la mise à l'épreuve d'hypothèses biologiques souvent négligées dans des systèmes où la fonction écologique des changements de couleur reste à découvrir.

Abstract

One of the most striking feature of animal colorations is their capacity to change in response to a variable environment. The reasons why animals acquired such a range of colors has always held a central position in biology. Even today, animal coloration is an active field of research and it requires multidisciplinary approaches to tackle the complex question of the adaptive value of colorations and color changes. This is especially true for pigments, whose properties and functions lie at the interface between chemistry and biology. Indeed, the electronic structure and the intracellular state of pigments are key factors that affect their optical properties, as well as their chemical reactivity. Therefore, the biochemistry and cell biology of pigments can inform on the functions of pigments and their color-changing capacities.

In this thesis, I focus on chemical colorations defined by the ommochrome pigments of insects, spiders and cephalopods. Ommochromes contribute to efficient color changes for several reasons. First, they possess the unique capacity among animal pigments to shift rapidly towards redder colors upon chemical reduction. Second, their structural diversity produces colors from yellow and red to purple. Finally, they are synthesized within intracellular organelles that can be dynamically rerouted toward production and degradation. Yet, despite their broad significance, the mechanisms behind these three properties are poorly understood. The biological functions, if any, of these color changes are seldom known despite decades of research, especially in crab spiders. In this work, I postulate that the multiscale structure–property relationship of ommochromes is an important aspect of their biology. Therefore, unravelling color-changing mechanisms at electronic, biochemical and intracellular levels should provide insight into the potential functions and uses of ommochromes.

For this purpose, I first review color changes in animals to compare their mechanisms, regulation and functions. I then review the biochemistry and cell biology of ommochromes, providing an update since the last major review more than 40 years ago. I finally study experimentally three biological systems related to the different color-changing properties of ommochromes, namely ommochrome biosynthesis in houseflies, nuptial coloration of dragonflies and reversible color changes of crab spiders. I employed mass spectrometry, quantum chemical modeling and nanoscale imaging techniques. The results strongly support the idea that ommochrome colors go along with other biologically relevant functions, such as antiradical capacities and metal storage. Therefore, ommochromes should not be seen only through the lens of coloration, but also in the light of their inherent chemical and cellular dynamics, in agreement with other pigmentary systems.

Overall, this study paves the way for testing new biological hypotheses in systems for which ecological functions of color changes remain to be discovered.

Liste des figures

Figures principales

Figure 1-1. Diversité des chromatophores de pigments d'animaux. 32

Figure 2-1. Model Organisms and Their Contributions to the Study of Colour Changes in the Animal Kingdom. 49

Figure 2-2. Morphological Colour Changes in a Crab Spider. 54

Figure 2-3. Environmental and Intrinsic Factors Controlling Morphological Colour Changes. 57

Figure 2-4. Physiological Colour Changes at the Tissue Level in Cephalopods. 59

Figure 2-5. Factors Regulating Physiological Colour Changes at the Cellular Level. 60

Figure 3-1. Examples of protostomes that produce ommochromes. 73

Figure 3-2. History of ommochrome study. 75

Figure 3-3. The ommochrome biosynthetic pathway. 79

Figure 3-4. The reactivity of ommochromes and related compounds. 83

Figure 3-5. Putative scheme of ommochromasome biogenesis. 103

Figure 3-6. Putative model for the formation and recycling of ommochromasomes and ommochromes. 107

Figure 3-7. Integrated biology of ommochromes and ommochromasomes. 113

Figure 4-1. Current knowledge of the tryptophan→ommochrome pathway of invertebrates. 129

Figure 4-2. Chromatographic profiles of synthesized xanthommatin before and after storage in acidified methanol. 138

Figure 4-3. Absorbance- and mass spectrometry-assisted elucidation of the structure of the five major ommatins detected after incubation in acidified methanol. 141

Figure 4-4. Alterations of synthesized ommatins in acidified methanol at 20 °C in darkness. 146

Figure 4-5. Structural elucidation of uncyclized xanthommatin, the labile intermediate in the synthesis of xanthommatin. 148

Figure 4-6. Biological localization of uncyclized xanthommatin and tryptophan→ommochrome metabolites from housefly eyes. 151

Figure 4-7. *In vitro* formation and alteration of ommatins. 154

Figure 4-8. Proposed biosynthetic pathway of ommochromes through the formation of uncyclized xanthommatin in ommochromasomes. 155

Figure 5-1. Set of substituted phenoxazin-3-ones and 3-methoxy-phenoxazines investigated in this study. 183

Figure 5-2. Computed vertical chromic shifts (ΔE^{vert} shift) of phenoxazinone/phenoxazine pairs as a function of two aromaticity indexes (A), cHOMHED (B) and NICS(0) (C), of phenoxazines. 186
Figure 5-3. Relationship between computed vertical excitation energies (ΔE^{vert}) chromic shifts of phenoxazinone/phenoxazine pairs. 189
Figure 5-4. Comparison of chromic shifts (ΔE^{vert} shift) of phenoxazinone/phenoxazine pairs with electron affinity (EA, A) and chemical hardness (η, B) of phenoxazines. 190
Figure 5-5. Comparison of computed chromic shifts (ΔE^{vert} shift) of phenoxazinone/phenoxazine pairs with geometric (A) and electronic (B-C) properties of electron-withdrawing auxochromes (EWA) in position 1. 193
Figure 5-6. Orbital diagrams of the bathochromic ommochrome pair xanthommatin/dihydroxanthommatin and the hypsochromic pair resorufin/dihydroresorufin. 195
Figure 5-7. Model of the effect of geometric and electronic couplings on chromic shifts and chemical behaviors of phenoxazinone/phenoxazine pairs upon reduction. 197
Figure 6-1. High-pressure freezing reveals labile ultrastructural features that relate pigment organelles of crab spiders to endolysosome-related organelles. 230
Figure 6-2. Correlative Synchrotron X-ray fluorescence and scanning transmission electron microscopy reveals metal accumulation in pigment organelles. 232
Figure 6-3. Ultrastructural diversity and typology of pigment organelles. 234
Figure 6-4. Pigment organelles differentially accumulate metals according to coloration and maturation stages. 236
Figure 6-5. Maturing a-type pigment organelles are associated to tubulo-saccular regions, which are associated to endosomes and enriched in vesicular and tubular carriers. 238
Figure 6-6. Evidence of homotypic fusion events between a-type pigment organelles in white spiders. 239
Figure 6-7. Evidence of intraluminal degradation and clustering of pigment organelles in yellow spiders. .. 241
Figure 7-1. Formules chimiques des phénazines et des phénoxazinones. 267
Figure 7-2. Composition chimique des ommochromasomes purifiés à partir des yeux de mouches domestiques. 272

Figures supplémentaires

Figure S4-1. ^{1}H-NMR spectrum of synthesized xanthommatin in acidic DMSO. 161

Figure S4-2. Optimization of cone voltages and collision energies for single reaction monitoring of ommochrome-related metabolites. 162

Figure S4-3. Determination of the wavelength at which ommatins absorb light equivalently. 163

Figure S4-4. Slow methoxylations of synthesized ommatins in acidified methanol at -20 °C in darkness. 164

Figure S4-5. Analytical characterization of dihydroxanthommatin. 165

Figure S4-6. Analytical characterization of uncyclized xanthommatin in methanolic extracts of housefly eyes. 166

Figure S4-7. Ommatins are altered by addition of β-mercaptoethanol. 168

Figure S5-1. Mean absolute errors in computed B3LYP bond lengths of 2-amino-7-methoxy-phenoxazine-3-one as a function of the basis set used. 206

Figure S5-2. Basis-set dependence of the first vertical excitation energy computed for the 2-amino-7-methoxy-phenoxazine-3-one molecule. 207

Figure S5-3. Mean absolute errors (MAE) in computed vertical excitation energies of phenoxazinones and phenoxazines for a series of functionals. 207

Figure S5-4. Comparison of M05-computed vertical excitation energies (ΔE^{vert}) with experimental maximum excitation energies (ΔE^{exp}). 208

Figure S5-5. Mean absolute error (MAE) in computed vertical chromic shifts of phenoxazinones/phenoxazines pairs for a series of functionals. 208

Figure S5-6. Comparison of M05-computed chromic shifts (ΔE^{vert} shift) with experimental shifts (ΔE^{exp} shift) of phenoxazinone/phenoxazine pairs. 209

Figure S5-7. Comparison of computed chromic shifts (ΔE^{vert} shift) of phenoxazinone/phenoxazine pairs with the sHOMHED values of corresponding reduced phenoxazines (red). 209

Figure S5-8. Comparison of computed chromic shifts (ΔE^{vert} shift) of phenoxazinone/phenoxazine pairs with the vertical excitation energies of corresponding oxidized phenoxazinones (ΔE_{ox}^{vert}). 210

Figure S5-9. Frontier orbital diagrams of two bathochromic phenoxazinone/phenoxazine pairs (1 and 2) and two hypsochromic ones (15 and 14). 210

Figure S5-10. Comparison of computed chromic shifts (ΔE^{vert} shift) with HOMO-LUMO gaps of phenoxazinone/phenoxazine pairs. 211

Figure S5-11. Molecular orbital diagrams of unsubstituted 2-hydro-phenoxazine-3-one, 2,3-dimethoxy-phenoxazine and of two electron-withdrawing auxochromes (EWA). 211

Figure S6-1. Ultrastructure of crab spider cells preserved by high-pressure freezing and freeze substitution. 248

Figure S6-2. Intraluminal vesicles and membrane tubulations of pigment organelles. 249

Figure S6-3. Recorded Synchrotron X-ray spectra of two intracellular regions within the same cell. 250
Figure S6-4. Various pigment organelle types observed within c-type clusters. 251
Figure S6-5. Examples of tubulo-saccular complexes in pigment cells of crab spiders. 252
Figure S6-6. Ultrastructural evidence of lysosomal degradation of pigment organelles. 253

Liste des tables

Tables principales

Table 2-1. Morphological and Physiological Colour Changes Are Widespread in the Animal Kingdom. 48

Table 3-1. Chemical characteristics of ommochromes. 80

Table 3-2. Enzymes involved in ommochrome biosynthesis and their related mutants in insects. 88

Table 3-3. Orthologues and functions of proteins encoded by ommochrome-related genes of the granule group in *Drosophila melanogaster*. 102

Table 4-1. Analytical characteristics of ommatin-related compounds found *in vitro* and in biological extracts. 139

Table 4-2. Diagnostic neutral losses of ommatins. 143

Table 5-1. Average values and dispersion of electronic and structural parameters computed for oxidized phenoxazinones and reduced phenoxazines. 187

Table 5-2. Computed chemical descriptors (in eV) of electron-withdrawing auxochromes (EWA) in relation with the chromic shifts they induce experimentally in phenoxazinone/phenoxazine pairs. 192

Table 6-1. Characteristics of pigment organelle types in relation to coloration. 235

Table 7-1. Paramètres influençant l'interaction entre la lumière et la matière et qui interviennent potentiellement dans le changement de couleur des pigments 262

Table 7-2. Calculs quantiques de l'électrochromisme de deux phénazines ayant des substituants différents. 269

Table 7-3. Le lien structure–propriété des organites apparentés aux endolysosomes (ELROs) et ses fonctions dans la pigmentation 283

Tables supplémentaires

Table S5-1. Electronic parameters of electron-withdrawing auxochromes in relation with the chromic shifts they induce theoretically. 212

Table S5-2. Computed electronic and structural parameters of oxidized xanthommatin and resorufin and their respective reduced forms. 213

Chapitre 1 – Introduction générale

Without absorption, […] the Earth would be a far less colorful place, with no paintings, flowers, leopard spots, or stained-glass windows.

Sönke Johnsen, *The Optics of Life* (2012)

1.0 Sommaire

CHAPITRE 1 – INTRODUCTION GENERALE 19

1.0 SOMMAIRE 20

1.1 UNE VIE HAUTE EN COULEUR 21

1.2 APERÇU DE L'HISTOIRE DE LA BIOLOGIE DE LA COULEUR 22

Avant Darwin : les couleurs n'ont pas d'importance pour les animaux 22

La seconde moitié du 19e siècle : les couleurs et le darwinisme 22

Le début du 20e siècle : le débat sur le camouflage provoqué par Thayer 23

La seconde moitié du 20e siècle : l'importance de la biochimie des pigments 24

1.3 LA CHIMIE DES COULEURS 26

La formation des couleurs : une interaction entre photons et électrons 26

Les méthodes d'étude des pigments : explorer leur relation structure–fonction 27

Analyse expérimentale par les techniques spectroscopiques 27

Analyses numériques avec la chimie quantique 29

1.4 L'IMPORTANCE BIOLOGIQUE DES PIGMENTS CHEZ LES ANIMAUX 31

La diversité et la distribution des pigments 31

Les pigments à l'intérieur de la cellule 34

L'état cellulaire des pigments 34

Les méthodes d'étude des organites pigmentés : étudier les couleurs à l'échelle subcellulaire 34

Les nombreuses fonctions biologiques des pigments 37

1.5 OBJECTIFS DE LA THESE 38

Questions, postulats et hypothèses 38

Plan de la thèse 39

1.1 Une vie haute en couleur

Les couleurs sont étonnamment diverses et importantes, aussi bien pour la nature que pour les sociétés humaines. Elles sont présentes dans tous les domaines scientifiques et artistiques, depuis la biologie évolutive (Mayr, 1999) jusqu'à la peinture (Schenk, 2009) et les technologies intelligentes (Caro, Stoddard, & Stuart-Fox, 2017a). En biologie, la grande variété de couleurs chez les animaux, les champignons, les plantes et les bactéries ont depuis plus d'un siècle attiré l'attention des scientifiques (Wallace, 1877; Poulton, 1890). L'étude du polymorphisme de couleurs a mené à un vaste nombre de découvertes dans bien des domaines (Caro, Stoddard, & Stuart-Fox, 2017b), depuis la génétique (ex. la couleur des pois et des yeux de drosophile) jusqu'à l'écologie évolutive (ex. le mélanisme industriel de la phalène du bouleau et le mimétisme des papillons du genre *Heliconius*). Comprendre comment et pourquoi les organismes sont colorés revêt donc une importance majeure (Caro *et al.*, 2017a; Cuthill *et al.*, 2017).

Le monde dans lequel nous vivons est non seulement coloré mais il est aussi dynamique. La couleur d'un seul individu peut varier en fonction de la lumière ambiante, du système visuel de l'observateur ou encore du mécanisme par lequel elle est produite (Björn, 2015). Les céphalopodes et les caméléons sont des maîtres en matière de changements de couleur rapides ; ils sont ainsi capables de se fondre dans leur environnement (Hanlon *et al.*, 2009) ou d'afficher leurs émotions (Teyssier *et al.*, 2015) en une fraction de seconde. Les autres organismes capables de changements de couleur, par exemple les arthropodes et les poissons, prennent généralement plus de temps mais ils peuvent tout de même produire une impressionnante palette de couleurs au cours de leur vie (Umbers *et al.*, 2014; Ligon & McCartney, 2016). Même nous êtres humains pouvons modifier en l'espace de quelques jours le ton de la couleur de notre peau en réponse à l'ensoleillement. Cette plasticité de couleur profère-t-elle une réponse adaptative à un environnement changeant ? Et si oui, comment ? Ce sont là des questions clés en biologie (Umbers *et al.*, 2014; Cuthill *et al.*, 2017) et qui vont m'intéresser dans cette thèse.

Afin d'étudier la biologie du changement de couleur, je présente en premier un bref historique de l'importance des couleurs depuis Darwin. Je discute ensuite de la chimie des couleurs en me concentrant sur les pigments. Je fournis aussi des informations concernant les techniques et les approches que j'ai utilisées pour étudier les propriétés chimiques des

pigments en relation avec leur couleur. Puis je discute de l'importance biologique des pigments chez les animaux en décrivant leur distribution, leurs états et leurs fonctions à l'intérieur de l'organisme. Je souligne en particulier l'importance de la biologie cellulaire des pigments et je présente quelques méthodes d'analyses associées. Enfin, je réduis la portée de mes travaux à une seule famille de pigments, les ommochromes, et je présente le plan de ma thèse.

1.2 Aperçu de l'histoire de la biologie de la couleur

Avant Darwin : les couleurs n'ont pas d'importance pour les animaux

Les raisons qui permettent d'expliquer la couleur des animaux ont fait l'objet de vifs débats chez les zoologistes, en particulier après que Darwin a exposé sa théorie de l'évolution en 1859 (Kingsland, 1978). Avant cela, on pensait que les couleurs avaient surtout une fonction esthétique, qu'elles avaient été créées pour plaire à l'œil humain. D'autres, qui étaient convaincus par le lamarckisme, défendaient que les couleurs n'étaient que le reflet de l'effet de la lumière et de la température sur les tissus (Wallace, 1877). En somme, la couleur n'avait pas de fonction pour celui qui l'arborait (Wallace, 1877; Kingsland, 1978).

La seconde moitié du 19^{e} siècle : les couleurs et le darwinisme

Peu après la publication de la théorie de l'évolution par Darwin, les trois célèbres naturalistes Henry W. Bates, Alfred R. Wallace et Fritz Müller décrivirent les colorations comme un moyen d'échapper aux prédateurs (Bates, 1862; Wallace, 1867; Müller, 1879). Wallace a été le premier à proposer une explication aux couleurs des plantes et des animaux qui soit entièrement basée sur « la sélection naturelle [qui] élimine en permanence les couleurs qui sont délétères pour les espèces, ou [qui] maintient et intensifie celles qui sont bénéfiques.[1] »

Edward B. Poulton suggéra pour sa part une vision plus nuancée en argumentant que des couleurs sans fonction existaient aussi. Il mentionna en particulier les couleurs observables à l'intérieur du corps : « le sang est rouge, la graisse est blanche […]. Dans de

[1] Traduit de (Wallace, 1877, p. 659) : « natural selection is constantly eliminating such tints as are injurious to the species, or preserving and intensifying such as are useful. »

tels cas, il n'y a pas de raison d'invoquer une utilité ou une signification à la couleur dans l'économie de l'animal.[2] » Il reconnut aussi que certaines couleurs pouvaient avoir une fonction en dehors de leurs effets visuels, telle que la thermorégulation et la photoperception. Cependant, dans l'ensemble, les couleurs avaient pour Poulton principalement un rôle dans le camouflage, l'avertissement et la parade nuptiale ; ce qui validait largement la théorie de Darwin à ses yeux (Poulton, 1890).

L'approche de Frank E. Beddard était, elle, bien moins darwinienne. En effet, il reprit la question de l'influence directe de l'environnement, y compris de la lumière, de l'humidité et de la nourriture, sur la production de la couleur et de ses changements : « Il y a de nombreux exemples où la couleur d'un animal est apparemment due directement à l'influence de son environnement, et n'a aucun lien possible avec la sélection naturelle.[3] » En somme, la différence d'opinion entre les naturalistes du 19^{e} siècle révèle à quel point la question de la couleur des animaux était déjà un sujet difficile (Kingsland, 1978).

En réponse à cette apparente complexité, Marion I. Newbigin affirma que « le sujet est aussi incomplet d'un point de vue théorique que physiologique. Il semble raisonnable de penser que ces deux carences sont liées, et qu'un peu plus de physiologie donnera de meilleures armes aux théoriciens.[4] » Elle souligna la nécessité d'obtenir « plus de données » (Newbigin, 1898, p. 325) pour éclaircir la fonction de la couleur, en particulier concernant la relation entre la chimie et la physiologie des pigments.

Le début du 20^{e} siècle : le débat sur le camouflage provoqué par Thayer

Au début du 20^{e} siècle, l'artiste Abbott H. Thayer se positionna dans le débat sur la fonction biologique des couleurs en argumentant que toutes les couleurs avaient une valeur adaptative en termes de camouflage (Kingsland, 1978). Ainsi, il écrivait : « on peut lire sur la

[2] Traduit de (Poulton, 1890, p. 12) : « blood is red, fat is white, […]. In such cases there is no reason why we should inquire as to the use or meaning of the colour in the animal economy. »
[3] Traduit de (Beddard, 1892, p. 42) : « There are numerous cases where the coloration of an animal appears to be due directly to the influence of the surroundings, and to have no possible relation to natural selection. »
[4] Traduit de (Newbigin, 1898, p. 325) : « the subject is as incomplete on the theoretical as on the physiological side. It seems reasonable to believe that the two deficiencies are related, and that a little more physiology will arm the theorists with better weapons. »

robe d'un animal les principales indications sur ses habitudes et son habitat, sans jamais le voir dans son milieu.[5] »

A l'inverse, le naturaliste et ancien président Theodore Roosevelt Jr. critique de manière virulente la théorie de Thayer postulant que « la doctrine semble […] poussée à un extrême incroyable et inclure tant de folles absurdités qu'il faut en appeler à appliquer le bon sens.[6] » Il reconnut en particulier que « […] nous n'en savons pas suffisamment pour être capables d'expliquer tout ou partie des différents types de couleur et leurs origines possibles.[7] »

La seconde moitié du 20e siècle : l'importance de la biochimie des pigments

La question de la fonction physiologique des pigments retint à nouveau l'attention des scientifiques avec les travaux, entre autres, de Francis B. Sumner qui déclara que les « substances colorées peuvent ou non avoir un rôle à jouer dans l'économie de l'organisme. Quand elles en ont un, ce rôle peut ou pas avoir un lien avec l'apparence extérieure de l'animal.[8] » Il suggéra la possibilité que l'apparence externe des animaux soit seulement un « simple produit dérivé du […] métabolisme.[9] » Cependant, il distinguait très clairement la propriété de coloration d'un pigment de sa fonction biologique : « Dans tous les cas, nous ne devons pas confondre la question de l'utilité d'une substance donnée qui est, par chance, colorée, avec l'utilité de la couleur visible que cette substance donne à l'animal qui la possède.[10] » Ainsi, il proposa d'appeler « pigments » uniquement les molécules qui ont un effet visuel et donc que les « pigments respiratoires » devaient nécessairement être renommés.

---

[5] Traduit de (Thayer & Thayer, 1909, p. 12) : « one may read on an animal's coat the main facts of his habits and habitat, without ever seeing him in his home. »
[6] Traduit de (Roosevelt, 1911, p. 122) : « the doctrine seems […] pushed to such a fantastic extreme and to include such wild absurdities as to call for the application of common sense thereto »
[7] Traduit de (Roosevelt, 1911, p. 219) : « we do not know enough to be able to explain all, or anything like all, the different kinds of coloration and their probable origins »
[8] Traduit de (Sumner, 1937, p. 351) : « Colored substances may or may not have a role to play in the economy of the organism. When they do, this role may or may not have anything to do with the animal's external appearance. »
[9] Traduit de (Sumner, 1937, p. 351) : « mere by-product of […] metabolism »
[10] Traduit de (Sumner, 1937, pp. 351–352) : « In any case, we must not confuse the question of the utility of a given substance which chances to be colored, and the utility of the visible color which this imparts to the animal possessing it. »

Denis L. Fox proposa, lui, une vue alternative dans laquelle la couleur des pigments, ou « biochromes » comme il préférait les appeler (Fox, 1944), ne pouvait pas être séparée de leurs fonctions biochimiques et physiologiques. Il écrivit ainsi : « La couleur et l'activité biochimique sont […] deux effets imbriqués issus du même phénomène moléculaire fondamental.[11] » Son opinion était donc alignée avec celle de Newbigin, qu'il citait par ailleurs, en demandant une « connaissance plus précise de la chimie et de la physique des systèmes qui produisent la couleur chez les animaux.[12] »

Arthur E. Needham offrit, selon moi, le travail le plus exhaustif sur l'importance fonctionnelle des pigments chez les animaux et son lien avec la biochimie, le métabolisme, la biologie cellulaire et la physiologie (Needham, 1974). Il partageait notamment l'avis de Fox en postulant que « La question principale, comment une molécule produit de la couleur, doit être traitée de la manière la plus complète possible puisque l'importance des biochromes en dépend probablement toujours, même lorsque la couleur elle-même parait inutile.[13] » À partir de là, les hypothèse évoquées pour expliquer la couleur des animaux à la fin du 20^{e} siècle prenaient systématiquement en compte les fonctions biochimiques des pigments (Burtt, 1981; Britton, 1983; Hoffmann, 1984; Oxford & Gillespie, 1998).

En conclusion, l'importance biologique des couleurs a fait l'objet d'âpres débats pendant plus d'un siècle et demi. Il y a eu une alternance d'hypothèses favorisant, d'un côté, la valeur adaptative de la couleur, en particulier en termes visuels, et, de l'autre côté, l'absence de fonctions aux couleurs. Ces différences d'opinion furent en partie résolues en prenant en compte la chimie intrinsèque des pigments pendant le 20^{e} siècle. Cette approche s'est traduite par de nombreuses monographies qui firent la part belle aux propriétés biochimiques des pigments et aux liens avec leurs fonctions biologiques [ex. (Britton, Liaaen-Jensen, & Pfander, 1995; Hill & McGraw, 2006; Borovanský & Riley, 2011)]. Sur la recommandation de Needham, je vais maintenant discuter des bases chimiques de la couleur.

---

[11] Traduit de (Fox, 1944, p. 471) : « Colour and biochemical activity are [...] two interlocked effects of the same fundamental molecular phenomenon. »

[12] Traduit de (Fox, 1976, p. 3) : « accurate knowledge of the chemical and physical systems which give rise to colour in animals »

[13] Traduit de (Needham, 1974, p. 4) : « The leading question, how a molecule produces colour, must be answered as fully as possible since the significance of biochromes is probably always dependent on this, even where colour itself seems irrelevant. »

1.3 La chimie des couleurs

La formation des couleurs : une interaction entre photons et électrons

Toutes les couleurs résultent d'une interaction entre la lumière (photons) et la matière [atomes, et plus particulièrement les électrons ; (Johnsen, 2012)]. Selon le type d'interaction, on différencie les couleurs en deux grandes classes : les couleurs structurales (ou physiques) et les couleurs pigmentaires (ou chimiques). Les couleurs structurales proviennent d'interférences produites par des surfaces à l'échelle microscopique lorsqu'elles diffusent la lumière (Johnsen, 2012). L'iridescence des plumes de paons est un des exemples les plus connus. Les couleurs chimiques, qui feront l'objet de cette thèse, sont produites par des molécules qui absorbent de manière sélective certaines longueurs d'onde de la lumière visible (entre 400 et 700 nm pour les humains, mais on peut étendre à 350 et 800 nm pour d'autres espèces). La lumière que nous percevons perd alors ces longueurs d'onde absorbées (Zollinger, 2003) et elle prend la couleur de toutes celles restantes ; c'est-à-dire la couleur complémentaire de celles manquantes [ex. si le violet est retiré, la lumière prend une teinte jaune ; (Needham, 1974)].

La raison pour laquelle seulement un certain type de molécules, qu'on appelle pigments, colorants ou chromes, peut absorber la lumière visible provient des bases électroniques de l'absorption lumineuse (Zollinger, 2003; Björn, 2015). Les molécules sont des assemblages ordonnés d'atomes liés entre eux par les électrons de leurs couches les plus élevées. Ces électrons dits de valence possèdent un certain niveau d'énergie à leur état fondamental (le plus stable), ainsi qu'un éventail d'autres niveaux énergétiques dits excités qui sont distribués de manière discrète et quantifiée. La lumière transporte de l'énergie sous forme de photons, qui peuvent être absorbés par les électrons si l'énergie photonique correspond exactement à la différence d'énergie entre l'état de base et un des états excités de ces électrons (Zollinger, 2003). Les énergies photoniques qui peuvent exciter les électrons de valence de la plupart des atomes et molécules sont de l'ordre de quelques eV, typiquement dans la région des ultraviolets (UV, en-dessous de 350 nm ou au-dessus de 3.5 eV). Cependant, la façon dont les électrons sont distribués dans la molécule (ce qu'on appelle la configuration électronique) peut stabiliser les états excités en abaissant leurs niveaux énergétiques. Ainsi, certaines configurations électroniques peuvent rendre possible l'absorption de photons entre 1.5 eV et 3.5 eV, ce qui correspond à des longueurs d'onde

entre 800 et 350 nm (Zollinger, 2003). Ces configurations électroniques très spéciales impliquent généralement une alternance de liaisons doubles et simples dans lesquelles les électrons ont une plus grande liberté de déplacement. On dit que ces électrons sont délocalisés autour de ces liaisons. La partie d'un pigment qui est composée d'un nombre suffisant de liaisons conjuguées est appelée le chromophore (ex. les cycles aromatiques). Les groupes chimiques qui affectent les énergies d'excitation en tirant (ou en poussant) les électrons depuis (ou vers) le chromophore sont appelés des auxochromes donneurs (ou accepteurs) d'électron [ex. -NO_2, -COOH, -OH, etc.; (Needham, 1974; Zollinger, 2003)]. En somme, les pigments, colorants et chromes (que j'appellerai collectivement pigments) peuvent être décrits comme un ensemble d'auxochromes attachés à un chromophore, dont les électrons de valence possèdent la capacité unique d'absorber des photons de faible énergie (donc dans le domaine visible de la lumière).

Du point de vue de la plasticité, cette chimie des pigments nous apprend que la configuration électronique est le paramètre clé qui influe sur leur couleur. La détermination colorimétrique du pH en est un exemple puisqu'ici les cations et les anions d'un pigment possèdent une couleur différente de l'état neutre suite au réarrangement des électrons lors de la perte ou l'ajout d'un proton (Zollinger, 2003). Dans cette thèse, j'étudie des phénomènes similaires mais dans des contextes biologiques.

Les méthodes d'étude des pigments : explorer leur relation structure–fonction

Analyse expérimentale par les techniques spectroscopiques

Comme discuté plus haut, la structure (électronique) des pigments joue un rôle central dans l'obtention de leurs propriétés colorantes. L'étude de la structure d'un pigment est donc un prérequis pour comprendre sa fonction dans la nature. Les techniques spectroscopiques ont une importance fondamentale puisqu'elles fournissent des informations sur la structure des molécules en se basant sur leur interaction avec la lumière (ex. la spectroscopie UV-Visible) ou avec toute autre forme d'énergie (ex. la spectrométrie de masse). Les méthodes théoriques et numériques complètent ces techniques expérimentales en modélisant les comportements électroniques. Dans ce qui suit, je décris brièvement les méthodes utilisées dans cette thèse.

La spectroscopie UV-Visible caractérise l'interaction entre les molécules et le rayonnement électromagnétique, souvent entre 200 et 700 nm (Zollinger, 2003). Ses résultats sont généralement donnés sous la forme de spectres d'absorption, qui montrent la quantité relative de lumière absorbée dans la lumière transmise par rapport à celle incidente en fonction de la longueur d'onde. Aussi bien l'intensité d'absorption que la longueur d'onde absorbée vont dépendre du chromophore et des auxochromes. Ainsi, les spectres d'absorption sont une signature des différents pigments qui permettent de les différencier (Britton, 1983). Cependant, le processus d'absorption dépend aussi de nombreux autres facteurs, tels que la température, le solvant, l'agrégation, l'état redox, etc. (Zollinger, 2003). Bien que ces paramètres puissent fournir des informations sur les propriétés du pigment en question, ils compliquent généralement les spectres d'absorption qui ne peuvent donc pas indiquer précisément la façon dont les électrons sont distribués. De plus, les autres groupes chimiques qui composent un pigment mais qui ne font pas partie des auxochromes et du chromophore ne participent pas au processus d'absorption UV-Visible. Ainsi, cette technique ne permet pas d'accéder à l'ensemble de la structure des pigments par définition.

Parmi les techniques analytiques qui permettent d'élucider plus précisément la structure chimique, la spectrométrie de masse (MS) en tandem (MS/MS) couplée à la chromatographie est une des plus versatiles puisqu'elle peut être appliquée sans trop de difficultés à une grande diversité de molécules, et ce jusqu'à des concentrations de l'ordre du femto-molaire (Boyd, Basic, & Bethem, 2008; Weissberg & Dagan, 2011; De Vijlder *et al.*, 2017). Le principe de base de la MS/MS est d'ioniser et de fragmenter des molécules. En mesurant le ratio masse-sur-charge (*m/z*) de ces ions, on peut en théorie en déduire leur formule chimique, en particulier celui de l'ion parent (non-fragmenté, donc la molécule initiale). En comparant les *patterns* de fragmentation obtenus avec ceux de molécules connues, on peut alors élucider la structure de molécules inconnues. Cependant, l'analyse est rendue compliquée par les nombreux et souvent imprédictibles réarrangements qui peuvent se produire lors de la fragmentation, en particulier pour les structures aromatiques tels que les chromophores, ainsi que par la résolution limitée des spectromètres de masse (Weissberg & Dagan, 2011; De Vijlder *et al.*, 2017). Les analyses MS/MS gagnent alors à être complétées par un couplage avec un spectroscope UV-Vis en amont de l'ionisation/fragmentation puisque les deux techniques donnent des informations indépendantes [dites orthogonales ; (De Vijlder *et al.*, 2017)]. En pratique, la MS/MS et la spectroscopie UV-Vis sont mieux à même de

valider une structure *a posteriori* que de l'élucider à partir de zéro (De Vijlder *et al.*, 2017). Enfin, la MS/MS est un outil puissant pour quantifier un composé une fois que les processus d'ionisation et de fragmentation ont été rigoureusement calibrés et définis (Boyd *et al.*, 2008).

Analyses numériques avec la chimie quantique

Une fois la structure d'un pigment connue, tout du moins supposée, elle peut alors servir à expliquer et à prédire les propriétés chimiques et optiques du pigment. Pour cela, les configurations électroniques peuvent être modélisées aussi bien à l'état de base qu'à l'état excité en utilisant la chimie quantique (Haywa, 2002; Jensen, 2017). Dans le cadre de la chimie quantique, les propriétés moléculaires sont dérivées du mouvement des électrons et des noyaux. En principe, ces mouvements s'obtiennent « simplement » en résolvant la fameuse équation d'onde de Schrödinger qui relie l'énergie d'une molécule à la position des noyaux et des électrons (je laisse ici de côté la question du *spin* des électrons). Théoriquement, n'importe quelle propriété chimique peut être déduite de l'énergie totale de la molécule en fonction de facteurs externes. Ainsi, les théories de la chimie quantique sont dites *ab initio* car elles ne nécessitent aucune valeur ou paramètre empirique. Cependant, excepté pour l'atome d'hydrogène qui ne contient que deux particules (un noyau et un électron), tous les autres systèmes chimiques se classent dans les systèmes à plusieurs corps (*many-body problems*) qui ne possèdent pas de solutions analytiques. De plus, le temps doit être inclus dans l'équation fondamentale pour pouvoir prendre en compte l'interaction électromagnétique avec la lumière et donc pour pouvoir modéliser les états photoexcités (Marques *et al.*, 2012), ce qui ajoute encore un degré de complexité.

Pour à la fois simplifier ces problèmes à plusieurs corps, dépendants du temps et pour les résoudre numériquement dans un laps de temps raisonnable, plusieurs transformations et approximations peuvent être faites (Jensen, 2017) ; ici, je me concentre uniquement sur celles qui sont les plus pertinentes dans le cadre de ma thèse. Tout d'abord, plutôt que de considérer les fonctions d'onde de N électrons interagissant ensemble (i.e. N fonctions d'onde corrélées avec 3 coordonnées spatiales chacune), on considère la densité électronique comme quantité fondamentale pour calculer l'énergie totale du système [d'après le théorème de Hohenberg–Kohn ; (Hohenberg & Kohn, 1964)]. La théorie de la fonctionnelle de la densité (*Density Functional Theory*, DFT) permet alors de simplifier le problème à plusieurs corps des théories

de la fonction d'onde à un problème à un seul corps, dont le nombre total de variables n'est que de trois (i.e. les coordonnées spatiales de la densité électronique). Alors que la complexité augmente exponentiellement avec la taille du système dans les théories de la fonction d'onde (N^7 pour le *gold standard* de la chimie quantique), elle devient en principe indépendante de la taille du système dans la DFT. Cependant, tous les termes énergétiques de l'équation de Schrödinger n'ont pas une expression analytique exacte en termes de densité électronique (Jensen, 2017). Il est donc nécessaire d'inclure des bases finies (*basis sets*) décrivant les orbitales électroniques [formalisme de Kohn–Sham ; (Kohn & Sham, 1965)] et des fonctionnelles approximées de la densité qui permettent respectivement de calculer l'énergie cinétique et l'énergie d'interaction dite d'échange–corrélation (Jensen, 2017). De ce fait, la complexité des calculs en DFT deviennent à nouveau dépendant de la taille du système, bien que le dimensionnement N^4 reste toujours plus favorable que pour les théories de la fonction d'onde (Santoro & Jacquemin, 2016). D'autre part, la principale difficulté issue du traitement d'une équation dépendante du temps est que la densité électronique à un instant *t* dépend de tous ses états précédents (effet mémoire). La solution est alors de considérer que le terme d'échange–corrélation réagit instantanément à la perturbation externe [approximation dite adiabatique ; (Zangwill & Soven, 1980)], ici le rayonnement électromagnétique lumineux. En ajoutant l'approximation considérant que la perturbation est suffisamment faible, cela a mené au régime de réponse linéaire de la DFT dépendante du temps formalisé par Casida (*Time-Dependent DFT*, TDDFT ; (Casida, 1995)]. Enfin, il y a bien d'autres approximations, telles que l'indépendance du mouvement des électrons par rapport à ceux du noyau [approximation de Born–Oppenheimer ; (Born & Oppenheimer, 1927)], la prise en compte de la solvatation de manière implicite [ex. le modèle du continuum polarisable, PCM ; (Adamo & Barone, 2000)] ou encore le gel de la géométrie pendant le processus d'excitation [approximation verticale ; (Santoro & Jacquemin, 2016)].

Bien que la TDDFT repose en pratique sur un certain nombre d'approximations qui affectent sa précision (Santoro & Jacquemin, 2016), son succès se matérialise par le nombre toujours plus grand d'études numériques qui relient les propriétés chimiques et optiques des pigments à leur structure (van Mourik, Bühl, & Gaigeot, 2014; Escudero, Laurent, & Jacquemin, 2015; Di Tommaso *et al.*, 2017). Le faible coût en termes de ressource informatique de la TDDFT permet de simuler des molécules de taille intermédiaire à très

grande, c'est-à-dire avec plus d'une dizaine d'atomes lourds, ce qui correspond à la grande majorité des biomolécules. Par exemple, la TDDFT a été utilisée pour décrire des systèmes aussi larges que les complexes photosynthétiques (König & Neugebauer, 2012; Barone *et al.*, 2014), pour expliquer les propriétés optiques des protéines fluorescentes telles que la GFP (Marques *et al.*, 2003) ou encore pour prédire la structure des polymères de mélanine (Kaxiras *et al.*, 2006).

1.4 L'importance biologique des pigments chez les animaux

La diversité et la distribution des pigments

Bien que la diversité des couleurs chez les animaux soit très grande, on ne compte finalement qu'une dizaine de familles de pigments, toutes caractérisées par des chromophores différents [**Figure 1-1**; (Needham, 1974)]. Les variations de couleur au sein de chacune de ces familles proviennent d'altérations du chromophore, telles que la conjugaison de différents auxochromes et métaux (Britton, 1983). La plupart de ces pigments sont largement distribués chez l'ensemble des animaux, citons par exemple les mélanines, les quinones, les tétrapyrroles (bilines, porphyrines, chlorophylles, etc.), les flavines et les ptérines. D'autres familles de pigments sont à l'inverse restreintes à un certain groupe d'animaux, telles que les ommochromes qui se trouvent uniquement chez les protostomiens [que j'appellerai invertébrés par la suite ; (Linzen, 1974)] ou encore les papiliochromes présents uniquement dans la famille de papillons des papilionidés (Umebachi, 1985). Il est à noter que nous ne savons toujours par pourquoi les vertébrés ne produisent pas d'ommochromes en conditions physiologiques [(Linzen, 1974) ; mais il est possible que la xanthommatine, l'ommochrome le plus répandu, se forme lors de l'apparition de la cataracte (Tomoda *et al.*, 1990)]. Si la plupart des animaux produisent leurs pigments *de novo*, certains pigments doivent être obtenus à partir de l'alimentation [ex. les flavonoïdes, les flavines et les caroténoïdes (Needham, 1974) ; bien que certains pucerons aient gagné la capacité de synthétiser les caroténoïdes suite à des transferts latéraux de gènes avec des champignons (Moran & Jarvik, 2010)].

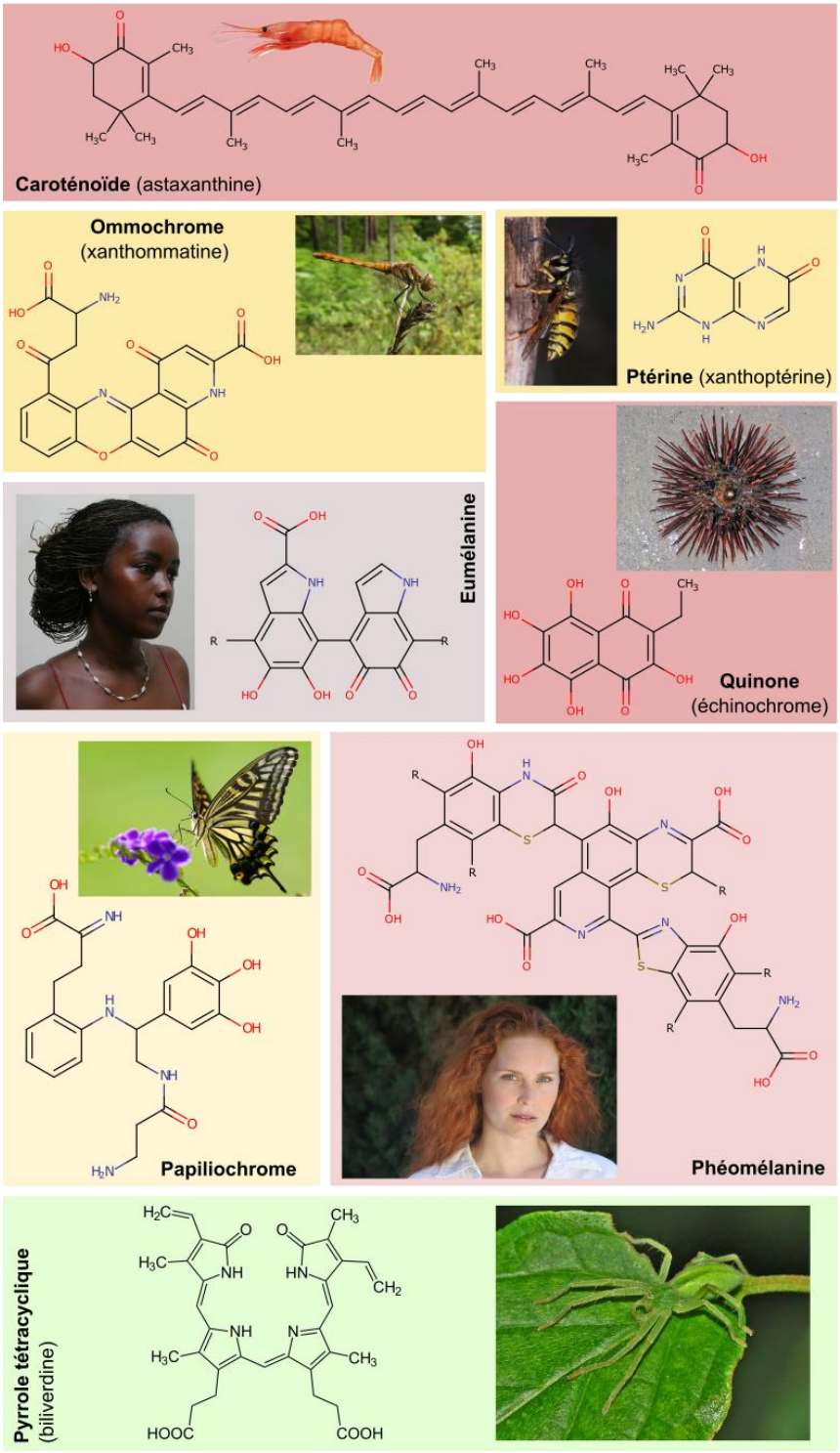

Figure 1-1. Diversité des chromatophores de pigments d'animaux.
Adapté de (Figon & Lorin, 2019). Source des photographies : *Pandalus borealis* : NOAA FishWatch/Wikimedia domaine public ; *Vespula vulgaris* : Jeroen Ruël/Wikimedia CC BY-SA ; couleur de la peau humaine : peter klashorst/Wikimedia CC BY ; femme rousse : dusdin on flickr/Wikimedia CC BY ; *Papilio xuthus* : Peellden/Wikimedia CC BY-SA ; *Arbacia punctulata* : James St. John/Wikimedia CC BY ; *Sympetrum darwinianum* : R78G addz/Wikimedia CC0 ; *Micromata virescens* : Ettore Balocchi/Wikimedia CC BY.

Les pigments sont non seulement largement distribués entre les animaux, mais ils sont aussi présents dans de nombreux types cellulaires et tissulaire [revus par (Needham, 1974)]. Les mélanines sont bien connues comme pigments à la surface du corps, mais elles se trouvent aussi dans la choroïde de l'œil, dans le système nerveux (sous forme de neuromélanine) ou dans le corps des insectes comme capsules immunitaires (Borovanský & Riley, 2011; Sugumaran & Barek, 2016). De même, les ommochromes se retrouvent dans les yeux composés, les écailles des ailes des papillons, les appareils génitaux, le cerveau ou encore le méconium des insectes (Linzen, 1974). Les tétrapyrroles cycliques sont des composants de l'hème (porphyrines) de l'hémoglobine et de la myoglobine, abondantes dans le sang et les muscles, et elles se retrouvent aussi dans diverses enzymes (ex. la cobalamine, aussi appelée vitamine B_{12}). Sous leur forme linéaire, les tétrapyrroles se retrouvent dans la bile (ex. la bilirubine) et les excrétions des vertébrés (ex. l'urobiline), ainsi que dans l'hémolymphe et les réserves d'ovocytes de certains arthropodes (ex. la micromatabiline de l'araignée *Micromata rosea* (Holl & Rüdiger, 1975)]. Les quinones sont ubiquitaires dans les cellules puisqu'elles font partie de la chaîne respiratoire mitochondriale (ex. l'ubiquinone, aussi appelée coenzyme Q_{10}). Les quinones sont aussi à l'origine de la couleur des pucerons (aphines) et des oursins (échinochromes). La flavine fait en même temps partie de la coenzyme redox flavine adénine dinucléotide (FAD) et elle donne sa couleur jaune aux tubes de Malpighi des insectes. Les caroténoïdes et leurs dérivés, en plus de leur rôle dans la couleur des oiseaux et des crevettes, sont bien connus pour faire partie des photorécepteurs à opsine (sous forme de rétinal). Enfin, les ptérines sont non seulement des pigments tégumentaires des insectes, crustacés, poissons, amphibiens et reptiles, mais aussi des cofacteurs enzymatiques ubiquitaires (ex. les folates, aussi appelés vitamines B_9, la tétrahydrobioptérine ou encore la molybdoptérine).

En conclusion, ce rapide aperçu de la diversité et de la distribution des pigments chez les animaux montre clairement qu'ils sont ubiquitaires et présents dans tous les tissus. En particulier, les pigments ne sont pas restreints aux téguments, ils se retrouvent en grande quantité à l'intérieur du corps (ex. les organes digestifs) où, bien entendu, ils n'interagissent pas avec la lumière. En d'autres termes, les pigments n'ont pas uniquement un rôle de signaux pour d'autres individus, ils ont aussi des fonctions au-delà de leur classique effet visuel.

Les pigments à l'intérieur de la cellule

L'état cellulaire des pigments

Dans l'environnement cellulaire, l'état des pigments est en partie dicté par leur chimie. Ainsi, les caroténoïdes et certaines quinones sont des composés lipophiles, ils se retrouvent donc préférentiellement dans les membranes ou dans des globules lipidiques cytoplasmiques (Hill & McGraw, 2006). Les autres pigments sont généralement peu hydrophiles et se retrouvent plutôt en association avec des protéines, en particulier lorsqu'ils circulent dans les fluides du corps (Needham, 1974). Les pigments se retrouvent à de rares occasions sous formes de cristaux cytoplasmiques [ex. l'hémoglobine des polychètes (Needham, 1974)]. Enfin, une large fraction des pigments impliqués dans la couleur du corps est déposée à l'intérieur d'organites membranaires, tels que les mélanosomes, les ptérinosomes, les ommochromasomes et les granules de riboflavine (Needham, 1974; Zhang *et al.*, 2018b). Cette compartimentation permet la synthèse d'une grande quantité de pigments à l'intérieur d'un espace clos sans que cela n'interfère avec le fonctionnement du reste de la cellule (Needham, 1974). Les organites pigmentés peuvent alors assurer la biosynthèse de polymères très larges, tels que l'eumélanine (Borovanský & Riley, 2011). De plus, la compartimentation permet de contrôler le métabolisme des pigments à travers la biogenèse, la sécrétion et possiblement la dégradation des organites pigmentés eux-mêmes (Borovanský & Elleder, 2003; Borovanský & Riley, 2011). Les organites pigmentés apparaissent donc comme des acteurs clés de la formation de la couleur et de la fonction des pigments.

Les méthodes d'étude des organites pigmentés : étudier les couleurs à l'échelle subcellulaire

L'étude des organites pigmentés à l'intérieur des tissus et dans des cellules repose sur des techniques d'imagerie capables de résoudre leur taille sub-micrométrique (Needham, 1974). Cela implique généralement des techniques d'imagerie subcellulaire, telles que la microscopie électronique (EM). Puisque l'EM ne peut être utilisée sur des animaux vivants, les tissus et les cellules doivent être fixés avant d'être imagés sous un faisceau d'électrons. Ce processus de fixation produit inévitablement des artefacts (Bozzola & Russell, 1999) ; c'est donc une étape cruciale dans la préparation des échantillons pour l'EM qui nécessite d'être planifiée soigneusement en fonction du but de l'étude. Enfin, d'autres modalités d'imagerie

sont capables d'élucider la biologie cellulaire des pigments à l'échelle subcellulaire, par exemple la cartographie chimique. Dans ce qui suit, je développe certains des aspects qui ont guidé mon choix des techniques d'imagerie et des protocoles utilisés dans mes travaux.

Dans les protocoles classiques d'EM, la fixation des tissus et des cellules est obtenue grâce à des fixateurs chimiques, tels que le paraformaldéhyde (PFA), le glutaraldéhyde (Glut) et le tétroxyde d'osmium (OsO_4), à température ambiante (Bozzola & Russell, 1999). Ils ont pour effet de coaguler et de réticuler les composants cellulaires (principalement les protéines et les lipides insaturés), ce qui arrête le métabolisme et assure que les structures restent autant que possible intactes durant la procédure de déshydratation (nécessaire pour l'infiltration de la résine hydrophobe). Le principal avantage des fixateurs chimiques est que leur utilisation est quasiment routinière et qu'il existe des protocoles optimisés pour fixer un grand nombre de tissus et de cellules différents. Cependant, la fixation chimique souffre d'un certain nombre d'inconvénients (Bozzola & Russell, 1999; Hurbain & Sachse, 2011). Premièrement, les fixateurs diffusent lentement dans les tissus et leur action chimique est assez lente ; le métabolisme et les activités dégradatives ne sont donc pas bloqués instantanément. Deuxièmement, tous les composants cellulaires ne sont pas aussi bien préservés, les sucres et les ions ont ainsi tendance à être extraits pendant l'étape de déshydratation. Enfin, les structures membranaires ont tendance à se déformer, ce qui est illustré par le *blebbing* de la membrane plasmique (Chandler, 1984) et la rétraction des compartiments endolysosomaux (Murk *et al.*, 2003). En théorie, toutes ces limites pourraient être surmontées par la cryofixation, c'est-à-dire la vitrification instantanée de l'eau cellulaire, puis l'imagerie avec un cryo-microscope électronique (Hurbain & Sachse, 2011). En pratique, on ne peut éviter la formation de cristaux de glace qui détruisent les structures cellulaires que sur des échantillons très fins (de l'ordre du micron) à pression ambiante ; ce qui signifie que cette technique n'est pas adaptée aux tissus. De plus, les cryo-microscopes électroniques ne sont pas aussi largement accessibles que leurs équivalents plus classiques, ce qui implique que les échantillons congelés doivent être réchauffés jusqu'à la température ambiante à un moment donné.

Afin d'allier le meilleur des deux mondes (chimique et congelé), la congélation à haute pression (*High-Pressure Freezing*, HPF) suivie de la substitution de congélation (*Freeze Substitution*, FS) est la technique de choix. En augmentant la pression à 210 MPa

pendant la congélation à -196 °C, la vitrification de l'eau est favorisée par rapport à sa cristallisation sur plus de quelques centaines de micromètres (Hurbain & Sachse, 2011), ce qui rend l'HPF compatible avec des tissus. Ensuite, en plaçant les échantillons vitrifiés dans de l'acétone refroidi à -90 °C et contenant de l'OsO_4, la déshydratation et la stabilisation des composants cellulaires peuvent être réalisées en prévision de l'infiltration de la résine à température ambiante. La FS permet d'éviter une partie des artefacts produits par la fixation chimique parce que (i) elle n'utilise pas de PFA ni de Glut, (ii) l'OsO_4 est inactif à -90 °C mais il peut tout de même diffuser librement avant de s'activer au-dessus de -70 °C, et (iii) le processus de déshydratation à froid qui remplace l'eau vitrifiée par l'acétone a moins tendance à déplacer les éléments les plus mobiles, tels que les ions et les métaux. Bien que des artefacts puissent quand même apparaître pendant l'HPF-FS et lors des étapes suivantes, l'état de préservation quasi-natif obtenu a grandement amélioré notre connaissance de l'architecture cellulaire, dont celle d'organites pigmentés comme les mélanosomes (Hurbain & Sachse, 2011).

Une fois que les tissus et les cellules pigmentés ont été vitrifiés, leur congélation substituée et la résine infiltrée, plusieurs modalités d'imagerie peuvent être utilisées pour étudier la biologie cellulaire des organites pigmentés. L'EM est une technique bien connue qui permet de visualiser en deux dimensions les composants ultrastructuraux (ex. les compartiments) et macromoléculaires (ex. les ribosomes) de la cellule (Bozzola & Russell, 1999). De plus, des informations en trois dimensions sont accessibles en imageant une section semi-fine de plusieurs centaines de nanomètres sous divers angles (McIntosh, Nicastro, & Mastronarde, 2005). La reconstruction tomographique des projections 2D aux différents angles permet d'obtenir un modèle 3D (McIntosh *et al.*, 2005). La tomographie électronique (ET) a, en particulier, permis d'élucider l'ultrastructure interne des mélanosomes en cours de maturation (Hurbain *et al.*, 2008), ainsi que la façon dont leur membrane limitante produit des invaginations vésiculaires et des extensions tubulaires (Hurbain *et al.*, 2008; Delevoye *et al.*, 2016; Ripoll *et al.*, 2018) ; des éléments qui ne sont pas visualisables dans leur entièreté en 2D avec des coupes ultrafines de 70 nm.

La cartographie de la distribution intracellulaire des métaux et des ions est particulièrement appropriée pour étudier la pigmentation puisqu'ils ont été associés aux pigments et à leurs organites à de nombreuses reprises, soit parce que les métaux et les ions

agissaient comme cofacteurs enzymatiques, soit parce qu'ils se lient à la structure des pigments (Needham, 1974; Borovanský & Riley, 2011). La principale limitation à l'imagerie chimique subcellulaire est la faible concentration des métaux à cette échelle, ce qui nécessite les techniques les plus résolutives et sensibles (McRae *et al.*, 2009; Decelle *et al.*, 2020), telles que la fluorescence des rayon X Synchrotron [SXRF; (Pushie *et al.*, 2014)]. Brièvement, le rayonnement Synchrotron provient d'électrons qui sont accélérés jusqu'à s'approcher de la vitesse de la lumière dans des machines circulaires à l'échelle industrielle. À chaque fois que les électrons sont déviés, ils perdent de l'énergie sous forme de photons, dont des rayons X durs (énergies de quelques keV). Les faisceaux Synchrotron se caractérisent par leur très petite taille et leur haute intensité, ce qui permet de détecter des matériaux très dilués à des échelles nanoscopiques. Quand un échantillon est illuminé par des rayons X durs, ces derniers excitent les électrons de cœur des métaux, qui réémettent des rayons X durs à plus faible énergie lors de leur désexcitation [ce qu'on appelle la fluorescence des rayons X ; (Pushie *et al.*, 2014)]. Les énergies de fluorescence sont spécifiques à chaque métal, ce qui permet d'imager de manière indépendante de multiples métaux en une seule fois. Enfin, le développement de nanosondes et de méthodes de balayage de plus en plus rapides ont permis la détection de métaux à des résolutions allant jusqu'à 50 nm (Medjoubi *et al.*, 2013; Gorniak *et al.*, 2014). L'utilisation de ces techniques de pointe a notamment mené à la description des mélanosomes comme des environnements hétérogènes en métaux, en particulier en calcium, cuivre et zinc (Gorniak *et al.*, 2014). De tels résultats sont par exemple à relier à la dynamique de déposition des différentes mélanines à l'intérieur des mélanosomes. Ainsi, je fais l'hypothèse l'imagerie chimique des métaux devrait donner des résultats importants concernant les changements de couleur à l'échelle subcellulaire.

Les nombreuses fonctions biologiques des pigments

Aujourd'hui, les pigments des animaux, en-dehors de leurs rôles visuels, sont connus pour avoir des fonctions aussi variées que [tirées de (Needham, 1974; Fox, 1976; Burtt, 1981; Britton, 1983; Hill & McGraw, 2006)] :

- cofacteurs redox (ex. flavines) ;
- pigments respiratoires (ex. porphyrines);
- photoprotecteurs (ex. mélanines) ;
- tampons du stress oxydatif (ex. caroténoïdes) ;

- durcisseurs (ex. mélanines) ;
- thermorégulateurs (ex. mélanines) ;
- anti-déshydratants (ex. mélanines) ;
- composés d'excrétion (ex. bilines) ;
- détoxifiants (ex. ommochromes) ;
- agents antimicrobiens (ex. mélanines) ;
- immunomodulateurs (ex. caroténoïdes) ;
- et possiblement de signaux intercellulaires (ex. caroténoïdes).

Comme je l'ai auparavant discuté, il a été soutenu à de nombreuses reprises que les mêmes propriétés chimiques responsables de la couleur des pigments étaient à l'origine de leurs fonctions biochimiques ; ce qui signifie que la coloration pourrait dans certains cas être un simple effet secondaire de la réactivité des pigments (Newbigin, 1898; Fox, 1944; Needham, 1974). De plus, les besoins métaboliques de la production (et de la dégradation) des pigments devraient être pris en compte pour apprécier les coûts et les bénéfices d'être colorés, d'autant plus quand c'est de manière variable (Oxford & Gillespie, 1998; Gawryszewski *et al.*, 2015). En somme, les pigments ont très probablement des effets multiples et pléiotropes *in vivo*, ce qui devrait être pris en considération, en plus de leurs effets visuels, quand on souhaite évaluer l'importance biologique de la coloration et des changements de couleur.

1.5 Objectifs de la thèse

Questions, postulats et hypothèses

Dans cette thèse, je m'intéresse aux changements de couleur des invertébrés, en particulier ceux basés sur les ommochromes. Mon objectif est triple, il s'agit :

1. de décrire les mécanismes sous-jacents aux capacités de changement de couleur des ommochromes ;
2. d'étudier comment ces propriétés sont reliées aux fonctions biologiques des ommochromes ;
3. de tirer des conclusions sur l'importance fonctionnelle du changement de couleur des ommochromes, que ce soit pour les sciences fondamentale ou appliquée.

Afin de remplir ces objectifs, mes travaux se basent sur une série de cinq postulats et hypothèses (**Encadré 1-1**).

Encadré 1-1. Postulats et hypothèses

Premièrement, les systèmes pigmentaires partagent des **caractéristiques communes**. Ainsi, une analyse comparative entre les ommochromes et les mélanines, qui sont les pigments les plus étudiés, devrait nous donner des indications sur la biologie des ommochromes.

Deuxièmement, les changements de couleur des ommochromes sont le résultat de **processus multi-échelles**. En effet, les changements de couleur peuvent être obtenus soit à l'échelle du pigment lui-même (à travers les voies biochimiques), soit à l'échelle des organites pigmentés (à travers leur trafic intracellulaire).

Troisièmement, **la structure chimique et l'organisation cellulaire** des ommochromes déterminent leurs propriétés biochimiques, depuis l'absorption lumineuse à la réactivité chimique ; elles sont donc des propriétés imbriquées.

Quatrièmement, l'étude des aspects chimiques et cellulaires des ommochromes peut nous informer sur de potentielles **fonctions pléiotropes**, et ainsi nous permettre de mieux comprendre des contextes que le seul aspect visuel des pigments échoue à expliquer.

Enfin, les propriétés multi-échelles des ommochromes pourraient se retrouver chez d'**autres systèmes pigmentaires**. Leur généricité implique que ces travaux auraient des répercussions au-delà du modèle d'étude.

Plan de la thèse

Dans le **Chapitre 2**, je présente une revue comparative des systèmes pigmentaires et des changements de couleur chez les animaux. Dans le **Chapitre 3**, je fais une revue de la biochimie et de la biologie cellulaire des ommochromes, en soulignant les problématiques que j'aborde dans mes travaux expérimentaux ultérieurs. Dans le **Chapitre 4**, je me concentre sur la biochimie des ommochromes et leurs voies de biosynthèse en utilisant la chimie analytique.

Dans le **Chapitre 5,** j'étudie les propriétés chimiques des ommochromes en lien avec leurs changements de couleur et leur réactivité chimique, en utilisant les outils de la chimie quantique numérique. Dans le **Chapitre 6**, j'explore le cycle de vie des organites pigmentés durant les changements de couleur des araignées crabes. Enfin, dans le **Chapitre 7**, je discute l'ensemble de mes résultats en les inscrivant dans une approche d'écophysiologie et je termine en abordant leurs implications sur l'évolution des systèmes pigmentaires chez les animaux.

Chapitre 2 – Les changements de couleur morphologique et physiologique des animaux

When marvelling at the extent of metamorphic colour-changes it should be appreciated that […] integrated over their life-span many animals experience massive changes in integumental chromes.

Needham (1974), *The Significance of Zoochromes*

2.0 Sommaire

CHAPITRE 2 – LES CHANGEMENTS DE COULEUR MORPHOLOGIQUE ET PHYSIOLOGIQUE DES ANIMAUX 41

2.0 SOMMAIRE 42

2.1 OBJECTIFS 43

2.2 REVUE DE LA LITTERATURE 44

Abstract 45

Introduction 46

Functions of Colour Changes in the Animal Kingdom 47

Thermoregulation 49

UV Protection 50

Aposematism 50

Intraspecific Communication 51

Crypsis 51

Mechanisms of Morphological Colour Changes 52

Morphological Colour Changes in the Crab Spider at the Tissue Level 52

Morphological Colour Changes in the Crab Spider at the Cellular Level 55

Morphological Colour Changes in the Crab Spider at the Molecular Level 55

Hormonal Control of Morphological Colour Changes 55

Mechanisms of Physiological Colour Changes 58

Physiological Colour Changes at the Tissue Level 58

Physiological Colour Changes at Cellular and Molecular Levels 61

Hormonal and Neuronal Controls of Physiological Colour Changes 62

Conclusion 63

Glossary 65

2.3 CONCLUSION 66

2.1 Objectifs

Les mécanismes de changement de couleur sont au moins aussi variés que les façons de produire de la couleur. Ainsi, une couleur structurale produite par un assemblage de particules ordonnées ne sera pas modifiée de la même manière qu'une couleur chimique issue de l'absorption sélective de longueurs d'onde par un pigment. Cette variété de mécanismes de changement de couleur peut avoir des impacts sur la vitesse, l'étendue ou encore la fonction du changement de couleur.

Dans ce chapitre, j'ai pour objectif de décrire les deux grands mécanismes de changements de couleur chez les animaux, c'est-à-dire les changements de couleur physiologiques et morphologiques. Plutôt que de se restreindre aux invertébrés, on s'intéresse ici à l'ensemble des animaux. Il y a plusieurs raisons à ce choix : (i) les mécanismes précis des changements de couleur n'ont été étudiés que dans un nombre restreint d'espèces, et ils ont peu été intégrés dans la physiologie, l'écologie et l'évolution des espèces en question ; (ii) cela permet de comparer des espèces produisant des pigments et des structures colorées différentes afin de faire ressortir les similarités et les différences ; et (iii) on peut alors tirer des conclusions évolutives sur les changements de couleur.

Pour répondre à cet objectif, j'ai réalisé une revue de la littérature sur les changements de couleur chez les animaux, depuis leurs mécanismes physico-chimiques jusqu'à leurs fonctions biologiques, en passant par leur régulation physiologique. J'ai particulièrement pris en compte les travaux publiés depuis la dernière grande revue à ce sujet (Umbers *et al.*, 2014). Je fais en particulier le lien entre les mécanismes physico-chimiques et les fonctions physiologiques dans une perspective de biologie intégrée des changements de couleur. En effet, ce n'est qu'une fois que les tenants et les aboutissants des changements de couleur auront été décrits et compris que leur écologie et leur évolution pourront être appréhendées.

2.2 Revue de la littérature

Le manuscrit suivant a été publié en tant que chapitre de l'encyclopédie en ligne *eLS*, éditée par Wiley-Blackwell.

FIGON, F. & CASAS, J. (2018) Morphological and Physiological Colour Changes in the Animal Kingdom. In *eLS* (ed JOHN WILEY & SONS LTD), pp. 1–11. John Wiley & Sons, Ltd, Chichester, UK.

Morphological and Physiological Colour Changes in the Animal Kingdom

Abstract

Colour change is the ability of an organism to modify its colouration in response to specific stimuli. Several biological functions have been proposed to explain colour changes, including UV protection, thermoregulation, crypsis, inter- and intraspecific communication. Changes in body colouration are mainly performed through two types of mechanisms referred to as morphological and physiological. Mechanistically, these two types of colour changes differ in their speed and the way coloured structures are altered. The proximal causes of these colour changes are identified in a handful number of species and demonstrate that common physiological, cellular and molecular actors are at play. However, the reasons why both colour change types are widespread in the animal kingdom and how they have evolved are still unknown. This is partly due to a lack of knowledge about the fitness implications of colour changes, particularly their energetic costs.

Keywords: Colour changes, morphological, physiological, evolution, animals, pigment, chromatophore, camouflage, melanin, ommochrome.

Key concepts

- Morphological and physiological colour changes are widespread in the animal kingdom.
- It has been suggested that both types of colour changes have the same biological functions, which are UV protection, thermoregulation, crypsis, inter- and intraspecific communication.
- Despite differences in speed and mechanisms, similar cellular and molecular actors are at play for both types of colour changes.
- Colour changes are triggered by environmental stimuli, mainly light, and are regulated by the neuronal and hormonal systems.
- The evolution of colour-changing abilities is still poorly understood because the consequences of colour changes on individual fitness remain to be investigated.

Introduction

Animal colouration has fascinated biologists for centuries. The famous naturalists Wallace and Poulton studied animal colours and their biological significance in the light of Darwin's natural selection theory of evolution (Poulton, 1890; Caro, 2017). Particularly, in his classic book entitled 'The colours of animals', Poulton acknowledged the importance of colour change in animal evolution (Poulton, 1890).

Colour changes are mediated by variations in either body brightness or hues (e.g. brown, yellow, red). This change in phenotype (phenotypic plasticity) during lifetime is called polyphenism, in contrast to polymorphism that designates the occurrence of individuals of the same species differing in their respective phenotype. Polyphenism of body colouration can occur at defined developmental stages, which is referred to ontogenetic colour changes. Here, we however restrict ourselves to colour changes that are dependent on environmental stimuli and that are in most cases reversible. These colour changes are classified as physiological and morphological depending on their mechanisms and speed (Umbers *et al.*, 2014). Physiological colour changes involve the rapid movements of coloured structures within seconds to hours. In contrast, morphological colour changes rely on the relatively slow production, degradation or chemical modification of pigments and is generally completed within hours to days.

Coloured cells, called chromatophores, are the main cellular actors of colour change. They produce the pigments and coloured structures involved in this process and generally store them. Chromatophores are named according to their hue: melano- (brown and black), erythro- (orange and red), xantho- (yellow), leuco- (white) and iridophores (iridescent). Depending on the species, pigments and coloured structures are either melanins, ommochromes, carotenoids, pterins, purines or proteins. Pigments are molecules that absorb specific wavelengths in the visible range of light and thus appear coloured to the eye. Photonic structures produce structural colours by generally creating phase interferences in the refracted light. Most blue colourations and iridescence, in which perceived colours depend on the viewing angle, are produced by structures and crystals of varying nature in animals (Mäthger, 2003; Mäthger *et al.*, 2009; Teyssier *et al.*, 2015).

Many animals can change their colouration in response to specific situations. The biological reasons of these colour changes are multiple, ranging from UV protection,

thermoregulation to communication. How to link the mechanisms (proximate causes) underlying reversible colour changes to these biological functions (ultimate causes) is still a key question in evolutionary biology. In this article, we review the main hypotheses that have been proposed so far to explain why some animals reversibly change their body colouration. We then describe the mechanisms of both morphological and physiological colour changes to conclude on their potential importance for the evolution of colour change in animals.

Functions of Colour Changes in the Animal Kingdom

Many biological functions have been assigned to both morphological and physiological colour changes (**Table 2-1**). However, few have really been proven and, when so, only in a handful number of species (**Figure 2-1**) (Umbers *et al.*, 2014; Duarte, Flores, & Stevens, 2017). In the following, we detail the plausible functions of colour changes in the animal kingdom by emphasizing the most emblematic cases (**Figure 2-1**). However, it has to be kept in mind that these functions are often hypotheses remaining to be properly tested, in these very model systems and even more so on a broader scale (i.e. phylogeny). The biological functions of colour changes comprise thermoregulation, UV protection, interspecific communication (aposematism), intraspecific communication (aggregation, sexual signals, etc.) and crypsis (camouflage, masquerade and mimicry; **Table 2-1**).

Table 2-1. Morphological and Physiological Colour Changes Are Widespread in the Animal Kingdom.

Type of colour change	Animal Group	Main changes in colouration	Biological functions
Morphological	Planarians	Whitening	?
	Crab spiders	Yellowing	Possibly crypsis
	Crustaceans	Darkening	Mainly crypsis and thermoregulation
	Insects	Changes in hues and brightness	Crypsis, intraspecific and interspecific communications
	Birds	Changes in hues and brightness	Intraspecific communication
	Mammals	Darkening	Mostly crypsis and UV protection
Physiological	Orb-web spiders	Appearance of white spots	Interspecific communication
	Crustaceans	Darkening, reddening	Mostly crypsis and UV protection
	Insects	Darkening	Thermoregulation
	Cephalopods	Changes in hues and brightness	Crypsis, intraspecific and interspecific communications
	Fishes	Changes in hues and brightness	Crypsis and interspecific communication in some species
	Amphibians	Darkening	Crypsis and thermoregulation?
	Reptiles	Changes in hues and brightness	Crypsis, thermoregulation and intraspecific communication

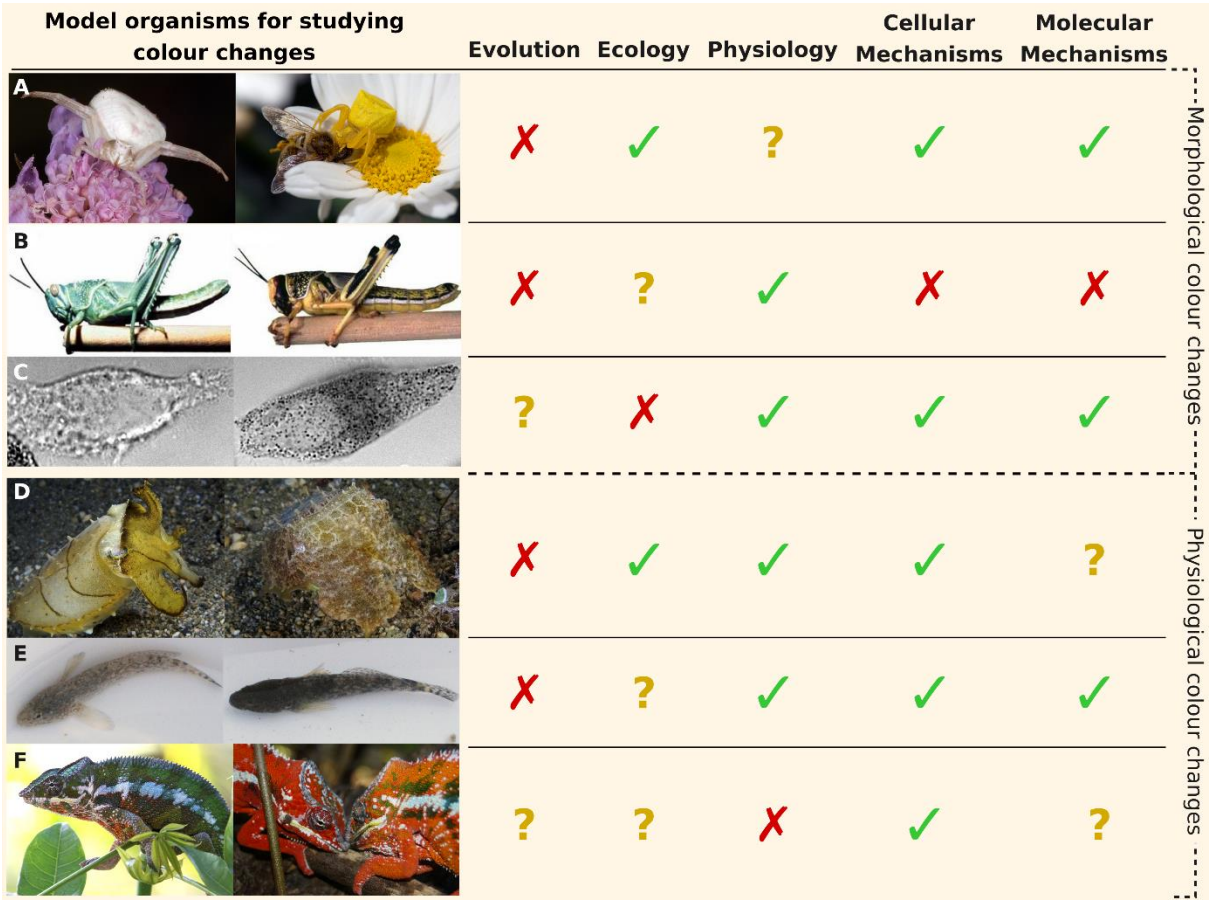

Figure 2-1. Model Organisms and Their Contributions to the Study of Colour Changes in the Animal Kingdom.

For each model species, contribution in the fields of evolution, ecology, physiology, cellular and molecular mechanisms of colour changes have been highlighted. A red cross indicates that no study has yet investigated this field for this particular species. A yellow question mark indicates that few studies have started to investigate this field. A green tick indicates that numerous studies have dealt with this field, even though many important biological questions may remain unanswered. (A) The colour-changing crab spiders *Thomisus onustus* and *Misumena vatia* (not shown). Size: few mm. (B) A desert locust (*Schistocerca gregaria*) in its solitarious (left) and gregarious (right) phases. Size: few cm. (C) Culture of human melanocytes producing melanin (from left to right) highlighting the process of tanning. Cell size: several µm. (D) Example of camouflage in a cephalopod, the cuttlefish. Size: several cm. (E) Rapid darkening of a rock pool goby (*Gobius paganellus*) subjected to a dark background (left to right). The same process has been studied in the frog *Xenopus laevi* (not shown). Size: several cm. (F) Reddening of a Panther chameleon (*Furcifer pardalis*) in the presence of a male rival. Size: tens of cm. Credits: A) CC BY SA Fritz Geller-Grimm, Paul-Henri Cahier and Hectonichus, B) Public domain, C) Florent Figon, D) CC BY SA Nick Hobgood, E) CC BY Stevens et al., 2014, F) CC BY SA Kris Norvig and Eric Mathieu.

Thermoregulation

Colour changes can theoretically provide thermoregulation because body temperature depends on light absorption, at least in ectotherms. Light, by the energy it carries and the effect of

infrared wavelengths on molecular vibration, is a source of thermal movements when it is absorbed; thus, under the sunlight, dark bodies get hotter and quicker than light ones.

Thermoregulation as a biological function of colour changes has been proposed for many animals, from damselflies, butterflies, ghost crabs to lizards (**Table 2-1**) (Umbers *et al.*, 2014). In the latter example, thermoregulation capacities not only vary daily but also seasonally, with the maximal colour change matching the highest peak activity season (i.e. brightness in luminous conditions) (Cadena *et al.*, 2017). This result indicates that animals do not only change their colour passively compared to temperature variation; they can also tune their colour-changing ability in function of their needs and their activity state.

UV Protection

Light is not only made of wavelengths in the visible range (400-700 nm), but also of ultraviolet radiations (UVs, below 400 nm). UVs carry more energy than longer wavelengths and are thus able to break molecular bonds, such as nucleic acid bonds in DNA. Such damage in the DNA of light-exposed cells is a threat that can potentially lead to cellular dysfunctions and uncontrolled replication (tumorigenesis). In humans, the UV-induced process of tanning protects skin-cells DNA and folate vitamins from harmful UVs via their absorption by epidermal melanins (López & Alonso, 2014). Similarly, shrimps of the Antarctic krill might change their colour in winter and summer to cope with seasonally and daily rhythms of UV (Auerswald *et al.*, 2008).

Aposematism

Aposematism is the production of conspicuous visual patterns by dangerous species to signal predators not to eat them. Variable aposematism could be advantageous in the context of species that are not always poisonous, particularly organisms relying on toxic molecules provided by their food (Umbers *et al.*, 2014). Furthermore, animals facing multiple predators in their environment may benefit from changing from a cryptic to an aposematic pattern if each pattern is better suited to a specific predator (Duarte *et al.*, 2017). Such a dynamic signalling toward multiple predators has been described in the mimic octopus (*Thaumoctopus mimicus*), which can resembles toxic banded soles, banded sea-snakes or lion-fishes, depending on the threat (Norman, Finn, & Tregenza, 2001).

Intraspecific Communication

Colour changes can be used for courtship and male-male fighting. These two intraspecific communications indeed use conspicuous signals that can be disadvantageous in terms of predation (Duarte *et al.*, 2017). This trade-off between being seen by conspecifics and hiding from preys or predators could be solved by colour changes. Chameleons and cephalopods are two famous groups of animals that use physiological colour changes for both intraspecific communication and camouflage (**Table 2-1**). Thanks to their iridescent cells, males of panther chameleon can become redder, independently of their current colour pattern, within a few minutes in the presence of rivals (**Figure 2-1**F) (Teyssier *et al.*, 2015).

Another colour change associated to intraspecific communication is the phase polyphenism of locusts, which generally become darker when they aggregate in the so-called gregarious phase (**Figure 2-1**B) (Tanaka *et al.*, 2016). Changing their colour might be a signal for nearby solitarious locusts to become gregarious (Anstey *et al.*, 2009). Testing the role of colour change in locust polyphenism is complex because this phase switch also triggers behavioural and metabolic changes whose effects on fitness can interfere with each other.

Crypsis

Together with intraspecific communication, crypsis is the other most popular hypothesis for explaining colour changes in animals (Umbers *et al.*, 2014; Duarte *et al.*, 2017). However, the crypsis hypothesis can be hard to test since remaining invisible to a specific organism (either a predator or a prey) directly depends on the visual system of the latter. For example, an animal that appears cryptic to humans might be highly conspicuous to bees as they perceive UVs. On the contrary, bees do not possess red-sensitive photoreceptors; thus, a red animal would remain unseen to them but not to humans. For instance, crab spiders can be spectacularly invisible to our eyes when they match the colour of the flower on which they hunt (**Figure 2-1**A). However, there is still no evidence for colour-matching as being beneficial in catching more preys (Brechbühl, Casas, & Bacher, 2010). This result might rely on the fact that flower-matching crab spiders are actually not invisible to bees and flies, their most abundant preys in the field (Defrize, Thery, & Casas, 2010). Few predation events on crab spiders have been recorded so far; yet, hiding from their predators has never been tested (Morse, 2007).

On the contrary, it is known that the physiological colour change of cephalopods is a highly efficient way of hiding to both preys and predators. Cephalopods can either use camouflage by disruptive patterns, mimicry, masquerade or a combination of these crypsis strategies (**Figure 2-1**D) (Hanlon *et al.*, 2009). As seen previously, their choice is highly dependent on the type of threat or prey.

The evolution of colour changes not only rely on the function they can provide to individuals but also on their costs. Changing body's colouration is likely to be an energy-demanding process with important implications on fitness. In the following two sections, we dissect the proximate mechanisms of colour changes, a necessary step to understand fully their evolution.

Mechanisms of Morphological Colour Changes

Morphological colour changes rely on the production, degradation or chemical modification of pigments. Hence, it is generally a slow process requiring reconfiguration of the cellular metabolism through the regulation of gene expression, enzyme synthesis, intracellular trafficking routes, etc. Morphological colour changes are widespread in the animal kingdom (**Table 2-1**). For example, some mammals and birds change their fur and plumage seasonally either for parade or camouflage, a process referred to as seasonal colour moulting (Zimova *et al.*, 2018). Humans produce melanin pigments under UV exposure through a reversible primary response of their skin termed tanning (López & Alonso, 2014). Ghost crabs are also known to vary their colour patterning during the day, matching the luminosity of their surroundings (Stevens, Rong, & Todd, 2013). Here, we focus on the case of crab spiders for which the morphological colour change has been comprehensively studied at the tissue, cellular and molecular levels. We then describe the hormonal control of locust phase polyphenism, as well as of seasonal colour moulting and tanning in mammals.

Morphological Colour Changes in the Crab Spider at the Tissue Level

Crab spiders have the unique ability to reversibly change their colour through the cyclic metabolism of ommochrome pigments and the related specialized organelles called ommochromasomes (Insausti & Casas, 2009). In white individuals, the layer of tegument

cells directly beneath the cuticle contains unpigmented organelles making it transparent to light (**Figure 2-2**A). Crab spiders are not transparent themselves because a second layer of cells called guanocytes produces and stores guanine crystals that refract the in-coming visible light (Gawryszewski *et al.*, 2015). Thus, they appear completely white to the human eye (**Figure 2-2**A). On the contrary, yellow individuals possess fully matured ommochromasomes in their chromatophores (**Figure 2-2**A) (Insausti & Casas, 2008). Their ommochromes absorb light radiations in the violet-blue range (around 440 nm; **Figure 2-2**C) (Linzen, 1974). All the remaining wavelengths are then refracted by the underlying layer of guanine crystals, which renders the spider yellow (the complementary colour of blue-violet) to the human eye. Depending on the flower on which it hunts, a crab spider can become either white or yellow within few days (Llandres *et al.*, 2013). This duration is directly linked to the switch in ommochromasome metabolism that requires major metabolic reconfiguration of the cell.

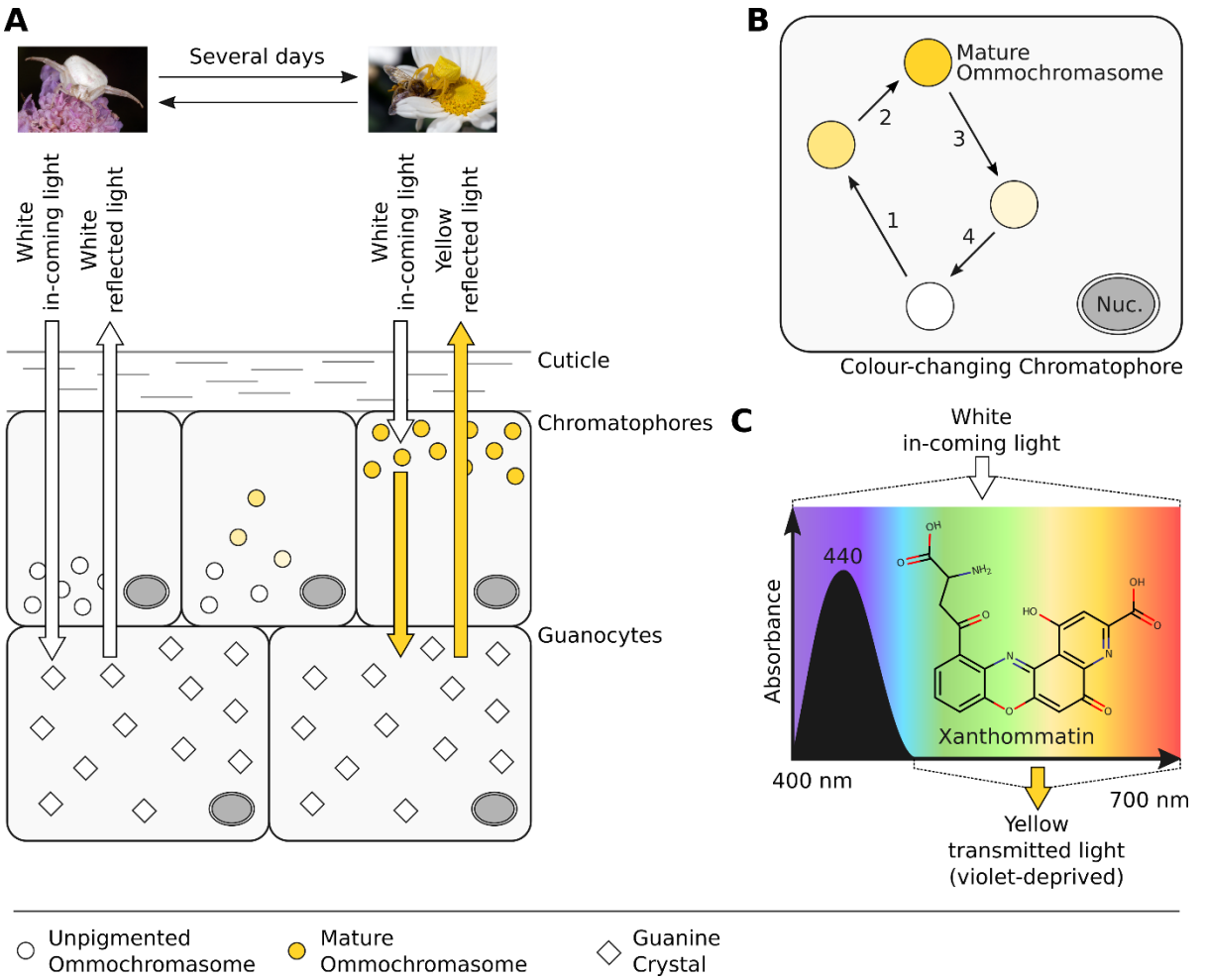

Figure 2-2. Morphological Colour Changes in a Crab Spider.
(A) At the tissue level, colour-changing chromatophores of crab spiders are beneath a transparent cuticle and on top of light-reflecting guanocytes. In white crab spiders, chromatophores possess unpigmented ommochromasomes that do not absorb the in-coming light, which is then fully reflected by guanine crystals in guanocytes. During morphological colour change, ommochromasomes progressively mature and acquire yellow ommochromes, such as xanthommatin. Hence, in yellow crab spiders, the in-coming light is first partly absorbed by mature ommochromasomes. This transmitted light deprived of blue and violet wavelengths is then reflected by guanine crystals and thus appears yellow to the eye. **(B)** In chromatophores of crab spiders, ommochromasomes can undergo a full cycle of pigmentation and depigmentation, which is the cellular basis of their morphological colour change. (1) During white-to-yellow transition, transparent pre-ommochromasomes acquire ommochrome precursors that are slightly yellow. (2) Precursors then form yellow ommochromes leading to a mature ommochromasome. (3) For yellow-to-white transition, ommochromasomes enter an autocatalytic process leading to the degradation of their pigments. (4) Degrading ommochromasomes are ultimately recycled into unpigmented organelles, ready for another cycle of ommochrome metabolism. **(C)** The production of xanthommatin within maturing ommochromasomes is the molecular basis of their yellow colouration. Thanks to its electronic delocalization structure, xanthommatin absorbs wavelengths between 400 and 500 nm (i.e. violet and blue). Thus, visible light passing through xanthommatin is deprived of these wavelengths making it yellow (the complementary colour of blue and violet) to the eye. See text for references. Nuc., Nucleus. Credits: CC BY SA Fritz Geller-Grimm, Paul-Henri Cahier and Hectonichus.

Morphological Colour Changes in the Crab Spider at the Cellular Level

The morphological colour change of crab spiders is based on the cyclic maturation and recycling of ommochromasomes (Insausti & Casas, 2009). During the white-to-yellow transition, unpigmented organelles are filled with ommochromes and their precursors, which all absorb blue-violet wavelengths (**Figure 2-2**B). For the yellow-to-white transition, these matured ommochromasomes undergo an autocatalytic process leading to the recycling of their pigment content (Insausti & Casas, 2009). Thus, they go back to their unpigmented state and are ready to go through a new cycle of maturation and recycling (**Figure 2-2**B).

Morphological Colour Changes in the Crab Spider at the Molecular Level

During the morphological colour change of crab spiders, ommochrome pigments are synthesised and degraded in a cycling process (**Figure 2-2**B). Ommochromes originate from tryptophan through the formation of precursors called kynurenines. 3-hydroxykynurenine, the direct precursor of most ommochromes, and the ommochrome xanthommatin both appear yellow in solution, with xanthommatin bearing a more intense colouration. Thus, depending on 3-hydroxykynurenine and xanthommatin concentrations in chromatophores, the colouration of a single individual ranges from pure white, beige to intense yellow.

Hormonal Control of Morphological Colour Changes

Colour changes that are dependent on light stimuli are further categorised into primary (pigmented cells directly respond to light) and secondary responses (the visual system is the intermediary between light and colour changing structures) (Duarte *et al.*, 2017). The colour change ability of crab spiders is a secondary response because blinded spiders can no longer turn yellow. Locust phase polyphenism depends not only on visual cues but also on mechanical and volatile stimuli, which all inform on conspecific density (Tanaka *et al.*, 2016). Both colour changes are under the control of the hormonal system. The injection to white crab spiders of 20-hydroxyecdysone, a common hormone of arthropods that regulates moulting among others, is sufficient to trigger a yellowing onset (Llandres *et al.*, 2013). In locust phase polyphenism, two main hormones are acting: juvenile hormones (JH) produced by the corpora allata and the dark-colour-inducing neurohormone (DCIN or [His^7]-corazonin) originating from the brain neurosecretory cells and the corpora cardiac (Tanaka *et al.*, 2016). DCIN and JH interact to produce a complex range of colourations in both solitarious and gregarious

phases but, in general, JH promotes yellowing while DCIN causes darkening (Tanaka *et al.*, 2016). To date, there is no confirmed link between hormones and changes in pigment metabolism in locusts. The cellular mechanisms of DCIN and JH effects on colouration (targeted tissues, signalling pathways, etc.) are unknown too.

The physiological control of morphological colour changes has been deeply investigated in mammals (**Figure 2-3**B). Their seasonal colour moulting is controlled by pituitary hormones, including prolactin, melatonin and alpha-melanocyte stimulating hormone (α-MSH), together with glucocorticoids, gonadal steroids and thyroid hormones (Zimova *et al.*, 2018). The action of α-MSH at the cellular level is the best understood of all (**Figure 2-3**C). This circulating hormone directly acts on the melanin-producing cells of the skin called melanocytes by binding to MC1R at their membrane. This causes a cascade of intracellular events that ultimately leads to the synthesis of melanogenic enzymes, as well as the concomitant biogenesis of melanin-containing organelles related to ommochromasomes and termed melanosomes. The same mechanisms are at stake during UV-induced tanning in humans (**Figure 2-3**A). Ratios in black eumelanins and red phaeomelanins are partly controlled by the balance in α-MSH and its antagonist, the agouti signalling protein (ASIP; **Figure 2-3**C). Fully pigmented melanosomes are then transferred to neighbouring keratinocytes contributing to hair and/or skin colouration (Zimova *et al.*, 2018).

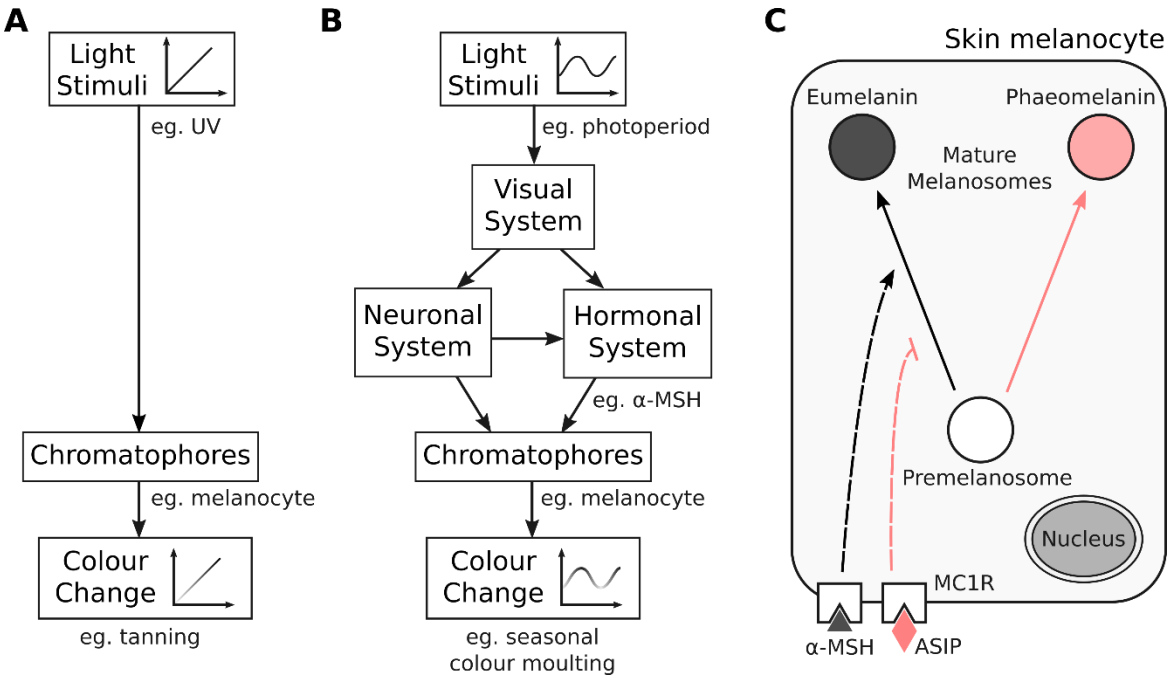

Figure 2-3. Environmental and Intrinsic Factors Controlling Morphological Colour Changes.
(A) When chromatophores directly sense light stimuli and trigger colour change, it is called a primary response. Colour change can be proportional to the light stimulus, such as in the tanning process of humans. (B) When the visual system is the intermediary between the light stimuli and the chromatophores response, it is called a secondary response. Both neuronal and hormonal systems can be involved in the regulation of colour-changing chromatophores. Hence, colour change pattern can match the light stimuli dynamics. For example, seasonal colour moulting is cyclic because it is linked to the change in photoperiod during the year. One hormonal factor involved in the regulation of skin melanocytes is α-MSH. (C) From the same pool of premelanosomes, skin melanocytes can produce either black melanosomes containing eumelanins or reddish ones with phaeomelanins. The fate of premelanosomes depends on the balance of two factors, α-MSH and ASIP; both bind to MC1R at the melanocytic membrane and activate antagonistic signalling cascades. See text for references. ASIP, Agouti signalling protein. α-MSH, α-melanocyte-stimulating hormone. MC1R, Melanocortin 1 Receptor. UV, ultraviolet radiation.

In the animal kingdom, morphological colour changes are mainly based on the formation and degradation of pigmented organelles. Such a process should be costly for the organism because it requires the production or mobilization of complex structures within chromatophores, as well as hormonal and intracellular signalling pathways. However, in the case of crab spiders, the recycling of pigment organelles might lead to a zero-sum process. This implies that energy budget studies should be performed on several colour-changing organisms before generalizing on the energetic cost of colour changes.

Mechanisms of Physiological Colour Changes

Physiological colour changes involve three main mechanisms: intracellular movements of pigmented structures, changes in the iridescence of nanophotonic structures and hydraulic-based changes of nanostructures (Umbers *et al.*, 2014). Physiological colour change based on the intracellular distribution of pigments is widespread in the animal kingdom, including spiders, crustaceans, insects, cephalopods, fishes, amphibians and chameleons (**Table 2-1**). Iridescent nanophotonic structures are mostly present in cephalopods, fishes and chameleons (**Table 2-1**). Hydraulic physiological colour change is rarer and mostly associated to the cuticle structure of insects, particularly in some beetles (Sun *et al.*, 2017a). In the following, we dissect the basic mechanisms of the two most emblematic cases of physiological colour changes, cephalopods and chameleons (**Figure 2-1**D, F). We also describe the regulation of darkening in fishes and amphibians (**Figure 2-1**E).

Physiological Colour Changes at the Tissue Level

In cephalopods, three layers of pigment cells contribute to their rapid colour-changing ability. The uppermost layer comprises superimposed xantho-, erythro- and melanophores. The two other layers comprise the light-reflecting leucophores and iridophores (**Figure 2-4**) (Mäthger *et al.*, 2009). Depending on their state of contraction/expansion, chromatophores variably filter parts of the visible light before it gets to the light-reflecting layers (**Figure 2-4**) (Mäthger & Hanlon, 2007). Hence, by independently regulating the expansion/retraction state of its chromatophores, a cephalopod can locally modify its colour pattern (Mäthger & Hanlon, 2007). This regulation is controlled by innervated muscles radially positioned around chromatophores. Upon contraction, they expand the chromatophores (**Figure 2-5**B). Thus, the fully contracted and colourless state is the rest state of chromatophores (Messenger, 2001).

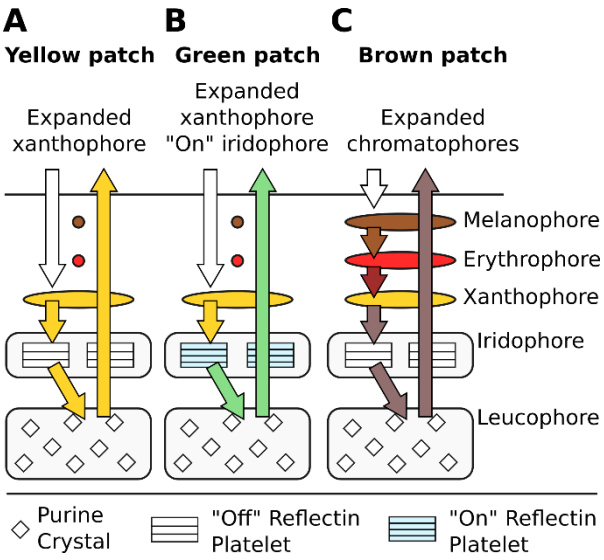

Figure 2-4. Physiological Colour Changes at the Tissue Level in Cephalopods.
In cephalopods, two layers of chromatophores are involved in colour change: pigmented chromatophores and iridophores. When leucophores are presents, they only reflect the in-coming light. Cephalopods can produce a wide array of coloured patches using a combination of expanded/retracted pigmented chromatophores together with activated/inactivated iridophores. **(A)** When pigmented chromatophores are expanded, the in-coming light is partly absorbed by pigments and thus appears coloured to the eye (e.g. yellow when absorbed by xanthophores). **(B)** When iridophore are in an activated state and xanthophores are expanded, a yellow (xanthophores) and a blue iridescent (iridophores) layers are superimposed leading to an overall green colouration. **(C)** Another combination is when all pigmented chromatophores are expanded and iridophores are inactivated, the in-coming light is then deprived of most of its wavelengths and will thus appear as dark brown.

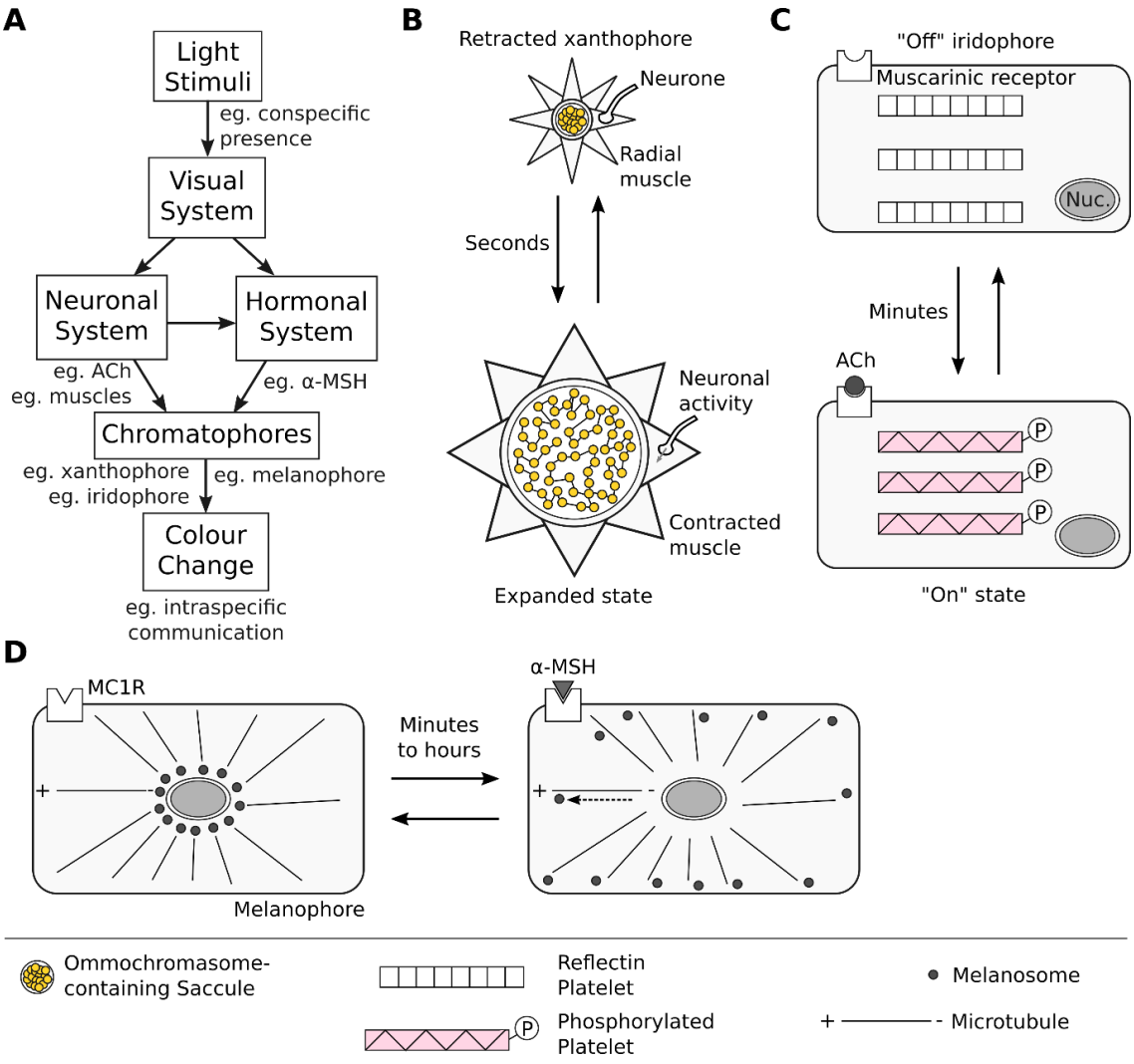

Figure 2-5. Factors Regulating Physiological Colour Changes at the Cellular Level.
(A) Physiological Colour Change is mostly a secondary response to light stimuli, although other types of stimuli can be involved, such as temperature (not shown). Both neuronal and hormonal systems can regulate chromatophores responses and thus colour change. (B) Pigmented chromatophores of cephalopods are under the control of a radial neuro-muscular system. When radial muscles are relaxed, chromatophores are in a retracted state that do not absorb light. Upon neuronal activity, radial muscles contraction forces chromatophores to expand. Since pigmented organelles of chromatophores are tethered together and that they are located within a cytoelastic saccule, the chromatophores expansion increases light absorption surface. This expanded and coloured state is fully reversible and allows for rapid colour change. (C) Cephalopod iridophores contain iridosomes made of reflectin platelets separated by layers of cytoplasm. In their inactivated "off" state, reflectin platelet structure and layers width do not create light interference and thus colouration. Upon activation of muscarinic receptors by the neurotransmitter acetylcholine, reflectin platelets are phosphorylated, change their conformation and layers of cytoplasm are reduced. The overall effect is the production of light interferences leading to red light. This activated "on" state of iridophores is fully and quickly reversible. (D) In fishes and amphibians, melanophores are the main pigmented cells providing physiological colour change. In their inactivated and unpigmented state, their melanosomes aggregates around the nucleus. Upon binding of α-MSH to MC1R, melanosomes are moved along microtubules toward their (+)-end by molecular motors. The dispersion of melanosomes to the edge of the cell increases the surface of light absorption. This activated and pigmented state of melanophores is fully and quickly reversible. See text for references. Ach, Acetylcholine. α-MSH, α-melanocyte-stimulating Hormone. MC1R, Melanocortin 1 Receptor. Nuc., Nucleus.

Interestingly, some orb-web spiders are also capable of physiological colour changes via a mechanism similar to the expansion/contraction of cephalopod chromatophores. By expanding their guanocytes, these orb-web spiders promote the total refraction of the in-coming light and thus are locally white rather than black, the colour of deeper integumental melanophores (Wunderlin & Kropf, 2013).

Furthermore, similarly to a soap bubble's iridescence, cephalopods iridophores produce phase interferences that further modify the colour of in-coming and reflected lights, which adds another layer of complexity in this system (**Figure 2-4**). Iridophores can be turned "on" and "off" during colour change making them either iridescent or colourless, respectively (**Figure 2-4**) (Mäthger & Hanlon, 2007; Mäthger *et al.*, 2009).

Physiological Colour Changes at Cellular and Molecular Levels

In cephalopods, expansion and contraction of chromatophores modify the intracellular distribution of pigmented organelles, the ommochromasomes (Messenger, 2001). These ommochrome-containing organelles are tethered together in an elastic saccule that expands and retracts concomitantly with the chromatophore (**Figure 2-5**B) (Deravi *et al.*, 2014). When this saccule is expanded, light is absorbed by a surface which is up to 500 times greater than in the retracted state, explaining why the chromatophore appears more coloured (Masthay, 1997).

Cephalopod iriodophores possess iridescent organelles called iridosomes that are made of thin reflectin platelets separated by layers of watery cytoplasm or extracellular space. Just like soap bubbles, iridosomes are ideal multilayer reflectors for producing phase interferences in light: their reflectin and cytoplasm layers have different refraction indexes and their widths match the wavelengths of visible light (Mäthger *et al.*, 2009; Ghoshal *et al.*, 2013). During physiological colour change, either reflectin platelets can be moved away from each other (**Figure 2-5**C) or water can be expulsed from extracellular spaces; both change the optical property of iridosomes and thus turn iridophores "on" or "off" (Mäthger *et al.*, 2009; DeMartini, Krogstad, & Morse, 2013). A comparable system is involved in the colour change of reflecting stripes of the paradise whiptail fish (Mäthger, 2003). Furthermore, cephalopod iridophores can change the 3D conformation and the phosphorylation state of reflectins

(**Figure 2-5**C). Reflectin's refractive index thus varies allowing a finer tuning of the iridescent property of iridosomes (DeMartini *et al.*, 2015).

In cephalopods, ommochromasomes may not only be effective light absorbers but could also act as photonic nanostructures since they possess reflectin proteins too (Williams *et al.*, 2016). Together with their geometrical distribution within the saccule, their spherical shape and their size, ommochromasomes could hence participate in reflecting light (Williams *et al.*, 2016); a property that could be rapidly altered during physiological colour change.

Chameleon's iridophores also possess multilayer reflectors, although they are made of guanine crystal lattices that are even more refracting than reflectins (Teyssier *et al.*, 2015). The colour produced by these photonic nanostructures changes upon modification of the distance between guanine crystals, similarly to reflectin platelets. Then, when this distance is increased, the reflected light shifts from blue to red hues, the latters being associated to the excited state of the chameleon (Teyssier *et al.*, 2015).

Changes in chromatophore brightness of insects, crustaceans, fishes, amphibians and lizards are mediated by the displacement of pigmented organelles within the cytoplasm (Umbers *et al.*, 2014). Their intracellular redistribution leads to either an increase or a decrease in light absorbance, making the chromatophore more or less coloured without directly altering its hue. The dispersion/aggregation and the displacement of pigmented organelles in general are mediated by molecular motors that anchor and move organelles along the cytoskeleton, especially microtubules (**Figure 2-5**D) (Ligon & McCartney, 2016).

Hormonal and Neuronal Controls of Physiological Colour Changes

Physiological colour changes are generally a secondary response to light stimuli and visual signals. Thus, the information must be transmitted from photoreceptors to chromatophores via the neuronal or the hormonal system (**Figure 2-5**A). In cephalopods, muscles controlling chromatophores are directly innervated by the brain (**Figure 2-5**B) (Messenger, 2001). This system allows colour changes in a few seconds. Alternatively, some iridophores can be turned "on" within minutes by acetylcholine (Mäthger *et al.*, 2009), a ubiquitous neurotransmitter in the animal kingdom that binds muscarinic membrane receptors of chromatophores (**Figure 2-5**C).

Similarly, the dispersion/aggregation of pigmented organelles in melanophores of some insects (particularly stick insects), crustaceans, amphibians, crocodiles and fishes is under the control of neurotransmitters and hormones, such as α-MSH (**Figure 2-5**D) (Ligon & McCartney, 2016).

In contrast to morphological colour changes, the mechanisms of physiological colour changes are highly diverse, spanning from muscle-driven expansion of chromatophores, organelle motility to changes in the conformation of iridescent structures. Noteworthy, neuro-muscular activities and organelle movements are two energy-consuming processes, which probably makes them costly to the organism. This said, the general benefits and costs of physiological colour changes are even less understood than those of morphological colour changes.

Conclusion

The two types of colour changes, morphological and physiological, are widespread in the animal kingdom (**Table 2-1**). Although the underlying mechanisms of morphological and physiological colour changes are quite different and lead to either slow or quick colour changes, respectively, the main actors are the same. Indeed, both morphological and physiological colour changes share chromatophores, pigmented organelles and pigments (e.g. ommochrome-containing xanthophores; **Figure 2-2** and **Figure 2-4**), except for iridophores that are almost exclusively involved in physiological colour changes. Furthermore, both morphological and physiological colour changes are under the control of similar external stimuli (light mainly) that often trigger a physiological response through similar neuronal and hormonal systems (e.g. α-MSH; **Figure 2-3** and **Figure 2-5**). Even the biological functions of both morphological and physiological colour changes (UV protection, thermoregulation, intra/interspecific communication and crypsis) are analogous (**Table 2-1**). Thus, one might assume that they have evolved under similar pressures.

Why those two types of colour changes have evolved independently several times during the evolution of animals is a key question. To answer it, there is still a need in more phylogenetic studies regarding colour changes (Umbers *et al.*, 2014; Duarte *et al.*, 2017). So

far, it was demonstrated that intraspecific communication, rather than camouflage, has been the main driver of dwarf chameleon colour evolution (Stuart-Fox & Moussalli, 2009). Thus, more phylogenetic studies will help understanding the actual function of colour changes in the animal kingdom. Furthermore, constraints on species metabolism, chromatophores capabilities, presence of iridophores, etc. might explain why some species can perform physiological rather than morphological colour changes.

The evolution of two different colour changes could also be due to differences in energetic costs for both types of colour changes. On one hand, morphological colour changes generally require *de novo* formation of pigments and organelles, which might be a costly process on the short term. On the other hand, physiological colour changes mainly involve the movements of pre-existing pigmented structures, a process that could be less costly, unless constantly used. However, to our knowledge, no study intended to quantify and to compare the costs of both morphological and physiological colour changes (Stuart-Fox & Moussalli, 2009). More generally, the impact of colour changes on individual fitness has rarely been investigated by studies linking proximate and ultimate causes in model organisms (**Figure 2-1**); it is therefore difficult to conclude on their evolutionary consequences.

Interestingly, colour changes are not exclusive to animals; bacteria, fungi and plant species are also able to modify their colouration. A well-known example being leaf senescence in autumn, during which leaves of deciduous trees turn from green to red with intermediary hues, such as yellow and orange. This process might not simply be a by-product of chlorophyll pigment degradation but could also provide benefits to the plant and hence be physiologically controlled (Archetti *et al.*, 2009). Particularly, senescent leaves might accumulate red anthocyanins and carotenoids that protect the recovery of their nutrients from harmful UVs; a function that reminds the protective role of tanning for folates in humans. Hence, the widespread occurrence of colour changes among different classes of organisms implies that there are general benefits of colour changes. Estimating these benefits and the associated costs is one of the most challenging questions of organismal and evolutionary biology.

Glossary

Morphological colour changes: Slow colour changes involving the formation, the degradation or chemical modifications of pigments.

Physiological colour changes: Rapid colour changes involving either tuneable iridescence, the contraction/expansion of chromatophores or intracellular movements of organelles.

Polyphenism: Changes in the phenotype of a single individual triggered by environment conditions. It is therefore a type of phenotypic plasticity.

Aposematism: Warning signals harboured by a dangerous organism toward predators.

Chromatophore: Coloured cell that produces pigments or coloured structures and usually stores them.

Ommochrome: Class of pigments that derives from tryptophan and that occurs in eyes and integuments of arthropods and cephalopods.

Crypsis: Ability of an individual to remain unseen from another organism, such as a predator or prey. Crypsis can be achieved by camouflage, masquerade or mimicry.

2.3 Conclusion

Cette revue de la littérature sur les changements de couleur morphologique et physiologique montre qu'ils possèdent de multiples points communs qui peuvent éclairer sur leur évolution. Ainsi, ils impliquent la plupart du temps les mêmes acteurs, qu'ils soient cellulaires ou moléculaires, à l'instar des ommochromes. Si les mécanismes physiologiques contrôlant les changements de couleur sont bien connus (et relativement conservés au sein des animaux), leur intégration avec toutes les autres échelles du vivant, de la molécule à l'écologie, n'est pas encore réalisée chez un nombre suffisant d'espèces. Ainsi, il manque des informations concernant les coûts et les bénéfices énergétiques des changements de couleur réversibles, qui sont pourtant nécessaires pour expliquer leur apparition et leur maintien. Ensuite, les nombreuses fonctions biologiques associées aux changements de couleur indiquent qu'il s'agit d'un processus complexe influencé par de nombreux facteurs, qu'ils soient biotiques (prédateur, partenaire sexuel, etc.) ou abiotiques (température, rayonnement UV, etc.). Ceci suggère que l'étude des changements de couleur nécessite une approche intégrative, prenant en compte toutes les propriétés conférées par les pigments et les structures colorées.

Dans la suite de ce travail, je m'intéresserai à la classe des ommochromes en étudiant leurs caractéristiques biochimiques et leur environnement cellulaire. La connaissance des mécanismes aux plus petites échelles (moléculaire et cellulaire) permettra de faire le lien entre les différentes propriétés de ces pigments, et donc de renseigner sur leur potentiel rôle dans les changements de couleur. Ces relations structure–fonction multi-échelles seront donc au cœur des prochains chapitres.

Chapitre 3 – Les ommochromes chez les invertébrés : biochimie et biologie cellulaire

As a whole, ommochrome pigmentation might still be expected to yield a number of interesting results.

Bernt Linzen (1974), in *Advances in Insect Physiology*

3.0 Sommaire

CHAPITRE 3 – LES OMMOCHROMES CHEZ LES INVERTEBRES : BIOCHIMIE ET BIOLOGIE CELLULAIRE 67

3.0 SOMMAIRE 68

3.1 OBJECTIFS 69

3.2 REVUE DE LA LITTERATURE 70

Abstract *71*

Introduction *72*

Ommochrome Biochemistry: From the Indole to the Phenoxazone Chromophore *77*

Ommochromes, a phenoxazone-based chrome family restricted to invertebrates 77

Extraction, analysis and identification of ommochromes 81

Ommochrome biogenesis: the tryptophan oxidation pathway 85

Enzymes of the Tryptophan→Ommochrome pathway 86

Putative cross-talk between ommochromes and other chromes 91

Ommochrome reactivity 93

Ommochromes within the Cell: the Ommochromasome Life Cycle *96*

Methods for studying ommochromasomes 96

Ommochromasome structure and composition 99

The origin of the ommochromasome, a lysosome-related organelle 100

Ommochromasome biogenesis 104

Ommochrome biosynthesis in relation to ommochromasome maturation 108

Ommochromasome recycling 110

Ommochromes in Context: the Fruit Fly Compound Eye *112*

Conclusions *115*

Acknowledgements *118*

3.3 CONCLUSION 119

3.1 Objectifs

Les ommochromes sont des pigments tout à fait particuliers, à plus d'un titre. D'une part, ils font partie de l'une des rares familles de pigments à être présents chez un seul groupe d'animaux (les invertébrés protostomiens). D'autre part, ils possèdent une physico-chimie atypique, comme en témoigne la couleur rouge des formes réduites par rapport aux formes oxydées jaunes. Finalement, les connaissances sur la biochimie et la biologie cellulaire des ommochromes restent en retrait par rapport à celles sur les caroténoïdes, les ptérines et surtout les mélanines, alors que les ommochromes ont été découverts il y a plus de 80 ans (Becker, 1939). La dernière revue sur les ommochromes, datant de 1974, peut en témoigner (Linzen, 1974). En revanche, la chimie des ommochromes (Williams *et al.*, 2016; Williams, Lopez, & Deravi, 2019a) et leur photochimie (Romero & Martínez, 2015) retiennent l'attention depuis quelques années, en particulier dans le cadre du biomimétisme du changement de couleur des céphalopodes (Kumar *et al.*, 2018). Intégrer ces nouvelles données à la biologie fonctionnelle des ommochromes devrait permettre de mieux comprendre l'importance de cette famille de pigments chez les invertébrés.

Ce chapitre a pour objectif de faire une revue de la littérature sur la biochimie et la biologie cellulaire des ommochromes, en les intégrant à leurs différents contextes biologiques. Je mets en parallèle les données moléculaires et biochimiques *per se* et les récentes avancées sur la chimie quantique des ommochromes, ce qui permet de revisiter la photochimie développée dans les années 1980. D'un point de vue pratique, je souhaite aussi mettre en avant les difficultés expérimentales propres à la chimie des ommochromes, ainsi que les nouvelles méthodes de chimie analytique qui pourraient aider à élucider la structure de nouveaux ommochromes. Finalement, en prenant appui sur les connaissances poussées à propos des mélanosomes (les organites qui contiennent la mélanine), je souhaite remettre en perspective les ommochromes dans leur environnement cellulaire. En effet, ceux-ci sont généralement produits et déposés dans des organites spécialisés, appelés ommochromasomes, dont le fonctionnement et l'architecture font partie intégrante de la biologie des ommochromes.

3.2 Revue de la littérature

Ce manuscrit a été publié dans le journal international à comité de lecture *Biological Reviews*.

FIGON, F. & CASAS, J. (2019) Ommochromes in invertebrates: biochemistry and cell biology. *Biological Reviews* **94**, 156–183.

Ommochromes in invertebrates: biochemistry and cell biology

Florent Figon and Jérôme Casas*

Institut de Recherche sur la Biologie de l'Insecte, UMR CNRS 7261, Université de Tours, 37200 Tours, France

*Author for correspondence (E-mail: jerome.casas@univ-tours.fr).

Abstract

Ommochromes are widely occurring coloured molecules of invertebrates, arising from tryptophan catabolism through the so-called Tryptophan→Ommochrome pathway. They are mainly known to mediate compound eye vision, as well as reversible and irreversible colour patterning. Ommochromes might also be involved in cell homeostasis by detoxifying free tryptophan and buffering oxidative stress. These biological functions are directly linked to their unique chromophore, the phenoxazine/phenothiazine system. The most recent reviews on ommochrome biochemistry were published more than 30 years ago, since when new results on the enzymes of the ommochrome pathway, on ommochrome photochemistry as well as on their antiradical capacities have been obtained. Ommochromasomes are the organelles where ommochromes are synthesised and stored. Hence, they play an important role in mediating ommochrome functions. Ommochromasomes are part of the lysosome-related organelles (LROs) family, which includes other pigmented organelles such as vertebrate melanosomes. Ommochromasomes are unique because they are the only LRO for which a recycling process during reversible colour change has been described. Herein, we provide an update on ommochrome biochemistry, photoreactivity and antiradical capacities to explain their diversity and behaviour both *in vivo* and *in vitro*. We also highlight new biochemical techniques, such as quantum chemistry, metabolomics and crystallography, which could lead to major advances in their chemical and functional characterisation. We then focus on ommochromasome structure and formation by drawing parallels with the well-characterised melanosomes of vertebrates. The biochemical, genetic, cellular and microscopic tools that have been applied to melanosomes should provide important information on the ommochromasome life cycle. We propose LRO-based models for ommochromasome biogenesis and recycling that could be tested in the future. Using the context of insect

compound eyes, we finally emphasise the importance of an integrated approach in understanding the biological functions of ommochromes.

Keywords: ommochrome, ommochromasome, pigment, photochemistry, antiradical capacity, phenoxazone, phenothiazine, melanosome, melanin, lysosome-related organelle.

Introduction

Colouration is one of the most striking traits observable in animals. It has caught the interest of scientists for centuries and was at the heart of the work of pioneers of evolutionary biology, particularly Alfred R. Wallace, Edward B. Poulton, Henry W. Bates and Johann F.T. Müller (Bates, 1862; Wallace, 1877; Müller, 1879; Poulton, 1890; Caro, 2017). The field of animal colouration has also inspired a wealth of ideas in applied sciences (Caro *et al.*, 2017a), including the investigation of biomimetic camouflage by the naturalist and artist Abbott H. Thayer (Thayer & Thayer, 1909). Therefore, understanding the proximate and ultimate causes of colouration in animals is of great importance (Endler & Mappes, 2017; Cuthill *et al.*, 2017).

Colours can arise from either physical or chemical processes (Cuthill *et al.*, 2017). Physical or structural colours are produced by interactions between light and photonic structures such as crystals. Chemical colours are mainly created by light-absorbing pigments and dyes, together referred to as chromes (Fox, 1944; Needham, 1974). Pigments differ from dyes by being in suspension whereas the latter are in solution. This difference in physical state can have dramatic consequences on colouration because particles in suspension can also produce structural colours. Because it is rarely known whether a coloured molecule is in a solid or a liquid matrix *in vivo* (Needham, 1974), we hereafter use the term ‘chrome’ rather than the more-common, but imprecise if not misleading, word ‘pigment’. Chromes are directly able to modify part of the wavelengths of visible, near-ultraviolet (UV) and near-infrared (IR) light. They do so by absorbing photons with a specific energy, and thus wavelength, via their chromophore (Needham, 1974). The molecular structure of chromophores is particular to each chrome family, and understanding how they work is necessary to comprehend the biological functions of chromes (Needham, 1974).

Ommochromes form a particular tryptophan-derived chrome family and have been described in protostomes (**Figure 3-1**), but are virtually absent from deuterostomes and plants [see (Takeuchi *et al.*, 2005) for possible ommochrome-related genes in the tunicate *Ciona intestinalis*] (Linzen, 1974; Needham, 1974). Interestingly, some bacteria produce the well-known ommochrome-like antibiotic compound, actinomycin D (Le Roes-Hill, Goodwin, & Burton, 2009). The ommochrome chromophore is based on phenoxazine and phenothiazine systems, which are heteropolyaromatic rings with either two N and O atoms or two N and S atoms, respectively. Phenoxazines are found in natural and synthesised chromes that have been used for centuries, such as orcein, and blue and red Niles, and also in more recent technologies, such as photovoltaic sensitizers (Li *et al.*, 2017). Thus, ommochromes are at a crossroads of basic and applied sciences.

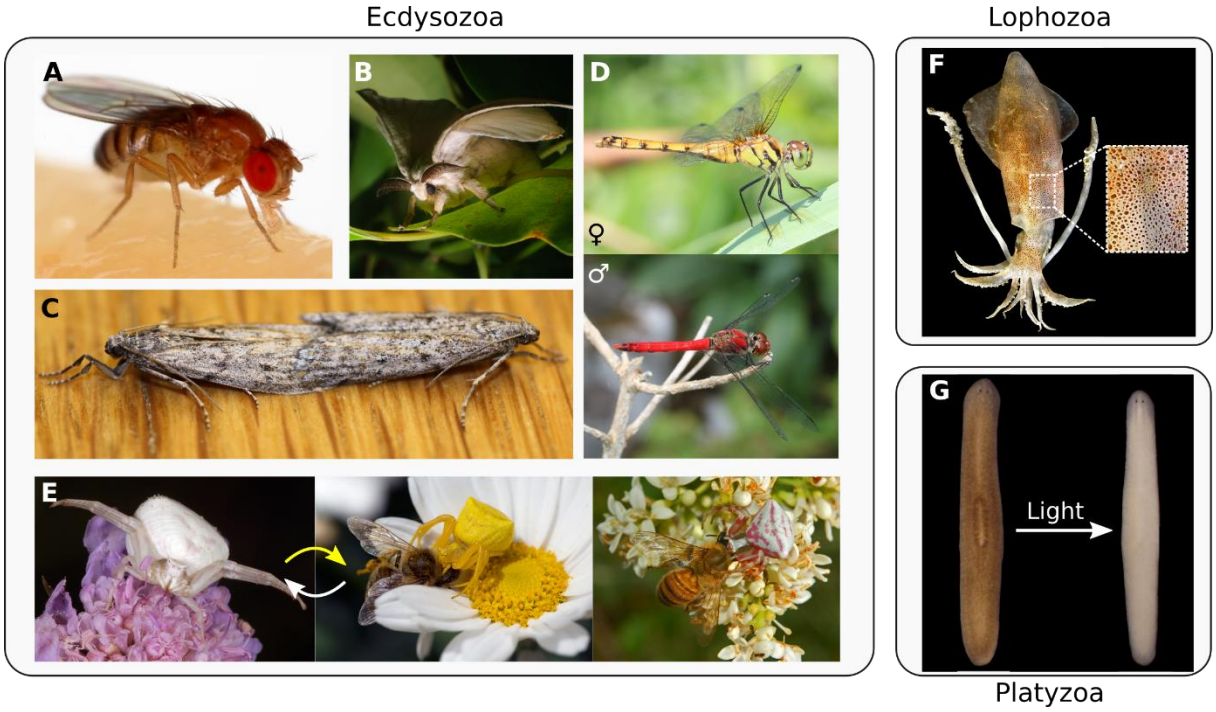

Figure 3-1. Examples of protostomes that produce ommochromes.
Ommochromes are found in the three main protostomian phyla: Ecdysozoa (insects and spiders), Lophozoa (cephalopods) and Platyzoa (flatworms). (A–C) Ommochromes generally function as eye pigments in insects, such as in *Drosophila melanogaster* (A; body length 3 mm), *Bombyx mori* (B; 20 mm) and *Ephestia kuehniella* (C; 10 mm). (D) Several *Sympetrum* species show sexual dimorphism, which results from different redox states of ommochromes: a yellow female and a red male of *S. darwinianum* are shown (body length 40 mm). (E) Some crab spiders, such as *Thomisus onustus* (body length 10 mm), can change their colour from white to yellow by producing and degrading ommochromes. Some individuals also show an irreversible purple-stripe pattern. (F) Cephalopods, such as *Loligo vulgaris* (body length 40 cm), can rapidly change their colour pattern by expanding or shrinking saccules of ommochromasomes, the ommochrome-containing organelles. The inset shows integumental chromatophores of different colours (from yellow to brown) corresponding to different

ommochromes. (G) The flatworm *Girardia dorotocephala* (body length 5 mm) possesses epithelial chromatophores producing ommochromes. In presence of light, these chromatophores are lost leading to an unpigmented animal. Photograph credits (all CC BY SA): (A) Sanjay Acharya, (B) Ash Bowie, (C) Magne Flåten, (D) Alpsdake, (E) Fritz Geller-Grimm, Paul-Henri Cahier and Hectonichus, (F) adapted from Hans Hillewaert, (G) adapted from Stubenhaus *et al.* (2016) https://doi.org/10.7554/eLife.14175.003.

The history of ommochrome study started almost 80 years ago with their first description in insect ommatidia by Becker (**Figure 3-2**) (Becker, 1939, 1942). In the 1950s and 1960s, the so-called Butenandt's school (one of Becker's collaborators) provided almost all we know about ommochrome chemistry. This analytical work was accompanied by genetic studies that unravelled the biogenesis pathway of ommochromes and their organelles in insects, particularly *Drosophila melanogaster*, *Ephestia kuehniella*, *Bombyx mori* and *Apis mellifera*. Since then, researchers lost interest in ommochromes (**Figure 3-2**A). A renaissance of interest is currently underway with studies dealing with ommochrome biological function and some of their chemical properties (**Figure 3-2**B). These biochemical studies have allowed physiologists to unravel the properties and the biological significance of ommochromes. Ecologists studied these chromes to unravel the proximal basis of colour-based behaviours such as mimicry and vision (Holl, 1987; Oxford & Gillespie, 1998; Stavenga, 2002; Théry & Casas, 2009; Umbers *et al.*, 2014). More recently, developmental biologists have used ommochromes of butterfly wings to tackle the mechanisms and the diversity of colour patterning (Sekimura & Nijhout, 2017). Today, ommochromes are also involved in transcriptomic studies of grasshoppers, butterflies, damselflies and spiders (Ooi *et al.*, 1997; Croucher *et al.*, 2013; Chauhan *et al.*, 2014; Connahs, Rhen, & Simmons, 2016; Wang *et al.*, 2017), as well as in clustered regular interspaced short palindromic repeats/CRISPR-associated protein 9 (CRISPR/Cas9)-mediated genome editing (Zhang & Reed, 2017; Khan, Reichelt, & Heckel, 2017; Xue *et al.*, 2017). Unfortunately, biochemical knowledge did not keep pace with this increase in functional studies. Thus, the latter are usually based on classical biochemical papers and reviews, while ommochromes appear to be more complex and reactive than previously thought (Bolognese & Liberatore, 1988).

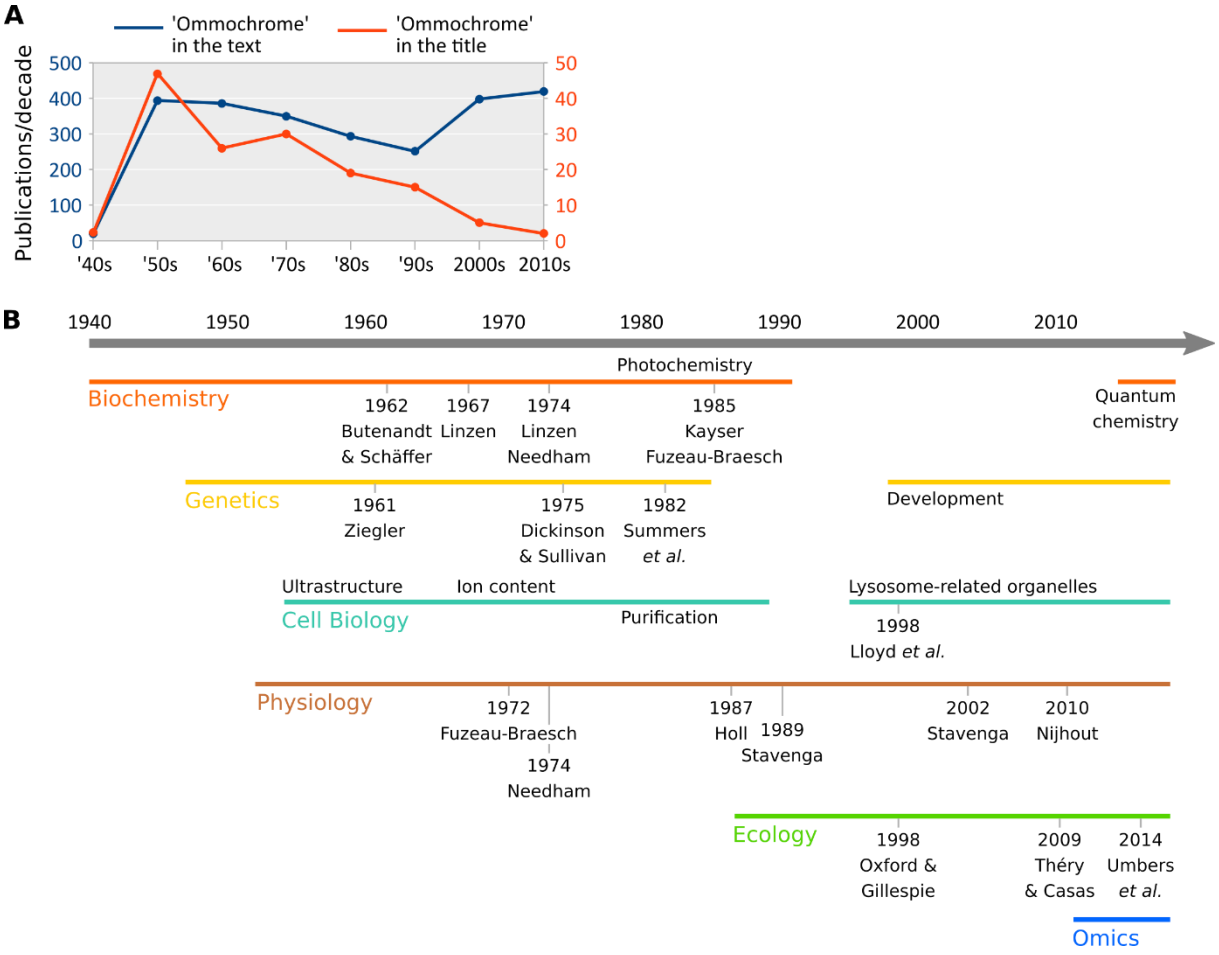

Figure 3-2. History of ommochrome study.
(A) The number of publications related to ommochromes since their first description. Results included papers found in *Google Scholar* with the term 'ommochrome' either in their whole content (blue line) or only in their title (red line). After a peak in the 1960s, the number of publications with ommochrome in the title decreased at a regular rate, reaching the lowest number in the last decade. By contrast, papers mentioning ommochromes in the main text reached a new peak during the last decade, after a low point in the 1990s. (B) Main periods in the history of ommochrome study. Major reviews for each topic are indicated. No review on ommochrome biochemistry and genetics has been published for almost 30 years. Interruption of lines implies almost no work on that topic.

The ommochrome-containing organelles were studied from the 1970s to the 1990s (**Figure 3-2**B), before researchers focussed their attention on the related vertebrate melanosomes. Ommochrome-containing organelles have been classically termed 'ommochrome granules' or 'pigment granules' (Linzen, 1974; Kayser, 1985). However, herein, we designate them as 'ommochromasomes' as proposed by Needham 40 years ago (Needham, 1974). This decision is motivated by the membrane-bound nature of these organelles and their close relationship to melanosomes, both in terms of structure and

biogenesis (Lloyd, Ramaswami, & Krämer, 1998). Considering both ommochromes and ommochromasomes in their chemical and cellular contexts should help in teasing apart the complexity of their biological functions.

Ommochromes are mainly found in insect ommatidia (from which their name is derived), in cephalopod eyes and in most protostomian integuments (**Figure 3-1**) (Linzen, 1974; Needham, 1974). They are known to mediate colour patterning and colour changes, often in association with other chromes (Fuzeau-Braesch, 1985; Kayser, 1985; Oxford & Gillespie, 1998). Their colours range from pale yellow to dull brown, as well as bright red and deep purple. Other chromes, like melanins and pterins, and structural colours, such as in butterfly wing scales, can alter the chemical colours of ommochromes (Stavenga, Leertouwer, & Wilts, 2014). Colour patterns associated with ommochromes and their precursors are involved in crypsis (Williams *et al.*, 2016), mimicry (Reed, McMillan, & Nagy, 2008; Ferguson & Jiggins, 2009; Bybee *et al.*, 2012), colour changes (Insausti & Casas, 2008; Llandres *et al.*, 2013; Umbers *et al.*, 2014; Williams *et al.*, 2016), sexual maturation and seasonal forms (Nijhout, 1997; Futahashi *et al.*, 2012), as well as many other colour-based functions.

Like most chromes, ommochromes not only produce colours, but also function in many metabolic and biological processes (Linzen, 1974; Needham, 1974). The chemical properties of chromophores often make them suitable for transporting electrons or reacting with oxidants, reducers and free radicals, as well as functioning in vision (Needham, 1974). All these functions have been proposed to be fulfilled by ommochromes in nature (Needham, 1974; Stavenga, 2002; Insausti, Le Gall, & Lazzari, 2013; Romero & Martínez, 2015), often without direct proof. Furthermore, protostomes generally lack the glutarate and nicotinamide biosynthesis pathway that catabolises the amino acid tryptophan (Linzen, 1974). In insects, tryptophan is toxic at high concentrations, such as those that occur during moulting (Linzen, 1974; Manoukas, 1981). Therefore ommochromes are also thought to be end-products of tryptophan detoxification (Linzen, 1974).

Most difficulties in studying ommochromes arise from their chemical behaviour. Not all of them are soluble in the same solvents, some tend to form aggregates and they usually react with the extraction mixture (Linzen, 1974; Bolognese & Liberatore, 1988). However,

they have led to many advances in biology. Their genetics paved the way for understanding the genome structure of eukaryotes and its inheritance (Morgan, 1910), the relationship between genes and enzymes (Beadle & Ephrussi, 1936; Butenandt, Weidel, & Becker, 1940) and the importance of cell interactions during development (Beadle & Ephrussi, 1936). This was made possible by studies of eye-colour mutants of *Drosophila melanogaster* that were impaired in particular steps of the ommochrome pathway. During recent decades, ommochromes also helped advance understanding of general developmental mechanisms of colour patterning in animals, especially in butterfly wings (Reed & Nagy, 2005; Reed *et al.*, 2008; Wittkopp & Beldade, 2009; Nijhout, 2010; Sekimura & Nijhout, 2017). Hence, ommochromes have been studied in many contexts since the most recent reviews, more than three decades ago (**Figure 3-2**B) (Linzen, 1974; Kayser, 1985). It is therefore now appropriate to provide an updated insight into the biochemistry and cell biology of ommochromes.

Ommochrome Biochemistry: From the Indole to the Phenoxazone Chromophore

Ommochromes, a phenoxazone-based chrome family restricted to invertebrates

Ommochromes are a class of chromes (pigments and dyes) restricted to Protostomes (referred to as invertebrates; **Figure 3-1**). Ommochromes are composed of three main families of molecules: ommatins, ommidins and ommins (**Figure 3-3**). They are based on either a phenoxazone (ommatins) or a phenothiazine (ommins and possibly ommidins) ring (**Figure 3-3**) (Linzen, 1974; Needham, 1974). Ommochromes were historically classified according to their dialysis profile: ommatins are small molecules that can be dialysed, ommins are large (and often aggregated) molecules unable to be dialysed, while ommidins are in between (Linzen, 1974). From the detailed chemical studies of Becker, Butenandt and their colleagues in the mid-1920s, six ommatins were identified and one ommin structure was proposed (**Table 3-1**; **Figure 3-3**B) (Linzen, 1974; Needham, 1974; Kayser, 1985). The most recently identified ommochromes are the decarboxylated forms of xanthommatin and H_2-xanthommatin, which were first found in *in vitro* oxidation of ommochrome precursors (Bolognese *et al.*, 1988b; Vogliardi *et al.*, 2004) but were subsequently described in extracts of crab spiders, dragonflies, silkworms and cephalopods (Riou & Christidès, 2010; Futahashi

et al., 2012; Osanai-Futahashi *et al.*, 2016; Williams *et al.*, 2016). Unfortunately, almost nothing is known about ommidins.

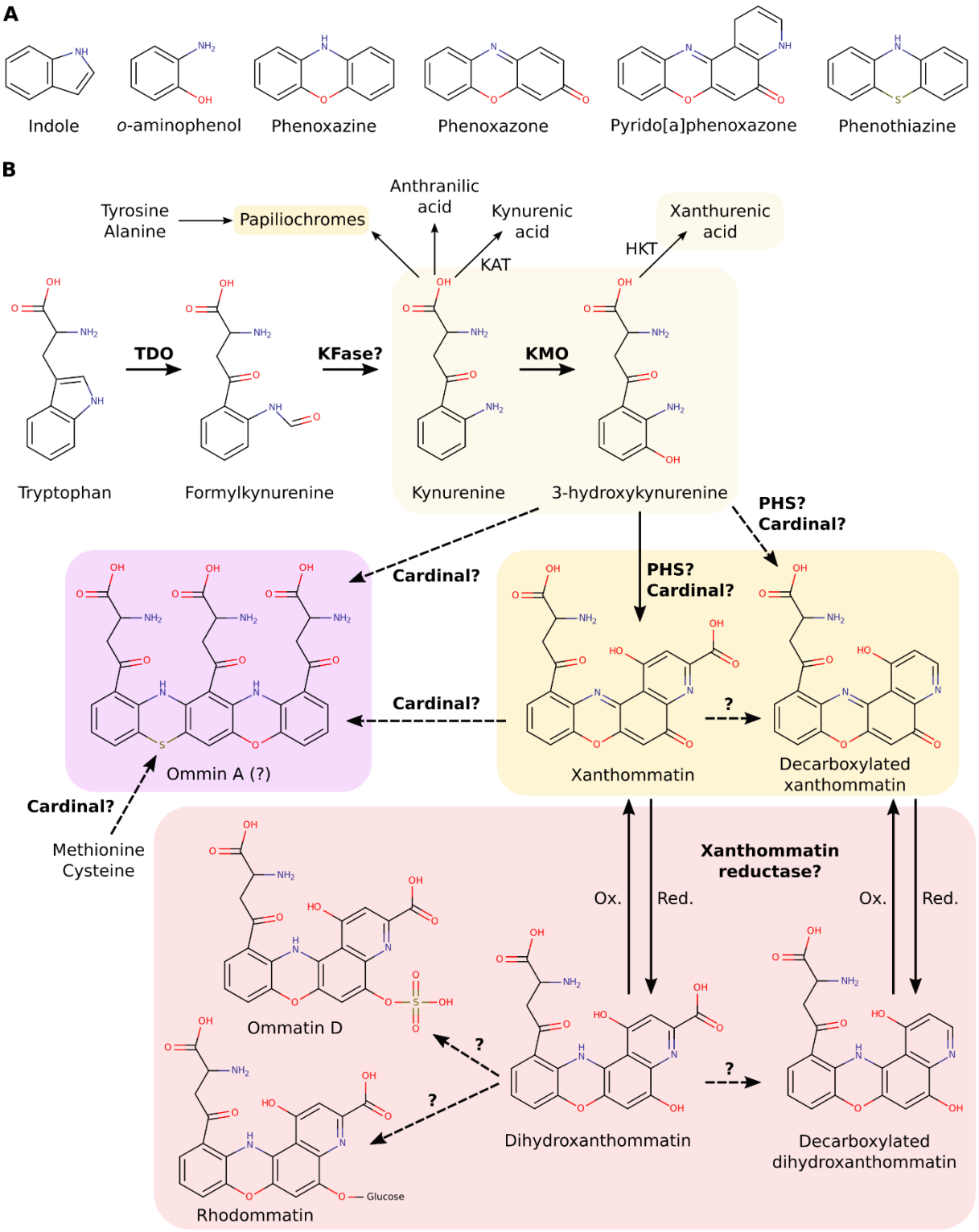

Figure 3-3. The ommochrome biosynthetic pathway.
(A) The cyclised chemical structure of ommochromes and their precursors. (B) Biochemical steps involved in ommochrome formation from tryptophan and their relationships with other kynurenine derivatives. Compounds that can be used as chromes are shown with a coloured background. Ommochrome formation starts with the breakdown of tryptophan *via* the oxidised opening of the indole ring, which is catalysed by TDO. Formylkynurenine is then transformed into kynurenine either through a spontaneous reaction or by the enzyme KFase. Kynurenine can be transformed into either anthranilic acid or kynurenic acid by HKT and KAT, respectively. It can also lead to the formation of papiliochromes by reaction with other amino acids. During ommochrome biosynthesis, kynurenine is processed into 3-hydroxykynurenine by the mitochondrial enzyme KMO. Both kynurenine and 3-hydroxykynurenine can be turned by HKT into xanthurenic acid, a yellow zoochrome. The condensation of two 3-hydroxykynurenines into the ommochrome xanthommatin may be either spontaneous or catalysed by a putative PHS. Both lead to the production of a phenoxazone ring, a ketone-derivative of phenoxazine. Redox reactions can lead to an equilibrium with the reduced state dihydroxanthommatin. The latter can be either *O*-sulphated or *O*-glycosylated to form ommatin D and rhodommatin, respectively. Both reduced and oxidised states of xanthommatin may be decarboxylated *in vivo* through an unknown mechanism. Ommin A formation involves two other amino acids, methionine and cysteine, which provide the sulphur atom for the phenothiazine system. Cardinal is thought to be the enzyme catalysing the late steps of ommin formation by using either 3-hydroxykynurenine or xanthommatin as substrates. HKT, 3-hydroxykynurenine transaminase; KAT, kynurenine aminotransferase; KFase, kynurenine formamidase; KMO, kynurenine 3-monooxygenase; Ox., oxidation; PHS, phenoxazone synthase; Red., reduction; TDO, tryptophan 2,3-dioxygenase.

Table 3-1. Chemical characteristics of ommochromes.

Ommochrome	Formula	Colour	Main absorbance peaks (nm)[a]	Theoretical MS $[M+H]^+$ *m/z*[b]	MS $[M+H]^+$ and MS^2 fragment *m/z*[c]
Ommatins					
Xanthommatin	$C_{20}H_{13}N_3O_8$	Yellow	230 450	424.07808	424.0761 407.0512 389.0410 361.0458 351.0614
Decarboxylated xanthommatin (Dc-xanthommatin)	$C_{19}H_{13}N_3O_6$	Yellow	230 440	380.08826	380.0865 363.0616 345.0511 317.0561 307.0713
Dihydroxanthommatin (H_2-xanthommatin)	$C_{20}H_{15}N_3O_8$	Red	230 380 495	426.09373	n/a
Decarboxylated dihydroxanthommatin (Dc-H_2-xanthommatin)	$C_{19}H_{15}N_3O_6$	Red	n/a	382.10391	n/a
Ommatin D (H_2-xanthommatin *O*-sulphate)	$C_{20}H_{15}N_3O_{11}S$	Red	230 370 490	506.05055	n/a
Rhodommatin (*O*-glucosyl-H_2-xanthommatin)	$C_{26}H_{25}N_3O_{13}$	Red	230 380 500	588.14656	n/a
Ommins					
Ommin A	$C_{30}H_{27}N_5O_{10}S$	Purple	520	650.15568	n/a
Ommidins	n/a	Yellow	230 320 430	n/a	n/a

[a] There can be shifts depending on the solvent (Linzen, 1974; Figon, F., personal observations).

[b] Calculated with MassBank (http://www.massbank.jp/MassCalc.html). MS, mass spectrometry; $[M+H]^+$ *m/z*, mass-to-charge ratio of the H adduct ion deriving from the considered molecule (M) after ionization.

[c] From postitive-mode electrospray source ionisation-based mass spectrometry coupled to high pressure liquid chromatography (HPLC-ESI^+-MS) and tandem MS (MS^2) data in Williams *et al.* (2016).

Phenoxazone and phenothiazine rings act as the main chromophores of ommochromes. These chromophores provide an electronic delocalisation system based on a polycyclic and asymmetric aromatic ring, which is composed of heteroatoms (N and O or S) and is associated with strong polar side-chains (**Figure 3-3**). These characteristics create a high dipole moment allowing the absorption of low-energy-carrying photons (Needham, 1974). Changes in side-chains (e.g. H_2-xanthommatin to ommatin D) or in redox states (e.g. xanthommatin to H_2-xanthommatin) modify the ability of these chromophores to absorb specific wavelengths and thus their colour (**Table 3-1**).

The typical absorption spectra of ommochromes show three peaks: two in the UV and near-UV regions and one in the 430–520 nm range (**Table 3-1**) (Linzen, 1974; Riou & Christidès, 2010). Therefore their colouration ranges from yellow (xanthommatin), to red (H_2-xanthommatin and its derivatives) to purple (ommins) (**Table 3-1**). Depending on the solvent used to measure ommochrome absorbance (5 *N* HCl, acidified methanol or phosphate buffer), there can be a shift of ~10 nm in their absorbance peaks (Linzen, 1974; Riou & Christidès, 2010). Interestingly, kynurenines are fluorescent whereas ommochromes only fluoresce in their crystal state (Linzen, 1974; Insausti & Casas, 2008). Internal or solvent-based quenching mechanisms have been proposed to explain this absence of fluorescence in solution (Linzen, 1974; Needham, 1974). Some studies have used the difference in fluorescence between kynurenines and ommochromes to detect an accumulation of kynurenines in tissues of white crab spiders and eye-colour mutants of fruits flies (Insausti & Casas, 2008; Harris *et al.*, 2011).

Extraction, analysis and identification of ommochromes

The chemistry of ommochromes is still largely unknown for one main reason: they are hard to extract and solubilise in conventional solvents (Linzen, 1974; Needham, 1974). Because ommidins and ommins tend to form aggregates and are thus hard to purify, these ommochromes are less characterised than ommatins. However, new analytical techniques, particularly liquid chromatography coupled with mass spectrometry, are now available to extract, identify and quantify ommochrome diversity more easily.

The most common solvent used to extract ommochromes is methanol acidified with 0.5–5% hydrochloric acid (MeOH–HCl) (Butenandt & Schäfer, 1962; Linzen, 1974; Kayser, 1985; Riou & Christidès, 2010; Williams *et al.*, 2016). It allows the extraction of ommochrome precursors, most ommatins and to some extent ommins. Only ommatin D and rhodommatin can be extracted with neutral aqueous solvents due to the presence of sulphate and glucose, respectively. Despite the convenience of MeOH–HCl extraction, photochemical studies (described in Section "Ommochrome reactivity"), demonstrated that, upon visible light radiation and at room temperature, ommochromes can undergo reversible transformation (photoreduction and methanol addition), as well as non-reversible reactions (phenoxazone opening, hydroxylation and methylation; **Figure 3-4**) (Bolognese *et al.*, 1988a, 1988b; Bolognese & Liberatore, 1988). This implies that not all compounds found in MeOH–HCl

extracts may be biologically relevant. It is also well known that ommatin D and rhodommatin spontaneously degrade into xanthommatin (Linzen, 1974; Nijhout, 1997). Thus, ommochrome extractions should be performed and stored in darkness at low temperature to avoid the production of chemical artefacts. Furthermore, it has been reported that the aspartic aminoacid chain is susceptible to deamination (forming fumaric acid) either in an acidic environment or by the action of aspartases (**Figure 3-4**B) (Bolognese *et al.*, 1988a). Finally, acidic solvents can also lead to the decarboxylation of the pyrido[a] ring of ommatins (**Figure 3-4**B) (Bolognese & Liberatore, 1988). Hence, extraction steps should be performed as rapidly as possible to ensure the identification of unaltered ommochromes.

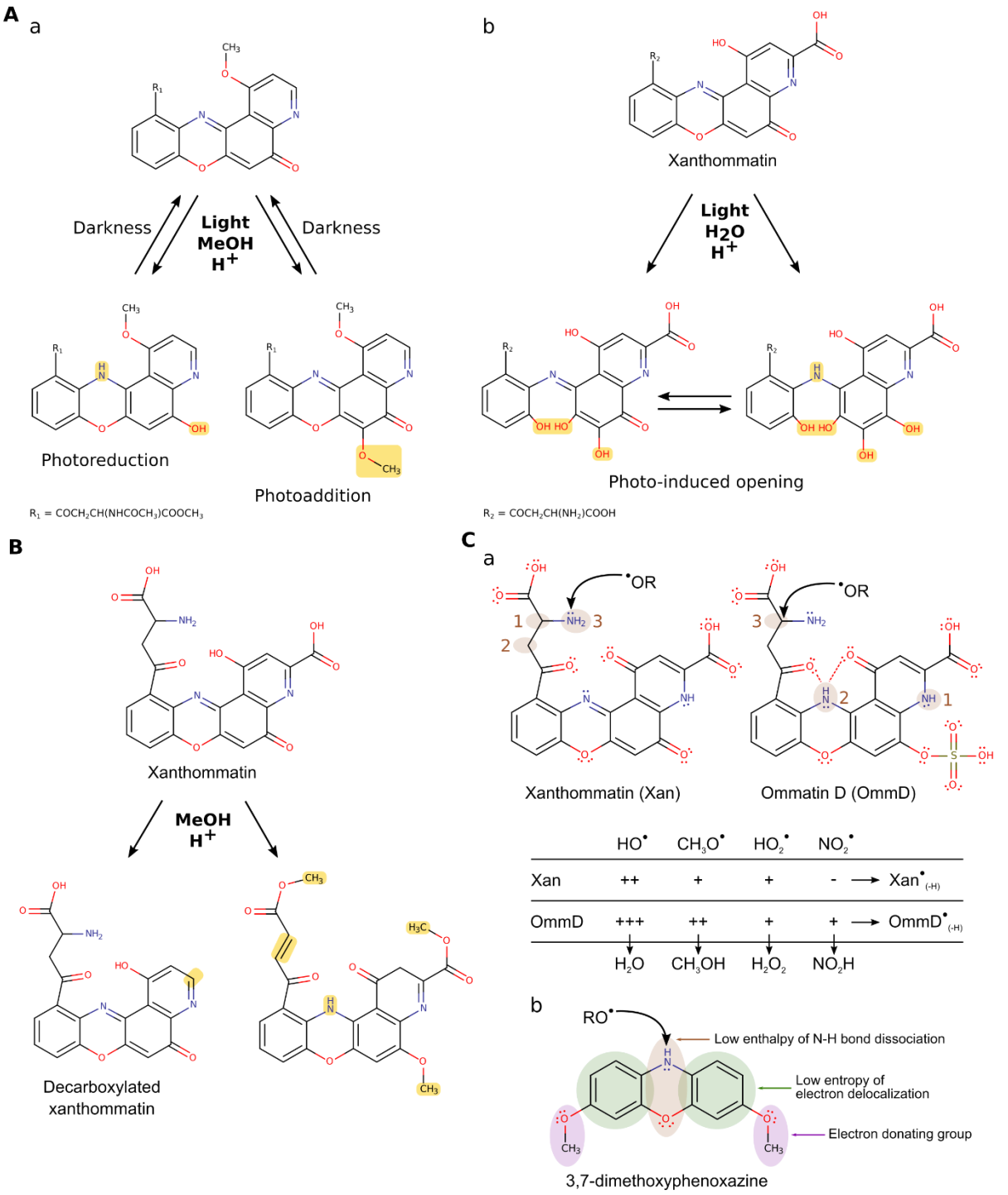

Figure 3-4. The reactivity of ommochromes and related compounds.
(A) The photoreactivity of xanthommatin and one of its derivatives in acidified solvents. Photo-induced modifications are highlighted in yellow. (a) Ommochrome-related compounds can undergo reversible reduction and solvent addition upon visible light irradiation. These transformations are not exclusive. In darkness, the initial compound is restored through spontaneous oxidation and demethylation. (b) In an acidified aqueous environment, where xanthommatin relatively insoluble, an irreversible opening of the phenoxazone ring can take place upon visible light irradiation. This is driven by the hydrolysis of O bonds and can be accompanied by photoreduction. Hence, subsequent closure of the phenoxazone ring can lead to the irreversible formation of new ommochrome compounds in xanthommatin mixtures (not shown). (B) Photo-independent reactions between

xanthommatin and acidified methanol can either lead to pyrido[a] decarboxylation, side-chain methylation or aspartyl-to-fumaryl transformation. (C) Antiradical properties of ommochromes and phenoxazone-based compounds. Ommochromes are able to quench free radicals, $RO^{\cdot}$, by a H-donor mechanism (curved arrow). (a) The three best H-donor sites (1–3), as calculated by computational chemistry, of xanthommatin and ommatin D are highlighted in brown. (b) Three chemical properties can explain the radical-trapping efficiency of phenoxazine-based compounds by decreasing the energy barrier of N–H bond dissociation.

The *in vivo* oxidized/reduced state of ommochromes depends directly on the redox state of their biological environment. This is of relevance regarding the role of red H_2-xanthommatin in filtering stray light within compound eyes and in the colour-changing ability of some dragonflies (Stavenga, 2002; Futahashi *et al.*, 2012). The redox conditions of an extraction solvent, which is in contact with the oxidising atmosphere, are likely to differ greatly from the buffered cytoplasm of a cell, which might also differ from the ommochromasome interior. Hence, reporting a ratio of xanthommatin/H_2-xanthommatin measured in a particular extraction solvent might not provide valid information regarding the real *in vivo* ratio of these two ommochromes (Futahashi *et al.*, 2012). Using standard samples (e.g. synthesised xanthommatin and H_2-xanthommatin) should provide information about the importance of redox reactions happening within the extract. The best approach would be to measure the redox potential of ommochrome-containing organelles as has been done for mitochondria (Go & Jones, 2008).

Historically, the identification of isolated ommochromes was performed with chromatography and spectrophotometry using, whenever possible, standard compounds (Linzen, 1974). It is important to note that no commercial ommochromes are available to date, meaning that ommochromes either have to be synthesised in the laboratory (Butenandt, Schiedt, & Biekert, 1954; Butenandt *et al.*, 1960, 1963) or purified from, for example, *Calliphora erythrocephala* eyes (xanthommatin), *Sepia officinalis* eyes (ommin A) and *Vanessa cardui* secretions (ommatin D and rhodommatin) (Butenandt & Schäfer, 1962). Migration profiles and absorption spectra of extracts can be compared to these standards, leading to a relatively precise identification of the compound of interest. This method is rather long, complex and error-prone. Today, with more sensitive detectors available, the absorption spectra of compounds even at very low concentrations can be measured using high-pressure liquid chromatography (HPLC) (Riou & Christidès, 2010; Llandres *et al.*, 2013). The increasing availability of mass spectrometry (MS) further enhances the identification power for both known and unknown ommochromes (**Table 3-1**) (Vogliardi *et al.*, 2004; Futahashi *et*

al., 2012; Daniels & Reed, 2012; Williams *et al.*, 2016). The ommochrome field would benefit from the creation of a community-based MS library (Dunn *et al.*, 2013) containing precursor and fragment ions from a large range of ommochromes and phenoxazone-based compounds (**Table 3-1**). As for plant metabolomics (Heiling *et al.*, 2016), such a library would help in the identification of new compounds and thereby in unravelling the diversity of ommochromes arising both *in vivo* and *in vitro* (Vogliardi *et al.*, 2004). Other analytical techniques [IR spectrometry, nuclear magnetic resonance (NMR), electron paramagnetic resonance (EPR)] have been used successfully to identify ommochrome-related compounds, which differ to ommochromes in methylation and side chains; unfortunately, natural ommochromes are largely unsuitable for these methods due to their low concentrations and poor solubility in neutral organic solvents, particularly chloroform (Bolognese *et al.*, 1988b).

Ommochrome biogenesis: the tryptophan oxidation pathway

The steps leading to ommatin formation from tryptophan (Trp) were first studied using the eye-colour mutants *vermilion* and *cinnabar* of *Drosophila melanogaster* (Summers, Howells, & Pyliotis, 1982), *Ephestia kuehniella* (Caspari, 1949), *Bombyx mori* (Uda, 1932; Kikkawa, 1953; Tanaka, 1953) and *Apis mellifera* (Dustmann, 1987) are also important genetic models that proved the generality of this ommochrome biosynthetic pathway. Supplementation of eye-colour mutants with tryptophan derivatives [*N*-formylkynurenine (FKyn), kynurenine (Kyn) and 3-hydroxykynurenine (3OHKyn)] allowed clarification of the so-called Tryptophan→Ommochrome pathway (**Figure 3-3**B) (Linzen, 1974). Xanthommatin biogenesis involves two spontaneous steps (loss of the formyl group, and the final cyclisation of the aspartyl chain), while the other steps rely exclusively on enzymatic activities (**Figure 3-3**B). It is still debated whether the condensation of two 3-hydroxykynurenines to form the phenoxazone ring takes place spontaneously *in vivo* (Phillips & Forrest, 1970; Yamamoto, Howells, & Ryall, 1976; Bolognese *et al.*, 1990; Li, Beerntsen, & James, 1999). It should be noted that a labile ommochrome precursor, thought to be non-cyclised xanthommatin, can be extracted in cold solvents from cephalopods, crustaceans and insects; this ommochrome spontaneously forms xanthommatin at room temperature (Bolognese & Scherillo, 1974). In this manner, non-cyclised xanthommatin might be stabilised within the cell. The final steps leading to the reduction of xanthommatin to H_2-xanthommatin and the addition of sulphate (ommatins D) or glucose (rhodommatin) are completely unknown (**Figure 3-3**B).

Compared to xanthommatin, the biogenesis of ommins is poorly understood. Early studies on radioactive incorporation of methionine and cysteine demonstrated that these two amino acids provide sulphur for the phenothiazine ring (**Figure 3-3**B) (Linzen, 1974), but at which step and how this sulphur addition occurs is not known (Linzen, 1974; Osanai-Futahashi *et al.*, 2012). Ommidins, which also seem to contain sulphur, might use the same pathway as ommins (Linzen, 1974). Recent studies on the silkworm *B. mori* and its eggs suggested that *cardinal*, a heme-peroxidase-encoding gene, is involved in the final steps of both ommatin and ommin synthesis (**Figure 3-3**B) (Harris *et al.*, 2011; Osanai-Futahashi *et al.*, 2016; Zhang *et al.*, 2017b). Since sulphur-containing ommochromes are found in a variety of animals and tissues (Linzen, 1974; Evans, Acosta, & Bolstad, 2015), further studies of their synthesis will be essential to a better understanding of the biological role of these animal chromes.

Several by-products of the tryptophan oxidation pathway have been described and might be of importance when considering the tryptophan-detoxification hypothesis. On the one hand, kynureninases can form anthranilic (or 3-hydroxyanthranilic) acid from kynurenine (or 3-hydroxykynurenine, respectively) (**Figure 3-3**B). Anthranilic acids could be used as end-catabolites, rather than intermediates, of tryptophan catabolism in the absence of the glutarate/nicotinamide biosynthesis pathway (Linzen, 1974). In *B. mori*, the kynureninase mutant *rb* accumulates 3-hydroxykynurenine and has a red body, suggesting that diverting the tryptophan flux towards either the 3-hydroxykynurenine or the anthranilic acid pathway can alter ommochrome production (Meng *et al.*, 2009). On the other hand, kynurenine and 3-hydroxykynurenine can be transaminated to form kynurenic acid and xanthurenic acid, respectively (**Figure 3-3**B) (Li & Li, 1997). In the crab spider *Thomisus onustus* and the butterfly *Junonia coenia*, the coloured intermediates 3-hydroxykynurenine and xanthurenic acid, respectively, may be directly responsible for integument colour patterns without involving ommochrome production (Daniels & Reed, 2012; Llandres *et al.*, 2013).

Enzymes of the Tryptophan→Ommochrome pathway

Enzymes of the tryptophan catabolism pathway have been known for several decades, mainly from the availability of two *D. melanogaster* mutants: *vermilion* and *cinnabar* (Linzen, 1974; Summers *et al.*, 1982). These enzymes and their genes have since been characterised in many

different insects (**Table 3-2**), and also in planarians (Stubenhaus *et al.*, 2016; He *et al.*, 2017), implying their conservation in protostomes (**Figure 3-1**). Recent years have seen the publication of crystal structures for these enzymes, including from *D. melanogaster*. Below, we detail the involvement of each enzyme in the formation of ommochromes from tryptophan. The precise description of these enzymatic steps, together with crystallographic data, should help in the design of new specific inhibitors and, therefore, in clarifying the roles of these enzymes, particularly in non-model organisms.

Table 3-2. Enzymes involved in ommochrome biosynthesis and their related mutants in insects.

Enzyme	Cofactor	Mutants	Crystallographic data	Inhibitors	References
Tryptophan 2,3-dioxygenase (TDO)	Heme	*vermilion* (*Drosophila melanogaster*), *green* (*Musca domestica*), *yellowish* (*Lucilia cuprina*), *ivory* (*Sarcophaga barbata*), *a* (*Ephestia kuehniella*), *snow* (*Apis mellifera*) and *vermilion*^{white} (*Tribolium castaneum*)	For *D. melanogaster*	LM10 (competitive inhibitor)	(Summers *et al.*, 1982; Lorenzen *et al.*, 2002; Huang *et al.*, 2013)
Kynurenine formamidase (KFase)	n/a	n/a[a]	For *D. melanogaster*	Diazoxon, PMSF[b] and diazinon	(Moore & Sullivan, 1978; Summers *et al.*, 1982; Han, Robinson, & Li, 2012)
Kynurenine 3-monooxygenase (KMO)	FAD[c]	*cinnabar* (*D. melanogaster*), *ocra* (*M. domestica*), *yellow* (*L. cuprina*), *w-1* (*Bombyx mori*), *kh*^{w} *(Aedes aegypti*) and *ivory* (*A. mellifera*)	No data for ommochrome-producing animals	See Smith *et al.* (2016)	(Summers *et al.*, 1982; Cornel *et al.*, 1997; Smith, Jamie, & Guillemin, 2016)
Phenoxazone synthase (PHS)?	n/a	*chartreuse*? (*A. mellifera*) and *alb*? (*E. kuehniella*)	n/a	n/a	(Phillips & Forrest, 1970; Phillips, Forrest, & Kulkarni, 1973; Yamamoto *et al.*, 1976; Rasgon & Scott, 2004)
Heme peroxidase[d]	Heme	*cardinal* (*D. melanogaster*, *B. mori* and *T. castaneum*)	n/a	n/a	(Howells, Summers, & Ryall, 1977; Harris *et al.*, 2011; Osanai-Futahashi *et al.*, 2016)
Xanthommatin reductase?	n/a	n/a	n/a	n/a	(Santoro & Parisi, 1987)

[a] Reduced activity of kynurenine formamidase in *vermilion*.

[b] Phenylmethylsulfonyl fluoride.

[c] Flavin adenine dinucleotide.

[d] Proposed to act as a PHS to form xanthommatin and ommins.

The first step of tryptophan catabolism is catalysed by the *vermilion*-encoded enzyme, tryptophan 2,3-dioxygenase (TDO or tryptophan pyrrolase; EC 1.13.11.11; **Table 3-2**). TDO accelerates the opening of the indole ring, the rate-limiting step of tryptophan catabolism (**Figure 3-3**B). Although this enzyme was first identified in the fruit fly several decades ago, its crystal structure has only been reported recently (Huang *et al.*, 2013). TDO is a tetrameric complex containing a heme that is important for tryptophan oxidation (Capece *et al.*, 2010). Three highly conserved loops are required for binding the heminic cofactor and for the induced-fit mechanism involved in binding tryptophan (Huang *et al.*, 2013; Michels *et al.*, 2016). Information on conserved sequences, structures and mechanisms are of great importance in the synthesis of new inhibitors of this enzymatic step (Huang *et al.*, 2013; Michels *et al.*, 2016). Hence, crystallographic data are needed if one intends to inhibit enzymes in both non-model organisms and model organisms for which no tryptophan pathway mutants are available.

The second step leading to the formation of kynurenine can be either spontaneous or catalysed by kynurenine formamidase (KFase; EC 3.5.1.9; **Table 3-2**; **Figure 3-3**B). The absence of isolated mutants for this step in insects, and particularly in *D. melanogaster* (Moore & Sullivan, 1978), suggests that KFase is either essential or expendable. Interestingly, *N*-formylkynurenine is unstable and thus rapidly converted into kynurenine *in vitro*. Hence, KFase might not be essential, but could be necessary in specific contexts for fine tuning of the tryptophan pathway or to produce kynurenine derivatives at a higher rate. The KFase structure of *D. melanogaster* was also described recently, meaning that its *in vivo* functions can now be investigated using purpose-designed inhibitors (Han *et al.*, 2012).

The third step involves the hydroxylation of kynurenine to 3-hydroxykynurenine by kynurenine 3-monooxygenase (KMO; EC 1.14.13.9; **Table 3-2**; **Figure 3-3**B), which is encoded by *cinnabar* in *D. melanogaster*. KMO reduces its cofactor flavin adenine dinucleotide (FAD) to $FADH_2$ by oxidising dihydronicotinamide adenine dinucleotide phosphate (NADPH) (or NADH) to $NADP^+$ (or NAD^+, respectively). $FADH_2$ and kynurenine are then both oxidised by O_2, leading to the recovery of FAD and the formation of 3-hydroxykynurenine (Smith *et al.*, 2016). Interestingly, KMO localises at the outer mitochondrial membrane, which links this enzyme and the ommochrome pathway to oxidative metabolism. To date, no crystal structure of any insect KMO exists; only yeast and

Pseudomonas KMO have been successfully purified and crystallised (Amaral *et al.*, 2013; Smith *et al.*, 2016; Gao *et al.*, 2018). New KMO inhibitors based on crystallographic data could provide tools to study the ommochrome pathway in model and non-model organisms. However, further studies on interspecific differences among KMOs are required because KMO inhibitors produce different effects in different species (Smith *et al.*, 2016).

There remains strong debate about the involvement of a phenoxazone synthase (PHS; EC 1.10.3.4; **Table 3-2**) in the ommochrome pathway. If present, PHS would catalyse the condensation of two 3-hydroxykynurenines into xanthommatin (**Figure 3-3**B). Some reports showed that ommochrome-containing organelles possess both enzymatic and non-enzymatic activity leading to xanthommatin formation (Phillips & Forrest, 1970; Phillips *et al.*, 1973; Yamamoto *et al.*, 1976; Rasgon & Scott, 2004). However, recent studies on mosquitoes suggested that PHS is unlikely to function in this pathway (Li *et al.*, 1999). The situation is even more complex because other enzymes (laccase, catalase or tyrosinase) are also able to form the phenoxazone ring from *o*-aminophenol compounds, such as xanthurenic acid (Le Roes-Hill *et al.*, 2009). Several studies on *D. melanogaster*, *B. mori* and *T. castaneum* have linked the *cardinal* mutation to a loss of ommochromes and an accumulation of 3-hydroxykynurenine in eyes (Howells *et al.*, 1977; Harris *et al.*, 2011; Osanai-Futahashi *et al.*, 2016). They all suggest that Cardinal, a heme peroxydase, is the PHS catalysing the final formation of ommatins and ommins (**Table 3-2**; **Figure 3-3**B). Interestingly, in *D. melanogaster* S9 cells, an overexpressed and tagged version of Cardinal was located to intracellular vesicles, which is coherent with ommochrome formation occurring in a specific cell compartment, the ommochromasome (Harris *et al.*, 2011). However, Cardinal acting as a PHS has been recently refuted in the hemipteran *Nilaparvata lugens*. We still lack sufficient biochemical data on the Cardinal enzyme to clarify its exact role in ommochrome biosynthesis. We hypothesise that Cardinal, as a redox enzyme, might be involved in the oxidative condensation of 3-hydroxykynurenine to xanthommatin. However, this catalysed step might complement other ways to produce xanthommatin (e.g. spontaneous oxidation, tyrosinase reaction, etc.) and might not act through the PHS reaction mechanism.

Only a few studies have investigated the formation of H_2-xanthommatin by reduction of xanthommatin. Xanthommatin was first proposed to be a cofactor of a soluble cytochrome c reductase that oxidised NADH (Harano & Chino, 1971). Reducing xanthommatin to H_2-

xanthommatin would thus lead to the oxidation of NADH to NAD^+. A mitochondrial process oxidising H_2-xanthommatin with O_2 was proposed to regenerate xanthommatin. Similarly, xanthommatin was proposed to be a cofactor of xanthine dehydrogenase in the biogenesis of pterins in fruit fly eyes (Parisi, Carfagna, & D'Amora, 1976a, 1976b). Finally, Santoro & Parisi suggested that H_2-xanthommatin was formed by the action of a specific enzyme, called xanthommatin reductase, that used NADH as a cofactor (Santoro & Parisi, 1987); in this case, pterins were involved as potent inhibitors of this redox reaction. To date, xanthommatin reductase has not been purified nor its gene identified. Its involvement in ommochrome formation remains therefore highly speculative.

Enzymes of the ommochrome pathway differ in their cellular and tissue localisation (Sullivan, Grillo, & Kitos, 1974). TDO and KFase are both present in the soluble fraction of cells, so they may localise to the cytosol. On the contrary, KMO is anchored to the outer membrane of mitochondria. If both PHS and xanthommatin reductase exist, they should be associated with ommochrome organelles. Thus, ommochrome biogenesis is a process that involves enzymes in various cell compartments, implying the involvement of transporters to deliver their substrates through membranes. Furthermore, not all steps of the ommochrome pathway occur in pigmented cells; it is known that precursors such as kynurenine and 3-hydroxykynurenine are taken up by ommochrome-producing cells from the haemolymph in insects (Linzen, 1974; Reed *et al.*, 2008). These precursors are produced by other organs containing TDO, KFase or KMO, such as the fat body, and are subsequently transported to target tissues. A comprehensive understanding of ommochrome biosynthesis thus requires a broad vision of cell and tissue processes.

Putative cross-talk between ommochromes and other chromes

Since it was discovered that the *white* mutant of *D. melanogaster* lacked two different eye zoochromes, ommochromes and pterins, it has been hypothesised that biochemical cross-talk exists between chromes (Summers *et al.*, 1982). At that time, when the function of the *white* gene was unknown, it was believed that either ommochromes or pterins were needed for the synthesis of the other class of chromes. Even though the hypothesis that both chromes shared a biochemical relationship was later ruled out by *white* encoding a transmembrane transporter and not a common enzyme, some studies have continued to focus on chemical interrelationships between ommochromes and three other insect chromes: pterins, melanins

and papiliochromes. In the following, we do not discuss the gene regulation and developmental patterns that can affect these chromogenic pathways because such signalling cross-talk is not directly related to the biochemistry of chromes [but see (Nijhout, 2010; Fujiwara & Nishikawa, 2016; Nadeau, 2016; Sekimura & Nijhout, 2017; Zhang, Mazo-Vargas, & Reed, 2017c)].

The red pterins are associated with ommochromes in *D. melanogaster* eyes (Shoup, 1966). Thus, mutants lacking pterins display brown eyes that only contain xanthommatin. Both pterin and ommochrome pathways can occur within the same cells; since they involve redox steps, ommochromes and their precursors were proposed to act as electron donors/acceptors for pterin biogenesis, and *vice versa* (Ziegler, 1961; Ziegler & Harmsen, 1970). To date, no metabolic connections between those pathways have been demonstrated *in vivo*. Changes in both chrome levels in some mutants are rather interpreted as a common defect in cell trafficking (Summers *et al.*, 1982; Reaume, Knecht, & Chovnick, 1991; Lloyd *et al.*, 1998).

The melanin pathway can be linked to the last step of xanthommatin biogenesis. As previously mentioned, tyrosinase, a key enzyme in the biosynthesis of melanins, is able to produce *in vitro* the phenoxazone ring, as well as xanthommatin, from *o*-aminophenols (Vogliardi *et al.*, 2004; Le Roes-Hill *et al.*, 2009). In the same way, dopaquinone, the product of tyrosinase, can convert two 3-hydroxykynurenine into xanthommatin; dopaquinone could then be converted back to 3,4-dihydroxyphenylalanine (DOPA) by tyrosinase and would thus act as a catalyst in the biogenesis of xanthommatin, at least *in vitro* (Needham, 1974). As for pterins, this chemical interrelationship between melanins and ommochromes has never been properly investigated *in vivo*.

Papiliochromes are a class of chromes only found in the wing of papilionid butterflies (Umebachi, 1985). Papiliochromes are formed from three amino acids: alanine, tyrosine and tryptophan (**Figure 3-3**B) (Koch, Behnecke, & ffrench-Constant, 2000; Nishikawa *et al.*, 2013)). These chromogenic amino acids tightly link papiliochromes to other chromes, including ommochromes and melanins. The enzyme catalysing the formation of papiliochrome II from kynurenine and *N*-β-alanyldopamine was purified some years ago (Yago, 1989). However, to date, no butterfly has been described to possess both

papiliochromes and ommochromes. Thus, a direct and *in vivo* relationship between these chromogenic pathways seems hard to address. Nonetheless, these observations indicate that producing ommochromes is not the only route to catabolise free tryptophan in insects; papiliochromes might serve as tryptophan detoxifiers in insects that do not have ommochromes. Why papilionid butterflies favour papiliochromes over ommochromes is not known and deserves to be studied in more detail.

Ommochrome reactivity

Once produced, ommochromes are not chemically inert, they can be further modified by interaction with radiation (visible light in particular) and through redox reactions. The reduction of xanthommatin to H_2-xanthommatin has been demonstrated to be of biological importance in dragonflies since it provides the chemical basis of colour change during sexual maturation (Futahashi *et al.*, 2012). It is noteworthy that kynurenines and their derivatives are also very reactive upon light exposure, in redox reactions and during radical scavenging. This field has already been extensively reviewed elsewhere (Giles *et al.*, 2003; Tsentalovich, Snytnikova, & Sagdeev, 2008; Colín-González, Maldonado, & Santamaría, 2013; Avila, Friguet, & Silva, 2015).

The photochemistry of ommochromes and of some of their synthesised derivatives was extensively in the 1980s [e.g. (Bolognese & Liberatore, 1988)]. These photochemical studies provided much of what we know about how ommochromes react to visible light. Since ommochromes are weakly soluble and can be extracted in only small amounts, Bolognese and coworkers examined the photostability of related compounds (**Figure 3-4**A, B). They showed that, in acidified methanol (a common extraction solvent for ommochromes), a reversible photoreduction process can lead to the formation of H_2-xanthommatin from xanthommatin (without any reducing agents and in the presence of O_2) (Bolognese *et al.*, 1988a; Bolognese, Liberatore, & Scherillo, 1988c). Photo-induced methylation (from the solvent) of the phenoxazone ring took place in parallel with this photoreduction (**Figure 3-4**A) (Bolognese *et al.*, 1988c). Methylations and acetylations are common modifications of biomolecules within the cell (Su, Wellen, & Rabinowitz, 2016) and they might therefore also affect ommochromes after their photoactivation. These reactions might explain the diversity of ommochrome-like spectra reported in some studies (Riou & Christidès, 2010; Llandres *et al.*, 2013).

Another unexpected result is the ease with which the phenoxazone ring could be opened upon irradiation, either by methylation in pure methanol or by water addition in acidified solvents (**Figure 3-4**B) (Bolognese *et al.*, 1988c; Bolognese, Liberatore, & Scherillo, 1988d; Bolognese & Liberatore, 1988). Compared to photoreduction and photoaddition, the photo-induced opening of the phenoxazone system was irreversible and led to new and stable ommochrome-related compounds. Interestingly, some ommochrome-like compounds could not undergo phenoxazone opening in methanol upon irradiation; it was only possible for molecules either with a pyrido[a] ring or with a methylated ketone group (Bolognese *et al.*, 1988d). This result means that rhodommatin and ommatin D might well fall into this class of openable ommochromes in methanol (**Figure 3-3**), whereas xanthommatin and H_2-xantommatin should not suffer from phenoxazone opening and subsequent conformational change in this solvent. However, in an acidified aqueous solvent, this opening occurred by photoaddition of water even with a complete ketone group (Bolognese & Liberatore, 1988). The open phenoxazone was highly unstable and could be hydroxylated (**Figure 3-4**B) before closing by methylation, acetylation or by reacting with other ommochromes in a redox reaction. Since ommochromes are deposited in an aqueous environment and are irradiated by sunlight, it is not improbable that natural ommochromes undergo multiple opening and closing episodes after conformational change, which would lead to a high diversity of ommochromes within the same cell. The large number of unidentified ommochrome-related compounds might be the result of these processes (Vogliardi *et al.*, 2004; Riou & Christidès, 2010).

Ommochromes are not only photosensitive, they can also perform redox reactions both *in vivo* and *in vitro*, as demonstrated by the colour shift of xanthommatin reduction to H_2-xanthommatin in dragonflies (Futahashi *et al.*, 2012). This bathochromic change (from short wavelengths to longer ones) upon reduction is uncommon in zoochromes (Needham, 1974). It occurs because the electronic delocalisation of the phenoxazine chromophore is increased in H_2-xanthommatin, leading to greater stabilisation by resonance of the oxonium ion (O_3^+) (Schäfer & Geyer, 1972). Recent studies suggested that these redox and related antiradical behaviours allow phenoxazine-based compounds to buffer oxidative stress (Romero & Martínez, 2015; Shah, Margison, & Pratt, 2017; Farmer *et al.*, 2017). The theoretical basis of this putative biological role was modelled using computational and quantum chemistry, as well as in biological assays. Engineers working in the field of organic matter preservation

acknowledge that phenoxazine-based compounds are one of the best radical-trapping antioxidants (Farmer *et al.*, 2017). *In vivo*, phenoxazines and phenothiazines were shown to be the most potent inhibitors of autoxidation and ferroptosis (iron-dependent oxidative stress) by trapping lipid radicals, thus breaking the propagation mechanism (Shah *et al.*, 2017). Interestingly, this antiradical property was directly linked to the N–H bond of phenoxazine/phenothiazine rings (**Figure 3-4**C) (Farmer *et al.*, 2017), meaning that only reduced ommochromes could act as potent antiradicals and antioxidants in cells. This result is consistent with *in silico* measurements of hydrogen-donor capacities of ommochromes (**Figure 3-4**C) (Romero & Martínez, 2015; Zhuravlev *et al.*, 2016). For xanthommatin, the three best H-donor sites localise to the aspartyl chain while the two best ones of ommatin D are within the pyrido[a]phenoxazone system (**Figure 3-4**C). This probably arises from the reduced state of ommatin D, which extends its electronic delocalisation. Interestingly, the antiradical power of the phenoxazone N–H (**Figure 3-4**C) may be partially inhibited in ommatin D by hydrogen bonds with the two carbonyl groups, making it less effective than the pyrido[a] N–H (**Figure 3-4**C). Using ommochrome-related compounds, another study proposed a chemical explanation for this antiradical property of phenoxazone N–H (Farmer *et al.*, 2017). First, stabilisation by resonance of the phenoxazine system decreases the N–H bond dissociation enthalpy. Then, a low increase in entropy during electronic delocalisation in this same phenoxazine system further decreases the energy barrier of N–H bond dissociation. Finally, electron-donating side-chains could reinforce electronic delocalisation (**Figure 3-4**C). Those three properties are maximised in ommatin D compared to xanthommatin, which explains why it is a better antiradical ommochrome. However, for ommatin D, hydrogen bonds increase N–H dissociation enthalpy; hence, it is not the best H-donor site in this molecule (**Figure 3-4**C). To assess whether ommochromes could act as antiradical compounds *in vivo*, free energies of reactions involving ommochromes and four relevant radicals were calculated *in silico* (Romero & Martínez, 2015). Ommatin D could react spontaneously and liberate more energy with the four different radicals compared to xanthommatin (**Figure 3-4**C) (Romero & Martínez, 2015). These results are in agreement with the differences in H-donor capacities of these two ommochromes. Thus, reduced ommochromes, which also are the reddest ones, may act as better antiradical compounds *in vivo* than their oxidised forms (Romero & Martínez, 2015; Zhuravlev *et al.*, 2016). To date, the ratio of these two redox forms within ommochrome-containing organelles is not known.

Ommochromes within the Cell: the Ommochromasome Life Cycle

Their chemical properties and low solubility in neutral aqueous solvents mean that ommochromes are deposited within intracellular membrane-bound organelles (Linzen, 1974). These organelles were first called 'ommochrome granules'. In an attempt to unify a science of chromes (chromatology), Needham proposed the name 'ommochromasome' in analogy with melanosomes, pterinosomes, and more generally chromasomes. (Needham, 1974) As we will discuss in Sections "Ommochrome biogenesis: the tryptophan oxidation pathway" and "Enzymes of the Tryptophan→Ommochrome pathway", the biogenesis of ommochrome-containing organelles is too complex to be summarised by the term 'ommochrome granule', which implies a rather static view of these organelles. In the following, we therefore adopt the term ommochromasomes. Furthermore, 'granule' is typically used to designate a membrane-less aggregate of molecules [e.g. melanin aggregates of cephalopod inks (Sun *et al.*, 2017b)] whereas known ommochrome organelles are membrane-bound. It is not known whether ommochromes are aggregated or fully soluble in this environment. Thus, to avoid confusion, we only use the term 'ommochromasome'.

Throughout this section, we compare ommochromasomes of invertebrates with the related and well-characterised melanosomes of vertebrates. Melanosomes are the melanin-containing organelles that mediate hair, skin and eye pigmentation, among others (Borovanský & Riley, 2011). Melanosomes have been widely studied for their role in skin colouration (Jablonski & Chaplin, 2017), as well as in melanomas (Dobry & Fisher, 2018) and various human pigmentation disorders (Yamaguchi & Hearing, 2014). The ultrastructure, biochemistry, cell biology and physiology of melanosomes are now relatively well understood (Borovanský & Riley, 2011), which makes these organelles an interesting subject for comparison with ommochromasomes. The genetics of ommochromasomes enlightened in the past the biology of melanosomes and related organelles (Lloyd *et al.*, 1998), in return, the melanosome field can provide important insights in understanding ommochromasomes.

Methods for studying ommochromasomes

Ommochromasomes were first identified in *D. melanogaster* and its eye-colour mutants (Ziegler-Günder & Jaenicke, 1959; Ziegler, 1960). Subsequently, ommochromasomes were described in all known ommochrome-producing groups, i.e. insects, spiders, crustaceans and

cephalopods (Mirow, 1972; Needham, 1974; Insausti & Casas, 2008). However, relative to ommochromes, ommochromasomes have been poorly studied, despite this being notted by Linzen more than forty years ago (Linzen, 1974). While several attempts to describe their ultrastructure, content and functions have been performed (**Figure 3-2**B), our knowledge of these specialised organelles does not match yet those of melanosomes (Raposo & Marks, 2007).

Ommochromasomes range from 200 nm to more than 1 µm in some species (Shoup, 1966; Linzen, 1974; Kayser, 1985; Stark & Sapp, 1988) and thus their structure is best studied using electron microscopy (EM). Ultrastructural studies allowing direct observation of ommochromasomes in tissues have been mainly performed using conventional EM approaches on chemically fixed and resin-embedded specimens. This *in situ* technique allowed the description, at least in part, of both ommochromasome anabolism and catabolism during morphological colour changes in crab spiders (Insausti & Casas, 2008, 2009). Recently, scanning EM allowed visualisation of the filamentous network that tethers ommochromasomes together in squid chromatophores, as well as their shrinkage upon ommochrome extraction (Williams *et al.*, 2016). Unfortunately, preparation techniques for EM often cause artifacts due to the fixation and cutting processes. It has been reported several times that ommochromes can be readily extracted and lost during fixation (Kolb, 1977; Cölln, Hedemann, & Ojijo, 1981; Stark & Sapp, 1988; Insausti & Casas, 2008). Furthermore, ommochromasome rigidity can lead to 'holes' in their content during the cutting process (Insausti & Casas, 2008). Modified EM protocols can be used to achieve better results, such as using faster fixation techniques (Prum, Cole, & Torres, 2004), reduced ethanol concentration (Mackenzie *et al.*, 2000) and avoiding glutaraldehyde that readily extracts ommochromes (Kolb, 1977). Interestingly, new EM methods like cryo-EM and particularly the development of high-pressure freezing (HPF), have not yet been applied to the study of ommochromasomes. These techniques allow a far better conservation of organelle ultrastructure (Studer, Humbel, & Chiquet, 2008), which led to major advances in the understanding of melanosomes when coupled with electron tomography or correlative light and electron microscopy (CLEM) (Hurbain *et al.*, 2008; Delevoye *et al.*, 2016). We anticipate that applying such techniques to ommochromasomes should also lead to major insights in their functional characterisation.

Purifying organelles is necessary when one seeks to understand how they work and what their specific components are. Early studies on ommochromasome-associated enzymes led to suggestions that mitochondrial, peroxisomal and lysosomal enzymes were present within ommochromasomes (Ziegler-Günder & Jaenicke, 1959). These discoveries were later refuted on the grounds that preparations were not devoid of other organelle types (Linzen, 1974). A specific purification method for ommochromasomes was thus needed to assess their exact composition. This was achieved for insect ommochromasomes more than 30 years ago (Cölln *et al.*, 1981). However, interest in ommochromes declined in the 1980s (**Figure 3-2**), meaning that this purification protocol has remained unused. Yet, this technique can be highly efficient; it represents a finely tuned protocol that minimises ommochrome extraction, ommochromasome aggregation and membrane contamination. By taking advantage of the high relative density of ommochromasomes (ranging from 1.32 to 1.38), ultracentrifugation steps on gradients of sucrose and metrizamide (now replaced by iohexol, also known as histodenz or nycodenz) allows removal of other membrane-bound organelles (Cölln *et al.*, 1981; Kayser, 1985). This purification protocol produces ommochromasome fractions that are suitable for performing cryo-EM, thus enabling characterisation of ommochromasome ultrastructure in detail. Other ultracentrifugation methods used to extract ommochromasomes from other tissues and organisms tend to be based on sucrose-only gradients or slow centrifugation, and might either lead to contaminated preparations (Sawada *et al.*, 1990; Sawada, 1994) and/or be only suitable for ommochromasomes of lower relative density, for example in squid (DiBona *et al.*, 2016).

Purifying ommochromasomes is not the only way to analyse their contents and their intraluminal environment. *In situ* spectroscopic studies using X-ray microprobes on ommatidia and single ommochromasomes were successfully carried out in mayflies, house crickets, migratory locusts, fruit flies and honeybees (Lhonoré, Anglo, & Marcaillou, 1973; Burovina *et al.*, 1978; Bouthier & Lhonoré, 1984; Gribakin *et al.*, 1987; Ukhanov, 1991). These studies demonstrated that ommochromasomes sequester K, Ca, Mg and possibly S, and could hence act as cationic reservoirs in the cell. Ca^{2+} is known to be required in ommochromasome extracts to stabilise them (Cölln *et al.*, 1981). It is not known whether ommochromes can sequester cations themselves; however, pirenoxine, a xanthommatin-derived drug used to treat cataracts, was shown to bind calcium (Liao *et al.*, 2011). Because ommochromes and pirenoxine share similar structures and chemical functions, ommochromes

may also bind calcium, which could explain ommochromasome stabilisation by Ca^{2+}. X-ray fluorescence studies using Synchrotron radiation have recently been applied to various organelles in order to map trace elements at the sub-100 nm scale (Gorniak *et al.*, 2014; Kashiv *et al.*, 2016; Zhu *et al.*, 2017). These studies revealed populations of melanosomes with different patterns of elemental heterogeneity (Gorniak *et al.*, 2014). Such techniques should also be suitable for ommochromasomes and would allow us to unravel their internal chemistry. In particular, their chemistry might change during ommochrome production as they may require calcium and other ions for ommochrome stabilisation and function.

Finally, to our knowledge, only two studies have succeeded in performing immuno-EM on ommochromasomes. Using this method, two proteins were localised to the ommochromasome membrane of the fruit fly: the transporter White, which is involved in ommochrome biosynthesis (Mackenzie *et al.*, 2000), and the small GTPase Ras-associated binding (RAB)-related protein 1 (RAB-RP1)/Lightoid, which is implied in ommochromasome biogenesis (Fujikawa *et al.*, 2002). Expanding immuno-EM to other ommochrome-related proteins, especially putative PHS, should help to decipher their role in the ommochrome pathway by clarifying their localisation to ommochromasomes.

Ommochromasome structure and composition

Ommochromasomes are sub-micrometric spherical organelles delimited by a single membrane (Langer, 1975). They can be found in the cytoplasm of primary and secondary pigment cells of ommatidia, in arthropod and cephalopod epidermis, and in butterfly brain and eggs (Shoup, 1966; Elofsson & Hallberg, 1973; Veron, O'Farrell, & Dixon, 1974; Langer, 1975; Sawada *et al.*, 1990, 2000; Insausti & Casas, 2008). Although ommochromes, especially ommatin D and rhodommatin, are present in butterfly wings, the existence of ommochromasomes in those tissues has never been investigated. Unravelling the subcellular localisation of these water-soluble ommochromes in butterfly scales will be of importance for a better understanding of colour patterning (Nijhout, 2010).

Compared to pterinosomes (pterin granules also present in pigment cells of insect eyes) and maturing melanosomes, the internal structure of ommochromasomes is often undistinguishable because of the electron-dense and osmiophilic material they contain. This material is thought to be made of precursors and/or ommochromes that are associated with

ommochrome-binding proteins (OBPs). In crab spiders, during colour change different stages of ommochromasomes can be identified on the basis of their osmiophilic properties and the presence of intraluminal vacuoles of varying sizes and electron-density (Insausti & Casas, 2008, 2009). It is not known whether these vacuoles are membrane-bound vesicles. If this is the case, they would be similar to the intraluminal vesicles of pre-melanosomes in stage I and II upon which melanin-nucleating fibrils form (Hurbain *et al.*, 2008). Interestingly, similar fibrils have been observed in pterinosomes (Shoup, 1966; Fuge, 1967; Hearl & Bruce Jacobson, 1984).

The most recent studies on ommochromasome ultrastructure were performed in squid [e.g. (Williams *et al.*, 2016)]. Ommochromasomes are important in these species because they provide one of the colouration systems facilitating their extraordinary and rapid colour-changing ability (Van Den Branden & Decleir, 1976; Messenger, 2001; Sutherland *et al.*, 2008). The shape, ommochrome content and protein composition, particularly of reflectins, of ommochromasomes controlled the refractive index of squid ommochromasomes (Deravi *et al.*, 2014; Williams *et al.*, 2016; Dinneen *et al.*, 2016). Ommochromasomes are thus not only light-absorbing granules but also very efficient and complex nanostructures that participate in modifying the optical properties of squid epidermis. These light scattering and absorption functions are based on three main characteristics. First, the tethering of ommochromasomes within saccules by a fibrous network allows expansion and contraction of the colouration of a single chromatophore (Deravi *et al.*, 2014). Second, the high refractive index of reflectins and, to some extent, of ommochromes efficiently scatters light (Dinneen *et al.*, 2016). Finally, the apparent contribution of both ommochromes and proteins in maintaining the spherical shape and diameter of ommochromasomes helps them to act as photonic nanostructures (Williams *et al.*, 2016). To date, it is not known whether the same conclusions can be drawn for other ommochromasome-producing animals because reflectins and neurologically controlled ommochromasomes saccules have only been described in cephalopods (Messenger, 2001; Guan *et al.*, 2017).

The origin of the ommochromasome, a lysosome-related organelle

As for melanosomes (Seiji *et al.*, 1963), the question of ommochromasome origins was a puzzling problem. Mitochondrial enzymatic activities of ommochromasome fractions (now known to be artefacts) led researchers to suggest that ommochromasomes originated from

mitochondria (Ziegler-Günder & Jaenicke, 1959); an hypothesis that was also proposed for melanosomes (du Buy, Showacre, & Hesselbach, 1963). Ultrastructural studies, however, suggested that ommochromes were first deposited within the endoplasmic reticulum (ER) (Fuge, 1967) or within the Golgi apparatus (Shoup, 1966); again, similar hypotheses were suggested for melanosomes (Wellings & Siegel, 1959). In the case of ommochromasomes, these conclusions were mainly drawn from the presence within the ER and Golgi apparatus of highly electron-dense granule-like deposits. However, in absence of biochemical evidence, it is impossible to determine the chemical nature of a deposit based solely on its electron-density. Thus, the origin of ommochromasomes remained speculative until a few decades ago.

Fruit fly mutants provided the answer. Some eye-colour mutants of *D. melanogaste*r are part of the so-called 'granule group' (**Table 3-3**) because they lack both ommochromasomes and pterinosomes. Sequence homologies and functional analogies demonstrated that granule group genes encoded orthologues of intracellular trafficking proteins (**Table 3-3**), which are involved in vacuole formation (the equivalent of lysosomes in yeast) and in the biogenesis of lysosome-related organelles (LROs, comprising lysosomes, melanosomes, lytic granules, etc.) in vertebrates (Raposo & Marks, 2007). Thus, ommochromasomes were proposed to be part of this LRO family, a subset of organelles with very different shapes and structures, but which share features with lysosomes such as an acidic lumen and lysosomal proteins (Schraermeyer & Dohms, 1993; Lloyd *et al.*, 1998). However, quantification of the ommochromasome pH has never been performed, nor has the detection of LRO markers such as the integral membrane protein lysosome-associated membrane protein 1 (LAMP-1) (Zhou *et al.*, 1993). All LROs receive materials from endosomes and most share a direct endosomal origin (Marks, Heijnen, & Raposo, 2013). Hence, ommochromasomes could primarily arise from endosomes and subsequently receive material from the ER and the Golgi apparatus (**Figure 3-5**). This is further supported by the many orthologues of known LRO biogenesis-related proteins that were recently assigned to fruit fly eye-colour mutants (see **Table 3-3** and references therein).

Table 3-3. Orthologues and functions of proteins encoded by ommochrome-related genes of the granule group in *Drosophila melanogaster*.

Fruit fly mutant	Orthologue protein[a]	References	Comments[b]
carmine	μ3	(Mullins *et al.*, 1999)	Subunits of the AP-3 complex that controls a vesicular sorting pathway
garnet	δ3	(Lloyd *et al.*, 1999)	
orange	σ3	(Mullins, Hartnell, & Bonifacino, 2000)	
ruby	β3	(Ooi *et al.*, 1997; Kretzschmar *et al.*, 2000)	
carnation	VPS33a	(Sevrioukov *et al.*, 1999; Suzuki *et al.*, 2003)	Subunits of the HOPS and CORVET complexes that control an endosomal and a Golgi-derived trafficking pathway to lysosomes and LROs
deep orange	VPS18p	(Shestopal *et al.*, 1997; Sevrioukov *et al.*, 1999)	
light	VPS41p	(Warner *et al.*, 1998)	
maroon	VPS16a	(Grant *et al.*, 2016)	
lightoid	RAB32/38 (RAB-RP1)	(Fujikawa *et al.*, 2002; Ma *et al.*, 2004)	Localizes at the limiting membrane of lysosomes and ommochromasomes, and regulates an AP-3-independent vesicular pathway
claret	RAB32 GEF?		Putative activator of RAB32/38
blos1	BLOC1S1	(Cheli *et al.*, 2010)	Subunit of BLOC-1
pink	HPS5	(Falcón-Pérez *et al.*, 2007)	Subunit of BLOC-2 that regulates eye pigmentation
dHPS4	HPS4	(Harris *et al.*, 2011)	Subunit of BLOC-3
mauve	CHS1/LYST	(Rahman *et al.*, 2012)	Prevents homotypic fusion of lysosomes and LROs
purpleoid	n/a		n/a

[a] BLOC1S1, biogenesis of lysosome-related organelle complex subunit 1. CHS1, Chediak-Higashi syndrome. GEF, guanine-exchange factor. HPS, Hermansky-Pudlak syndrome. LYST, lysosomal trafficking regulator. RAB, Ras-associated binding protein. RAB-RP1, RAB-related protein 1. VPS, vacuolar protein sorting-associated protein.

[b] AP, adaptor protein. BLOC, biogenesis of lysosome-related organelle complex. CORVET, class C core vacuole/endosome tethering. HOPS, homotypic fusion and protein sorting. LRO, lysosome-related organelle. RAB, Ras-associated binding protein.

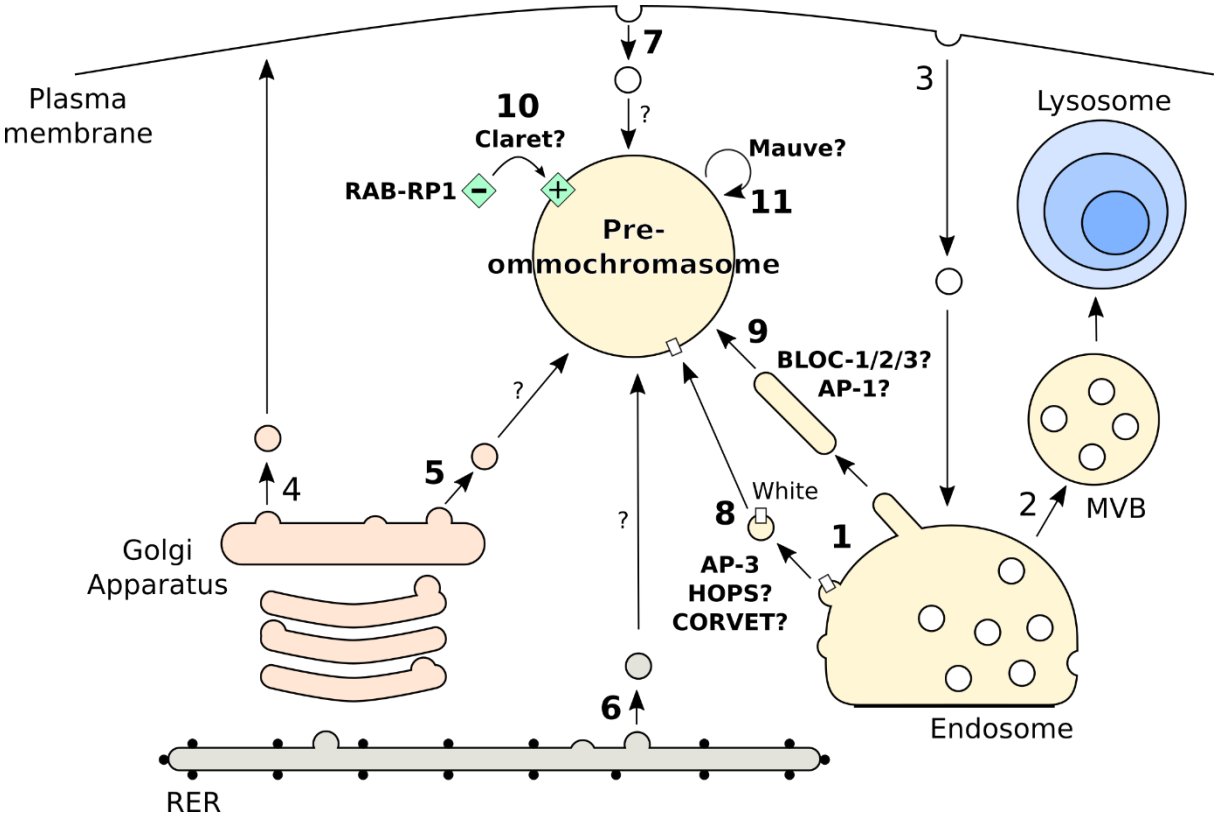

Figure 3-5. Putative scheme of ommochromasome biogenesis.
Ommochromasomes, the organelles that produce and store ommochromes, are part of the lysosome-related organelle (LRO) family. LROs are derived from endosomes (1), which give also rise to multivesicular bodies (MVBs) and thence lysosomes (2). Endosomes receive material from the plasma membrane (endocytic pathway, 3) and the Golgi apparatus (link not shown). The latter can also directly target carriers to the plasma membrane (secretory pathway, 4) or to LROs (5). The rough endoplasmic reticulum (RER) is often associated with maturing ommochromasomes, suggesting that it can also participate in their biogenesis (6). The plasma membrane might also be directly involved in ommochromasome formation (7). The ommochrome precursor transporter White is the only protein known to travel from endosomes to ommochromasomes in an AP-3-dependent pathway (8). This endosomal trafficking route might also involve the HOPS and CORVET complexes (8). An AP-3-independent pathway, which is regulated by BLOCs, AP-1 and RAB-RP1, might bring other cargoes from endosomes to ommochromasomes (9). RAB-RP1/Lightoid associates with the ommochromasome membrane and is necessary for their proper maturation. The GEF Claret potentially activates this RAB GTPase promoting its association with ommochromasomes (10). Finally, Mauve could prevent the homotypic fusion of ommochromasomes, and hence could regulate their size (11). AP, adaptor protein; BLOC, biogenesis of lysosome-related organelle complex; CORVET, class-C core vacuole/endosome tethering; GEF, guanine-nucleotide exchange factor; HOPS, homotypic fusion and protein sorting; RAB-RP1, Ras-associated binding-related protein 1.

Altogether, these results on the relationship between ommochromasomes, melanosomes and LROs lead us to propose for the first time a LRO-based model of ommochromasome biogenesis (**Figure 3-5**). This model is neither definitive nor complete and it should be tested in coming years. In the following, we detail this model, emphasising its limitations and how they could be overcome.

Ommochromasome biogenesis

As a LRO, ommochromasome precursors (pre-ommochromasomes) should be derived from an endosomal compartment (**Figure 3-5**) (Klumperman & Raposo, 2014) although no ultrastructural study has yet shown this lineage. HPF-EM, which allows very good preservation of membrane-bound organelles (Hawes *et al.*, 2007; Hurbain *et al.*, 2017), might be the technique of choice to assess this endosomal origin. Furthermore, this cellular process would be easier to study in cell cultures that are able to synthesise ommochromasomes (Li & Meinertzhagen, 1997) rather than in complex organs, such as insect eyes. Maturing pre-ommochromasomes may then receive materials (membrane, lipids, proteins, etc.) mainly from endosomal compartments, which sort proteins (or cargoes) to the plasma membrane, late endosomes, lysosomes and LROs (**Figure 3-5**) (Klumperman & Raposo, 2014). The Golgi apparatus, the ER and the plasma membrane could also provide materials to maturing ommochromasomes (**Figure 3-5**). These pathways would be controlled by a set of molecular actors, such as adaptor proteins (APs), homotypic fusion and protein sorting proteins (HOPS), class-C core vaculole/endosome tethering (CORVET), Ras-associated binding (RAB) proteins and biogenesis of lysosome-related organelles complexes (BLOCs) (**Table 3-3**; **Figure 3-5**).

During the last decade, several of these molecular actors have been specifically studied in *D. melanogaster* to understand how they regulate the endolysosomal system, and, more precisely, ommochromasome biogenesis. The RAB32/38 orthologue Lightoid/RAB-RP1, an important small GTPase involved in LRO biogenesis, localises at the ommochromasome membrane (**Table 3-3**; **Figure 3-5**) (Fujikawa *et al.*, 2002). When a negative dominant version of RAB-RP1 was overexpressed in fruit fly eyes, RAB-RP1-positive autophagosomes and multivesicular endosomes accumulated in pigment cells, suggesting that RAB-RP1 is involved in an endolysosomal pathway that possibly controls ommochromasome biogenesis (Fujikawa *et al.*, 2002). RAB-RP1 activation might be under the control of the guanine-nucleotide exchange factor (GEF) Claret, another protein of the granule group (**Table 3-3**; **Figure 3-5**) (Ma *et al.*, 2004). The latter authors also suggested that this RAB-RP1/Claret pathway is independent of AP-3, a complex first described in fruit fly eye-colour mutants and known to regulate the sorting of specific cargoes from early endosomes to LROs (**Table 3-3**). During melanosome biogenesis, BLOC-1/2/3, AP-1 and,

more interestingly, RAB32/38 define an AP-3-independent endosomal pathway, which sorts specific cargoes from endosomes to melanosomes (Sitaram & Marks, 2012). To our knowledge, no *D. melanogaster* eye-colour mutant of AP-1 has been reported, however, orthologues of AP-1 subunits exist in the fruit fly genome (Gramates *et al.*, 2017). Interestingly, AP-1 works in the endosomal trafficking pathway of developmental genes and in the formation of mucin-containing secretory granules of *D. melanogaster* (Benhra *et al.*, 2011; Burgess *et al.*, 2011; Kametaka *et al.*, 2012). Subunits of BLOC-1, the BLOC1S1 orthologue BLOS1, of BLOC-2, the HPS5 orthologue Pink, and of BLOC-3, the HPS4 orthologue dHPS4, are directly involved in eye-colour mutant phenotypes (**Table 3-3**) (Falcón-Pérez *et al.*, 2007; Cheli *et al.*, 2010; Harris *et al.*, 2011). Other subunit genes of these three complexes were found in the fruit fly genome without involvement in any natural or artificial eye-colour mutant (Falcón-Pérez *et al.*, 2007). Thus, the parallel pathways controlling LRO biogenesis, i.e. the AP-3- and the BLOCs-AP-1-RAB32/38-dependent trafficking routes, might function in a similar way during ommochromasome biosynthesis (**Figure 3-5**). It is noteworthy that the production of uric acid-containing organelles in the silkworm relies on orthologues of BLOC-1, BLOC-2 and the BLOC-3-interacting Vps9-domain ankyrin repeat protein (VARP) (Ito *et al.*, 2009; Fujii *et al.*, 2010; Wang *et al.*, 2013; Zhang *et al.*, 2017a). This further supports the idea that LROs and their related molecular complexes play a major role in colour patterning in animals.

In the endolysosomal system, trafficking pathways also define, partly at least, to which organelles specific cargoes are targeted (Luzio *et al.*, 2014). This is of great importance because lysosomes and LROs, whose respective functions are very different, often coexist within the same cell (Raposo & Marks, 2007). This is even truer in *D. melanogaster* eyes since lysosomes, ommochromasomes and pterinosomes were described in the same pigment cells (Shoup, 1966). Thus, studying ommochromasome biogenesis in the context of the fruit fly eye should help to unravel the cell trafficking pathways that ensure the concomitant biogenesis of three different LROs.

LROs are not only known to fuse with carriers of the endocytic pathway, but also with vesicles budding from the Golgi apparatus through a co-opted secretory pathway (Patwardhan *et al.*, 2017). In the *D. melanogaster* eye, this explains why the Golgi apparatus was suggested to be a precursor of ommochromasomes (Shoup, 1966)). The close proximity of ER to

ommochromasomes in several species also indicates that both organelles might directly exchange materials (Insausti & Casas, 2008); an hypothesis that still requires proper testing.

Unlike melanosomes, no specific cargo of ommochromasomes has been clearly demonstrated to be transported *via* endosomal pathways. It is a problem of growing concern for the complete understanding of ommochromasome biogenesis. Earlier studies on ommochrome precursor transport suggested two putative cargoes: White and Scarlet, two intramembrane transporters from the ATP binding cassette (ABC) family (Lloyd *et al.*, 1998). It is now well established that White specifically localises at the ommochromasome membrane (**Figure 3-5**) (Mackenzie *et al.*, 2000). The putative function of these two ABC transporters would be to incorporate ommochrome precursors (especially 3-hydroxykynurenine) from the cytosol to the ommochromasome lumen by an ATP-driven mechanism (**Figure 3-6**) (Mackenzie *et al.*, 2000). The incorporation of White and Scarlet (as well as Brown and Ok in the case of pterinosomes and uric-acid-containing organelles, respectively) within ommochromasome membranes should rely on a fusion process between a tubulo-vesicular carrier and the ommochromasome itself (**Figure 3-5**). This hypothesis is supported by a cryptic allele of the *white* gene, *enhancer of garnet* (AP-3) (Lloyd *et al.*, 2002). When this allele was mutated in *D. melanogaster*, White was not dysfunctional but rather mis-localised, suggesting that White is transported through an AP-3-dependent route to ommochromasomes (Lloyd *et al.*, 2002). Whether White travels directly from Golgi or endosomes to ommochromasomes remains to be determined. Evidence for an endosomal route comes from the fact that White tagged with a green fluorescent protein (GFP) localised to the membrane of vesicular compartments resembling endosomes in Malpighian tubules of fruit flies (Evans *et al.*, 2008). Thus, overexpressing a tagged version of White in the eye of wild-type flies, AP-3 mutants and *enhancer of garnet* mutants should provide sufficient evidence for White being sorted in an AP-3-dependent way from endosomes to ommochromasomes. Interestingly, White was also proposed to take an alternative route by travelling first to the plasma membrane and then undergoing endocytosis to reach ommochromasomes (Lloyd *et al.*, 2002); a behaviour that has been described for the premelanosome protein (PMEL) (Raposo & Marks, 2007).

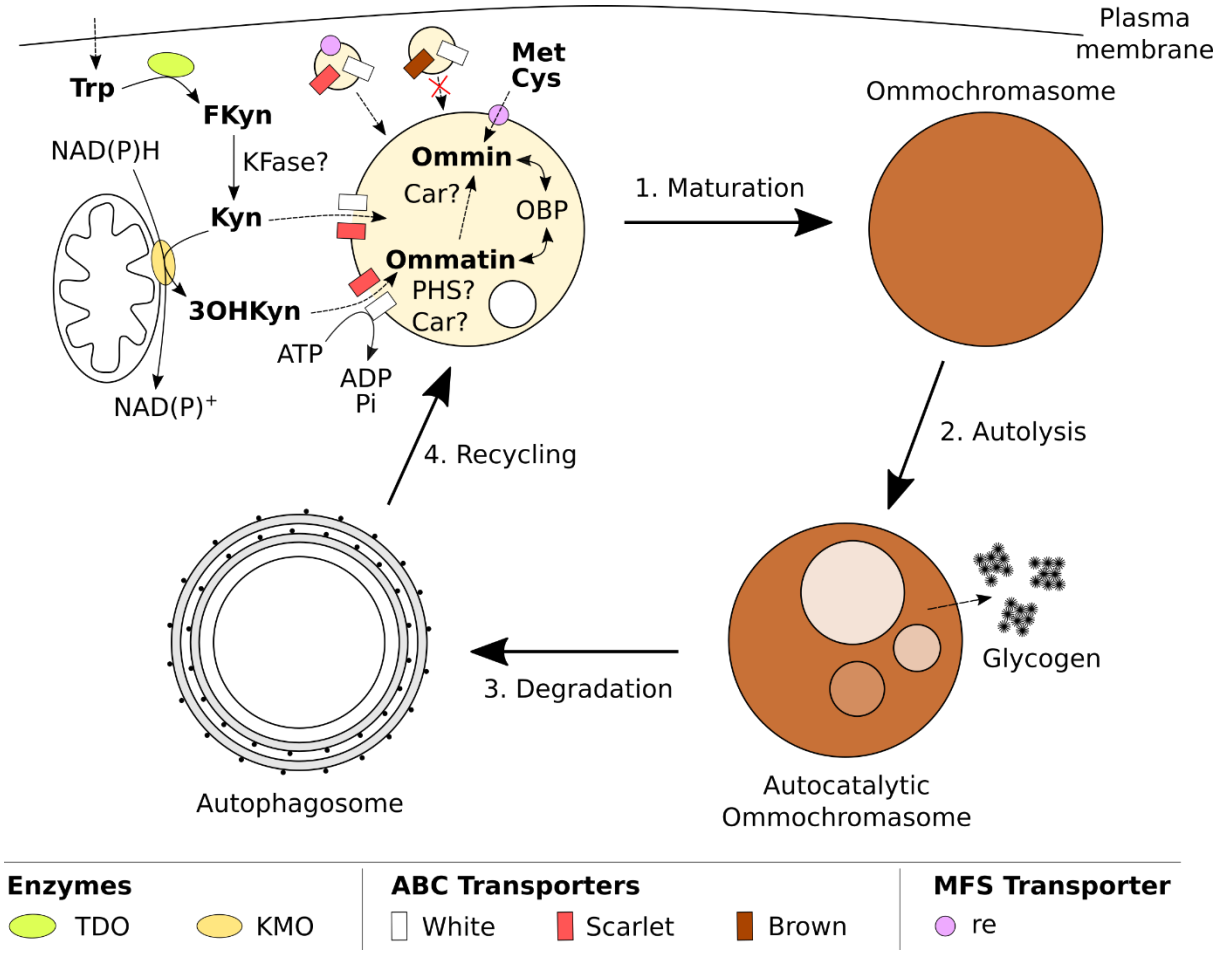

Figure 3-6. Putative model for the formation and recycling of ommochromasomes and ommochromes. Following or concomitantly with ommochromasome formation (**Figure 3-5**), ommochrome biosynthesis begins with the uptake of tryptophan into the pigment cell. Tryptophan is further processed into kynurenines by cytosolic and mitochondrial enzymes, TDO, KFase and KMO. Kynurenines can also be taken up from the extracellular space (not shown here). Kynurenines can be translocated to ommochromasomes by dimers of the ABC transporters, White and Scarlet. By hydrolysing ATP into ADP and Pi, they transport ommochromasome precursors within ommochromasomes. In their lumen, PHS might catalyse the condensation of two 3-hydroxykynurenines into ommatins. Another enzyme, Cardinal, might form ommins from ommatins and methionine/cysteine; those amino acids could be transported by another class of transporters, the MFS transporter re. Ommochrome-binding proteins could stabilise ommochromes and form a proteinaceous matrix within the ommochromasome. During their maturation, ommochromasomes might be able to fuse with White/Scarlet/re-transporting vesicles, but not with White/Brown-transporting vesicles that are specific to pterinosomes. In some organisms, ommochromasomes might be recycled through a two-step process. First, ommochromasomes become autocatalytic and promote glycogen formation in the cytosol. Intraluminal vesicles can be seen. Layers of endoplasmic reticulum forming an autophagosome then surround such autocatalytic ommochromasomes. These autophagosomes do not fuse with lysosomes; degraded ommochromasomes are rather thought to be recycled and then refilled with ommochromes. 3OHkyn, 3-hydroxykynurenine; ABC, ATP-binding cassette; Car, Cardinal; Cys, cysteine; FKyn, formylkynurenine; KFase, kynurenine formamidase; KMO, kynurenine 3-monooxygenase; Kyn, kynurenine; Met, methionine; MFS, major facilitator superfamily; OBP, ommochrome-binding protein; PHS, phenoxazone synthase; TDO, tryptophan 2,3-dioxygenase; Trp, tryptophan.

Ommochrome biosynthesis in relation to ommochromasome maturation

In all eukaryotic cells, compartmentalisation allows specific metabolic pathways to proceed in a controlled environment (Martin, 2010). The best-known examples of cellular compartmentalisation are gene expression (nuclear transcription and cytosolic translation) and aerobic respiration (cytosolic glycolysis and mitochondrial oxidation). In all these processes, compartmentalisation allows fine tuning of the rates of enzymatic reactions in response to the cell environment (Barbier-Brygoo *et al.*, 1997). In the same way, the ommochrome pathway is compartmentalised between the cytosol, mitochondria and ommochromasomes. Its first step, the production of formylkynurenine from tryptophan, occurs in the cytosol (**Figure 3-6**), which is in accordance with TDO being in the soluble fraction of centrifuged cells. By contrast, KMO localises to the outer membrane of mitochondria (**Figure 3-6**) meaning that 3-hydroxykynurenine should occur at the highest intracellular concentration near these organelles. Finally, the only known site of ommochrome production is within ommochromasomes (**Figure 3-6**), which is correlated to the specific presence of ommochrome precursor transporters in their delimiting membrane (Mackenzie *et al.*, 2000). Interestingly, mitochondria are often found in close proximity to ommochromasomes (Insausti & Casas, 2008, 2009), which suggests that these two organelles might cooperate tightly in producing ommochromes (**Figure 3-6**). Physical contact between mitochondria and melanosomes has recently been described to be involved in melanogenesis (Daniele *et al.*, 2014). Further investigations are needed to assess whether ommochromasome biogenesis also requires such inter-organelle contacts.

ABC transporters play a key role in the biosynthesis of insect chromes, as has been demonstrated in the genetic models *D. melanogaster*, *B. mori*, *Helicoverpa armigera* and *Tribolium castaneum* (Ewart *et al.*, 1994; Tatematsu *et al.*, 2011; Grubbs *et al.*, 2015; Khan *et al.*, 2017). These model species, especially the lepidopteran models, are highly useful in terms of their suitability for CRISPR/Cas9-based genome editing (Zhang & Reed, 2017). This method is of great interest now that there are candidate genes to test, which are already known to work in the ommochrome pathway or in ommochromasome biogenesis in other species. ABC transporters are likely to drive the influx of 3-hydroxykynurenine, pterins and uric acid by an ATP-driven mechanism (Mackenzie *et al.*, 2000; Tatematsu *et al.*, 2011; Grubbs *et al.*, 2015). Their specificity to one of these molecules is based on the heterodimerization of White

with either Scarlet, Brown or Ok, respectively (**Figure 3-6**). Since ommochromasomes and pterinosomes only accumulate ommochromes and pterins, respectively, this means that specific intracellular routes are taken by Scarlet and Brown to reach their organelles (**Figure 3-6**). Whether only these ABC transporters define the identity of chromasomes within pigment cells or other molecular patterns are involved is not known. Interestingly, during colour change in crab spiders, different stages of ommochromasome maturation were described based on the content of ommochromasomes. The initial stages appeared to contain kynurenine, then 3-hydroxykynurenine and lastly ommochromes themselves (Insausti & Casas, 2008). These results imply that kynurenine, along with 3-hydroxykynurenine, can be incorporated within ommochromasomes, probably through the same ABC heterodimer. We suggest that measuring the levels of ommochrome precursors in purified ommochromasomes should provide an answer to the question of which of these acts as an ABC substrate. If kynurenine is incorporated within ommochromasomes, it is not known whether it then leaves ommochromasomes to be hydroxylated or is further processed within the organelles.

Another transporter, from the major facilitator superfamily (MFS), was shown to mediate the synthesis of ommochromes in both *B. mori* and *T. castaneum* (Osanai-Futahashi *et al.*, 2012). This transporter, called Re because its mutation led to the red egg phenotype in silkworms, is thought to incorporate sulphur-containing precursors, such as cysteine and methionine, within ommochromasomes (Osanai-Futahashi *et al.*, 2012; Zhang *et al.*, 2017b). Hence, ommin synthesis, which requires sulphur, may rely on the presence and activity of Re at the ommochromasome membrane (**Figure 3-6**). To date, this MFS transporter has not been described in the fruit fly, which would explain why this insect does not produce ommins in its eyes. Interestingly, another MFS transporter, BmmucK, was shown to be involved in the formation of melanin in silkworms (Ito *et al.*, 2012; Zhao *et al.*, 2012). Thus, studying ommochromasome transporters might provide information on chromogenesis that is also relevant for melanosomes and other LROs.

How ommochromes are deposited within ommochromasomes is poorly understood. Studies on the development of these organelles during colour changes in crab spiders suggested that ommochromes formed around membrane-bound intraluminal vesicles; ommochromes then completely filled the lumen with only a highly electron-dense material visualisable by EM (Insausti & Casas, 2008). Early work on ommochromes proposed that

they were bound to proteins within the cell (**Figure 3-6**) (Shoup, 1966; Fuge, 1967; Riddiford & Ajami, 1971a). Such OBPs were purified and identified in butterflies (Riddiford & Ajami, 1971a; Yepiz-Plascencia *et al.*, 1993; Sawada, Iino, & Tsuué, 1997; Sawada *et al.*, 2002, 2007). These glycosylated proteins are rather large (13–30 kDa), and have an affinity for phenoxazone-based molecules. They might play a role in stabilising the reduction state of H_2-xanthommatin or the uncyclised form of ommatins. In the same way, if 3-hydroxykynurenine does serve as a chrome (Llandres *et al.*, 2013), the presence of specific proteins within ommochromasomes might preserve it from oxidation and condensation (Reed *et al.*, 2008). Interestingly, a glycosylated OBP of 31 kDa has been found in the haemolymph of *M. sexta*, with an increase in concentration at pupation onset (Martel & Law, 1991, 1992). This OBP could be bound to ommatin D, and thus would define the colour change of caterpillars during their growth. This finding suggests that ommochromasome contents could be released, possibly by an exocytosis and secretion mechanism, within the body circulation. Since ommatin D is normally found in butterfly wings and excreta, it could also mean that ommochromes undergo chemical transformations, such as *O*-glycosylations that make them water soluble, prior to their secretion (Martel & Law, 1991).

Ommochromasome recycling

If our knowledge of ommochromasome biogenesis is still incomplete, our understanding of their catabolism is nearly non-existent. This also applies to other LROs, including melanosomes (Borovanský & Elleder, 2003). However, crab spiders, which are able to change their colour within a few days depending on the flower in which they forage (Morse, 2007; Llandres *et al.*, 2013), concomitantly produce and degrade ommochromasomes within the same cells (Insausti & Casas, 2008, 2009). Thus, crab spiders might well be a suitable model to study how LROs are degraded and/or recycled to produce new LROs. However, since crab spiders are difficult to breed and given that very little is known about their genetics, future research should also focus on finding new model organisms or cell cultures with which to address this question.

In their ultrastructural studies using EM on crab spiders, Insausti & Casas suggested that a single ommochromasome could undergo several cycles of ommochrome production and degradation (Insausti & Casas, 2009). They describe the catabolic process as taking place in two steps (**Figure 3-6**). First, part of the ommochromasome content is degraded by an

autocatalytic mechanism, which might give rise to the production of glycogen, a possible source of energy for ommochrome reformation (Insausti & Casas, 2009). Interestingly, all LROs share characteristics with lysosomes, such as an acidic pH and lysosomal enzymes (Klumperman & Raposo, 2014). Thus, if ommochromasomes are indeed LROs, thus lysosomal properties might be acting during the putative autocatalytic process of ommochromasomes. In whitening crab spiders, degraded ommochromasomes lost their electron-dense content and accumulated as electron-lucent vacuoles at the base of the cell (Insausti & Casas, 2009). Before the ommochromasome content is completely degraded, an intermediate step exists in which vacuoles of different electron-dense properties are present within the ommochromasome lumen (**Figure 3-6**). Subsequently, onion-shaped ER layers sequester these electron-lucent vacuoles, as well as the surrounding cytosol; these structures are reminiscent of autophagosomes (**Figure 3-6**) (Insausti & Casas, 2009), which indicates that an active degradative process is occurring. Lysosomes were often seen close to these autophagocytic structures, without any evidence of fusion events leading to the formation of autolysosomes (Insausti & Casas, 2009), in which autophagosome content would be entirely degraded by the lysosomal content. Thus, the vacuolar structure of electron-lucent ommochromasomes was preserved; on this basis, the authors suggested that catabolic ommochromasomes could be reused for another round of ommochrome production and degradation during colour change (Insausti & Casas, 2009). To date, this is the only evidence for a cyclic turnover of chromes and their related organelles within the same cell (**Figure 3-6**) and it might be related to the colour-changing ability of this group. This hypothesis still needs further experimental confirmation both in crab spiders and in other ommochrome-producing organisms. Interestingly, these crab spiders can develop an irreversible purple colour after moulting (Figon, F., personal observations) perhaps suggesting that not all ommochromes can undergo this cyclic turnover, and highlighting the complexity and the plasticity of LRO metabolism.

Autophagy has also been linked to ommochromasome homeostasis in the fruit fly. This organism has been used to study autophagy in relation to endolysosomal pathways (Lőrincz *et al.*, 2016). Recently, loss-of-function of the autophagy-related gene *Atg2* was shown to ameliorate the eye-colour phenotype of AP-3, BLOC-1 and RAB-RP1 mutants (Rodriguez-Fernandez & Dell'Angelica, 2015). Thus, autophagy might also be required during pigmentation to control the quantity of ommochromes that are produced by

ommochromasomes. Such a link between autophagy and pigmentation has also been shown for melanosomes, which can be differentially degraded after being transferred to skin keratinocytes (Ho & Ganesan, 2011; Murase *et al.*, 2013). Hence, studying both melanosomes and ommochromasomes could help in unravelling how LROs are catabolised.

Ommochromes in Context: the Fruit Fly Compound Eye

Ommochromes are best known in the context of light capture in ommatidia, which are the optical units of compound eyes in insects and some crustaceans (Nilsson & Kelber, 2007). Each ommatidium perceives light coming from a single point leading to the formation of a mosaic image (Cronin, 2014). Ommatidia are separated from each other by pigment cells that produce screening chromes, such as ommochromes and pterins (Stavenga, 1989). Screening chromes perform two functions in fruit fly ommatidia: absorbing stray light, hence limiting light from entering adjacent ommatidia (**Figure 3-7**A), and promoting the photogeneration of metarhodopsins back to rhodopsins, the light-sensor molecules of rhabdomeres (Stavenga, 2002). In the following, we take an integrative approach to draw links between ommochrome and ommochromasome characteristics with their biological functions in compound eyes.

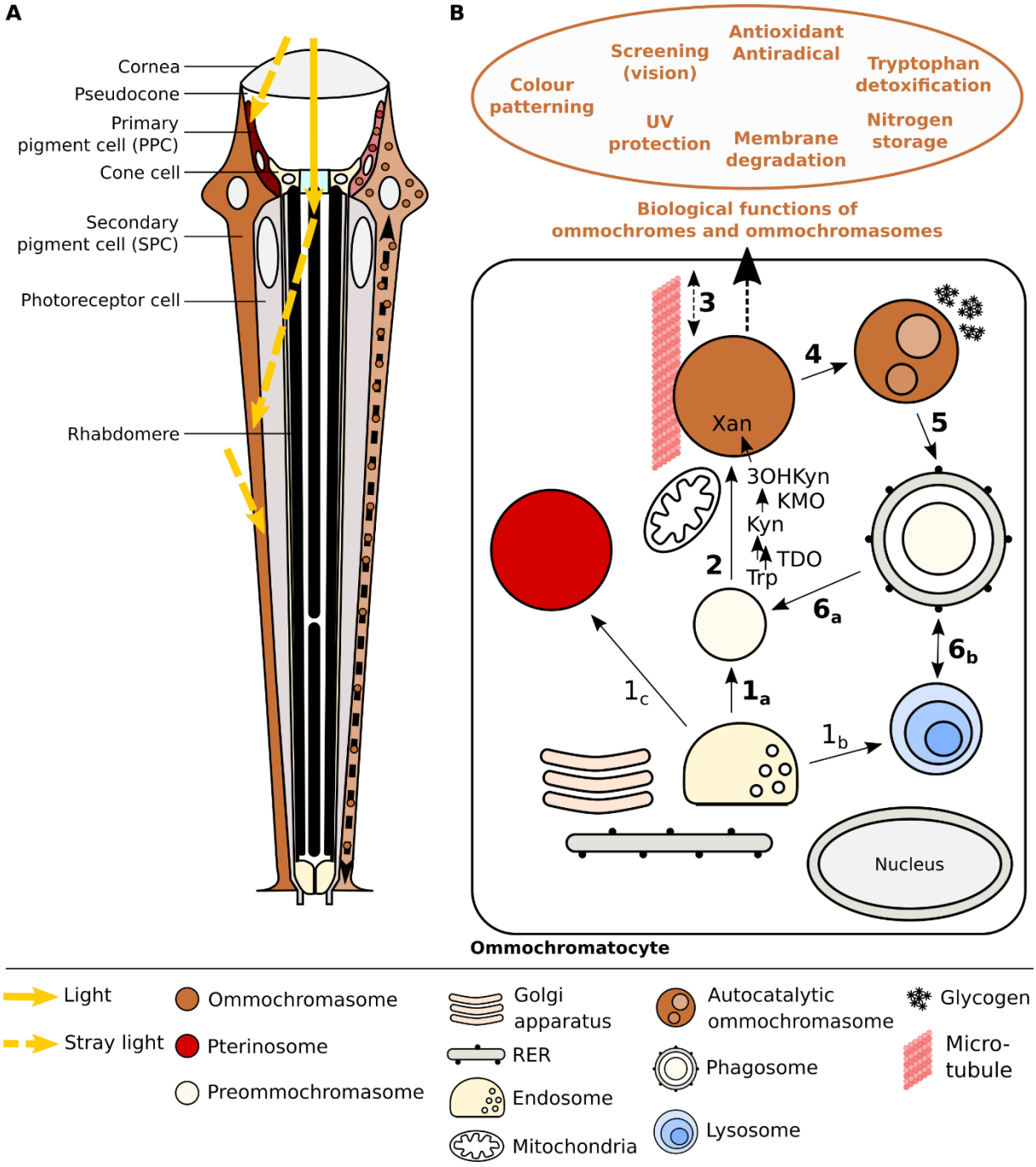

Figure 3-7. Integrated biology of ommochromes and ommochromasomes.
(A) View of an insect ommatidium showing the different parts, cells and organelles involved in vision. Direct light is perceived by the rhabdomeres of photoreceptor cells. Stray light, either out of the ommatidial axis or coming from another ommatidium, is absorbed by ommochromasomes, as well as pterinosomes, of primary and secondary pigment cells. Both organelles can be moved along the cytoskeleton of these cells (black dashed double-headed arrow). Thus, an ommatidium receives light from only one direction. (B) Biological functions of ommochromes and ommochromasomes in relation to their biochemistry and cell biology in ommochrome-producing cells (ommochromatocytes). (1) Endosomes can become either (a) preommochromasomes, (b) lysosomes or (c) pterinosomes. (2) The tryptophan→ommochrome pathway leads to the formation of 3-hydroxykynurenine in coordination with mitochondria. This ommochrome precursor is loaded into maturing ommochromasomes and then condenses into xanthommatin to form mature ommochromasomes. (3)

Ommochromasomes can be moved within the cells *via* microtubule tracks. (4) Prior to their degradation or recycling, ommochromasomes enter into an autocatalytic process, which is associated with depigmentation and glycogen formation. (5) Autocatalytic ommochromasomes then transform into autophagosomes that either (6a) lead to recycled ommochromasomes or (6b) fuse with lysosomes that degrade their content. Note that not all these steps might be present in all ommochromatocytes. 3OHKyn, 3-hydroxykynurenine; KMO, kynurenine 3-monooxygenase; Kyn, kynurenine; RER, rough endoplasmic reticulum; TDO, tryptophan 2,3-dioxygenase; Trp, tryptophan; Xan, xanthommatin.

In *D. melanogaster*, primary pigment cells (PPCs) produce both chromasomes and pterinosomes, while secondary pigment cells (SPCs) only form ommochromasomes (**Figure 3-7**A) (Shoup, 1966). This indicates that a single cell can produce at least three different LROs, namely ommochromasomes, pterinosomes and lysosomes in the fruit fly, without confusing their biogenesis (**Figure 3-7**B). Thus, mechanisms to sort LRO type-specific materials within the cell must be present. Similarly, melanosomes and lysosomes coexist in melanocytes (Raposo & Marks, 2007), thus SPCs might a good model to study how these sorting mechanisms work.

In dark-adapted eyes, ommochromasomes migrate on microtubules within pigment cells (**Figure 3-7**A), which allows the leaking of stray light to adjacent ommatidia, thus enhancing eye sensitivity (Stavenga, 1989, 2002). Actin filaments and microtubules are two important players in the formation and proper function of LROs such as melanosomes (Hume & Seabra, 2011). It is not known whether cytoskeletons participate in the maturation of ommochromasomes, but they certainly regulate ommochromasome functions by modifying their intracellular localisation (**Figure 3-7**B).

In light-adapted eyes, ommochromasomes and ommochromes are known to be involved in the maintenance of photoreceptors. In the blowfly *Lucilia* sp., degraded rhabdomere membranes seem to be transported to pigment cells (Schraermeyer & Dohms, 1993). Residual bodies originating from this degradation might then fuse with ommochromasomes (Schraermeyer, Rack, & Stieve, 1993). The function of this membrane exchange between photoreceptors and pigment cells is not known. We can hypothesise that the possible lysosomal characteristics of ommochromasomes, i.e. an acidic pH and the presence of hydrolases, might help in degrading photoreceptor materials. Antioxidant and antiradical properties of ommochromes might also serve to quench harmful products arising from the degradation of membrane lipids and photo-activated rhodopsins. In red-eye mutants of triatomine bugs lacking ommochromes, UV exposure led to severely damaged ommatidia,

especially when bugs were blood-fed, and thus experienced high oxidative stress (Insausti *et al.*, 2013). Furthermore, in wild-type bugs, light exposure induced a major increase in ommochrome synthesis. Thus, these results link ommochromes to the protection of the eye structure against both light and oxidation.

Similarly to crab spiders, degradative ommochromasomes associated with glycogen occur naturally in ommatidia of horseshoe crabs, crickets and mantis shrimps (Fahrenbach, 1969; Wachmann, 1969; Perrelet, Orci, & Baumann, 1971). However, in these species, ommochromasomes do not seem to be recycled, but are localised to autophagic vacuoles and lysosomal compartments with acid phosphatase activity, indicating that these ommochromasomes are intended for degradation. Thus, depending on the cellular context, mature ommochromasomes could be diverted toward either a fully degradative or a recycling process (**Figure 3-7**B). The choice between these two routes might rely on a last fusion step of ommochromasome-containing autophagosomes with lysosomes (**Figure 3-7**B).

Overall, the study of compound eyes demonstrates the importance of taking an integrative approach when one seeks to unravel the biological role of ommochromes. Their functions are directly linked to their chromophores and to ommochromasomes. Thus, as noted over 40 years ago (Needham, 1974), there is a strong requirement to understand the biochemistry, as well as the cell biology, of ommochromes in order to link them to their biological function.

Conclusions

(1) Since the nineteenth century, animal colouration has been an ever-growing field of research with important implications for both basic and applied sciences. Thus, understanding the mechanisms underlying colouration and its related functions is of great importance. In invertebrates, chemical colours are often produced by coloured molecules of the ommochrome family. These chromes and the related ommochromasomes have been implied in a broad range of biological functions, including camouflage, vision and cell homeostasis, as well as in many general biological processes, such as colour pattern development and lysosome-related family biogenesis. Furthermore, the phenoxazine-derived chromophore of ommochromes has been used in a wide array of classic and new technologies, from histological dyes to photovoltaic sensitizers. Hence, future studies on

the biochemistry of ommochromes will shed light on their biological and technological use.

(2) Ommochromes are widespread coloured compounds in invertebrates and they have been studied for almost 80 years. With their unique phenoxazone-based chromophore, ommochromes perform different functions from vision and colour patterning to amino acid detoxification. Ommochromes are products of tryptophan metabolism, which involves the formation and the condensation of ommochrome precursors, called kynurenines, in four biochemical steps. These steps are either spontaneous or catalysed by specific enzymes, for some of which crystallographic structures are now available. The Tryptophan→Ommochrome pathway might be biochemically linked to other chromogenic pathways either through common precursors or through redox reactions.

(3) Ommochromes are classified into three compound families: ommatins, ommins and ommidins. Ommatin structure and chemistry are now well understood, but almost nothing is known about the two other groups. Following recent studies on silkworms, future research should focus on unravelling the chemical structure of ommochromes and how they are produced, especially for ommidins that are abundant in several model species for both basic and applied biology.

(4) Ommochromes are photosensitive molecules and can undergo redox reactions, two characteristics shared by chromes in general. Hence, ommochromes can be modified by light exposure and chemical reactions. Thus, their stability both *in vivo* and *in vitro* is questionable and further studies should address the way ommochromes are spontaneously modified in cells, as well as during extraction and identification. Moreover, the putative biological role of ommochromes in buffering oxidative stress may rely on their light and redox reactivity.

(5) Even though the formation of ommochrome precursors has been well described, we still lack considerable understanding of the last steps leading to ommochrome biosynthesis. In particular, whether a phenoxazone synthase is involved in

the *in vivo* condensation of 3-hydroxykynurenine to xanthommatin is still highly debated. Future studies should also address the mechanisms by which H_2-xanthommatin derivatives, such as rhodommatin and ommatin D, are produced. These ommochromes differ from other ommochromes by being water soluble. Thus, rhodommatin and ommatin D might perform different biological functions from other ommochromes.

(6) Ommochrome precursor loading and ommochrome deposition both take place in specialised membrane-bound organelles termed ommochromasomes. Ommochromasomes also contain cations and proteins, especially ommochrome-binding proteins. Ommochromasomes are thought to belong to the lysosome-related organelle (LRO) family and therefore could originate from endosomes. Ommochromasome biogenesis and maturation rely on the functioning of highly conserved traffic-regulating complexes: APs, BLOCs, RABs, HOPS and CORVET. Many other organelles and membrane systems might also play a role in the proper formation of ommochromasomes. Mitochondria have a significant role by hosting in their outer membrane a key enzyme of the Tryptophan→Ommochrome pathway. This highlights the importance of cell compartmentalisation in ommochrome production.

(7) Ommochromasome structure and content has only been deciphered in the context of organisms and tissues. Purifying them and identifying appropriate cell models will also be required to fully appreciate their intrinsic characteristics. Hence, future studies should perform morphological, biochemical and analytical studies, as successfully done for melanosomes, on highly purified fractions of ommochromasomes.

(8) How the different lysosome-related organelles (LROs), i.e. ommochromasomes, pterinosomes and lysosomes, can coexist within the same cell is not known. Even though endosomal complexes are known to control ommochromasome formation, how they do this has only been described through the study of other LROs, in particular the melanosomes of vertebrates. It is now necessary to unravel the specific details of their involvement in the ommochrome context by precisely describing the endosomal routes taken by ommochromasome-specific proteins.

(9) The fate of LROs is a key question in cell biology. Even for melanosomes, whether they are degraded or recycled and how these processes happen remain unknown. Mature ommochromasomes may be recycled and re-loaded with ommochromes under specific conditions. This part of the ommochromasome life cycle might involve an autocatalytic process of ommochromasome content degradation, followed by the formation of autophagosomes. In other contexts, ommochromasome-containing autophagosomes might fuse with lysosomes leading to the complete degradation of ommochromasomes.

(10) An integrated approach is needed to understand the biological role of ommochromes. Their functions depend directly on their chemistry and their organelles. Thus, future ecological and physiological studies on ommochromes should take into account recent advances in understanding their biochemistry and cell biology to clarify their involvement in biological processes.

Acknowledgements

We are grateful to Cédric Delevoye, Teresita Insausti and two anonymous reviewers for their comments on the manuscript. This study formed part of the doctoral dissertation of F.F. under the supervision of J.C. The ENS de Lyon is thanked for its financial support.

3.3 Conclusion

Cette revue de la littérature a montré que, si les études centrées sur les ommochromes ont périclité depuis les années 1970-1980, ils restent impliqués dans des contextes biologiques divers. Ils ont permis des avancées dans les domaines de la génétique, de la biologie cellulaire et, plus récemment, du biomimétisme. Il semble donc nécessaire de poursuivre les recherches sur leurs caractéristiques physico-chimiques et sur leur environnement cellulaire afin de pouvoir les intégrer aux nombreuses données développementales, physiologiques et écologiques.

Dans la perspective d'une biologie intégrative des ommochromes, une dizaine de pistes de recherche (pp. 115-118) qui paraissent les plus importantes et prometteuses ont été identifiées. Dans le reste de cette étude, j'en aborde quelques-unes. Ainsi, dans le **chapitre 4**, les *points 4 à 8* (pp. 116-117) sont abordés par l'analyse de la stabilité des ommochromes dans les solvants d'extraction (*point 4*, p. 116) afin de vérifier quels métabolites sont effectivement présents *in vivo* dans les ommochromasomes (*points 6 et 8*, p. 117). Cela permettra en particulier de savoir si la biosynthèse des ommatines est bien réalisée par la condensation de la 3-hydroxykynurénine en une forme non-cyclisée de la xanthommatine (*point 5*, p. 116). La méthodologie emploiera la spectrométrie de masse couplée à la synthèse de standards d'ommochromes, dont j'ai déjà discuté l'intérêt et l'importance pour élucider leurs structures, ainsi qu'un protocole de purification des ommochromasomes, étape nécessaire à la description de leur contenu. Dans le **chapitre 5**, les méthodes de la chimie quantique déjà discutées seront utilisées afin de comprendre les mécanismes d'absorption de la lumière à l'échelle moléculaire et électronique. Cette approche permettra d'aborder les *points 1 et 4* (pp. 115 et 116) en faisant le lien entre les caractéristiques optiques des ommochromes, leur utilisation en biomimétisme et leurs fonctions biologiques qui dépendent de leurs états électroniques, c'est-à-dire le changement de couleur et les capacités anti-radicalaires. Dans le **chapitre 6**, la prédiction du *point 6* (p. 117) sera testée en vérifiant si les organites pigmentés des araignées crabes sont bien des LROs. En particulier, le rayonnement Synchrotron permettra de tester la présence de métaux (par fluorescence des rayons X) à l'intérieur des organites pigmentés. De plus, en étudiant des araignées crabes de différentes couleurs et dont les tissus auront été préservés dans un état quasi-natif (par cryofixation), le modèle du cycle de vie de leurs organites pigmentés (*point 9*, p. 118) sera testé en cherchant

des indices ultrastructuraux et chimiques (métaux) de leur anabolisme, de leur catabolisme et de leur recyclage. Finalement, dans le **chapitre 7**, je ferai une synthèse de l'ensemble des résultats de cette thèse en proposant une biologie intégrative des ommochromes dans le contexte du changement de couleur, comme préconisé par le *point 10* (p. 118).

Chapitre 4 – La xanthommatine non-cyclisée est un intermédiaire clé dans la coloration des invertébrés

Whatever it is, the outlet of ommochrome synthesis has endowed insects […] with a most valuable and variable means of handling light

Linzen (1974), in *Advances in Insect Physiology*

4.0 Sommaire

CHAPITRE 4 – LA XANTHOMMATINE NON-CYCLISEE EST UN INTERMEDIAIRE CLE DANS LA COLORATION DES INVERTEBRES 121

4.0 SOMMAIRE 122
4.1 OBJECTIFS ET METHODOLOGIES 124
4.2 TRAVAIL EXPERIMENTAL 125
Abstract *128*
Introduction *128*
Material and Method *132*
Insects 132
Reagents 132
In vitro synthesis of xanthommatin 132
Oxidative condensation of 3-hydroxykynurenine under anoxia 132
Solubilization and analyses of synthesized ommatins 133
Nuclear Magnetic Resonance (NMR) Spectroscopy 133
Ultra-Pressure Liquid Chromatography coupled to Diode-Array Detector and Electrospray Ionization Source-based Mass Spectrometer (UPLC-DAD-ESI-MS) 134
System 134
Chromatographic conditions 134
Spectroscopic conditions 134
Thermal reactivity of ommatins in acidified methanol in darkness 134
Conditions of solubilization and incubation 134
Quantification of ommatins 135
Extraction and content analysis of housefly eyes 135
Biological extractions 135
Chromatographic profile 135
Purification and content analysis of ommochromasomes 136
Isolation protocol 136
Extraction of ommochrome-related metabolites from purified ommochromasomes 136
Metabolic analysis of purified ommochromasomes 136
Statistical analysis 137
Results *137*
UPLC-DAD-MS/MS structural elucidation of synthesized xanthommatin and its in vitro derivatives 137
The ommatin profile is rapidly and readily modified overtime by artifactitious methoxylations in acidified methanol 144
UPLC-DAD-MS/MS structural elucidation of uncyclized xanthommatin, the labile intermediate in the synthesis of ommatins from 3-hydroxykynurenine 146
Biological localization of the metabolites from the tryptophan→ommochrome pathway 149

Discussion *152*
UPLC-DAD-MS/MS structural elucidation of new ommatins 152
Biological extracts are prone to yield artifactitious ommatins 153
The metabolites of the tryptophan→ommochrome pathway in ommochromasomes 154
Uncyclized xanthommatin is a potential key branching point in the biogenesis of ommatins and ommins 158
Acknowledgments *161*
Supplemental Data *161*
Supplemental Figures 161
File S1. Supplemental Materials and Methods 168
Homogenization of housefly eyes 168
Differential centrifugation 168
Ultracentrifugation 169
Analytical characterization of dihydroxanthommatin 169
Reactivity of synthesized ommatins with β-mercaptoethanol 169
Sample preparation 169
Quantifications 170
File S2. Report of statistical analyses 170
4.3 CONCLUSION 171

4.1 Objectifs et méthodologies

Nous avons vu dans les chapitres précédents que la fonction des ommochromes est intimement liée à leur structure. Or, la biochimie des ommochromes n'a que peu avancé depuis la description de la voie des kynurénines et l'élucidation de la structure de la rhodommatine dans les années 70. J'ai dès lors souligné que des outils de chimie analytique à la pointe, telles que la spectrométrie de masse en tandem couplée à la chromatographie liquide ultra-haute performance, devraient permettre de surmonter certaines difficultés propres à la chimie des ommochromes, telles que leur instabilité dans les solvants d'extraction et leur difficile analyse par RMN.

L'objectif de ce chapitre est d'investiguer expérimentalement la biochimie des ommochromes dans un contexte biologique bien connu, celui des yeux de mouches où les ommochromes (en particulier la xanthommatine) sont produits en abondance. Ce modèle permet de tester plusieurs hypothèses quant à la voie de biosynthèse des ommochromes : (i) les ommochromes dérivent de la dimérisation de la 3-hydroxykynurénine ; (ii) cette dimérisation se produit à l'intérieur des ommochromasomes ; et (iii) il y a un lien structurel qui relie la biosynthèse des ommatines à celle des ommines. L'hypothèse de la dimérisation de la 3-hydroxykynurénine impose la formation d'un intermédiaire de synthèse, la xanthommatine non-cyclisée. Pour pouvoir tester sa présence biologique, la spectrométrie de masse en tandem est d'abord appliquée à un produit de synthèse issu de la condensation de la 3-hydroxykynurénine en conditions oxydantes, qui sont connues pour former des dimères d'*ortho*-aminophénols. Une fois la méthode de détection mise en place, l'objectif est de quantifier la xanthommatine non-cyclisée dans les ommochromasomes purifiés des yeux de mouche par rapport à un extrait total de ces mêmes yeux ; ceci afin de savoir si cet intermédiaire est enrichi, et donc spécifiquement produit, dans les ommochromasomes. Finalement, je cherche à relier la présence de la xanthommatine non-cyclisée dans la voie de biosynthèse des ommatines à celle des ommines.

4.2 Travail expérimental

Le manuscrit suivant a été accepté le 27 avril 2020 dans le journal international à comité de lecture *Insect Biochemistry and Molecular Biology*.

FIGON, F., MUNSCH, T., CROIX, C., VIAUD-MASSUARD, M.-C., LANOUE, A. & CASAS, J. (2020) Uncyclized xanthommatin is a key ommochrome intermediate in invertebrate coloration. *Insect Biochemistry and Molecular Biology* **124**, 103403. DOI: 10.1016/j.ibmb.2020.103403

La version soumise (avant révision) a été déposée en tant que prépublication sur le serveur *bioRxiv*.

FIGON, F., MUNSCH, T., CROIX, C., VIAUD-MASSUARD, M.-C., LANOUE, A. & CASAS, J. (2019) Uncyclized xanthommatin is a key ommochrome intermediate in invertebrate coloration. preprint, bioRxiv. DOI: 10.1101/666529

Uncyclized xanthommatin is a key ommochrome intermediate in invertebrate coloration

Short title: Uncyclized xanthommatin in ommochrome biosynthesis

Florent Figon[1]*, Thibaut Munsch[2], Cécile Croix[3], Marie-Claude Viaud-Massuard[3], Arnaud Lanoue[2], and Jérôme Casas[1]

From the [1]Institut de Recherche sur la Biologie de l'Insecte, UMR CNRS 7261, Université de Tours, 37200 Tours, France; [2]Biomolécules et Biotechnologies Végétales, EA 2106, Université de Tours, 37200 Tours, France; [3]Génétique, Immunothérapie, Chimie et Cancer, UMR CNRS 7292, Université de Tours, 37200 Tours, France

*To whom correspondence should be addressed: Florent Figon: Institut de Recherche sur la Biologie de l'Insecte, UMR CNRS 7261, Université de Tours, 37200 Tours, France; florent.figon@univ-tours.fr; Tel. +33 (0)2 47 36 69 81; Fax. +33 (0)2 47 36 69 66.

Author contributions: F. F., A. L. and J. C. conceptualization; F. F. data curation; F. F. formal analysis; M.-C. V.-M., A. L. and J. C. funding acquisition; F. F., T. M. and C. C. investigation; F. F., T. M., C. C., A. L. and J. C. methodology; F. F., A. L. and J. C. project administration; M.-C. V.-M., A. L. and J. C. resources; J. C. supervision; F. F., A. L. and J. C. validation; F. F. visualization; F. F. and J. C. writing – original draft; F. F., T. M., C. C., M.-C. V.-M., A. L. and J. C. writing – review & editing.

Abbreviations: CE, collision energy; CV, cone voltage; DAD, diode-array detector; ESI^+, positive-mode electron spray ionization; LC, liquid chromatography; MeOH-HCl, acidified methanol with 0.5 % hydrochloric acid; MRM, multiple reaction monitoring; MS, mass spectrometry; MS/MS, tandem mass spectrometry; MW, molecular weight; *m/z*, mass-to-charge ratio; NMR, nuclear magnetic resonance; RT, retention time; SD, standard deviation; SE, standard error; SIR, single ion recording; UV, ultraviolet.

Highlights

1. Ommochromes are widespread invertebrate pigments
2. Mass and UV-Visible spectroscopies help elucidating the structure of ommochrome
3. Uncyclized xanthommatin is identified in ommochrome organelles of fly ommatidia
4. Uncyclized xanthommatin is a key branching metabolite in ommochrome biosynthesis
5. Provides insight into ommochrome diversification in insects and other invertebrates

Graphical Abstract

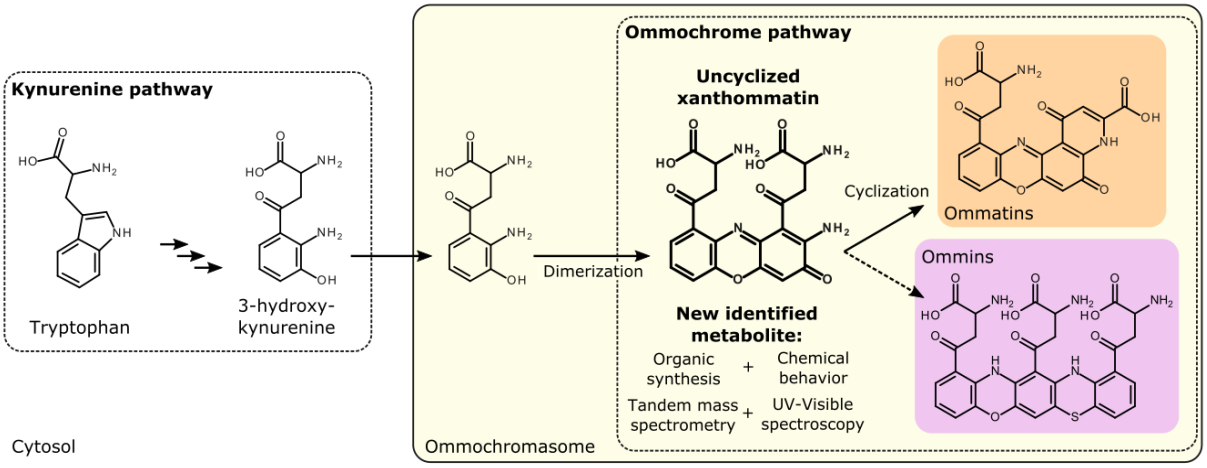

Abstract

Ommochromes are widespread pigments that mediate multiple functions in invertebrates. The two main families of ommochromes are ommatins and ommins, which both originate from the kynurenine pathway but differ in their backbone, thereby in their coloration and function. Despite its broad significance, how the structural diversity of ommochromes arises *in vivo* has remained an open question since their first description. In this study, we combined organic synthesis, analytical chemistry and organelle purification to address this issue. From a set of synthesized ommatins, we derived a fragmentation pattern that helped elucidating the structure of new ommochromes. We identified uncyclized xanthommatin as the elusive biological intermediate that links the kynurenine pathway to the ommatin pathway within ommochromasomes, the ommochrome-producing organelles. Due to its unique structure, we propose that uncyclized xanthommatin functions as a key branching metabolite in the biosynthesis and structural diversification of ommatins and ommins, from insects to cephalopods.

Keywords: high-performance liquid chromatography (HPLC), kynurenine, mass spectrometry (MS), ommin, ommochromasome, ultraviolet-visible spectroscopy (UV-Vis spectroscopy)

Introduction

Ommochromes are widespread phenoxazinone pigments of invertebrates. They act as light filters in compound eyes and determine the integumental coloration of a large range of invertebrates (Figon & Casas, 2019). Ommochromes are also of particular interest in applied sciences as their scaffold has been used to design antitumor agents (Bolognese *et al.*, 2002b) and, very recently, to manufacture biomimetic color changing electrochromic devices (Kumar *et al.*, 2018). The two major families of natural ommochromes are the yellow-to-red ommatins and the purple ommins that contain a supplemental phenothiazine ring. Ommatins are currently the best described family of ommochromes and occur throughout invertebrates. Ommins are much less characterized, although they are virtually ubiquitous in insects and cephalopods (Riddiford & Ajami, 1971b; Needham, 1974). After nearly 80 years and despite their broad significance, the structural and chemical relationships between these two abundant families of ommochromes remain surprisingly mysterious (Figon & Casas, 2019).

The early steps of the biosynthesis of ommochromes in invertebrates cover the oxidation of tryptophan into kynurenines (**Figure 4-1**B) (Figon & Casas, 2019), from insects (Linzen, 1974) and spiders (Croucher *et al.*, 2013) to planarians (Stubenhaus *et al.*, 2016) and cephalopods (Williams *et al.*, 2019b). These oxidative steps are homologous to the kynurenine pathway of vertebrates in which the last enzyme, the mitochondria-bound kynurenine 3-monooxygenase, catalyzes the formation of 3-hydoxykynurenine. This *ortho*-aminophenolic amino acid is the currently accepted last common precursor of all known ommochromes, from ommatins to ommins (**Figure 4-1**B) (Figon & Casas, 2019). The catabolism of tryptophan then diverges from vertebrates because invertebrates lack the glutarate pathway but possess the ommochrome pathway (Linzen, 1974).

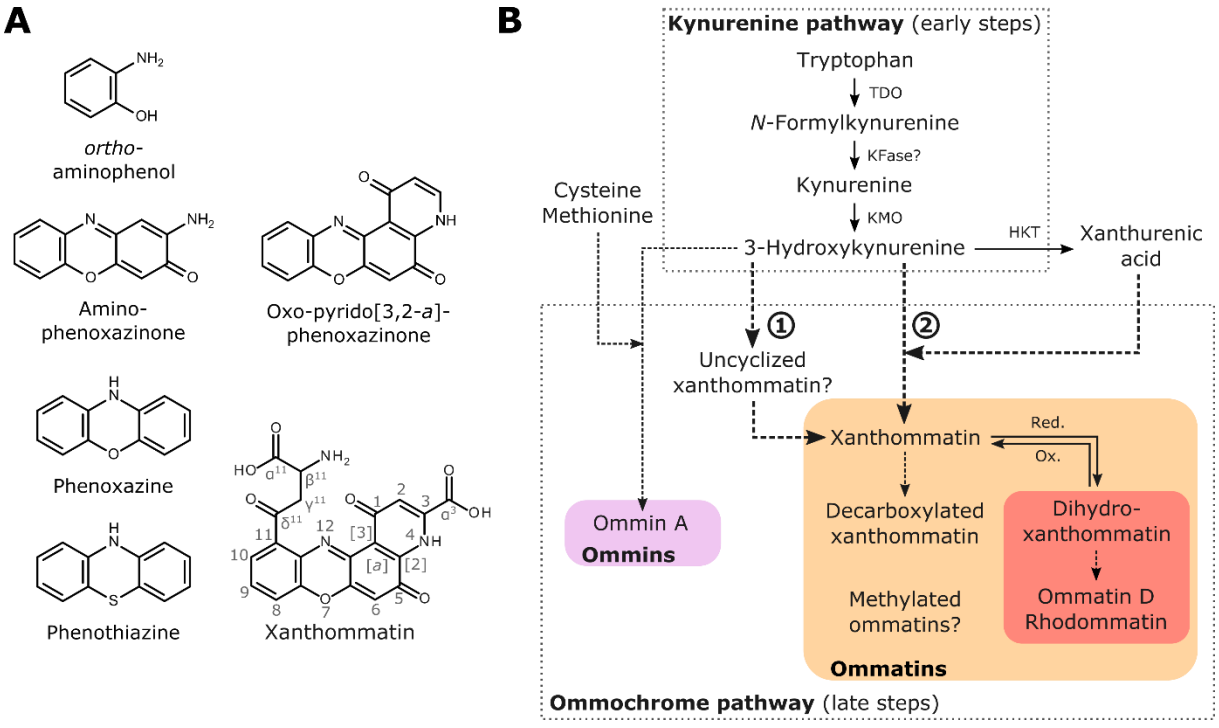

Figure 4-1. Current knowledge of the tryptophan→ommochrome pathway of invertebrates.
A) Main chemical structures and chromophores of the tryptophan→ommochrome pathway. Numbering of ommatins used in this study is indicated on the structure of xanthommatin. B) Kynurenine and ommochrome pathways form the early and late steps of the tryptophan→ommochrome pathway, respectively. Ommatins are possibly biosynthesized via two routes: (1) the dimerization of 3-hydroxykynurenine into the intermediary uncyclized xanthommatin, or (2) the direct condensation of 3-hydroxykynurenine with its cyclized form, xanthurenic acid. Ommatin and ommin pathways share 3-hydroxykynurenine as a precursor, but at which step they diverge is not known. Dashed arrows, steps for which we lack clear biological evidence. HKT, 3-hydroxykynurenine transaminase. KFase, kynurenine formamidase. KMO, kynurenine 3-monooxygenase. Ox., oxidation. Red., reduction. TDO, tryptophan 2,3-dioxygenase.

Ommochromes are produced within specialized intracellular organelles, called ommochromasomes, most likely after the incorporation of 3-hydroxykynurenine (Mackenzie *et al.*, 2000; Figon & Casas, 2019). Two hypotheses have been proposed to explain how ommatins originate from there. (1) It has been suggested very early, but on weak evidence, that the oxidative dimerization of 3-hydroxykynurenine into uncyclized xanthommatin and its subsequent intramolecular cyclization account for the biosynthesis of ommochromes (**Figure 4-1**B) (Butenandt and Schäfer, 1962). (2) The condensation of *ortho*-aminophenols with xanthurenic acid has been proposed to form directly the oxo-pyrido[3,2-*a*]phenoxazinone chromophore of ommatins (**Figure 4-1**B) (Linzen, 1974; Panettieri *et al.*, 2018). Hypothesis 1 is currently more accepted because ommatins can be synthesized *in vitro* by the oxidative condensation of 3-hydroxykynurenine, which is predicted to form an unstable intermediate, the 3-hydroxykynurenine dimer called uncyclized xanthommatin (Butenandt & Schäfer, 1962; Iwahashi & Ishii, 1997; Zhuravlev, Vetrovoy, & Savvateeva-Popova, 2018; Figon & Casas, 2019; Williams *et al.*, 2019a). Furthermore, uncyclized xanthommatin was speculated in biological extracts (Bolognese & Scherillo, 1974), putatively identified in the *in vitro* oxidation of 3-hydroxykynurenine (Iwahashi & Ishii, 1997) and its enzymatic formation predicted *in silico* by quantum calculations (Zhuravlev *et al.*, 2018). However, it has never been formerly extracted and characterized in biological samples. Alternatively, hypothesis 2 does not involve the formation of any intermediate between the kynurenine pathway and the ommatin pathway. Hence, to discriminate between the two hypotheses, one needs to determine whether uncyclized xanthommatin is produced *in vivo* (**Figure 4-1**B). Finding this still-elusive intermediate in biological extracts would therefore be a major step in characterizing the actual biosynthetic pathway of ommochromes.

Deciphering the ommochrome pathway requires the characterization of metabolites in biological extracts. However, biological ommochromes are remarkably refractory to NMR spectroscopy, partly because of their poor solubility in most conventional solvents (Bolognese *et al.*, 1988b; Parrilli & Bolognese, 1992; Crescenzi *et al.*, 2004). It was only very recently that the first ^{1}H-NMR spectrum of xanthommatin, whose structure has been known for 60 years, was published after extensive purification and optimization steps (Kumar *et al.*, 2018). However, from a theoretical point of view, mere ^{1}H-NMR data cannot provide enough information on the exact structure of ommochromes. Indeed, they are rather poor in carbon-bonded hydrogens, which prevents access to all positions in the structure. Furthermore, they

are redox/pH sensitives and prone to tautomerization, which complicate ^{1}H spectra greatly. Since our main target compound, uncyclized xanthommatin, is unstable in solution (Bolognese & Scherillo, 1974; Bolognese *et al.*, 1988a), it is highly improbable that gold-standard techniques for structural elucidation, such as ^{13}C- and 2D-NMR, can be used because they suffer from too low sensitivity. In order to elucidate the biological diversity of ommochromes, one should therefore look for a combination of more sensitive analytical techniques that provide orthogonal information, such as mass spectrometry and UV-Visible spectroscopy. For nearly a decade, mass spectrometry (MS) has been used to elucidate the structure of both known and unknown ommochromes from biological samples (Futahashi *et al.*, 2012; Williams *et al.*, 2016; Panettieri *et al.*, 2018; Reiter *et al.*, 2018). Yet, evidence for common and compound-specific fragmentation patterns of ommochromes are scarce [but see (Panettieri *et al.*, 2018; Reiter *et al.*, 2018)]. Together with the seldom use of synthesized ommochromes, this lack of analytical data accounts for the very little progress made since four decades to unravel the biological diversity of ommochromes (Figon & Casas, 2019).

In this study, we synthesized xanthommatin and its decarboxylated form by the oxidative dimerization of 3-hydroxykynurenine. Knowing that ommatins are methoxylated in acidified methanol (MeOH-HCl), we incubated synthesized xanthommatin in MeOH-HCl to produce a range of ommatin-derivatives. We constructed an analytical dataset of those ommatins by a combination of UV-Visible spectroscopy, and (tandem) mass spectrometry after separation by liquid chromatography. From this dataset, we derived a fragmentation pattern with valuable structural information, especially when combined with UV-Visible spectra, to infer the structure of new ommochromes with strong confidence. Hence, we could elucidate the structure of three methoxylated ommatins and, more importantly, of uncyclized xanthommatin. Our experiments demonstrated that ommatins are easily and rapidly methoxylated leading to artifacts in conditions matching standard extraction procedures from biological samples. By combining our analytical tools with an artifact-free extraction protocol and a subcellular fractionation of ommochromasomes, we reinvestigated the ommochromes of housefly eyes. We could identify xanthommatin, decarboxylated xanthommatin and uncyclized xanthommatin in ommochromasomes. Our results provide strong support to the hypothesis that ommatin biosynthesis occurs in subcellular organelles through the dimerization of 3-hydroxykynurenine and its subsequent intramolecular cyclization (hypothesis 1, **Figure 4-1**B). Furthermore, the unique structure of uncyclized xanthommatin

makes it a good candidate to link the biosynthetic pathways of ommatins and ommins, which has important implications on how ommochromes have diversified in a wide range of phylogenetically-distant species.

Material and Method

Insects

Houseflies (*Musca domestica*) were obtained at the pupal stage from Kreca. After hatching, houseflies were either directly processed for ommochromasome purification or stored at -20 °C for ommochrome extraction.

Reagents

Sodium dihydrogen phosphate, sodium hydrogen phosphate, L-kynurenine (≥ 98 %), 3-hydroxy-D,L-kynurenine, trifluoroacetic acid (TFA), Triton X-100, tris(hydroxymethyl)aminomethane (Tris), potassium ferricyanide, magnesium chloride, potassium chloride, potassium pentoxide and cinnabarinic acid (≥ 98 %) were purchased from Sigma-Aldrich. Methanol, potassium chloride and hydrochloric acid (37 %) were purchased from Carlo Erba reagents. Nycodenz® was purchased from Axis Shield. L-tryptophan (≥ 99 %) and xanthurenic acid (≥ 96 %) were purchased from Acros Organics. Sucrose (99 %) and sulfurous acid (≥ 6 % SO_2) were purchased from Alfa Aesar. β-Mercaptoethanol was purchased from BDH Chemicals. Acetonitrile and formic acid were purchased from ThermoFischer Scientific.

In vitro *synthesis of xanthommatin*

Oxidative condensation of 3-hydroxykynurenine under anoxia

A mixture of ommatins was synthesized by oxidizing 3-hydroxy-D,L-kynurenine with potassium ferricyanide as previously described (Butenandt *et al.*, 1954; Hori & Riddiford, 1981), with some modifications. In a round bottom flask under argon, a solution of 44.6 mM of 3-hydroxy-D,L-kynurenine was prepared by dissolving 455 µmol (102 mg) in 10.2 mL of 0.2 M phosphate buffer at pH 7.1 (PB). In a second round bottom flask under argon, 174 mM of potassium ferricyanide (303 mg) were dissolved in 5.3 mL of PB. Both solutions were

purged with argon and protected from light. The potassium ferricyanide solution was added slowly to the solution of 3-hydroxy-D,L-kynurenine. The resulted reaction mixture was stirred at room temperature for 1 h 30 in darkness. Then, 10 mL of sulfurous acid diluted four times in PB was added. The final solution was brought to 4 °C for 30 min during which red flocculants formed. The suspension was then transferred into a 50 mL centrifuge tube. The round bottom flask was rinsed with 8 mL of sulfurous acid previously diluted four times in PB to ensure the complete reduction and flocculation of synthesized ommatins, as well as to remove ferrocyanide. The final suspension was centrifuged for 10 min at 10 000 × g and at 4 °C. The solid was desiccated overnight under vacuum over potassium hydroxide and phosphorus pentoxide. 104 mg of a reddish brown powder was obtained and kept at 4 °C in darkness until further use.

Solubilization and analyses of synthesized ommatins

A solution of synthesized ommatins at 1 mg/mL of was made in methanol acidified with 0.5 % HCl and pre-cooled at -20 °C (MeOH-HCl). The solution was mixed for 30 s and filtered on 0.45 µm filters. All steps were performed, as much as possible, at 4 °C in darkness. The overall procedure took less than two minutes. Immediately after filtration, the solution was subjected to absorption and mass spectrometry analysis (see below). The filtered solution was then stored at 20 °C in darkness and subjected to the same analysis 24 hours later.

Nuclear Magnetic Resonance (NMR) Spectroscopy

One milligram of synthesized product was solubilized in 600 µL of d6-DMSO acidified with 25 µL of TFA, as previously described (Kumar *et al.*, 2018; Williams *et al.*, 2019a). NMR spectra were recorded on Bruker AVANCE AV 300 instruments and the NMR experiment was reported in units, parts per million (ppm), using residual solvent peaks d6-DMSO (δ = 2.50 ppm) for ^{1}H NMR as internal reference. Multiplicities are recorded as: s = singlet, d = doublet, t = triplet, dd = doublet of doublets, m = multiplet, bs = broad singlet. Coupling constants (J) are reported in hertz (Hz).

^{1}H NMR (300 MHz, d6-DMSO + 0.04 % TFA) δ 8.37 (bs, 3H, H_1), 8.21 (bs, 1H, NH_8), 8.04 (t, *J* = 4.5 Hz, 1H, H_5), 7.83 - 7.82 (m, 2H, H_4, H_6), 7.69 (s, 1H, H_7), 6.67 (s, 1H, H_9), 4.46 - 4.42 (m, 1H, H_2), 3.89 (bs, 2H, H_3).

Ultra-Pressure Liquid Chromatography coupled to Diode-Array Detector and Electrospray Ionization Source-based Mass Spectrometer (UPLC-DAD-ESI-MS)

System

A reversed-phase ACQUITY UPLC® system coupled to a diode-array detector (DAD) and to a Xevo TQD triple quadrupole mass spectrometer (MS) equipped with an electrospray ionization source (ESI) was used (Waters, Milford, MA). Tandem mass spectrometry (MS/MS) was performed by collision-induced dissociation with argon. Data were collected and processed using MassLynx software, version 4.1 (Waters, Milford, MA).

Chromatographic conditions

Analytes were separated on a CSH™ C18 column (2.1 x 150 mm, 1.7 µm) equipped with a CSH™ C18 VanGuard™ pre-column (2.1 x 5 mm). The column temperature was set at 45 °C and the flow rate at 0.4 mL/min. The injection volume was 5 µL. The mobile phase consisted in a mixture of MilliQ water (eluent A) and acetonitrile (eluent B), both prepared with 0.1 % formic acid. The linear gradient was set from 2 % to 40 % B for 18 min.

Spectroscopic conditions

The MS continuously alternated between positive and negative modes every 20 ms. Capillary voltage, sample cone voltage (CV) and collision energy (CE) were set at 2 000 V, 30 V and 3 eV, respectively, for MS conditions. CE was set at 30 eV for tandem MS conditions. Cone and desolvation gas flow rates were set at 30 and 1 000 L/h, respectively. Absorption spectra of analytes were continuously recorded between 200 and 500 nm with a one-nm step. Analytes were annotated and identified according to their retention times, absorbance spectra, mass spectra and tandem mass spectra (**Table 4-1**).

Thermal reactivity of ommatins in acidified methanol in darkness

Conditions of solubilization and incubation

Solutions (n = 5) of synthesized ommatins at 1 mg/mL were prepared in MeOH-HCl. The solutions were mixed for 30 s and filtered on 0.45 µm filters. Aliquots of 50 µL were prepared for each sample and stored at either 20 °C or -20 °C in darkness. All steps were performed, as

much as possible, in darkness and at 4 °C. The overall procedure for each sample took less than two minutes. During the course of the experiment, each aliquot was analyzed only once by UPLC-ESI-MS/MS, representing a single time point for each sample.

Quantification of ommatins

Unaltered (*i.e.* xanthommatin and its decarboxylated form) and their methoxylated forms were detected and quantified by absorption and MS/MS (single reaction monitoring [MRM] mode) spectrometry. MRM conditions were optimized for each ommatin based on the following parent-to-product ion transitions: xanthommatin $[M+H]^+$ 424>361 *m/z* (CV 38 V, CE 25 eV), α^3-methoxy-xanthommatin $[M+H]^+$ 438>375 *m/z* (CV 37 V, CE 23 eV), α^3,α^{11}-dimethoxy-xanthommatin $[M+H]^+$ 452>375 *m/z* (CV 38 V, CE 25 eV), decarboxylated xanthommatin $[M+H]^+$ 380>317 *m/z* (CV 34 V, CE 28 eV) and decarboxylated α^{11}-methoxy-xanthommatin $[M+H]^+$ 394>317 *m/z* (CV 34 V, CE 28 eV). See **Figure S4-2** for detailed information on MS/MS optimization. Peak areas for both absorption and MRM signals were calculated by integrating chromatographic peaks with a "Mean" smoothing method (window size: ± 3 scans, number of smooths: 2). Absorbance values at 414 nm of unaltered ommatins were summed and reported as a percentage of the total absorbance of unaltered and methoxylated ommatins. The decay at -20 °C of uncyclized xanthommatin was followed by integrating both the absorbance at 430 nm and the 443 *m/z* SIR signals associated to the chromatographic peak of uncyclized xanthommatin at RT 6.7 min.

Extraction and content analysis of housefly eyes

Biological extractions

Five housefly (*M. domestica*) heads were pooled per sample (n = 5), weighted and homogenized in 1 mL MeOH-HCl with a tissue grinder (four metal balls, 300 strokes/min for 1 min). The obtained crude extracts were centrifuged for 5 min at 10 000 × g and 4 °C. The supernatants were filtered on 0.45 µm filters and immediately processed for absorption and MS analyses. All steps were performed, as much as possible, in darkness at 4 °C. The overall extraction procedure took less than 20 min.

Chromatographic profile

The chromatographic profile of housefly eyes that includes L-tryptophan, xanthurenic acid, 3-D,L-hydroxykynurenine, uncyclized xanthommatin, xanthommatin and decarboxylated xanthommatin is reported based on their optimized MRM signals. L-Tryptophan and xanthurenic acid were quantified based on their optimized MRM signals: $[M+H]^+$ 205>118 *m/z* (CV 26 V and CE 25 eV) and $[M+H]^+$ 206>132 *m/z* (CV 36 V and CE 28 eV), respectively. See **Figure S4-2** for detailed information on MS/MS optimization. 3-D,L-Hydroxykynurenine and uncyclized xanthommatin were quantified based on their absorption at 370 and 430 nm, respectively. L-Tryptophan, 3-D,L-hydroxykynurenine and xanthurenic acid levels were converted to molar concentrations using calibrated curves of commercial standards. Molar concentrations of uncyclized xanthommatin are reported as cinnabarinic equivalent, since both metabolites possess the same chromophore and presented similar absorbance spectra (see **Figure 4-5**C).

Purification and content analysis of ommochromasomes

Isolation protocol

Ommochromasomes from housefly eyes were purified as previously described (Cölln *et al.*, 1981), with slight modifications. The isolation buffer was prepared with MgCl2 instead of CaCl2, metrizamide was replaced by Nycodenz® (iohexol) and the final ultracentrifugation step was performed on Nycodenz layers solely since Nycodenz mixes with sucrose layers. See Supplemental File S1 for a more detailed protocol.

Extraction of ommochrome-related metabolites from purified ommochromasomes

Pellets (n = 5) were resuspended in 50 µL MeOH-HCl and directly subjected to UPLC-DAD-ESI-MS/MS analysis. All steps were performed, as much as possible, in darkness and at 4 °C. The overall extraction procedure took less than 2 min per sample.

Metabolic analysis of purified ommochromasomes

The chromatographic profile of purified ommochromasomes that includes L-tryptophan, xanthurenic acid, 3-D,L-hydroxykynurenine, uncyclized xanthommatin, xanthommatin, decarboxylated xanthommatin and β-mercaptoethanol-added ommatins is reported based on their optimized MRM signals. L-Tryptophan, 3-D,L-hydroxykynurenine, xanthurenic acid

and uncyclized xanthommatin were quantified as described for crude extracts of housefly eyes.

Statistical analysis

Statistical analyses were performed using the R software, version 3.4.1 (www.r-project.org). Statistical threshold was set to 0.05. For kinetic analyses, changes of metabolite quantities overtime were first tested by correlation tests assuming monotonic variations (Sperman's rank correlation test). Depending on the shape of the variation, either linear or logarithmic in this study, we performed linear regressions on either unchanged or log-scaled time points, respectively. For comparisons of two samples, we first assessed whether normality and homoscedasticity criteria were met with Shapiro-Wilkinson normality tests and Fligner-Killeen tests of homogeneity of variances, respectively. When data were heteroscedastic, we used Welch *t*-test rather than Student *t*-test. For multiple comparisons, we also tested normality and heteroscedasticity. Since the normality criteria was not met in that case, we performed a Kruskal-Wallis rank sum test followed by pairwise comparisons using a Wilcoxon rank sum test with the Holm adjustment method. Detailed results of all statistical analyses are reported in File S2.

Results

UPLC-DAD-MS/MS structural elucidation of synthesized xanthommatin and its in vitro *derivatives*

Since xanthommatin is commercially unavailable, we achieved its *in vitro* synthesis by oxidative condensation of 3-hydroxykynurenine under anoxia as previously reported (Butenandt *et al.*, 1954). ^{1}H-NMR spectroscopy on the product validated that the main synthesized compound was xanthommatin (see Material and Methods and **Figure S4-1**) (Williams *et al.*, 2019a). The synthesized product was then solubilized in methanol acidified with 0.5 % HCl (MeOH-HCl) and analyzed by Liquid Chromatography (LC) coupled to Diode-Array Detection (DAD) and Mass Spectrometry (MS) (**Figure 4-2**). The product was solubilized extemporaneously to avoid any chemical degradation before LC-DAD-MS analyses (**Figure 4-2**A, B). Chromatograms showed two main peaks corresponding to xanthommatin (retention time [RT]: 11.8 min, $[M+H]^+$ at *m/z* 424) and decarboxylated

xanthommatin (RT: 9.1 min, $[M+H]^+$ at *m/*z 380) (**Table 4-1**). Two co-eluting peaks were present in trace amounts at RT 8.5 and 11.9 min and were associated to $[M+H]^+$ at *m/*z 460 and $[M+H]^+$ at *m/*z 504, respectively. The detailed analysis of this sample enabled the detection of a small peak at RT 6.7 min ($[M+H]^+$ at *m/*z 443) with its corresponding chromatogram at 430 nm (**Figure 4-2**A). A detailed analysis of this particular compound is presented further in the text.

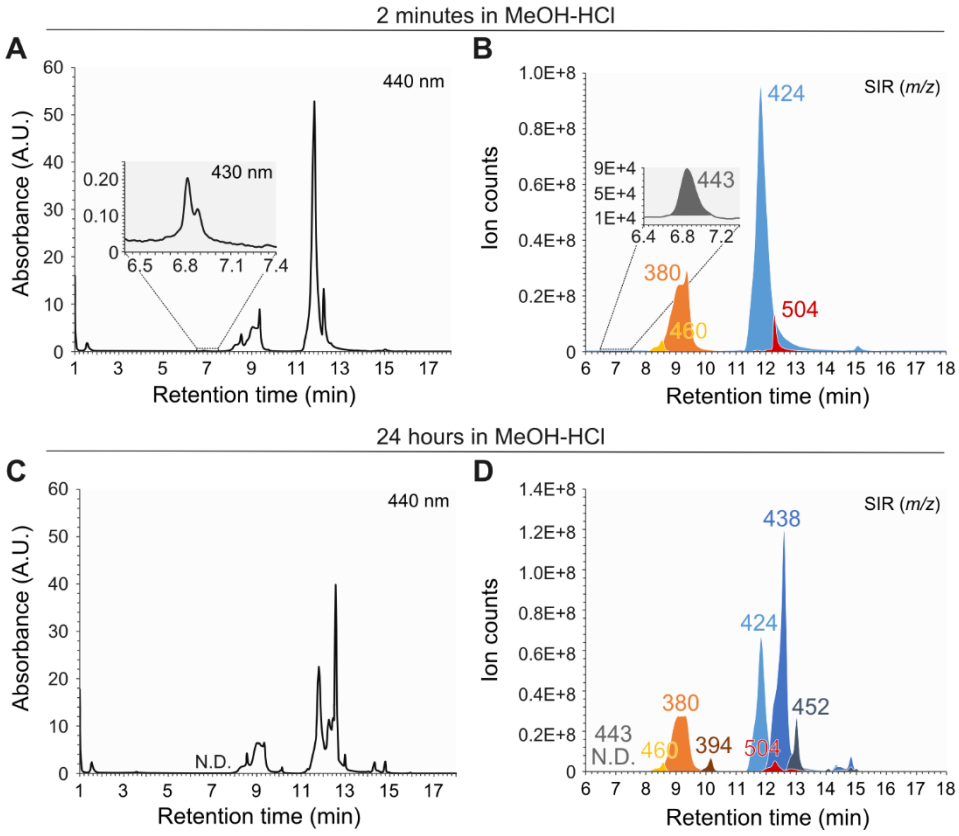

Figure 4-2. Chromatographic profiles of synthesized xanthommatin before and after storage in acidified methanol.

Xanthommatin was synthesized by oxidizing 3-hydroxykynurenine with potassium ferricyanide. **(A-B)** The ommatin solution was subjected to liquid chromatography (LC) two minutes after solubilization in methanol acidified with 0.5 % HCl (MeOH-HCl). The eluted compounds were detected by their absorbance at 440 and 430 nm (A). The main molecular ions (electrospray ionization in positive mode) associated to each peak were monitored by a triple quadrupole mass spectrometer running in single ion reaction (SIR) mode (B). **(C-D)** The same ommatin solution was left for 24 hours at 20 °C in complete darkness. Compounds were separated by LC and detected using the same absorbance (A) and MS modalities (B) as described above.

Table 4-1. Analytical characteristics of ommatin-related compounds found *in vitro* and in biological extracts.

Annotation (Formula, calculated MW)	**RT (min)**	**Absorbance peaks**	**Monocharged ions (*m/z* loss)**	**Double-charged ions (*m/z* loss)**	**MS/MS fragments (*m/z* loss)**
Detected in synthesized ommatins, crude extracts of housefly eyes and ommochromasome extracts					
3-Hydroxykynurenine ($C_{10}H_{12}N_2O_4$, 224.21)	1.6	231; 264; 376	224.9 $[M+H]^+$; 207.9 (-17); 161.9 (-63); 152.0 (-73)	Not detected	207.7 (-17); 161.9 (-63)
Uncyclized xanthommatin ($C_{20}H_{18}N_4O_8$, 442.38)	6.7	235; 420-450	442.9 $[M+H]^+$; 425.9 (-17); 408.8 (-34); 353.0 (-90)	213.6 $[M-17+2H]^{2+}$	425.9 (-17); 409.0 (-34); 390.9 (-52); 363.1 (-80); 353.0 (-90); 344.9 (-98); 335.1 (-108); 317.0 (-126); 307.0 (-136)
Xanthommatin ($C_{20}H_{13}N_3O_8$, 423.33)	11.8	234; 442	423.9 $[M+H]^+$; 406.8 (-17); 377.9 (-46); 350.9 (-73)	212.5 $[M+2H]^{2+}$; 189.5 (-23)	406.3 (-17; -18); 360.7 (-63); 350.8 (-73); 316.8 (-107); 304.8 (-119); 288.9 (-135)
Decarboxylated xanthommatin ($C_{19}H_{13}N_3O_6$, 379.32)	9.1	234; 442	379.9 $[M+H]^+$; 362.9 (-17); 333.9 (-46); 306.9 (-73)	190.5 $[M+2H]^{2+}$; 167.5 (-23)	362.7 (-17; -18); 333.7 (-46); 316.8 (-63); 306.8 (-73); 290.9 (-89)
Only detected in synthesized ommatins					
Xanthommatin sulphate/phosphate ester ($C_{20}H_{13}N_3O_{11}S$, 503.40; $C_{20}H_{14}N_3O_{11}P$, 503.31)	12.4	236; 445	503.9 $[M+H]^+$; 453.6 (-50); 430.5 (-73?); 379.8 (-124); 350.7 (-153)	252.5 $[M+2H]^{2+}$; 229.5 (-23)	487.0 (-17); 440.6 (-63); 430.8 (-73); 422.8 (-81); 396.5 (-107?); 384.9 (-119)
Decarboxylated xanthommatin sulphate/phosphate ester ($C_{19}H_{13}N_3O_9S$, 459.39; $C_{19}H_{14}N_3O_9P$, 459.30)	8.5	236; 443	459.8 $[M+H]^+$; 442.8 (-17); 413.8 (-46); 386.7 (-73)	230.4 $[M+2H]^{2+}$; 207.4 (-23)	442.8 (-17); 413.7 (-46); 396.8 (-63); 386.8 (-73)
Detected in synthesised ommatins incubated in MeOH-HCl in darkness					
α^3-Methoxy-xanthommatin ($C_{21}H_{15}N_3O_8$, 437.36)	12.6	217; 303; 452	437.9 $[M+H]^+$; 420.9 (-17); 391.9 (-46); 364.9 (-73)	219.4 $[M+2H]^{2+}$; 196.5 (-23)	420.7 (-17); 391.8 (-46); 374.8 (-63); 364.8 (-73); 314.8 (-123); 304.8 (-133)
α^3, α^{11}-Dimethoxy-xanthommatin ($C_{22}H_{17}N_3O_8$, 451.39)	13.0	217; 303; 452	451.9 $[M+H]^+$; 434.9 (-17); 391.9 (-60); 364.9 (-87)	226.5 $[M+2H]^{2+}$; 196.4 (-30)	434.9 (-17); 374.8 (-77); 364.9 (-87); 314.8 (-137); 304.8 (-147)
Decarboxylated α^{11}-methoxy-xanthommatin ($C_{20}H_{15}N_3O_6$, 393.35)	10.1	234; 442	393.9 $[M+H]^+$; 376.9 (-17); 333.9 (-60); 307.0 (-87)	197.6 $[M+2H]^{2+}$; 167.4 (-30)	376.7 (-17; -18); 333.8 (-60); 316.8 (-77); 306.9 (-87); 290.9 (-105)
Unknown altered xanthommatin (455)	14.4	242; 442	455.9 $[M+H]^+$	228.4 $[M+2H]^{2+}$; 205.4 (-23)	340.1 (-116); 324.6 (-131?); 295.0 (-161); 205.2 (-251)
Unknown altered methoxy-xanthommatin (469)	14.9	243; 390; 452	469.8 $[M+H]^+$	235.5 $[M+2H]^{2+}$; 212.4 (-23)	353.7 (-116); 338.8 (-131); 294.7 (-175); 204.8 (-265)
Unknown altered dimethoxy-xanthommatin (483)	15.0	242; 388; 450	484.0 $[M+H]^+$	242.5 $[M+2H]^{2+}$; 212.5 (-30)	353.9 (-130); 338.8 (-145); 294.8 (-189); 204.9 (-279)
Detected in synthesized ommatins incubated with β-mercaptoethanol in darkness and in ommochromasome extracts					
β-mercaptoethanol-added xanthommatin ($C_{22}H_{17}N_3O_9S$, 499.45)	11.7	238; 415	499.9 $[M+H]^+$; 426.8 (-73)	250.4 $[M+2H]^{2+}$; 227.5 (-23); 218.4 (-32)	482.7 (-17); 464.7 (-35)
β-mercaptoethanol-added decarboxylated xanthommatin ($C_{21}H_{17}N_3O_7S$, 455.44)	9.1	232; 412	455.9 $[M+H]^+$; 420.0 (-36); 382.8 (-73); 343.8 (-112)	228.4 $[M+2H]^{2+}$; 205.4 (-23); 196.5 (-32)	438.8 (-17); 421.0 (-35); 392.7 (-63)

With the aim to produce more ommatins and thus manipulate their molecular structure, we incubated synthesized ommatins for 24 h in MeOH-HCl at 20 °C in darkness (**Figure 4-2**C, D). Based on previous studies (Bolognese & Liberatore, 1988), we expected ommatins to get methoxylated, mainly on their carboxylic acid functions. The comparative analysis of **Figure 4-2**A, B (2 minutes in MeOH-HCl) and **Figure 4-2**C, D (24 h later) highlights different sets of peaks that appeared or disappeared over the 24 h of incubation. Three major newly formed compounds were observed at RT 10.1, 12.6 and 13 min corresponding to $[M+H]^+$ at *m/z* 394, 438 and 452, respectively. We compared the UV and MS characteristics of these compounds with those of xanthommatin and decarboxylated xanthommatin. Absorbance spectra of the five compounds revealed strong similarities, particularly in the visible region (> 400 nm, **Figure 4-3**A) suggesting that these three newly formed molecules shared their chromophores with xanthommatin and decarboxylated xanthommatin. Mass spectra of the five compounds also showed strong similarities (**Figure 4-3**B). They all experienced an in-source neutral loss of -17 *m/z* ($-NH_3$) and formed a double-charged molecular ion $[M+2H]^{2+}$. 452 and 394 *m/z*-associated compounds typically lost 14 units more than xanthommatin and decarboxylated xanthommatin, respectively, during in-source fragmentation. Additionally, their double-charged fragmentations were 7 units higher than for xanthommatin and decarboxylated xanthommatin (= 14/2; **Figure 4-3**B). Overall, gains of 14 *m/z* in the newly formed compounds compared to xanthommatin and decarboxylated xanthommatin suggested methylation reactions occurring in acidic methanol.

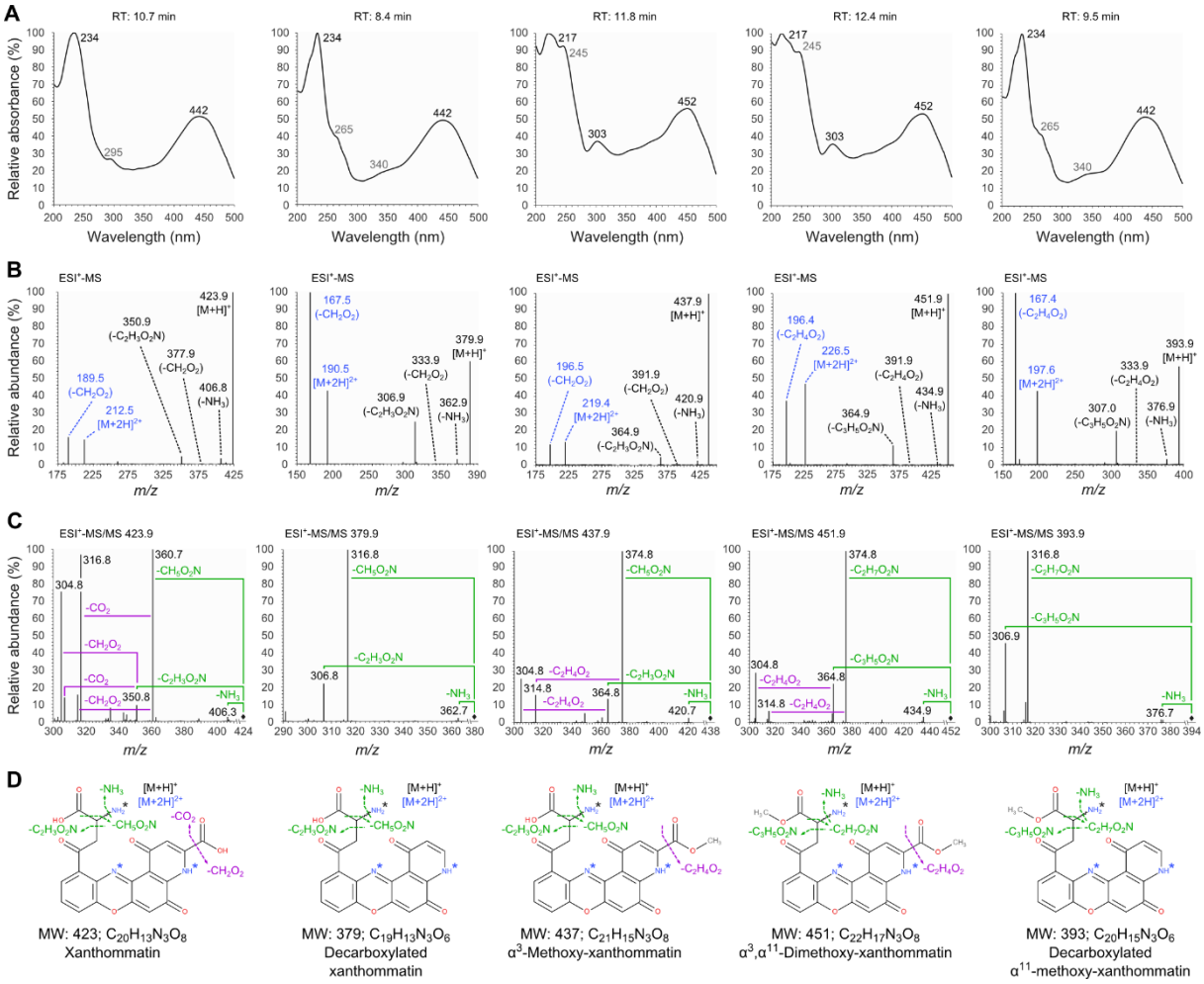

Figure 4-3. Absorbance- and mass spectrometry-assisted elucidation of the structure of the five major ommatins detected after incubation in acidified methanol.
Ommatins incubated for 24 hours in acidified methanol were analysed by liquid chromatography coupled to a photodiode-array detector and a triple quadrupole mass spectrometer. (A) Absorbance spectra. For each metabolite, absorbance values were reported as percentages of the maximum absorbance value recorded in the range of 200 to 500 nm. Major and minor absorbance peaks are indicated in black and grey fonts, respectively. (B) Mass spectra showing molecular ions and in-source fragments. Black fonts, monocharged ions. Blue fonts, double-charged molecular ions. (C) Tandem mass (MS/MS) spectra of molecular ions obtained by collision-induced dissociation with argon. Black diamonds, $[M+H]^+$ *m/z*. Green fonts, fragmentations of the amino acid chain. Purple fonts, fragmentations of the pyridine ring are indicated. (D) Elucidated structures of the five ommatins. MS/MS fragmentations are reported in green and purple like in panel C. Black asterisk, main charged basic site. Blue asterisks, potential charged basic sites of the double-charged molecular ions.

Because we did not succeed in purifying each compound to analyze them separately by NMR spectroscopy, we subjected the main $[M+H]^+$ to MS/MS fragmentation and compared it with previously reported fragmentation patterns of kynurenine, 3-hydroxykynurenine, xanthommatin and decarboxylated xanthommatin (Vazquez *et al.*, 2001; Williams *et al.*, 2016; Guijas *et al.*, 2018; Panettieri *et al.*, 2018; Reiter *et al.*, 2018)

(http://metlin.scripps.edu, METLIN ID: 365). In these molecules, the main ionization site is the amine function of the amino acid branch, which is also the most susceptible to fragmentation. For both xanthommatin and decarboxylated xanthommatin, we observed similar patterns of fragmentation of the amino acid branch with three neutral losses corresponding to $-NH_3$ (-17 *m/z*), $-CH_5O_2N$ (-63 *m/z*) and $-C_2H_3O_2N$ (-73 *m/z*) (**Table 4-1**). Those fragmentations have been reported for these two ommatins (Williams *et al.*, 2016; Panettieri *et al.*, 2018; Reiter *et al.*, 2018), as well as for kynurenines (Vazquez *et al.*, 2001), indicating that they are typical of compounds with a kynurenine-like amino acid chain. Additionally, two neutral losses corresponding to $-CO_2$ (-44 *m/z*) and $-CH_2O_2$ (-46 *m/z*) were observed only for xanthommatin (**Figure 4-3**C) due to the presence of the carboxyl function on the pyridine ring (**Figure 4-3**D). We categorized those predictable MS fragments into different successive fragmentation signatures called F_A to F_E (**Table 4-2**) and we used them to assign the structure of unknown ommatins. The fragmentation of $[M+H]^+$ 394 *m/z* showed neutral losses corresponding to $-NH_3$ (-17 *m/z* = F_A), $-C_2H_7O_2N$ (-77 = -63 -14 *m/z* = $F_A + F_B + F_C - CH_2$) and $-C_3H_5O_2N$ (-87 = -73 -14 *m/z* = $F_A + F_B + F_C + F_D - CH_2$) on the amino acid branch. These results strongly indicated that, in the 394 *m/z*-associated compound, the carboxyl function of the amino acid branch was methoxylated (α^{11} position). Consequently, this compound was assigned to decarboxylated α^{11}-methoxy-xanthommatin (**Figure 4-3**C). Those conclusions are in accordance with the similar absorbance spectra of decarboxylated α^{11}-methoxy-xanthommatin and decarboxylated xanthommatin (**Figure 4-3**A), as the amino acid branch is unlikely to act on near-UV and visible wavelength absorptions of the chromophore. The fragmentation of $[M+H]^+$ 438 *m/z* showed the xanthommatin-like neutral losses, $-NH_3$ (-17 *m/z* = F_A), $-CH_5O_2N$ (-63 *m/z* = $F_A + F_B + F_C$) and $-C_2H_3O_2N$ (-73 *m/z* = $F_A + F_B + F_C + F_D$), highlighting that this compound shared the same unaltered amino acid branch with xanthommatin. However, this compound experienced the neutral loss $-C_2H_4O_2$ (-60 = -46 -14 *m/z* = $F_E - CH_2$) on the pyridine ring instead of $-CH_2O_2$ (-46 *m/z* = F_E) (**Figure 4-3**C), which strongly indicated a methoxylation on the pyrido-carboxyl group (α^3 position). This is in accordance with the associated absorbance spectrum being different from that of xanthommatin, which has a carboxylated chromophore (**Figure 4-3**A). Hence, we proposed that this compound was α^3-methoxy-xanthommatin (**Figure 4-3**D). The 452 *m/z*-associated compound showed neutral losses corresponding to $-NH_3$ (-17 *m/z* = FA), $-C_2H_7O_2N$ (-77 *m/z* = $F_A + F_B + F_C - CH_2$) and $-C_3H_5O_2N$ (-87 *m/z* = $F_A + F_B + F_C + F_D - CH_2$) on the amino acid

branch and -$C_2H_4O_2$ (-60 *m/z* = F_D - CH_2) on the pyridine ring, which strongly indicated methoxylations on both pyridine ring and amino acid branch in positions α^3 and α^{11}, respectively. This is in accordance with the associated absorbance spectrum being similar to that of α^3-methoxy-xanthommatin, which has a methoxylated chromophore. Thus, we proposed this compound to be α^3,α^{11}-dimethoxy-xanthommatin (**Figure 4-3**D). Overall, such positions of methoxylation agree well with the reactivity of ommatins in MeOH-HCl (Bolognese & Liberatore, 1988).

Table 4-2. Diagnostic neutral losses of ommatins.

Annotation	Fragmented structure	Neutral loss	*m/z* loss
F_A	Amino acid	-NH_3	-17
F_B	Amino acid	-H_2O	-18
F_C	Amino acid	-CO	-28
F_D	Amino acid	-C+2H	-10
F_E	Pyridine ring	-CO_2H	-46

Using the same DAD-MS combination approaches, we annotated other ommatin-like compounds produced during *in vitro* synthesis and after incubation in MeOH-HCl (**Table 4-1**). The 504 and 460 *m/z*-associated compounds differed from xanthommatin and decarboxylated xanthommatin by 80 Da, respectively. The associated double-charged ions $[M+2H]^{2+}$ and $[M-CH_2O_2+2H]^{2+}$ accordingly differed by 40 *m/z* from those of xanthommatin and decarboxylated xanthommatin, respectively. Their absorbance spectra were identical to the two ommatins. Their MS and MS/MS spectra revealed identical losses to xanthommatin and decarboxylated xanthommatin: -NH_3 (-17 *m/z* = F_A), -CH_2O_2 (-46 *m/z* = F_D), -CH_5O_2N (-63 *m/z* = F_A + F_B + F_C) and -$C_2H_3O_2N$ (-73 *m/z* = F_A + F_B + F_C + F_D; see **Table 4-2**). Furthermore, the $[M+H]^+$ 504 *m/z* experienced the same neutral losses -$C_2H_5O_4N$ (-107 m/z) and -$C_3H_5O_4N$ (-119 *m/z*) than xanthommatin. Alternatively, the $[M+H]^+$ 504 *m/z* experienced a unique in-source neutral loss of -153 *m/z* that could correspond to -$C_2H_3O_5NS$ or -$C_2H_4O_5NP$ (-73 -80 *m/z*). All those results suggested that the 504 and 460 *m/z*-associated compounds were sulphate or phosphate esters of xanthommatin and decarboxylated

xanthommatin, respectively. This in accordance with the use of phosphate buffer for the *in vitro* synthesis and of sulfurous acid to precipitate ommatins. To our knowledge, these two esters have never been described. Finally, during the incubation in MeOH-HCl, minor ommatin-like compounds (classified as ommatins based on their absorbance and the presence of double-charged ions) were formed and were associated to the 456, 470 and 484 *m/z* (**Table 4-1**). The differences of 14 units of their respective molecular ion *m/z*, as well as their neutral losses in MS/MS being either similar or differing by 14 units, indicated that they were methylated versions of each other. However, due to their very low amounts, we could not unambiguously propose a structure.

These results showed that, in storage conditions mimicking extraction procedures with MeOH-HCl, xanthommatin and its decarboxylated form are methoxylated, even in darkness. Those reactions are likely to result from solvent additions with acidified MeOH-HCl (the most efficient solvent for ommatin extraction). To further characterize the importance of those artifactitious reactions, we followed the kinetic of the five ommatins described in **Figure 4-3**D in MeOH-HCl at 20 °C and in darkness.

The ommatin profile is rapidly and readily modified overtime by artifactitious methoxylations in acidified methanol

Because absorbance spectra of all five considered compounds did not differ significantly and because some of them were co-eluted (**Figure 4-2**), their detection and quantification were performed by MS/MS in multiple reaction monitoring (MRM) mode. MRM conditions were independently optimized for each compound based on the fragmentation of their amino acid branch (**Figure S4-2**).

The MRM signal of xanthommatin rapidly decreased overtime in a linear fashion, with a near 40 % reduction after only one day of incubation (**Figure 4-4**A). On the contrary, the MRM kinetics of α^3-methoxy-xanthommatin had a logarithmic-shape, sharply increasing during the first day before reaching a plateau during the two following days (**Figure 4-4**B). Both decarboxylated α^{11}-methoxy-xanthommatin and α^3,α^{11}-dimethoxy-xanthommatin appeared after a few hours of incubation. Their MRM signal then linearly increased overtime (**Figure 4-4**C, E). In parallel, the MRM signal of decarboxylated xanthommatin stayed nearly constant, with only a small increase by 1.13 % over the five first hours (**Figure 4-4**D). Those

results further validate that xanthommatin was readily methoxylated in darkness, primarily in position α^3. A slower methoxylation on the amino acid branch could account for the delay in the appearance of the two other methoxylated forms. The levels of decarboxylated xanthommatin did not vary much overtime although its methoxycarbonyl ester was produced (**Figure 4-4**D, E). This result could be explained by the concomitant and competitive slow decarboxylation of xanthommatin, a reaction that has already been described in MeOH-HCl upon light radiations (Bolognese *et al.*, 1988b).

Because we cannot compare MRM signal intensities of different molecules, we took benefit of their similar absorption in the visible region, especially at 414 nm (**Figure 4-3**A**Figure S4-3**), to quantify their relative amounts. Although less sensitive and less specific than MRM-based detection, the absorbance at 414 nm strongly indicated that, after only one day of incubation, one third of ommatins was methoxylated (**Figure 4-4**F). Most of the methoxylated ommatins accumulated during the first 24 hours (**Figure 4-4**B). As expected, rates of methoxylation were significantly decreased by incubating synthesized ommatins in MeOH-HCl at -20 °C (**Figure S4-4**A, B). After storage of a month at -20 °C, the methoxylated ommatins represented nearly 1.2 % of ommatins (**Figure S4-4**C).

To conclude, our results showed that decarboxylated xanthommatin was mostly stable in MeOH-HCl. By contrast, xanthommatin was rapidly converted into methoxylated derivatives. Since, MeOH-HCl is the most efficient solvent for ommatin extraction, the conditions for extraction and analysis of ommatins from biological samples should avoid wherever possible the formation of artifactitious methoxylated ommatins.

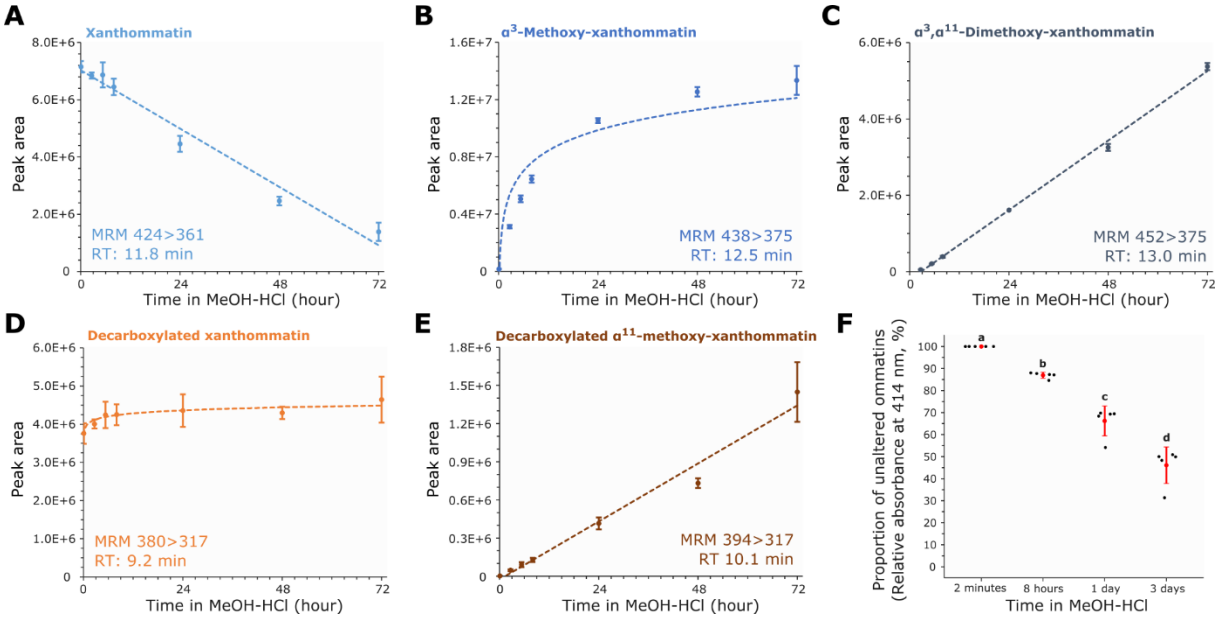

Figure 4-4. Alterations of synthesized ommatins in acidified methanol at 20 °C in darkness.
Synthesized ommatins were solubilized in methanol acidified with 0.5 % HCl (MeOH-HCl) and stored for up to three days at 20 °C and in complete darkness. **(A-E)** Kinetics of alterations were followed by multiple reaction monitoring (MRM) mode of xanthommatin (A), α^3-methoxy-xanthommatin (B), α^3,α^{11}-dimethoxy-xanthommatin (C), decarboxylated xanthommatin (D) and decarboxylated α^{11}-xanthommatin (E). Values are mean ± SD of four to five samples. (A) Linear regression (R^2 = 0.96, F = 813.5, df = 1 and 32, p-value < 2.2e-16). (B) Linear regression with log-scaled time (R^2 = 0.83, F = 159.8, df = 1 and 32, p-value = 5.5e-14). (C) Linear regression (R^2 = 0.98, F = 1665, df = 1 and 32, p-value < 2.2e-16). (D) Linear regression with log-scaled time (R^2 = 0.35, F = 17.16, df = 1 and 32, p-value = 0.00023). (E) Linear regression (R^2 = 0.95, F = 651.2, df = 1 and 32, p-value < 2.2e-16). **(F)** Relative quantifications of methoxylated ommatins compared to unaltered ones (i.e. xanthommatin and decarboxylated xanthommatin) were performed by measuring the absorbance of ommatins at 414 nm for each time point. Values are mean ± SD of five samples. Different letters indicate statistical differences (Kruskal-Wallis rank sum test: χ^2 = 17.857, df = 3, p-value = 0.00047; pairwise comparisons using Wilcoxon rank sum test and Holm adjustment: p-values < 0.05).

UPLC-DAD-MS/MS structural elucidation of uncyclized xanthommatin, the labile intermediate in the synthesis of ommatins from 3-hydroxykynurenine

The *in vitro* synthesis of xanthommatin by oxidizing 3-hydroxykynurenine additionally yielded a minor compound at RT 6.7 min. It was characterized by a peak of absorbance at 430 nm and was associated to the 443 *m/z* feature (**Figure 4-2**A, B). Upon solubilization in MeOH-HCl, the unidentified compound was labile and disappeared after the 24h-incubation at 20 °C in darkness (**Figure 4-2**C, D). A similar 443 *m/z* feature was described two decades ago during oxidations of 3-hydroxykynurenine in various conditions (Iwahashi & Ishii, 1997). Based on its MS spectrum, it was assigned putatively to the 3-hydroxykynurenine dimer called uncyclized xanthommatin. However, there was a lack of analytical evidence to support

its structural elucidation. No study has ever since reported the presence of uncyclized xanthommatin, either *in vitro* or *in vivo*. Because this compound could be an important biological intermediate in the formation of ommatins (Bolognese *et al.*, 1988b; Iwahashi & Ishii, 1997), we further characterized its structure based on its chemical behavior, absorbance and fragmentation pattern. We note that the apparent lability and the very low amounts of this unidentified product precluded its characterization by NMR spectroscopy.

The absorbance and MS kinetics of the unidentified synthesized compound showed that it was very labile (insets of **Figure 4-5**A, B). Indeed, we could not detect it after a week of storage at -20 °C anymore. This behavior resembled that of a photosensitive ommatin-like isolated 40 years ago from several invertebrates, which rapidly turned into xanthommatin after extraction (Bolognese & Scherillo, 1974). The absorbance spectrum of this unidentified compound matched almost exactly the UV-Visible spectrum of cinnabarinic acid measured in the same conditions (**Figure 4-5**C), and both are similar to those reported for actinomycin D and 2-amino-phenoxazin-3-one (Nakazawa *et al.*, 1981). This result indicated that this compound contained the amino-phenoxazinone chromophore rather than the pyrido[3,2-*a*]phenoxazinone scaffold of ommatins or the *ortho*-aminophenol core of 3-hydroxykynurenine. Furthermore, its ionization pattern revealed striking similarities with ommatins. Along with the molecular ion $[M+H]^+$ at 443 *m/z* (corresponding to MW 442 and to the formula $C_{20}H_{18}N_4O_8$), we detected the double-charged ion $[M-NH_3+2H]^{2+}$ at 213.6 *m/z* (**Figure 4-5**D). We then targeted the molecular ion for MS/MS to compare the obtained fragments with those reported above (**Table 4-2**). If the compound was uncyclized xanthommatin, we predicted that F_A, F_B, F_C and F_D would appear each twice, because uncyclized xanthommatin possesses two 3-hydroxykynurenine-like amino acid chains. Only F_E should be absent, because no aromatic carboxylic acid exist in uncyclized xanthommatin. Indeed, from two MS^2 spectra obtained at different collision energies, we could assign each F_X twice and we did not find any fragmentation event corresponding to F_E. Hence, by starting from the amino-phenoxazinone backbone suggested by the UV-Visible spectrum, the uncyclized form of xanthommatin could be reconstructed after adding each F_{Xx} successively (**Figure 4-5**F).

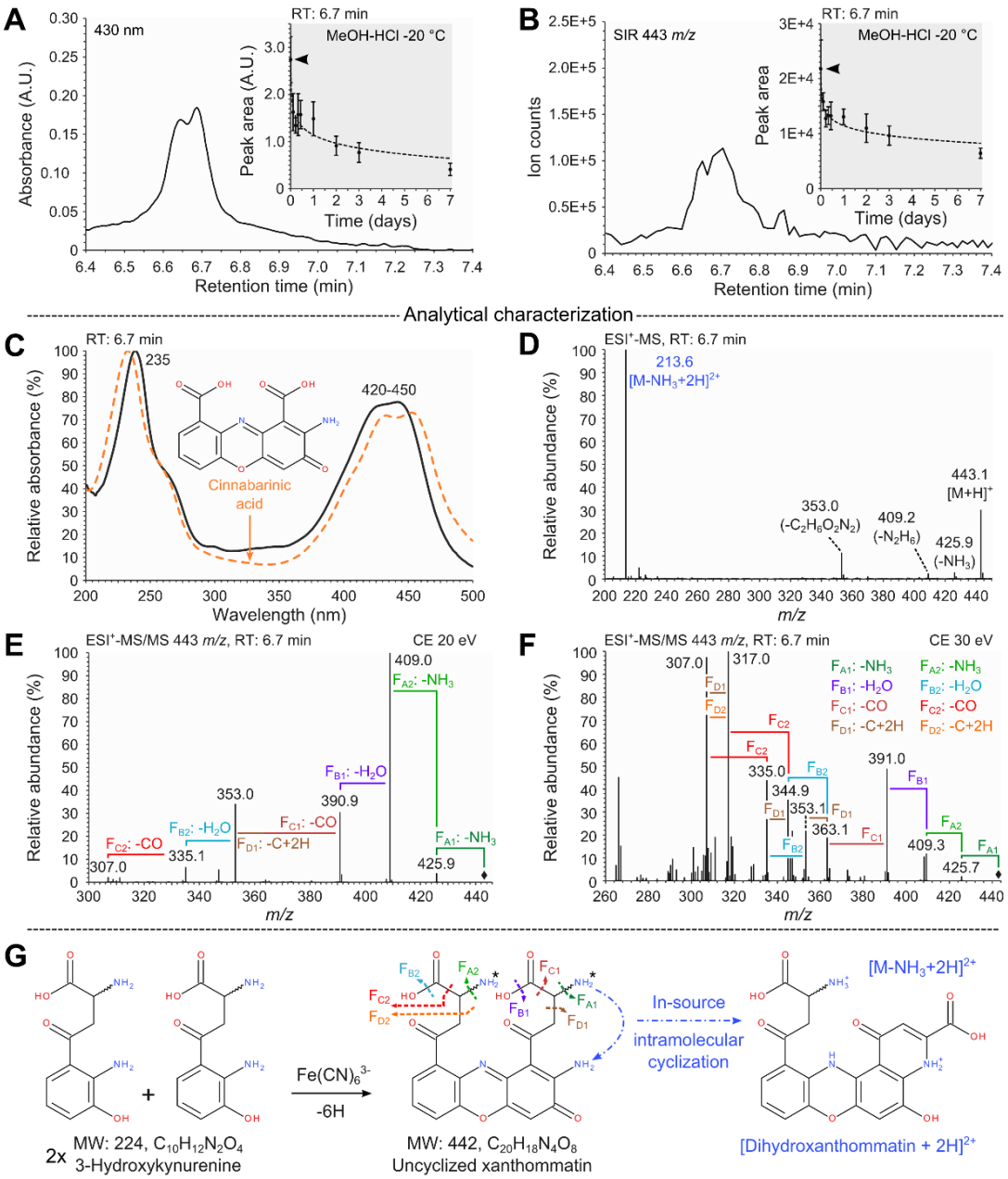

Figure 4-5. Structural elucidation of uncyclized xanthommatin, the labile intermediate in the synthesis of xanthommatin.

(A-B) Chromatographic peaks (absorbance at 430 nm [A] and $[M+H]^+$ 443 m/z recorded in single ion reaction [SIR] mode [B]) corresponding to the labile ommatin-like compound detected in in vitro synthesis of xanthommatin by the oxidation of 3-hydroxkynurenine with $Fe(CN)_6^{3-}$. Insets show the decay of chromatographic peaks during storage in methanol acidified with 0.5 % HCl at -20 °C in darkness. Values are mean ± SD of five samples. (A) Linear regression with log-scaled time (R^2 = 0.75, F = 131.4, df = 1 and 43, p-value = 1.2e-14). (B) Linear regression with log-scaled time (R^2 = 0.72, F = 111.5, df = 1 and 43, p-value = 1.6e-13). **(C)** Absorbance spectra. Solid line, labile ommatin-like compound. Dashed line, the aminophenoxazinone cinnabarinic acid. **(D)** Mass spectrum showing molecular ions and in-source fragments. Black fonts, monocharged ions. Blue font, double-charged ion. **(E-F)** Tandem mass spectra of the molecular ion obtained by collision-induced dissociation with argon at collision energies of 20 eV (E) and 30 eV (F). Fragmentations were classified in four types (F_A to F_D) that occurred twice (F_{X1} and F_{X2}). Black diamonds, $[M+H]^+$ *m/z*. **(G)** Evidence

for the structural elucidation of uncyclized xanthommatin. Colors of the MS/MS fragmentation pattern correspond to those in panels D-F. Black asterisks, potential charged basic sites.

All these analytical characteristics strongly supported that this labile compound was the phenoxazinone dimer of 3-hydroxykynurenine (**Figure 4-5**G), called uncyclized xanthommatin (Figon & Casas, 2019). This structural assignment was further supported by the two following chemical behaviors. First, the oxidation of an *ortho*-aminophenol (here 3-hydroxykynurenine) by potassium ferricyanide is known to induce its dimerization through the loss of six electrons and protons (here 2x $MW_{3\text{-hydroxykynurenine}}$ [224 Da] - 6 Da = MW_{dimer} [442 Da] = $MW_{Uncyclized\ xanthommatin}$). Second, the spontaneous intramolecular cyclization involving the amine functions of the amino-phenoxazinone core and the closest amino acid branch could explain the lability of uncyclized xanthommatin in cold MeOH-HCl (insets of **Figure 4-5**A, B) (Williams *et al.*, 2019a), as well as the formation of a major double-charged ion corresponding to that of the reduced form of xanthommatin (dihydroxanthommatin; **Figure 4-5**G and **Figure S4-5**). The lability of uncyclized xanthommatin questions how we could detect it. We believe there are three main reasons. First, our UHPLC-DAD-MS approach use some of the most sensitive analytical techniques so far. Second, we used rather concentrated samples that allowed us to inject it in sufficient amounts for chromatography, despite the steep decrease in uncyclized xanthommatin during the first hours after extraction. Third, abiotic and biotic factors likely stabilize uncyclized xanthommatin before and during extraction. In particular, we kept all extraction steps at 4 °C and in the darkness as much as possible to avoid increased rates of cyclization (Bolognese & Scherillo, 1974; Bolognese *et al.*, 1988a). Furthermore, ommochromes are known to bind to specific proteins, such as ommochrome binding protein and reflectins, which protect them from degradation (Williams *et al.*, 2019b); it is therefore possible that uncyclized xanthommatin is stabilized in vivo by binding to proteins. In conclusion, we have now the tools to identify uncyclized xanthommatin in other samples, particularly biological materials.

Biological localization of the metabolites from the tryptophan→ommochrome pathway

Using our chemical and analytical knowledge of synthesized ommatins, we reinvestigated the content of housefly eyes in ommochromes and their related metabolites. We chose this species because it is known to accumulate xanthommatin and some metabolites of the kynurenine pathway in its eyes (Linzen, 1974). However, nothing is known about

decarboxylated xanthommatin and uncyclized xanthommatin because they were recently described [(Figon & Casas, 2019) and this study], even though the presence of uncyclized xanthommatin has been suspected (Bolognese & Scherillo, 1974). Furthermore, a protocol to extract and purify ommochromasomes from housefly eyes is available (Cölln *et al.*, 1981), thus we can address the question of the localization of the metabolites from the tryptophan→ommochrome pathway. Finally, we designed an extraction protocol in which all steps were performed in darkness, at low temperature and in less than half an hour. In those conditions, we were confident that artifactitious methoxylated ommatins would represent less than one percent of all ommatins and that we could still detect uncyclized xanthommatin.

Based on MRM signals, we detected in methanolic extractions of housefly eyes (called crude extracts; **Figure 4-6**A) the following metabolites of the tryptophan→ommochrome pathway: tryptophan, 3-hydroxykynurenine, xanthurenic acid, xanthommatin, decarboxylated xanthommatin and uncyclized xanthommatin (**Figure 4-6**B, **Table 4-1**). We ascertained the identification of uncyclized xanthommatin by acquiring its absorbance, MS and MS/MS spectra in biological samples. They showed the same features as synthesized uncyclized xanthommatin (**Figure S4-6**).

We then purified ommochromasomes from housefly eyes by a combination of differential centrifugation and ultracentrifugation, and we compared the extracted compounds with those of crude extracts (**Figure 4-6**A). The main metabolites of ommochromasomes were xanthommatin and its decarboxylated form (**Figure 4-6**D), in accordance to the function of ommochromasomes as ommochrome factories (Figon & Casas, 2019). Based on the absorbance at 414 nm, decarboxylated xanthommatin represented 5.3 ± 0.1 % (mean ± SD, n = 5) of all ommatins detected in extracts of ommochromasomes. In comparison, decarboxylated ommatins represented 21.5 ± 0.2 % (mean ± SD, n = 10) of all ommatins synthesized *in vitro*, a percentage four times higher than in methanolic extracts of purified ommochromasomes (Welch two sample *t*-test, t = 219.99, df = 12.499, p-value < $2.2e^{-16}$). Regarding the precursors of ommochromes in housefly eyes, we could only detect tryptophan and 3-hydroxykynurenine but not the intermediary kynurenine. Tryptophan remained undetectable in extracts of ommochromasomes (**Figure 4-6**D). Xanthurenic acid, the product of 3-hydroxykynurenine transamination, was particularly present in crude extracts of housefly eyes but much less in ommochromasomes relatively to 3-hydroxykynurenine (**Figure 4-6**C

vs. **Figure 4-6**E). We also detected the uncyclized form of xanthommatin in ommochromasomes (**Figure 4-6**D). We calculated an enrichment ratio of 3-hydroxykynurenine compared to either xanthurenic acid or uncyclized xanthommatin in both crude and ommochromasome extracts, allowing a meaningful comparison between xanthurenic acid and uncyclized xanthommatin in the two extracts. The lower this enrichment ratio is, the more xanthurenic acid or uncyclized xanthommatin is present in the extract. We found that xanthurenic acid was more enriched in crude extracts (mean enrichment of 2.1) than in ommochromasomes (mean enrichment of 11; Student's *t*-test, t = -8.88, df = 8, p-value = $2.04e^{-5}$), while uncyclized xanthommatin was more enriched in ommochromasomes (mean enrichment of 6.2) than in crude extracts (mean enrichment of 21; Student's *t*-test, t = 5.71, df = 8, p-value = 0.00045).

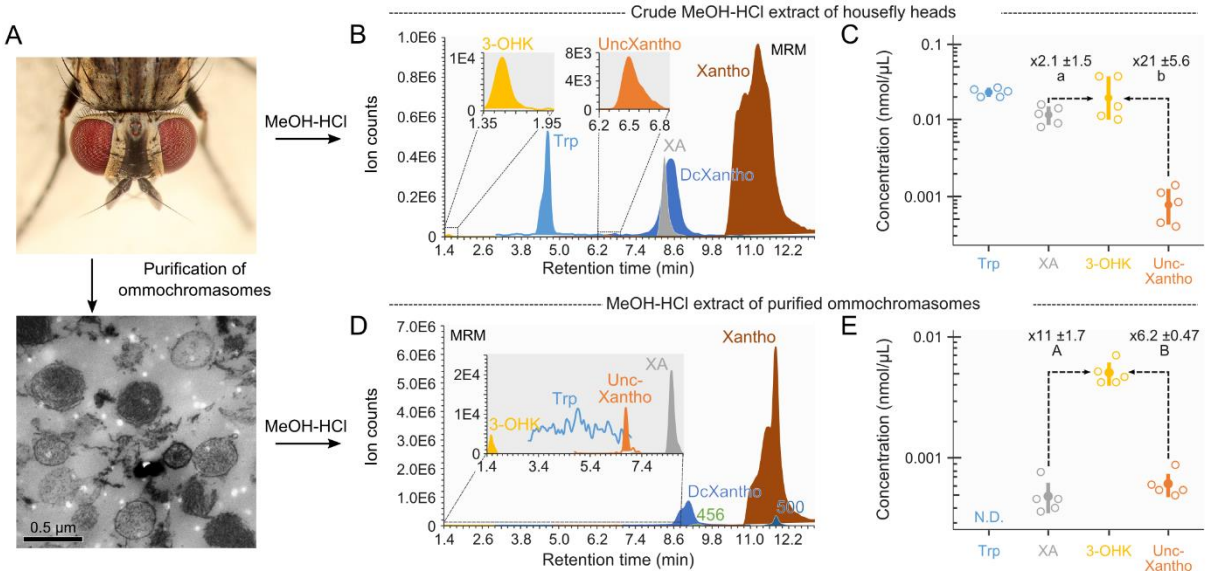

Figure 4-6. Biological localization of uncyclized xanthommatin and tryptophan→ommochrome metabolites from housefly eyes.

(A) Overview of the purification and extraction protocols of ommochromes from housefly eyes. **(B)** Chromatographic profile in Multiple Reaction Monitoring (MRM) mode of the six main metabolites of the tryptophan→ommochrome pathway detected in acidified methanol (MeOH-HCl) extracts of housefly eyes (crude extracts). DcXantho, decarboxylated xanthommatin, 3-OHK, 3-hydroxykynurenine, Trp, tryptophan, UncXantho, uncyclized xanthommatin. Xantho, xanthommatin. XA, xanthurenic acid. **(C)** Five µL of crude extract were injected in the chromatographic system and absolute quantifications of tryptophan, xanthurenic acid, 3-hydroxykynurenine and uncyclized xanthommatin were performed based on available standards (uncyclized xanthommatin levels are expressed as cinnabarinic acid equivalents). Open circles, measures of five independent extracts. Filled circles and error bars, means ± SD of five samples. Ratios of 3-hydroxykynurenine to xanthurenic acid and to uncyclized xanthommatin are shown (mean ± SD, N = 5). **(D-E)** Same as panels B (D) and C (E) but for MeOH-HCl extracts of purified ommochromasomes from housefly eyes. The tryptophan signal was below the signal-to-noise ratio. Statistical differences (p-value < 0.05) between ratios within panels (paired *t*-test) and between panels (unpaired *t*-test) are indicated by different letters and capitals, respectively. N.D., not

detected. See Supplemental File S2 for information on statistical analyses. Photograph credits: (A) Sanjay Acharya (CC BY SA).

We detected in ommochromasomes two minor ommatin-like compounds associated to the molecular ions 500 and 456 *m/*z (**Table 4-1**), which co-eluted with xanthommatin and its decarboxylated form, respectively (**Figure 4-6**D). Both unknown compounds were undetectable in crude extracts of housefly eyes. Their associated *m/z* features differed from those of xanthommatin and decarboxylated xanthommatin by 76 units, respectively (**Table 4-1**). Because the isolation buffer used for ommochromasome purifications contained β-mercaptoethanol (MW 78 Da), we tested whether those unknown ommatins could be produced by incubating synthesized ommatins with β-mercaptoethanol in a water-based buffer. We did find that 456 and 500 *m/z*-associated compounds were rapidly formed in those *in vitro* conditions and that their retention times matched those detected in ommochromasome extracts (**Figure S4-7**). Therefore, the 456 and 500 *m/z*-associated ommatins detected in ommochromasome extracts were likely artifacts arising from the purification procedure via the addition of β-mercaptoethanol. These results further demonstrate that ommochromes are likely to be altered during extraction and purification procedures, a chemical behavior that should be controlled by using synthesized ommochromes incubated in similar conditions than biological samples.

Discussion

UPLC-DAD-MS/MS structural elucidation of new ommatins

Biological ommochromes are difficult compounds to analyze by NMR spectroscopy (Bolognese *et al.*, 1988b). Only xanthommatin, the most common and studied ommochrome, has been successfully subjected to ^{1}H-NMR (although no ^{13}C- and 2D-NMR data exist to date, to the best of our knowledge) (Kumar *et al.*, 2018; Williams *et al.*, 2019a). The NMR-assisted structural elucidation of unknown ommochromes remains therefore extremely challenging and deceptively difficult. To tackle this structural problem, we used a combination of absorption and mass spectroscopies, which offer high sensitivities and orthogonal information, after separation by liquid chromatography. We report here the most comprehensive analytical dataset to date of ommatins, based on their absorbance, mass and tandem mass spectra (**Table 4-1**). This dataset allowed us to elucidate with strong confidence

the structure of four new ommochromes, including three methoxylated forms and one labile biological intermediate, and to propose structures for eight new other ommatins.

Studies reporting the MS/MS spectra of ommatins demonstrated that they primarily fragment on their amino acid chain (Williams *et al.*, 2016) and then on the pyrido-carboxylic acid, if present (Panettieri *et al.*, 2018). We confirmed those results for other ommatins, which indicates that ommatins fragment in a predictable way despite being highly aromatic compounds. We took a step further by positioning methoxylations based on the differences in fragmentation between methoxylated ommatins and (decarboxylated) xanthommatin. Besides, xanthommatin not only formed a 307 *m/z* fragment but also a major 305 *m/z* fragment (**Figure 4-3**C; **Table 4-1**). This sole fragment was used in a previous study to annotate a putative new ommochrome called (iso-)elymniommatin, an isomer of xanthommatin (Panettieri *et al.*, 2018). Our results prove that MS/MS spectra cannot distinguish (iso-)elymniommatin and xanthommatin unambiguously. The use of synthesized ommatins and further experiments are thus needed to verify the existence of (iso-)elymniommatin in butterfly wings.

Overall, this analytical dataset will help future studies to identify known biosynthesized and artifactitious ommatins in biological samples, as well as to elucidate the structure of unknown ommatins by analyzing their absorbance and mass spectra in the absence of NMR data. Furthermore, it is now possible to look for uncyclized xanthommatin in a wide variety of species.

Biological extracts are prone to yield artifactitious ommatins

It has long been reported that ommatins are photosensitive compounds that react with acidified methanol (MeOH-HCl) upon light radiation, leading to their reduction, methylation, methoxylation, decarboxylation and deamination (Bolognese *et al.*, 1988c, 1988d; Bolognese & Liberatore, 1988; Figon & Casas, 2019). Nevertheless, incubating tissues in MeOH-HCl for several hours at room temperature has been commonly used to extract ommatins from biological samples efficiently (Bolognese *et al.*, 1988a; Riou & Christidès, 2010; Zhang *et al.*, 2017b). Our results demonstrate that, even in the absence of light radiation, ommatins are readily and rapidly methoxylated by thermal additions of methanol, primarily on the carboxylic acid function of the pyridine ring and secondarily on the amino acid chain (**Figure 4-7**). The $[M+H]^+$ 438 *m/z* of α^3-methoxy-xanthommatin identified in our study could

correspond to the same $[M+H]^+$ previously reported in extracts of butterfly wings (Panettieri *et al.*, 2018). Hence, artifactitious methoxylations during extraction should first be ruled out before assigning methoxylated ommatins to a new biosynthetic pathway. We also show that ommatins react with other extraction buffers since we detected β-mercaptoethanol-added ommatins when synthesized ommatins were incubated in a phosphate buffer containing that reducing agent. Overall, these results emphasize the need to control for potential artifactitious reactions when performing any extraction or purification protocol of biological ommochromes.

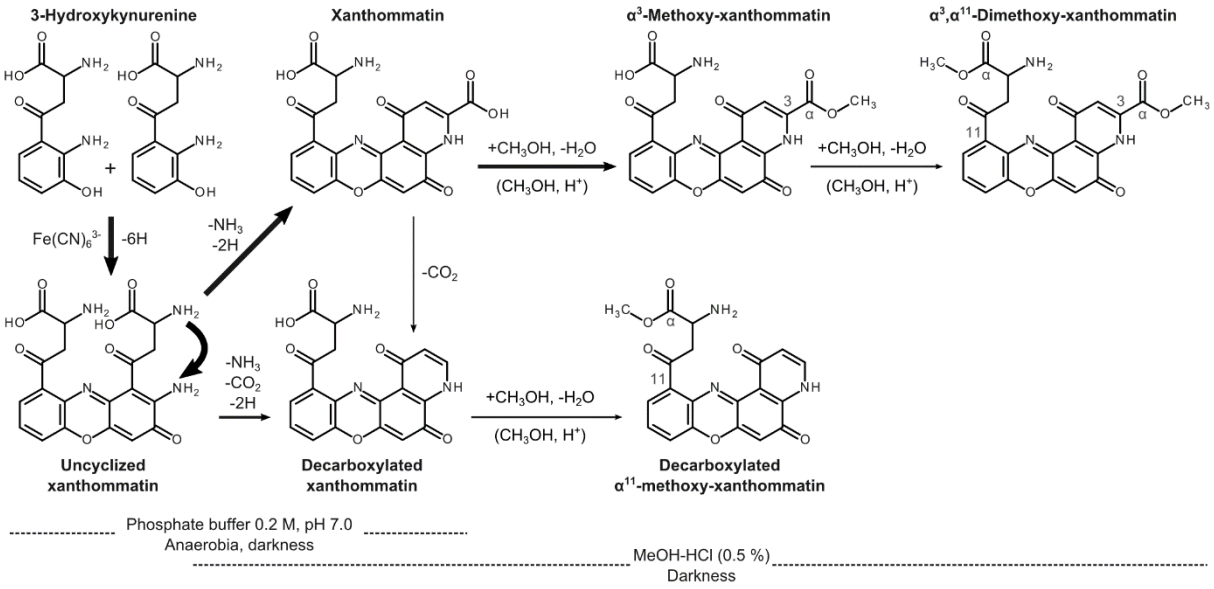

Figure 4-7. *In vitro* formation and alteration of ommatins.
Oxidative condensation of the *ortho*-aminophenol 3-hydroxykynurenine proceeds through the loss of six electrons, leading to the formation of the amino-phenoxazinone uncyclized xanthommatin. Uncyclized xanthommatin then rapidly undergoes intramolecular cyclization and oxidation, forming the two pyrido[3,2-*a*]phenoxazinone xanthommatin and decarboxylated xanthommatin. Decarboxylated xanthommatin could also be produced from the direct decarboxylation of xanthommatin. In acidified conditions, ommatins readily undergo thermal additions of methanol, which leads to their methoxylation. In solution, uncyclized xanthommatin also decays by intramolecular cyclization and xanthommatin slowly decarboxylates. Relative sizes of arrows are indicative of reaction rates.

The metabolites of the tryptophan→ommochrome pathway in ommochromasomes

It has long been hypothesized that precursors of ommochromes are translocated within ommochromasomes by the transmembrane ABC transporters White and Scarlet (Ewart *et al.*, 1994; Mackenzie *et al.*, 2000). Here, we clearly demonstrate that 3-hydroxykynurenine, but

not tryptophan, occurs in ommochromasome fractions of housefly eyes, confirming that 3-hydroxykynurenine is the precursor imported into ommochromasomes by White and Scarlet transporters (**Figure 4-8**).

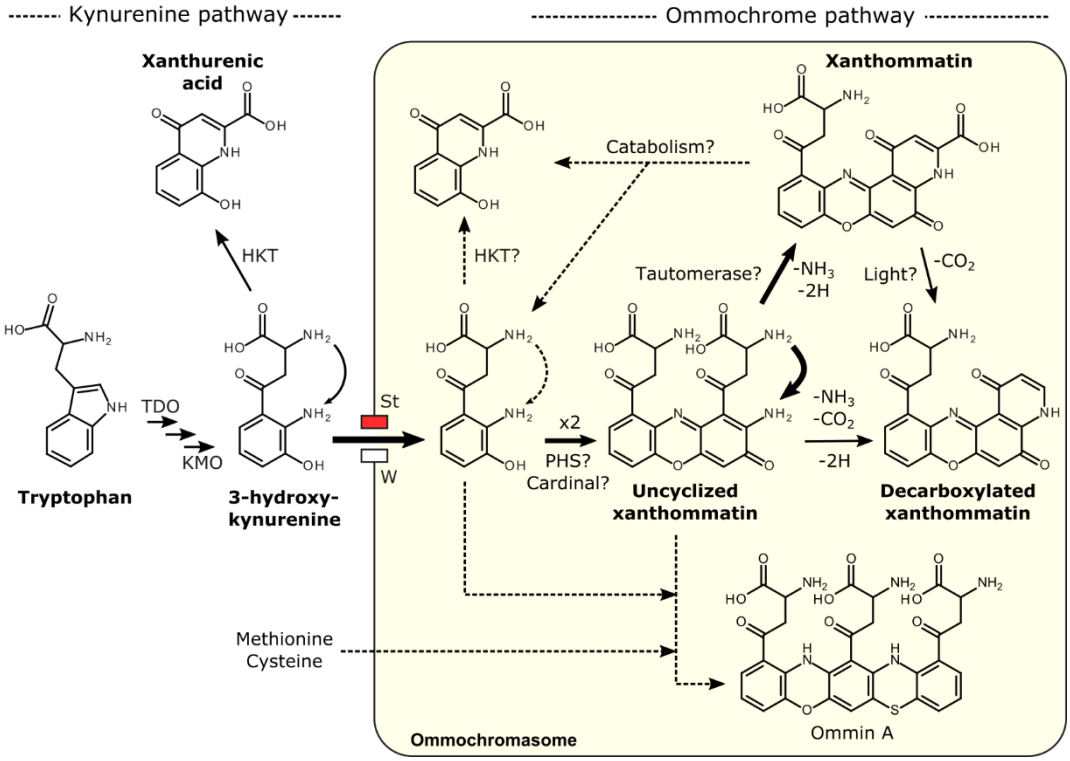

Figure 4-8. Proposed biosynthetic pathway of ommochromes through the formation of uncyclized xanthommatin in ommochromasomes.
See text for more details on each step**.** Relative sizes of arrows are indicative of reaction rates. TDO, tryptophan 2,3-dioxygenase. KMO, kynurenine 3-monooxygenase. St, ABC transporter scarlet. W, ABC transporter white. PHS, phenoxazinone synthase. HKT, 3-hydroxykynurenine transaminase.

Our results confirm that xanthommatin is the main ommatin in ommochromasomes of housefly eyes. We also showed that decarboxylated xanthommatin was present in significant amounts, which could not be solely due to the slow decarboxylation of xanthommatin in MeOH-HCl. This result indicates that both xanthommatin and its decarboxylated form are produced from 3-hydroxykynurenine within ommochromasomes (**Figure 4-8**). We also detected xanthurenic acid, the cyclized form of 3-hydroxykynurenine, in housefly eyes. Compared to 3-hydroxykynurenine, xanthurenic acid was present in minute amounts within ommochromasomes. We hypothesize that xanthurenic acid is produced within ommochromasomes via two non-exclusive pathways (**Figure 4-8**). The first route is the *in situ* intramolecular cyclization of 3-hydroxykynurenine, which requires a cytosolic

transaminase activity (HKT; **Figure 4-8**) (Han, Beerntsen, & Li, 2007). The second route is the degradation of xanthommatin that would produce 3-hydroxykynurenine and xanthurenic acid. The phenoxazinone structure of ommatins is indeed known to undergo ring-cleavage, particularly in slightly basic water-based buffers (Butenandt & Schäfer, 1962). Hence, traces of xanthurenic acid might either come from degradation during the purification protocol or from biological changes in ommochromasome conditions (enzymatic activities or basification) leading to the cleavage of xanthommatin. To the best of our knowledge, no biological pathways for the degradation of the pyrido-phenoxazinone structure of ommatins have been described. The detection of xanthurenic acid in ommochromasomes might therefore be the first step towards understanding the *in situ* catabolism of ommatins (**Figure 4-8**).

Experimental and computational chemists have long hypothesized that the pyrido[3,2-*a*]phenoxazinone structure of ommatins should be synthesized *in vivo* by the dimerization of 3-hydroxykynurenine and a subsequent spontaneous intramolecular cyclization (Butenandt, 1957; Zhuravlev *et al.*, 2018). However, the associated dimer of 3-hydroxykynurenine, called uncyclized xanthommatin, proved to be difficult to characterize and to isolate from biological samples because of its lability (Bolognese & Scherillo, 1974). In our study, we synthesized uncyclized xanthommatin by the oxidative condensation of 3-hydroxykynurenine with potassium ferricyanide, an oxidant known to form amino-phenoxazinones from *ortho*-aminophenols (Bolognese & Scherillo, 1974). We used a combination of kinetics and analytical spectroscopy (DAD, MS and MS/MS) to confirm the *in vitro* and biological occurrence of uncyclized xanthommatin. Because we detected xanthommatin, its decarboxylated form, their precursor 3-hydroxykynurenine and the intermediary uncyclized xanthommatin in both *in vitro* and biological samples, we argue that the *in vitro* synthesis and the biosynthesis of ommatins proceed through a similar mechanism (compare **Figure 4-7** and **Figure 4-8**). An alternative biosynthetic pathway for ommatins has been proposed to occur through the condensation of 3-hydroxykynurenine with xanthurenic acid (hypothesis 2, **Figure 4-1**B) (Linzen, 1974; Panettieri *et al.*, 2018). Under the hypothesis that 3-hydroxykynurenine and xanthurenic acid condense into xanthommatin, we would expect them to be in similar quantities within ommochromasomes (i.e. enrichement ratio of 1), which was not the case since their concentrations differed by an order of magnitude. On contrary, under the hypothesis that uncyclized xanthommatin is the intermediate form between 3-

hydroxykynurenine and xanthommatin, we would expect it to be enriched in ommochromasomes compared to crude extracts, which was the case either. Furthermore, the fact that the unstable uncyclized xanthommatin was more enriched in ommochromasomes than the stable xanthurenic acid indicates that the flux of 3-hydroxykynurenine dimerization is high enough to counterbalance the disappearance of uncyclized xanthommatin by intramolecular cyclization. Thus, uncyclized xanthommatin is unlikely solely a by-product. At the very least, our results show that xanthurenic acid is tightly linked to the ommochrome pathway and therefore cannot be considered as a marker of a distinct biogenic pathway. Lastly, as far as we know, there has been no experimental evidence for the formation of xanthommatin by condensing 3-hydroxykynurenine with xanthurenic acid. In conclusion, the formation of uncyclized xanthommatin by the oxidative dimerization of 3-hydroxykynurenine is likely to be the main biological route for the biosynthesis of ommatins within ommochromasomes (**Figure 4-8**).

Whether the *in vivo* oxidative dimerization of 3-hydroxykynurenine is catalyzed enzymatically remains a key question in the biogenesis of ommochromes (Figon & Casas, 2019). Theoretical calculations suggested that both enzymatic and non-enzymatic oxidations of 3-hydroxykynurenine would lead to the formation of the phenoxazinone uncyclized xanthommatin (Zhuravlev *et al.*, 2018; Williams *et al.*, 2019a). There was some evidence of a phenoxazinone synthase (PHS) activity associated to purified ommochromasomes of fruitflies (Yamamoto *et al.*, 1976). However, no corresponding PHS enzyme has ever been isolated nor identified in species producing ommochromes (Figon & Casas, 2019). PHS is not the only enzyme capable of forming aminophenoxazinones from *ortho*-aminophenols. Tyrosinase, laccase, peroxidase and catalase can also catalyze these reactions (Le Roes-Hill *et al.*, 2009). Particularly, peroxidase can produce xanthommatin and its decarboxylated form from 3-hydroxykynurenine *in vitro* (Ishii *et al.*, 1992; Iwahashi & Ishii, 1997; Vazquez *et al.*, 2000; Vogliardi *et al.*, 2004), likely through the formation of uncyclized xanthommatin (Iwahashi & Ishii, 1997). This result relates to the long-known fact that insects mutated for the heme peroxidase Cardinal accumulate 3-hydroxykynurenine without forming ommochromes (Howells *et al.*, 1977; Osanai-Futahashi *et al.*, 2016). Hence, our data support the hypothesis that the biosynthesis of ommatins could be catalyzed by a relatively unspecific peroxidase such as Cardinal (**Figure 4-8**) (Osanai-Futahashi *et al.*, 2016; Liu *et al.*, 2017), without the requirement of a specialized PHS.

Uncyclized xanthommatin is a potential key branching point in the biogenesis of ommatins and ommins

The relatively recent description of decarboxylated xanthommatin in several species indicates that it is a common biological ommatin (Figon & Casas, 2019). Yet, little is known about how decarboxylation of ommatins proceeds *in vivo*. In this study, we show that decarboxylated xanthommatin is unlikely to arise solely from the artifactitious decarboxylation of xanthommatin in MeOH-HCl, and that the level of decarboxylated xanthommatin is lower in biological extracts (5.3 %) than *in vitro* (21.5 %). Three biological mechanisms could account for the biosynthesis of decarboxylated xanthommatin (**Figure 4-8**). (1) The decarboxylation of xanthommatin in water-based environments and upon light radiations possibly accounted for the formation of decarboxylated xanthommatin (**Figure 4-8**). Indeed, some aromatic compounds are known to be decarboxylated by the action of water (Mundle & Kluger, 2009), and kynurenic acid, which is structurally related to xanthommatin, is decarboxylated upon light radiations (Zelentsova *et al.*, 2013). (2) Enzymatic and non-enzymatic syntheses of ommatins might differ in their products and exact molecular steps (Ishii *et al.*, 1992; Zhuravlev *et al.*, 2018). Thus, the proposed involvement of the heme peroxidase Cardinal in the biosynthesis of ommatins (Howells *et al.*, 1977) might lead to the natural formation of xanthommatin over its decarboxylated form. (3) Bolognese and colleagues proposed that decarboxylation happens by a rearrangement of protons, consecutively to the intramolecular cyclization of uncyclized xanthommatin (Bolognese *et al.*, 1988b). Such mechanism has been well described for the biogenesis of eumelanin monomers, in which the non-decarboxylative rearrangement of dopachrome is favored by the dopachrome tautomerase (Solano *et al.*, 1996). Hence, this analogy raises the intriguing possibility that a tautomerase might catalyze the formation of xanthommatin from uncyclized xanthommatin (**Figure 4-8**), thereby controlling the relative content of decarboxylated xanthommatin in ommochromasomes, which is known to vary among species, individuals and chromatophores (Futahashi *et al.*, 2012; Williams *et al.*, 2016; Zhang *et al.*, 2017b). Why decarboxylated xanthommatin levels depend on the biological context may rely on its biological functions, which we now discuss.

Few studies have addressed the biological function of decarboxylated xanthommatin. Its ratio to xanthommatin is known to vary among species and individuals (Futahashi *et al.*, 2012; Williams *et al.*, 2016). In cephalopods, the ratio of xanthommatin to its decarboxylated

form within a chromatophore has been suggested to determine its color, ranging from yellow to purple (Williams *et al.*, 2016). However, our absorbance data do not support this hypothesis because the experimental absorbance spectrum of decarboxylated xanthommatin was not different from that of xanthommatin in the visible region. Moreover, purple colors are produced by chromophores that absorb wavelengths around 520 nm, which has not been described for any ommatin in contrast to ommins (Figon & Casas, 2019). Another study focusing on the quantum chemistry of pirenoxine, a xanthommatin-like drug, proposed that the carboxylic acid function present on the pyrido[3,2-*a*]phenoxazinone of pirenoxine could enhance its binding to divalent cations (Liao *et al.*, 2011). This is coherent with the fact that ommochromasomes accumulate and store cations, such as Ca^{2+} and Mg^{2+} (Gribakin *et al.*, 1987; Ukhanov, 1991). Thus, favoring xanthommatin over its decarboxylated form *in vivo* might enhance the storage of metals in ommochromasomes, as proposed for eumelanins that contain high proportions of the carboxylated monomers DHICA (Hong & Simon, 2007). To which extent the binding of metals modifies the physical and chemical properties of ommatins, therefore their biological roles, remains to be determined.

How ommatins and ommins, the two most abundant families of ommochromes, are biochemically connected to each other is still a mystery (Figon & Casas, 2019). Purple ommins have higher molecular weights than ommatins and derive from both 3-hydroxykynurenine and cysteine/methionine, the latter providing sulfur to the phenothiazine ring of ommins (Linzen, 1974; Needham, 1974). The best-known ommin is called ommin A, whose structure was proposed to be a trimer of 3-hydroxykynurenine in which one of the phenoxazine ring is replaced by phenothiazine (**Figure 4-8**) (Needham, 1974). Since the pyrido[3,2-*a*]phenoxazinone cannot be reopen to an amino-phenoxazinone in anyway (Bolognese & Liberatore, 1988), it is unlikely that the biosynthesis of ommins is a side-branch of ommatins. Thus, the biochemical relationship between ommatins and ommins should be found upstream in the biosynthetic pathway of ommochromes. Older genetic and chemical studies demonstrated that ommins and ommatins share the kynurenine pathway and Linzen proposed that the ratio of xanthommatin to ommins could depend on the level of methionine-derived precursors (Linzen, 1974). The distinct structure of uncyclized xanthommatin raises the interesting hypothesis that uncyclized xanthommatin is the elusive intermediate between the *ortho*-aminophenol structure of 3-hydroxykynurenine, the pyrido-phenoxazinone chromophore of xanthommatin and the phenoxazine-phenothiazine structure

of ommins. We propose that the biosynthesis of ommins first proceeds with the dimerization of 3-hydroxykynurenine into uncyclized xanthommatin, then with the stabilization of its amino acid chain to avoid a spontaneous intramolecular cyclization, and finally with the condensation with a sulfur-containing compound derived from methionine/cysteine (**Figure 4-8**). Although this mechanism is hypothetical at this stage, it can explain two apparently unrelated observations. First, it clarifies the reason why *cardinal* mutants of insects, which lack the heme peroxidase Cardinal that possibly catalyzes the formation of uncyclized xanthommatin, lack both ommatins and ommins, and accumulate 3-hydroxykynurenine (Howells *et al.*, 1977; Osanai-Futahashi *et al.*, 2016). Second, it could explain how a single cephalopod chromatophore can change its color from yellow (ommatins) to purple (ommins) across its lifetime (Reiter *et al.*, 2018). The biochemical mechanism might be analogous to the casing model of melanins (Ito & Wakamatsu, 2008), in which pheomelanins and eumelanins (in this case ommins and ommatins, respectively) are produced sequentially from the same precursors (uncyclized xanthommatin) through changes in sulfur (methionine/cysteine) availability within melanosomes (ommochromasomes).

Overall, uncyclized xanthommatin appears as a key metabolite in the ommochrome pathway by leading to either ommatins, decarboxylated ommatins or ommins (**Figure 4-8**). Therefore, the formation of uncyclized xanthommatin might represent a key step in the divergence between the post-kynurenine pathways of vertebrates and invertebrates, as well as in the structural diversification of ommochromes in phylogenetically-distant invertebrates.

Acknowledgments

We thank Kévin Billet, Cédric Delevoye and Emmanuel Gaquerel for fruitful discussions. We are grateful to Antoine Touzé for his technical assistance and for access to the ultracentrifuge. We thank Rustem Uzbekov for providing the electron micrograph. The ENS de Lyon is thanked for financial support (to F. F.). This study formed part of the doctoral dissertation of F. F. under the supervision of J. C.

Conflict of interest: The authors declare that they have no conflicts of interest with the contents of this article.

Supplemental Data

Supplemental Figures

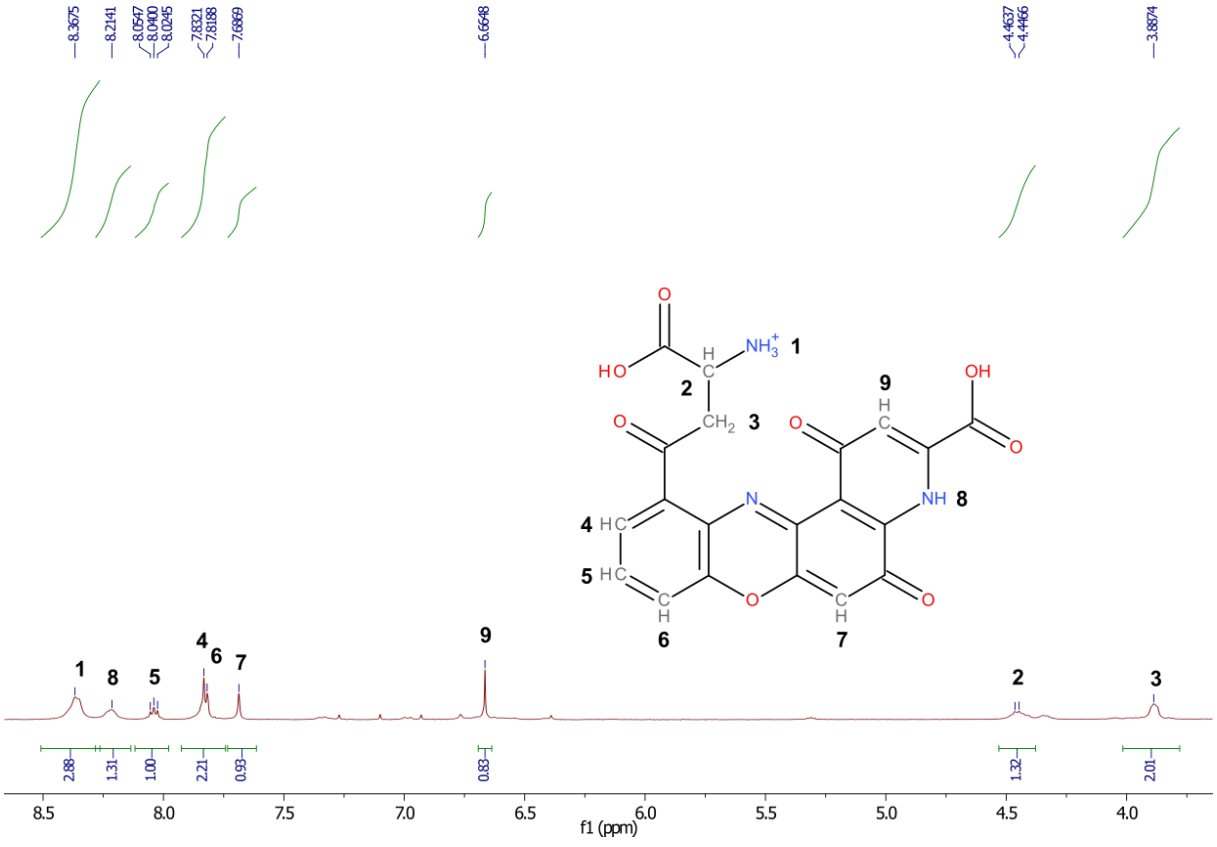

Figure S4-1. ^{1}H-NMR spectrum of synthesized xanthommatin in acidic DMSO.

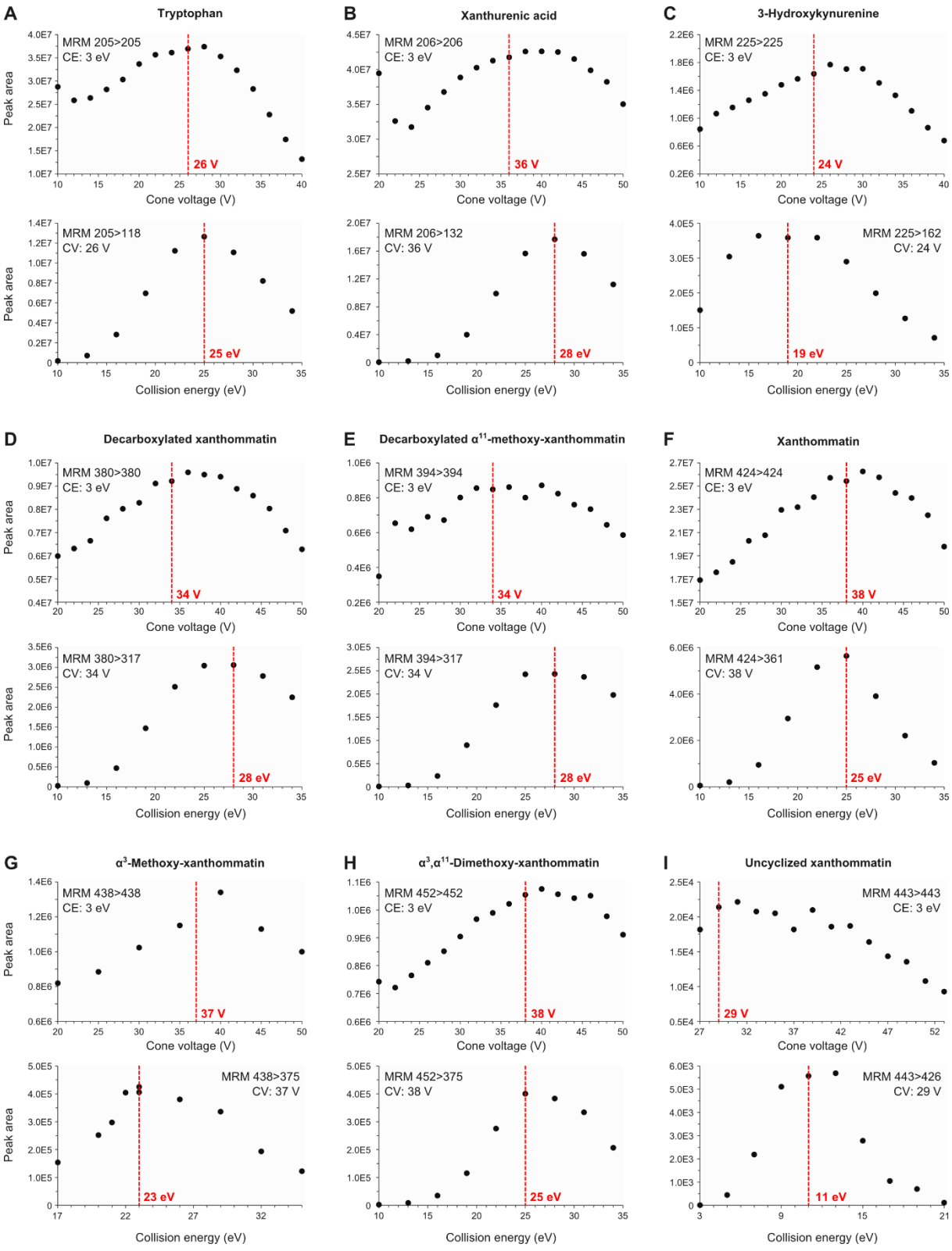

Figure S4-2. Optimization of cone voltages and collision energies for single reaction monitoring of ommochrome-related metabolites.

Optimization of cone voltages (CV) was achieved by monitoring the parent-to-parent ion transition for different CV at the minimum collision energy (CE = 3 eV) during the same run. The optimum CV was defined as the CV

just before the maximum peak area. Optimization of CE was achieved by monitoring a specific parent-to-product ion transition for different CE at the corresponding optimized CV during the same run. The optimum CE was defined as the CE corresponding to the maximum peak area.

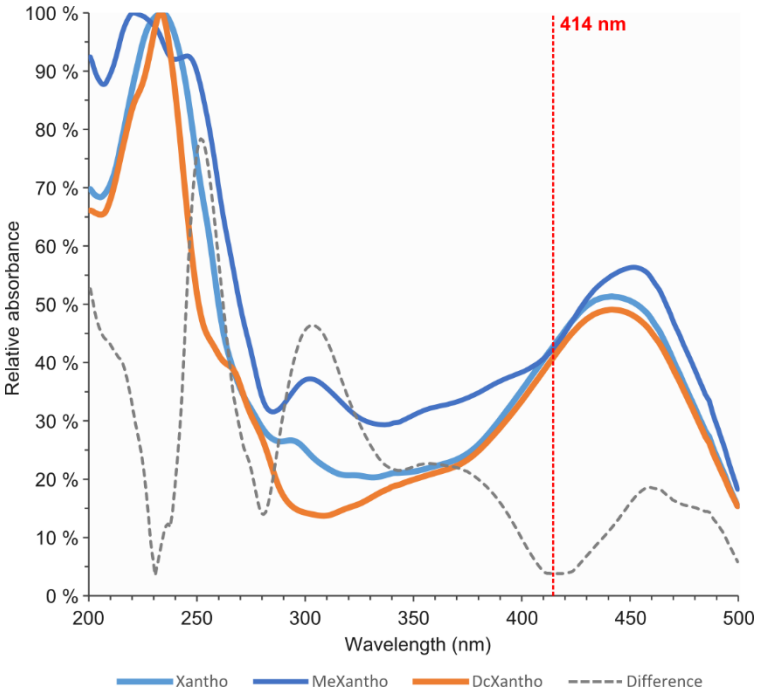

Figure S4-3. Determination of the wavelength at which ommatins absorb light equivalently.
Synthesized ommatins incubated in acidified methanol were separated by liquid chromatography and analyzed by absorption spectroscopy. Relative absorbance spectra of xanthommatin (Xantho), α^3-methoxy-xanthommatin (MeXantho) and decarboxylated xanthommatin (DcXantho) were reported relatively to their respective maximum absorbance value. Gray dashed curve, difference between the three relative absorbance spectra calculated with the Manhattan formula: $Difference(x) = |Abs_{Xantho}(x) - Abs_{MeXantho}(x)| + |Abs_{Xantho}(x) - Abs_{DcXantho}(x)| + |Abs_{MeXantho}(x) - Abs_{DcXantho}(x)|$. The chromophores of the three ommatins absorb light equivalently at the wavelength for which this difference is minimal, i.e. 414 nm.

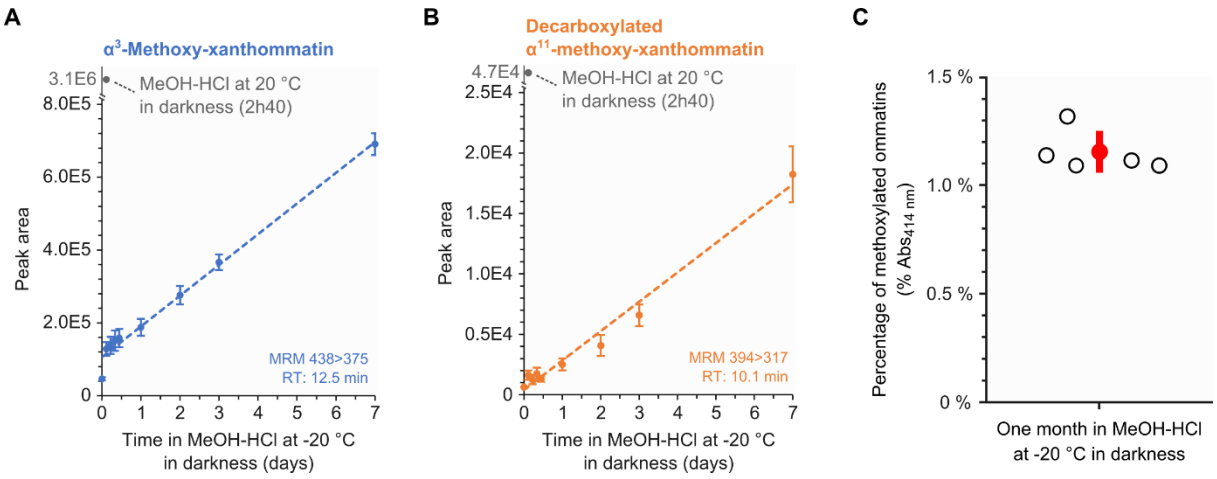

Figure S4-4. Slow methoxylations of synthesized ommatins in acidified methanol at -20 °C in darkness. Synthesized ommatins were solubilized in methanol acidified with 0.5 % (MeOH-HCl) and stored at -20 °C in darkness. Incubated ommatins were then separated by liquid chromatography. (**A**) Multiple reaction monitoring (MRM) signal of α^3-methoxy-xanthommatin. Values are mean ± S.D. of five samples. Linear regression (R^2 = 0.87, F = 286.6, df = 1 and 43, p-value < 2.2e-16). (**B**) MRM signal of decarboxylated α^{11}-methoxy-xanthommatin. Values are mean ± S.D. of five samples. Linear regression (R^2 = 0.92, F = 519.4, df = 1 and 43, p-value < 2.2e-16). **C)** Relative quantities of methoxylated ommatins (i.e. α^3-methoxy-xanthommatin, α^3, α^{11}-dimethoxy-xanthommatin and decarboxylated α^{11}-xanthommatin) in synthesized ommatins incubated in MeOH-HCl for one month at -20 °C in darkness. Quantifications were based on the absorbance of ommatins at 414 nm. Open circles, sample value. Red circle and error bar, mean value ± S.D. of five samples.

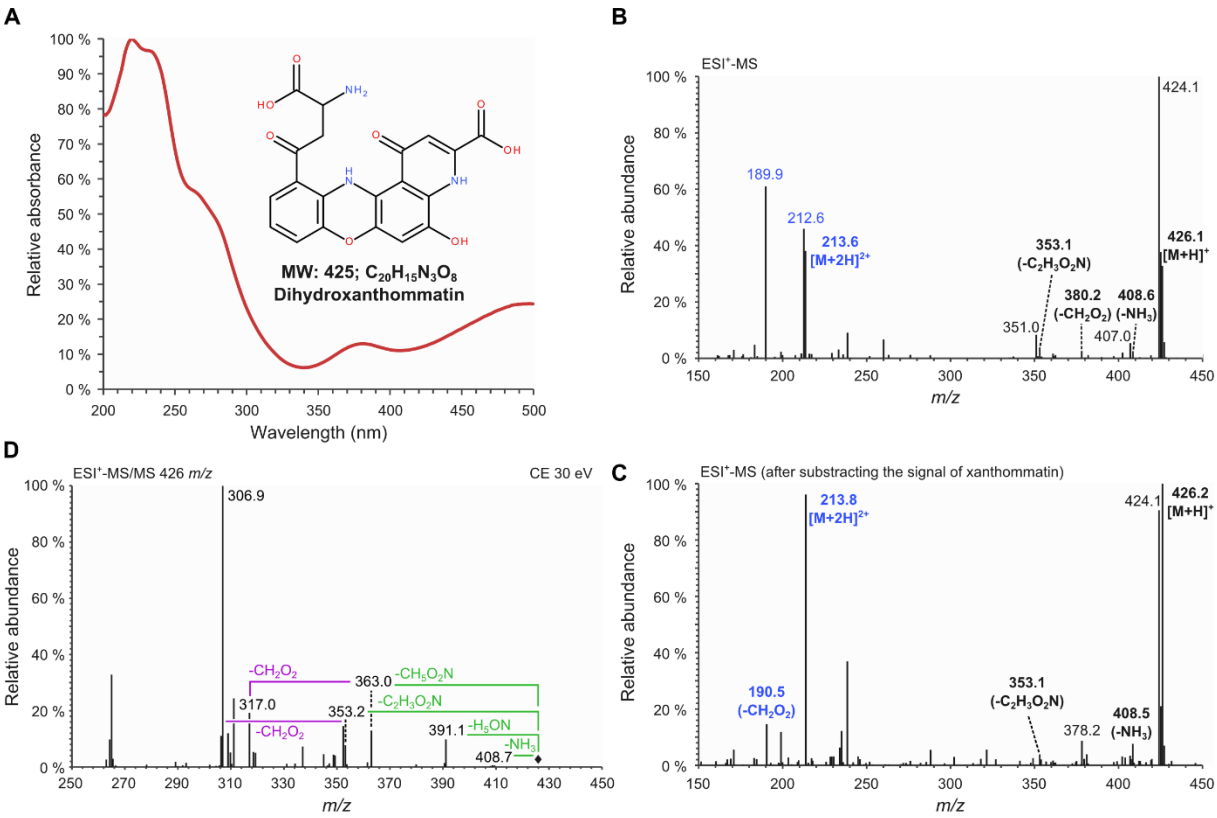

Figure S4-5. Analytical characterization of dihydroxanthommatin.
Synthesized ommatins were solubilized in acidified methanol with 0.5 % HCl and separated by liquid chromatography (see File S1 for the experimental procedure). (**A**) Absorbance spectrum of dihydroxanthommatin. The peak at 480 nm makes dihydroxanthommatin appearing red in solution. (**B-C**) Raw mass spectrum (B) and mass spectrum with the signal of xanthommatin from the same run subtracted (C) of dihydroxanthommatin in positive mode. Ions associated to dihydroxanthommatin are indicated in bold fonts. Monocharged and double-charged ions are indicated in black and blue fonts, respectively. Mass losses of in-source fragments are indicated in parenthesis. (**D**) Tandem mass spectrum of dihydroxanthommatin obtained by the fragmentation of the molecular ion $[M+H]^+$ 426 *m/z* at a collision energy (CE) of 30 eV. Losses corresponding to the typical fragmentation of the amino acid chain of ommatins are indicated in green. Losses corresponding to the fragmentation of the pyrido-carboxylic acid are reported in purple.

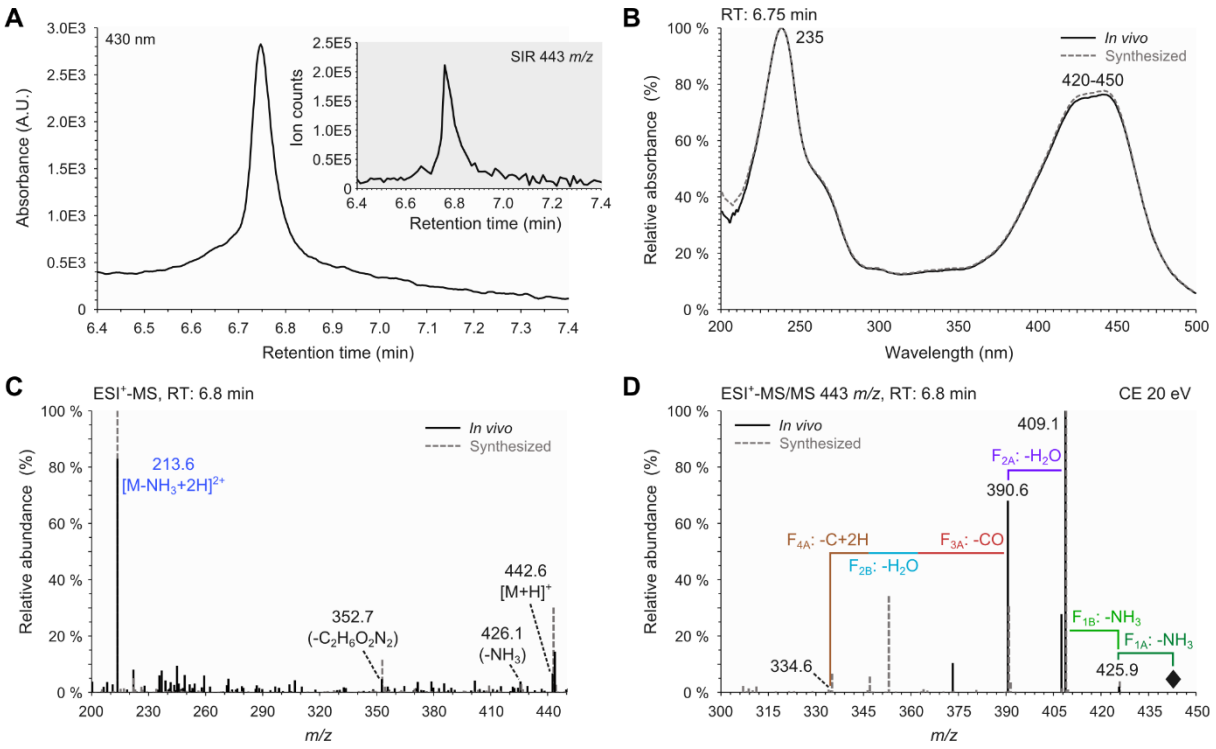

Figure S4-6. Analytical characterization of uncyclized xanthommatin in methanolic extracts of housefly eyes.

(**A**) Chromatographic peak of absorbance at 430 nm. Inset, corresponding chromatographic peak of the associated $[M+H]^+$ 443 *m/z* acquired in Single Ion Recording (SIR) mode. (**B**) Solid curve, absorbance spectrum corresponding to the chromatographic peak shown in panel A. Dashed curve, absorbance spectrum of synthesized uncyclized xanthommatin. (**C**) Solid lines, mass spectrum (MS) corresponding to the chromatographic peak shown in the inset of panel A. Dashed lines, MS of synthesized uncyclized xanthommatin. Black fonts, monocharged ions. Blue fonts, double-charged ion. (**D**) Solid lines, tandem mass (MS/MS) spectrum corresponding to the chromatographic peak shown in the inset of panel A. Dashed lines, MS/MS spectrum of synthesized uncyclized xanthommatin. F_{1A}, F_{1B}, F_{2A}, F_{2B}, F_{3A} and F_{4A} correspond to the fragmentations described in **Figure 4-5**.

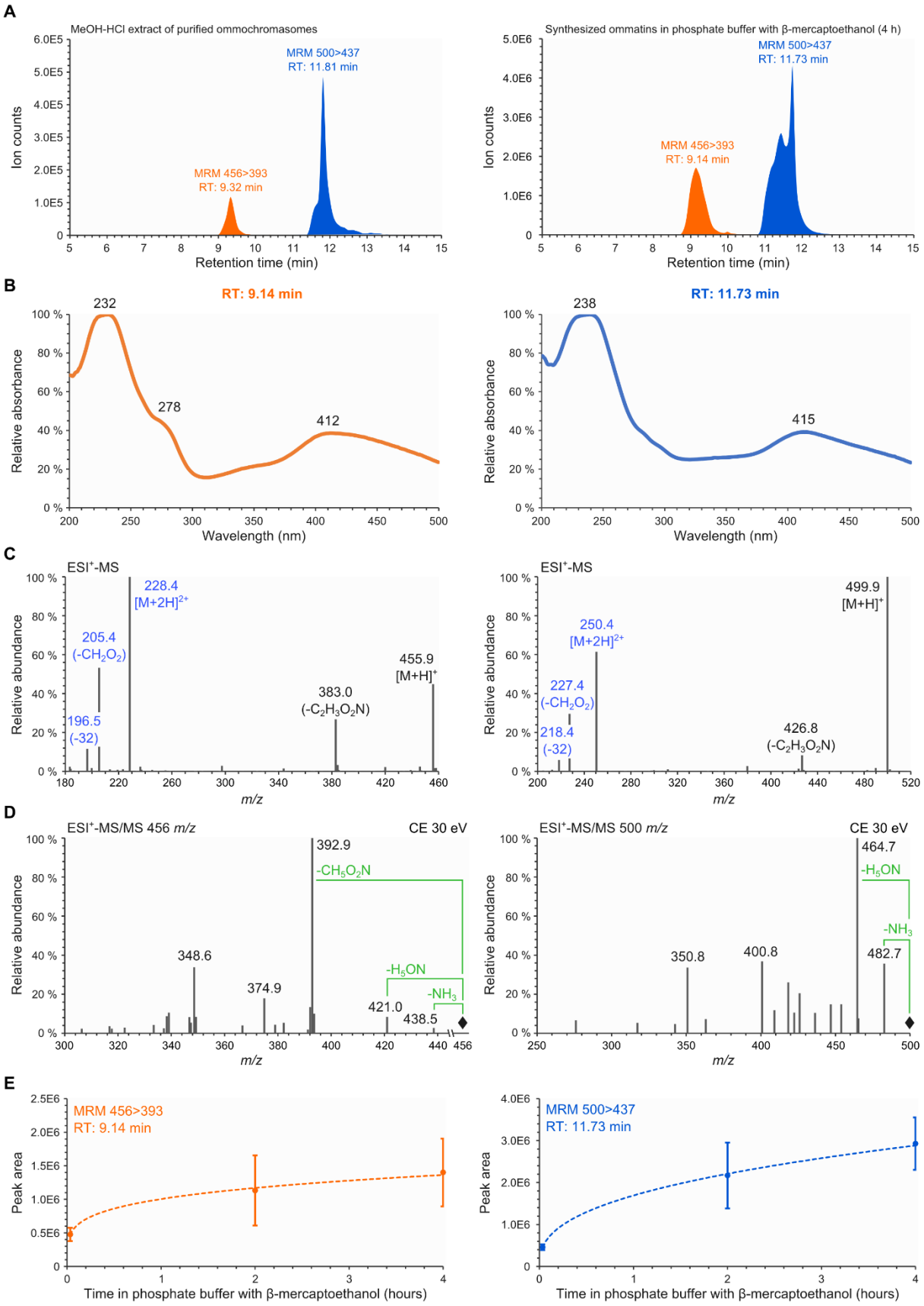
A
MeOH-HCl extract of purified ommochromasomes
MRM 500>437
RT: 11.81 min
MRM 456>393
RT: 9.32 min
Ion counts
Retention time (min)
Synthesized ommatins in phosphate buffer with β-mercaptoethanol (4 h)
MRM 500>437
RT: 11.73 min
MRM 456>393
RT: 9.14 min
Ion counts
Retention time (min)
B
RT: 9.14 min
232
278
412
Relative absorbance
Wavelength (nm)
RT: 11.73 min
238
415
Relative absorbance
Wavelength (nm)
C
ESI+-MS
228.4
[M+2H]2+
205.4
(-CH2O2)
196.5
(-32)
383.0
(-C2H3O2N)
455.9
[M+H]+
Relative abundance
m/z
ESI+-MS
499.9
[M+H]+
250.4
[M+2H]2+
227.4
(-CH2O2)
218.4
(-32)
426.8
(-C2H3O2N)
Relative abundance
m/z
D
ESI+-MS/MS 456 m/z
CE 30 eV
392.9
-CH5O2N
348.6
374.9
-H5ON
-NH3
421.0
438.5
Relative abundance
m/z
ESI+-MS/MS 500 m/z
CE 30 eV
464.7
-H5ON
-NH3
350.8
400.8
482.7
Relative abundance
m/z
E
MRM 456>393
RT: 9.14 min
Peak area
Time in phosphate buffer with β-mercaptoethanol (hours)
MRM 500>437
RT: 11.73 min
Peak area
Time in phosphate buffer with β-mercaptoethanol (hours)

Figure S4-7. Ommatins are altered by addition of β-mercaptoethanol.
Ommatins were separated by liquid chromatography and analysed by absorption, mass and tandem mass spectroscopies. (**A**) Chromatograms of acidified methanol (MeOH-HCl) extract of purified ommochromasomes and synthesized xanthommatin solubilized in phosphate buffer with β-mercaptoethanol. Only the signals of the multiple reaction monitoring (MRM) for the 456- and 500 *m/z*-associated compounds are shown. (**B-D**) Analytical characterization of the 456- and the 500-*m/z*-associated compounds present in phosphate buffer with β-mercaptoethanol. (B) Absorbance spectra. Wavelengths of peaks are reported. (C) Mass spectra in positive mode. Monocharged and double-charged ions are indicated in black and blue fonts, respectively. Mass losses of in-source fragments are indicated in parenthesis. (D) Tandem mass spectra in positive mode of the molecular ions $[M+H]^+$. Main fragments are indicated in black fonts. Losses corresponding to the typical fragmentation of the amino acid chain of ommatins are reported in green. (**E**) Kinetics of formation of the 456- and 500-*m/z*-associated compounds in phosphate buffer with β-mercaptoethanol at 20 °C in darkness. The two compounds were monitored and quantified by MRM. Values are mean ± S.D. of four samples. Left panel, linear regression with log-scaled time ($R^2 = 0.52$, F = 10.67, df = 1 and 10, p-value = 0.0085). Right panel, linear regression with log-scaled time ($R^2 = 0.78$, F = 36.43, df = 1 and 10, p-value = 0.00013).

File S1. Supplemental Materials and Methods

The isolation buffer (IB) was prepared with 10 mM Tris, 1 mM $MgCl_2$, 25 mM KCl and 14 mM β-mercaptoethanol in distilled water. β-mercaptoethanol maintains a reducing environment that stabilizes ommochromasomes (Cölln *et al.*, 1981). The pH was brought to 7.0 with 1 M HCl. Isolation buffer with sucrose (IB sucrose) was prepared by adding 0.25 M sucrose to IB. IB and IB sucrose were kept at 4 °C no longer than a day to avoid β-mercaptoethanol degradation (Stevens, Stevens, & Price, 1983). All steps of the purification procedure were performed at 4 °C.

Homogenization of housefly eyes

A total of 416 fresh housefly heads were homogenized in 12 mL of IB sucrose with a glass potter Elvehjem homogenizer. The suspension was filtered on gauze and the filtrate recovered. The potter was rinsed with 6 mL of IB sucrose, filtered and the filtrate recovered.

Differential centrifugation

The two filtrates were combined and centrifuged for 2 min at 400 × g. The supernatant was recovered. The pellet was resuspended in 6 mL IB sucrose, centrifuged for 2 min at 400 × g and the supernatant recovered. The supernatants were combined and centrifuged for 5 min at 180 × g. The supernatant was recovered and centrifuged for 12 min at 10 000 × g. The obtained pellet was stored overnight at 4 °C. To limit membrane destabilization and loss of pigments by the action of detergents, the pellet was only resuspended in 12 mL IB sucrose

with 30 µL Triton X-100 immediately before ultracentrifugation. The suspension containing Triton X-100 was further centrifuged for 1 min at 100 × g and the supernatant recovered.

Ultracentrifugation

The supernatant was layered onto two discontinuous gradients of (from bottom to top): 2.5 M, 2.25 M, 2 M, 1.75 M, 1.5 M, 1.25 M and 1 M sucrose in IB. The tubes were ultracentrifuged for 45 min at 175 000 × g in a Beckman LE-70 ultracentrifuge with a SW32 rotor. The obtained pellets were resuspended in 3 mL of IB sucrose, combined and layered onto a discontinuous gradient of (from bottom to top): 0.99 M, 0.83 M and 0.73 M Nycodenz® (iohexol) in IB. The tube was ultracentrifuged for 2 h 40 at 175 000 × g with a SW41Ti rotor. Purified ommochromasomes were recovered from the 0.83 M layer (corresponding density around 1.4) and centrifuged for 10 min at 23 000 × g. The obtained pellet was rinsed with IB sucrose, resuspended in 1 mL IB sucrose and fractionated into 0.1 mL aliquots. Those aliquots were centrifuged for 20 min at 12 000 × g. The supernatants were discarded and one pellet was directly processed for electron microscopy to check for the absence of membrane contaminants and other organelles, particularly mitochondria and lysosomes (**Figure 4-6**A). The remaining obtained pellets of purified ommochromasomes were stored at -20 °C until further use.

Analytical characterization of dihydroxanthommatin

Dihydroxanthommatin, the reduced form of xanthommatin, was not detectable using the CSH™ C18 column, most likely because dihydroxanthommatin was oxidized into xanthommatin by the chemistry of the column. Therefore, we analytically characterized dihydroxanthommatin after separation on a HSS T3 C18 column (2.1 x 150 mm, 1.7 µm) equipped with a HSS T3 C18 VanGuard™ pre-column (2.1 x 5 mm). All other analytical conditions were the same than those described in the experimental procedure section.

Reactivity of synthesized ommatins with β-mercaptoethanol

Sample preparation

Solutions of synthesized ommatins were prepared at 1 mg/mL in phosphate buffer 0.2 M, pH 7.0 and 14 mM β-mercaptoethanol (n = 4). The samples were mixed for 30 s and filtered

using 0.45 µm filters. Aliquots of 50 µL were prepared for each sample and stored in darkness at 20 °C. Each aliquot was analyzed only once and represented a single time point for each sample.

Quantifications

β-Mercaptoethanol-added forms were detected and quantified by MS/MS (multiple reaction monitoring [MRM] mode) spectrometry. The following parent-to-product ion transitions were monitored: $[M+H]^+$ 456>393 *m/z* (cone voltage 43 V, collision energy 25 eV) and $[M+H]^+$ 500>437 *m/z* (cone voltage 43 V, collision energy 25 eV). Peak areas were calculated by integrating chromatographic peaks with a "Mean" smoothing method (window size: ± 3 scans, number of smooths: 2).

File S2. Report of statistical analyses

4.3 Conclusion

Ce travail expérimental a permis de tester plusieurs hypothèses concernant la chimie et la biochimie des ommochromes. Il a tout d'abord été démontré que les ommochromes sont instables dans les conditions d'extraction, même en l'absence de lumière (*point 4* du **chapitre 3**, p. 116). Il faut donc prendre avec précaution la détection d'ommochromes méthylés dans des extraits biologiques. Cela étant dit, la diversité d'ommochromes produits dans le méthanol acide a permis de mettre au point une méthode d'identification et d'élucidation de la structure des ommatines, en particulier lorsqu'elles possèdent des chaînes latérales substituées (carboxylation, méthoxylation, double chaîne acide aminé, etc.). Dès lors, la xanthommatine non-cyclisée a pu être identifiée en conditions de synthèse *in vitro* et dans les yeux de mouche domestique, validant ainsi la condensation oxydative de la 3-hydrokynurénine comme étape clé de la biosynthèse des ommatines (*point 5* du **chapitre 3**, p. 116). Enfin, après avoir purifié les ommochromasomes des yeux de mouche domestique, la 3-hydroxykynurénine, la xanthommatine non-cyclisée, la xanthommatine et sa forme décarboxylée ont pu être identifiées ce qui valide l'hypothèse que les ommochromasomes sont le lieu de synthèse privilégié des ommochromes via l'import de 3-hydroxykynurénine dans leur lumen (*points 6 et 8* du **chapitre 3**, p. 117). Finalement, la formation de la xanthommatine non-cyclisée renseigne sur le lien potentiel entre la biosynthèse des ommatines et celle des ommines dans un contexte de changement de couleur, celui du vieillissement des chromatophores de céphalopode qui deviennent jaunes, puis rouges et enfin violets au cours de leur vie. Ces résultats suggèrent donc que les chromatophores de céphalopodes modifient dynamiquement le métabolisme des ommochromes en produisant d'abord des ommatines, puis des ommines. Cette transition se ferait en fournissant les précurseurs soufrés des ommines, tout en maintenant la synthèse de xanthommatine non-cyclisée à partir de 3-hydroxykynurénine.

D'un point de vue méthodologique, l'identification de la xanthommatine non-cyclisée s'est basée sur des *patterns* de fragmentations en spectrométrie de masse (simple et en tandem), en spectroscopie UV-Vis, et sur sa labilité. En pratique, cette élucidation structurale a pu être réalisée car nous avions une idée de sa formule chimique et que l'élément clé de sa structure était la double chaîne d'acides aminés, dont la fragmentation était prédictible dans les conditions de cette étude. L'identification des composés méthoxylés a de même pu se faire car les modifications affectaient la chaîne acide aminé ou encore la fonction acide

carboxylique. En l'absence de RMN, il aurait par contre été difficile de réaliser cette identification sur des ommochromes où des fonctions méthyles, hydroxyles, etc. auraient été placées directement sur les cycles aromatiques. Ces derniers ont effectivement tendance à fragmenter de manière plus complexe, avec de nombreux réarrangements empêchant de prévoir avec certitude la structure des fragments produits, et donc la position exacte des substituants. Cette méthodologie ne pourra donc en aucun cas remplacer la RMN comme *gold standard* pour déterminer la structure de l'ensemble des ommochromes. Cependant, les données de RMN pour les ommochromes biologiques sont très éparses et ne concernent que les protons en une dimension. Malgré nos tentatives, nous n'avons pas pu développer de méthode de chromatographie pour isoler les ommochromes les uns des autres en quantité suffisante. Or, l'obtention de molécules purifiées dans des concentrations de l'ordre du mg/mL est une étape nécessaire à la spectroscopie RMN, surtout pour la détection des carbones et les analyses en deux dimensions. Un développement de protocoles de purification et de solvants spécifiques pour l'analyse en RMN des ommochromes s'avérera donc nécessaire pour non seulement valider définitivement les résultats de ce chapitre, mais aussi pour assurer l'élucidation structurale de tous les autres ommochromes biologiques encore inconnus et pourtant si répandus, à l'instar des ommines.

Chapitre 5 – Le changement de couleur des ommochromes repose sur les couplages électroniques de la forme réduite

Like love, molecular absorption is simple in principle,
but difficult in practice.

Sönke Johnsen, *The Optics of Life* (2012)

5.0 Sommaire

CHAPITRE 5 – LE CHANGEMENT DE COULEUR DES OMMOCHROMES REPOSE SUR LES COUPLAGES ELECTRONIQUES DE LA FORME REDUITE 173

5.0 SOMMAIRE 174
5.1 OBJECTIFS ET METHODOLOGIES 175
5.2 TRAVAIL EXPERIMENTAL 177
Abstract *179*
Introduction *180*
Computational Details *182*
Computational Approaches and Benchmarks 182
Computation of Descriptors 184
Results *185*
Schäfer and Geyer's Phenoxazine Series 185
Application to Ommochromes and Other Phenoxazinone Dyes 194
Discussion *195*
Conclusions *198*
Acknowledgments *200*
Supplemental Information *201*
Supplemental Text 201
Basis Set and Functional Benchmarks 201
Computation of Descriptors 202
Exceptions in the Phenoxazinone/Phenoxazine Series 203
Calculation of the HOMHED index 203
E_{XC} Functional Benchmark results 204
Description of the phenoxazine chromophore 205
Supplemental Figures 206
Supplemental Tables 212
Computed Data 214
Optimized Structures 214
5.3 CONCLUSION 215

5.1 Objectifs et méthodologies

La capacité des ommochromes à devenir rouges à l'état réduit alors qu'ils sont jaunes à l'état oxydé est un changement de couleur atypique. Une explication de ce changement de couleur à l'échelle moléculaire a été proposée par Schäfer et Geyer il y a près de 50 ans (Schäfer & Geyer, 1972). La bathochromie des ommochrommes reposerait sur l'augmentation du nombre de formes de résonnance (donc une délocalisation électronique plus étendue) à l'état réduit par rapport à l'état oxydé. Cependant, ce modèle qualitatif ne permet pas d'expliquer simplement toutes les observations que ces auteurs ont pu faire sur divers couples redox de modèles d'ommochromes. Une meilleure description des phénomènes électroniques qui mènent à cette bathochromie plutôt qu'à une hypsochromie permettrait pourtant de comprendre pourquoi les ommochromes ont ce comportement optique, et de savoir comment ces phénomènes électroniques peuvent être contrôlés dans des contextes aussi bien biologiques que technologiques (biomimétisme).

L'objectif de ce chapitre est d'étudier les différences électroniques qui existent entre l'état oxydé et l'état réduit pour différents couples redox de modèles d'ommochromes (c'est-à-dire des phénoxazinones/phénoxazines substituées). Ces derniers ont été choisis car ils présentent des changements de couleur après réduction soit hypsochromiques (vers le jaune) soit bathochromiques (vers le rouge), selon leurs substituants. Pour décrire ces états excités, je me suis tourné vers des méthodes numériques issues de la chimie quantique. Ce choix se justifie par les raisons suivantes : (i) la série de modèles d'ommochromes a été produite et analysée expérimentalement par Schäfer et Geyer de manière exhaustive, donnant accès à toutes les informations nécessaires (spectres UV-Vis, solvant, structures, etc.) ; (ii) la chimie quantique appliquée aux états excités par la lumière a depuis quelques années fait un très grand pas en avant, en particulier grâce à des théories *ab initio* dont les implémentations récentes rendent les temps de calculs très favorables pour des biomolécules aussi grosses que les ommochromes (plusieurs dizaines d'atomes lourds) ; et (iii) ces théories, en particulier la *Time-Dependent Density Functional Theory* (TDDFT), ont déjà démontré leur efficacité pour estimer la longueur d'onde d'absorbance maximale de la xanthommatine et de l'ommatine D (Romero & Martínez, 2015). Cependant, bien que la TDDFT soit une théorie *ab initio*, ses implémentations numériques nécessitent des approximations et sont donc semi-empiriques. Dans les faits, la plupart de ces approximations sont généralement suffisantes pour comparer

le comportement optique des pigments, mais il s'avère aussi que certaines approximations sont dépendantes du système investigué. En particulier, le terme décrivant le potentiel d'échange–corrélation des électrons n'est jamais connu précisément. Son choix doit donc généralement être validé a posteriori. Pour cela, un ensemble de fonctionnelles caractérisées, entre autres, par différents taux d'échange–corrélation, est testé en comparant les valeurs d'absorbance prédites avec celles mesurées expérimentalement. C'est à partir de ce critère qu'est choisie la fonctionnelle la plus adéquate pour modéliser les états électroniques des ommochromes et de leurs modèles redox.

5.2 Travail expérimental

Le manuscrit suivant a été déposé en tant que prépublication sur le serveur preprint *ChemRxiv*.

FIGON, F., CASAS, J., CIOFINI, I. & ADAMO, C. (2020) Electronic Couplings in the Reduced State Lie at the Origin of Color Changes of Ommochromes. preprint ChemRxiv. DOI: 10.26434/chemrxiv.12294146.v1

Une version révisée a été acceptée le 19 juin 2020 dans le journal international à comité de lecture *Dyes and Pigments*.

FIGON, F., CASAS, J., CIOFINI, I. & ADAMO, C. (2021) Electronic Coupling in the Reduced State Lies at the Origin of Color Changes of Ommochromes. *Dyes and Pigments* **185**, 108661. DOI: 10.1016/j.dyepig.2020.108661

Electronic couplings in the reduced state lie at the origin of color changes of ommochromes

Florent Figon[1], Jérôme Casas[1], Ilaria Ciofini[2]* and Carlo Adamo[2]*

[1]Institut de Recherche sur la Biologie de l'Insecte, UMR CNRS 7261, Université de Tours, 37200 Tours, France

[2]Chimie ParisTech, PSL University, CNRS, Institute of Chemistry for Life and Health Sciences, 75005 Paris, France

*Correspondence:

Florent Figon, Institut de Recherche sur la Biologie de l'Insecte, UMR CNRS 7261, Université de Tours, Faculté des Sciences et Techniques, Parc Grandmont, 37200 Tours, France; Email: florent.figon@univ-tours.fr

Ilaria Ciofini, Chimie ParisTech, PSL University, CNRS, Institute of Chemistry for Life and Health Sciences, 11 rue Pierre et Marie Curie, 75005 Paris, France. Email: ilaria.ciofini@chimie-paristech.fr

Highlights

1. Ommochrome pigments in insects uniquely display red shift upon reduction
2. Color changes were modelled at quantum level using TDDFT
3. Electron-withdrawing auxochromes affect optical properties only in reduced states
4. Electronic couplings that facilitate charge-transfer transitions drive red shifts
5. Larger red shifts are associated to higher antiradical behavior in reduced states

Graphical Abstract

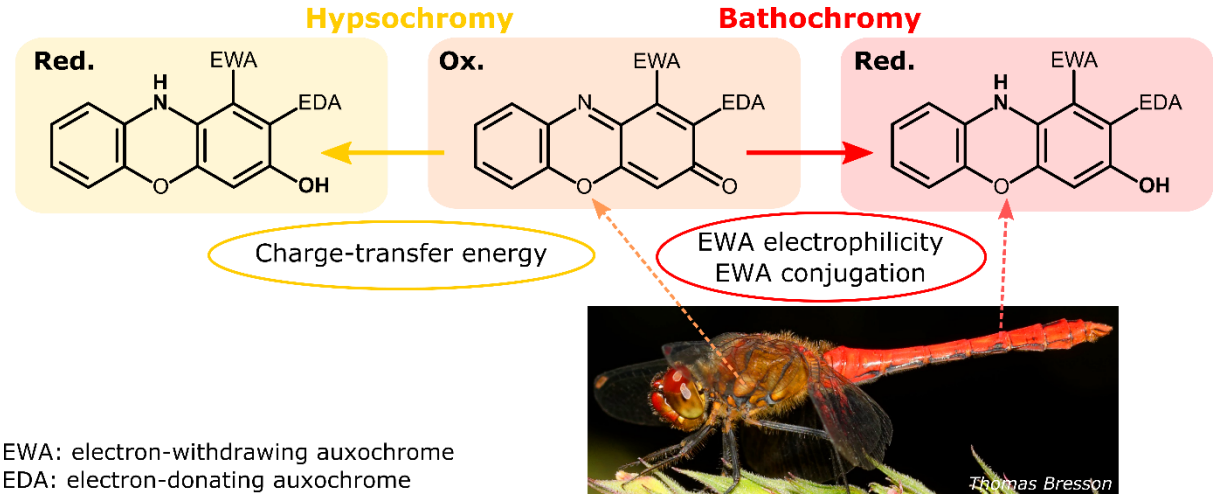

Abstract

In the colorful world of pigments and dyes, the chemical reduction of chromophores usually leads to bleaching because of π-conjugation interruption. Yet, the natural phenoxazinone-based ommochrome pigment called xanthommatin displays a bathochromic (i.e. red) shift upon two-electron reduction to its corresponding phenoxazine, whose electronic origins are not completely disclosed. In this study, we investigated, at quantum chemical level, a series of phenoxazinone/phenoxazine pairs that was previously explored by UV-Vis spectroscopy (Schäfer and Geyer, 1972), and which displays different hypsochromic and bathochromic shifts upon reduction. Density Functional Theory (DFT) and Time-Dependent DFT (TDDFT) have been applied to compute their optical properties in order to find a rational explanation of the observed photophysical behavior. Based on our results, we propose that the electro-accepting power of auxochromes and their conjugation facilitate intramolecular charge-transfers across the phenoxazine bridge by lowering unoccupied molecular orbitals via electronic and geometric couplings, leading ultimately to bathochromy. Our findings therefore suggest new potential ways to adjust the color-changing ability of phenoxazinones in technological contexts. Overall, this model extends our mechanistic understanding of the many biological functions of ommochromes in invertebrates, from tunable color changes to antiradical behaviors.

Keywords: Antiradical, Bathochromy, Insect pigment, Ommochrome, Phenoxazine, Time-Dependent Density Functional Theory

Introduction

Chemical colors in animals are mostly produced by π-conjugated organic molecules, which contain a chromophore with alternating single and double bonds. Extending the electronic conjugation of chromophores usually leads to bathochromic shifts (i.e. absorption at longer wavelengths), while breaking the π-system induces hypsochromic shifts (i.e. absorption at shorter wavelengths) (Needham, 1974; Nassau, 1987). Therefore, even limited chemical reduction of organic dyes and pigments can result in their bleaching due to the saturation of double bonds (Needham, 1974). However, one class of biological pigments –the phenoxazinone-based ommochromes– has appeared to be an exception to this rule (Figon & Casas, 2019). Xanthommatin, the best-known and most-widespread ommochrome, is yellow in its oxidized state (oxo-pyrido[3,2-*a*]phenoxazinone; absorption at 440 nm) but red when reduced to dihydroxanthommatin (oxo-pyrido[3,2-*a*]hydroxyphenoxazine; absorption at 480 nm) (Figon & Casas, 2019). This unusual color-changing molecular property mediates important biological functions (Linzen, 1974), such as nuptial colorations in dragonflies (Futahashi *et al.*, 2012), light filtering in insect eyes (Langer, 1975), as well as electron transfers in a marine worm (Horowitz & Baumberger, 1941; Linzen, 1959) and various insects (Bellamy, 1958; Linzen & Bückmann, 1961; Harano & Chino, 1971). Besides, the bathochromic reduction of xanthommatin has shown biomimetic potential to craft color-changing electrochromic devices (Kumar *et al.*, 2018). Thus, unraveling the chemical origin of this distinct bathochromic reduction may have implications for both biologists and material scientists.

In 1972, Schäfer and Geyer synthesized a series of bathochromic and hypsochromic phenoxazinone/phenoxazine pairs to mimic ommochromes, and analyzed them by UV-Vis spectroscopy (Schäfer & Geyer, 1972). They showed that only 1-acetyl-2-[amino/hydroxy]-phenoxazin-3-ones (see Figure 1 for the numbering of phenoxazinones) underwent bathochromic reduction. They concluded that this bathochromic shift was due to an increased resonance in the molecular reduced states, in relation to the dipolar structure of the 1-acetyl auxochrome (Schäfer & Geyer, 1972; Linzen, 1974). Unfortunately, after this pioneering experimental study, the model proposed was never further validated, nor rationalized making use of quantum chemical approaches. Yet, understanding the correlation between geometrical and electronic molecular structures with chromatic shifts in phenoxazinonic dyes and pigments hold great promises to further unravel their natural functions and technological uses.

The recent advances in quantum chemical methods for the description of ground and excited electronic states has greatly helped to rationalize and to predict the optical properties of molecules, especially in the case of organic dyes (Jacquemin *et al.*, 2009a; Di Tommaso *et al.*, 2017). In particular, the advent of Density Functional Theory (DFT) and Time-Dependent DFT (TDDFT), together with an increased availability of computational resources, has enabled to successfully model a vast number of biochromes, pigments and dyes [see for instance references (Adamo & Barone, 2000; Barone *et al.*, 2014; Ferré, Filatov, & Huix-Rotllant, 2016)]. Because of its favorable cost-to-accuracy ratio, we selected TDDFT to investigate the properties of phenoxazinone/phenoxazine pairs firstly to test the validity of Schäfer and Geyer's model and then to rationalize the link between the structure and photophysical properties of ommochromes. However, since TDDFT performances may quantitatively depend on the exchange correlation functional used (Laurent & Jacquemin, 2013; Di Tommaso *et al.*, 2017), a preliminary benchmark of commonly applied functionals has been performed on both phenoxazinones and phenoxazines. In particular, we tested a set of global hybrid functionals with various percentages of exact exchange, as well as range-separated hybrids (RSH), which usually perform better for excited states with a substantial amount of non-local charge transfer (CT). Once the computational approach set, several structural (e.g. planarity) and electronic properties (e.g. aromaticity indexes and CT character) were analyzed to establish the structure-property relationship of chromic shifts upon reduction. By applying the same techniques to ommochromes and resorufin, an important hypsochromic biotechnological dye, we rationalized their color-changing behavior upon reduction in terms of electronic and geometric couplings in the reduced phenoxazine state. Finally, our electronic model of ommochromes provides a mechanistic understanding of their unique optical properties, which helps rationalizing their widespread and various uses in invertebrates, as well as in new biomimetic applications.

Computational Details

Computational Approaches and Benchmarks

All quantum chemical calculations were performed with the Gaussian program (Frisch *et al.*, 2016) at the DFT level (Kohn, Becke, & Parr, 1996) while molecular orbitals were visualized using the Gabedit program (Allouche, 2011).

The B3LYP functional (Becke, 1993) was used to locate minima since it generally provides reliable geometric parameters for organic compounds (Jacquemin *et al.*, 2011), while Grimme's dispersion correction using the D3(BJ) model (Becke & Johnson, 2007; Grimme, Ehrlich, & Goerigk, 2011) was also introduced to account for weak interactions. Bulk solvent effects were considered using the COSMO approach to polarizable continuum models [CPCM; (Cossi *et al.*, 2003)]. Different solvents were considered depending on experimental conditions (Schäfer & Geyer, 1972; Linzen, 1974; Song *et al.*, 2014), as specified in Supporting Information (SI).

Each structural optimization was followed by a harmonic frequency calculation, ensuring that all computed vibrational frequencies were positive, as they should be for an energy minimum on the potential energy surface. The optimized coordinates of all investigated compounds investigated are listed in SI. The 6-311G(d,p) basis set was chosen for all structural optimizations, after a careful test (see SI for details).

Using these molecular structures optimized at the identified theoretical level (B3LYP-D3(BJ)/6-311G(d,p), vertical absorption energies (ΔE^{vert}) were then computed within the linear response Time-Dependent DFT (TDDFT) framework (Casida, 2009) using the non-equilibrium approximation of CPCM (Cossi *et al.*, 2003). It is well known that the computed electronic adsorption energies depend on the chosen DFT approach. While some general trends appear from previous detailed benchmarks (Jacquemin *et al.*, 2009b; Laurent & Jacquemin, 2013), it is a better practice to verify the performances on the systems under investigations. To this end, as functionals based on local-density (LDA) and generalized gradient approximation (GGA) are known to perform poorly for the calculation of vertical excited states (Jacquemin *et al.*, 2009b), TDDFT calculations were carried out only considering 12 functionals, chosen among the most representative (see SI for details)

All 18 phenoxazinone/phenoxazine pairs depicted in **Figure 5-1** were used for this TDDFT benchmark, while the experimental values were taken from (Schäfer & Geyer, 1972). If a compound in this dataset showed broad/unresolved absorbance peaks, the one with the highest wavelength was systematically used. The performance of the selected functionals was evaluated suing the following criteria: mean absolute errors (MAE) on ΔE^{vert} (target to be below 0.2 eV), comparable errors for both phenoxazinones (ΔE^{vert}_{ox}) and phenoxazines (ΔE^{vert}_{red}), MAE on chromic shifts (defined as ΔE^{vert} shift = $\Delta E^{vert}_{red} - \Delta E^{vert}_{ox}$; target to be below 0.2 eV), comparable errors for both bathochromic and hypsochromic redox pairs, high correlations with experimental values for both absorption energies and chromic shifts, and high number of well-predicted chromic shifts.

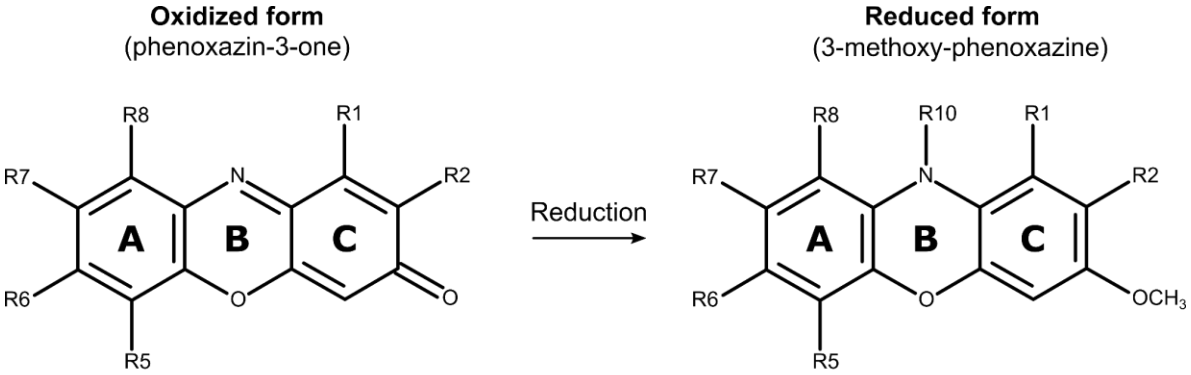

(**1o**) R1 = $COCH_3$; R2 = OH
(**2o**) R1 = R8 = $COCH_3$; R2 = OH
(**3o**) R1 = R8 = $COCH_3$; R2 = NH_2

(**6o**) R1 = R8 = $COCH_3$; R2 = Cl
(**7o**) R1 = $COCH_3$; R2 = OH; R8 = C_2H_2-$COCH_3$
(**8o**) R1 = $COCH_3$; R2 = OH; R6 = C_2H_2-$COCH_3$
(**9o**) R1 = $COCH_3$; R2 = OH; R8 = $COOCH_3$
(**10o**) R1 = R6 = $COCH_3$; R2 = NH_2
(**11o**) R1 = R8 = $COCH_3$; R2 = NH-C_6H_5
(**12o**) R1 = R8 = $COCH_3$; R2 = NH-C_6H_4-*p*OCH_3
(**13o**) R1 = CN; R2 = OH
(**14o**) R1 = CO-$C(CH_3)_3$; R2 = OH
(**15o**) R1 = $COOCH_3$; R2 = OH
(**16o**) R1 = $COOCH_3$; R2 = OH; R7 = CH_3
(**17o**) R1 = $COOCH_3$; R2 = OH; R6 = $COCH_3$
(**18o**) R1 = $COOCH_3$; R2 = OH; R5 = $COCH_3$

(**1r**) R1 = $COCH_3$; R2 = OCH_3
(**2r**) R1 = R8 = $COCH_3$; R2 = OCH_3
(**3r**) R1 = R8 = $COCH_3$; R2 = NH_2
(**4r**) R1 = R8 = $COCH_3$; R2 = $NHCH_3$
(**5r**) R1 = R8 = $COCH_3$; R2 = $N(CH_3)_2$
(**6r**) R1 = R8 = $COCH_3$; R2 = Cl
(**7r**) R1 = $COCH_3$; R2 = OCH_3; R8 = C_2H_2-$COCH_3$
(**8r**) R1 = $COCH_3$; R2 = OCH_3; R6 = C_2H_2-$COCH_3$
(**9r**) R1 = $COCH_3$; R2 = OCH_3; R8 = $COOCH_3$
(**10r**) R1 = R6 = $COCH_3$; R2 = $N(CH_3)_2$; R10 = CH_3
(**11r**) R1 = R8 = $COCH_3$; R2 = NH-C_6H_5
(**12r**) R1 = R8 = $COCH_3$; R2 = NH-C_6H_4-*p*OCH_3
(**13r**) R1 = CN; R2 = OCH_3
(**14r**) R1 = CO-$C(CH_3)_3$; R2 = OCH_3
(**15r**) R1 = $COOCH_3$; R2 = OCH_3
(**16r**) R1 = $COOCH_3$; R2 = OCH_3; R7 = CH_3
(**17r**) R1 = $COOCH_3$; R2 = OCH_3; R6 = $COCH_3$
(**18r**) R1 = $COOCH_3$; R2 = OCH_3; R5 = $COCH_3$

Figure 5-1. Set of substituted phenoxazin-3-ones and 3-methoxy-phenoxazines investigated in this study.

Based on this benchmark, whose results are reported and commented in the SI, the M05 functional (Zhao, Schultz, & Truhlar, 2005) results as the best compromise and the most reliable functional for predicting the chromic reduction of phenoxazinones to phenoxazines.

Following previous experience (Ciofini & Adamo, 2007) and the test carried out for the 2-amino-7-hydroxy-phenoxazin-3-one molecule (see SI for details), all the vertical transition energies were computed using the 6-31+G(d) basis set.

Computation of Descriptors

Several descriptors were considered in order to assess the relationship between the structural and electronic parameters of the considered dyes and their optical behavior.

The Harmonic oscillator model of aromaticity for heterocycle electron delocalization (HOMHED) is a geometric index of aromaticity that evaluates bond conjugation by comparing bond lengths of a compound to those of an ideal aromatic compound (Frizzo & Martins, 2012). The closer to 1 HOMHED is, the more conjugated, and thus aromatic, the compound is. The HOMED values were computed using the Gabedit program and the parameters described in reference (Frizzo & Martins, 2012).

Another commonly applied index is the so-called nucleus-independent chemical shifts (NICS) which is based on the deshielding induced at a center of an aromatic ring by the ring current (Chen *et al.*, 2005). The more deshielded NICS is, the more aromatic the compound. The NICS indexes were computed at the center of each ring (NICS(0)) using the above mentioned level of theory and the gauge-including atomic orbital (GIAO) method (Cheeseman *et al.*, 1996).

The third descriptor is the charge-transfer distance (D_{CT}) that evaluates the hole-electron mean distance associated to an electronic excitation, thus unraveling its nature (local or charge transfer). It is easily computed measuring the distance between the barycenters of charge distributions corresponding to a density depletion and a density increase upon excitation (Le Bahers, Adamo, & Ciofini, 2011).

Finally, some descriptors, issued from the so-called conceptual DFT (De Proft & Geerlings, 2001), were also considered, including electron affinity (EA), hardness (η) and electro-accepting power (ω^+). The latter measures the local charge-acceptance of a compound

and thus its capacity to accept fractions of electron during charge-transfer phenomena (Pearson, 1992; Gázquez, Cedillo, & Vela, 2007).

Results

A total of 15 molecular pairs from Schäfer and Geyer's series (Schäfer & Geyer, 1972) were considered for a detailed analysis (see SI for the explanation on this choice). Electronic and geometric properties of the bathochromic ommochrome pair xanthommatin/dihydroxanthommatin and the hypsochromic dye pair resorufin/dihydroresorufin were also investigated for sake of completeness. Experimental UV-Visible data for these molecules were taken from (Figon & Casas, 2019) and (Kitson, 1998), respectively.

Schäfer and Geyer's Phenoxazine Series

Nearly 50 years ago, Schäfer and Geyer proposed that the bathochromic shifts of some substituted phenoxazinones upon reduction could be related to an increase of resonance forms (Schäfer & Geyer, 1972), and thus to a greater conjugation of the phenoxazine chromophore. To test this hypothesis, we computed two indices that can be related to the degree of delocalization and aromaticity in a molecule, namely the HOMHED and NICS(0) indexes (De Proft & Geerlings, 2001).

The HOMHED index basically considers computed structural parameters, namely related to bond length alternation between single and double bonds, to evaluate the degree of electron delocalization, as detailed in the computational section. This index has been evaluated for two possible delocalization patterns in the molecule as highlighted in Figure 2A and Figure S7 namely: i) the pattern involving delocalization along ring C (cHOMHED, **Figure 5-2**A) and ii) the delocalization pattern along all bonds involved in the resonant forms produced by substituents in position 1, 2 and the phenoxazine nitrogen (sHOMHED, **Figure S5-7**). In contrast with the experimental hypothesis, no clear correlation with chromic shifts can be drawn in the case of the sHOMHED pathway (**Figure S5-7**) while, in the case of the cHOMHED index, a partial positive correlation (R^2 = 0.77) can be found (**Figure 5-2**B). According to this index, hypsochromicity is associated with an increase in aromaticity of ring C. This partial correlation is nonetheless lost when considering the NICS(0) index, an index based on electronic properties. While considering only bathochromic pairs (**Figure 5-2**C), a

positive correlation between aromaticity and bathochromicity can be found (R^2_{batho} = 0.79), in agreement with the experimental hypothesis, no correlation can be found if both batho and hypsochromic pairs are considered. Indeed three hypsochromic phenoxazines show the lowest NICS(0) and thus the highest aromaticity. In short, these two measures of the aromaticity, which are different in nature (electronic and structural origin), do not support the hypothesis of Schäfer and Geyer on the observed color change of ommochromes and, particularly on the different batho and hypsochromic behavior.

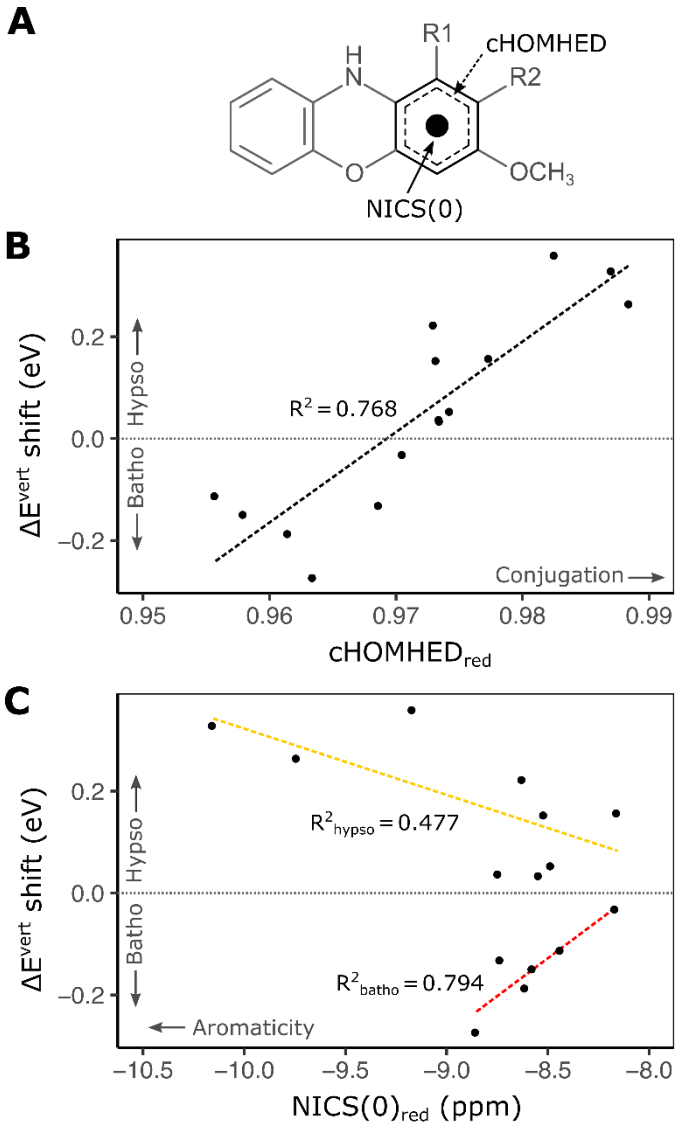

Figure 5-2. Computed vertical chromic shifts (ΔE^{vert} shift) of phenoxazinone/phenoxazine pairs as a function of two aromaticity indexes (A), cHOMHED (B) and NICS(0) (C), of phenoxazines.
Batho, bathochromy. Hypso, hypsochromy. Red, reduced state (i.e. phenoxazine).

In order to have a general picture of these behaviors and to propose a more general rationalization of the chromic reduction of phenoxazinones to phenoxazines, we analyzed the general trends arising from the mean values and dispersion of the set of structural and electronic parameters chosen, as reported in **Table 5-1**.

Table 5-1. Average values and dispersion of electronic and structural parameters computed for oxidized phenoxazinones and reduced phenoxazines.

	Phenoxazinone (mean ± SD)	**Phenoxazine** (mean ± SD)
ΔE^{exp} (eV)[a]	2,80 ± 0,10	2,91 ± 0,20
ΔE^{vert} (eV)	2,71 ± 0,09	2,75 ± 0,23
Phenoxazinone/Phenoxazine dihedral angle (°)	0,6 ± 0,3	12,0 ± 5,9
HOMO energy (eV)	-6,84 ± 0,14	-5,37 ± 0,10
LUMO energy (eV)	-3,34 ± 0,13	-1,64 ± 0,25
HOMO-LUMO gap (eV)	3,50 ± 0,08	3,73 ± 0,26
Oscillator strength	0,83 ± 0,21	0,40 ± 0,15
Transition dipole moment (D)	12,45 ± 3,41	5,85 ± 2,58
Dipole moment of GS (D)	6,34 ± 1,98	6,52 ± 2,56
Dipole moment of ES (D)	8,29 ± 2,70	12,35 ± 4,19
NICS(0) of ring C (ppm)	-0,87 ± 0,64	-8,77 ± 0,54
cHOMHED of ring C	0,65 ± 0,05	0,97 ± 0,01
D_{CT} (Å)	1,71 ± 0,30	2,61 ± 0,60

[a] Experimental values are taken from (Schäfer & Geyer, 1972)

First, we note a significant structural difference between phenoxazines and phenoxazinones, the first being sizably less planar that the latter (+11.5°; **Table 5-1**), in agreement with the expected sp^3 configuration of the phenoxazine nitrogen. Consistently, in average, both the cHOMHED and the NICS(0) indicate an increased aromaticity in the reduced systems (**Table 5-1**). Nonetheless, no correlation between chromicity and structural parameters can be directly established.

At the ground electronic state (GS), reduction leads to the destabilization of both the highest occupied molecular orbital (HOMO, +1.47 eV) and the lowest unoccupied molecular orbital (LUMO, +1.7 eV; **Table 5-1**). The HOMO-LUMO gap is only slightly higher in phenoxazines (+0.23 eV) but the spreading of values for these systems is computed to be three times larger than for phenoxazinones (**Table 5-1**), thus indicating that phenoxazines present both significantly lower and higher HOMO-LUMO gaps than phenoxazinones. This pattern is mirrored by those of ΔE^{vert} and ΔE^{exp}, consistently with the presence of batho and hypsochromic pairs. Looking at properties involving excited states, reduction leads to oscillator strengths and transition dipole moments more than twice lower than in phenoxazinones (**Table 5-1**). These data are in agreement with the hypochromic shift (i.e. less intense absorption) observed upon reduction to phenoxazines (Schäfer & Geyer, 1972). Finally, dipole moments and, consistently, the charge-transfer distances (D_{CT}) associated to excited states are computed to be higher in phenoxazines (+4.06 D and +0.9 Å, respectively; **Table 5-1**). This latter finding indicates a larger intramolecular charge transfer (ICT) character associated to electronic transitions in phenoxazines than in phenoxazinones.

More interestingly, we note that dispersion of the values associated to most of the electronic and structural parameters is greatly larger in phenoxazines (**Table 5-1** and **Figure 5-3**A). Therefore, we can formulate the hypothesis that different chromic shifts are essentially driven by differences in the reduced systems independently of the corresponding oxidized ones. Consistently to this hypothesis, chromic shifts show a relatively strong linear correlation ($R^2 = 0.84$) with ΔE^{vert}_{red} (**Figure 5-3**B) but no correlation at all with ΔE^{vert}_{ox} (**Figure S5-8**). In line with these results, there is a clear distinction between ΔE^{vert}_{red} of bathochromic and hypsochromic compounds, while ΔE^{vert}_{ox} do no significantly differ (**Figure 5-3**A).

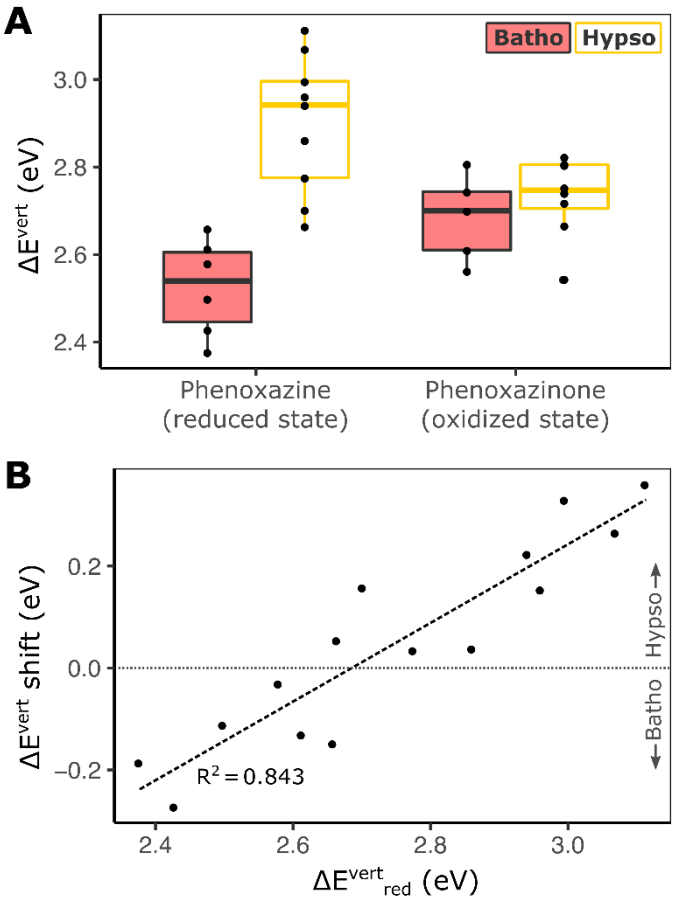

Figure 5-3. Relationship between computed vertical excitation energies (ΔE^{vert}) chromic shifts of phenoxazinone/phenoxazine pairs.
Batho, bathochromy. Hypso, hypsochromy. Red, reduced state (i.e. phenoxazine).

To further validate the hypothesis that chromicity is mainly linked to properties of the reduced forms, the electronic properties of four representative pairs, including two bathochromic (**1** and **2**) and two hypsochromic phenoxazines (**14** and **15**), were considered (**Figure S5-9**). In all cases, since the π-π* excited states of interest have a dominant HOMO-LUMO character for both oxidized and reduced compounds, energies of the HOMO and LUMO were firstly analyzed. Consistently with the results presented in **Table 5-1**, only the molecular orbital energies of the reduced compounds vary consistently with chromic shifts (**Figure S5-10**). Furthermore, the range of HOMO-LUMO gap values in phenoxazines is primarily associated to a wider variation in LUMO than in HOMO energies (**Table 5-1** and **Figure S5-10**).

All these data suggest that a simple correlation could link chromic shifts to LUMO energies of reduced phenoxazines, which are *in fine* directly related to their electron affinity

(EA) and thus to their reactivity and antiradical properties (Martínez *et al.*, 2008; Romero & Martínez, 2015). Indeed, a clear correlation is found between computed chromic shift and electron affinity of phenoxazines (EA_{red}, **Figure 5-4**A; R^2 = 0.61). This correlation is further improved by considering chemical hardness in the reduced states (η_{red}, **Figure 5-4**B; R^2 = 0.82), which implicitly takes into account also the variation of the energy of the HOMO level.

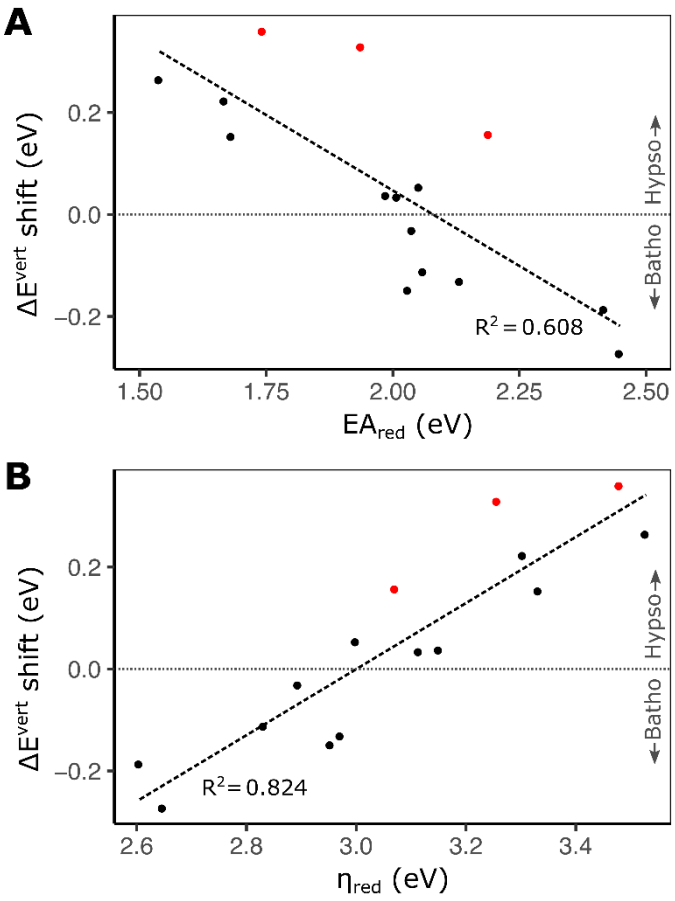

Figure 5-4. Comparison of chromic shifts (ΔE^{vert} shift) of phenoxazinone/phenoxazine pairs with electron affinity (EA, A) and chemical hardness (η, B) of phenoxazines.
Batho, bathochromy. Hypso, hypsochromy. Red, reduced state (i.e. phenoxazine).

Since LUMOs energies can be tuned by the presence of electron-withdrawing auxochromic groups (EWA) (Mao, Head-Gordon, & Shao, 2018), we computed the frontier orbital energies of the different EWA that can be placed in positions 1 and 8 (**Figure 5-1**). Consistently with our hypothesis, the two EWA (i.e. acetyl and γ-oxobutenyl) with the lowest LUMO energies and highest electro-accepting powers, ω^+, are associated to bathochromic shifts, while EWA with high LUMO energies (such as cyano or carboxy substituted) induce hypsochromic shifts

(**Table 5-2**). Of note, the *tert.*butyl-carbonyl EWA shows a hypsochromic shift whereas its LUMO energy is close to that of acetyl. This result indicates that other parameters than the LUMO stabilization may play a role in the observed shifts. In particular, *tert.*butyl-carbonyl is a bulky EWA compared to acetyl and carbomethoxy. In this case, as already proposed by Schäfer and Geyer, steric hindrance can altered excitation energies by constraining the carbonyl out-of-plane (Schäfer & Geyer, 1972). Such an effect is observed in the case of compound **14r** for which a large dihedral angle between ring C and carbonyl in position 1 is computed (59° in **14r** *vs* 8° in **1r**) (**Figure S5-11**). To test whether this torsion destabilized the LUMO and thereby induced the hypsochromic shift, we computed the ΔE^{vert} as a function of the torsional angle for compounds **1r**, **14r** and **15r** (**Figure 5-5**A). The results show that for dihedral angles greater than 30° there is a significant hypsochromic effect, with the maximum hypsochromy obtained around 90° (from 0.30 eV for **1r** to 0.83 eV for **15r**; **Figure 5-5**A). Below 60°, **14r** becomes less hypochromic than **15r** in its optimized geometry (**Figure 5-5**A), in agreement with the lower LUMO energy of *tert*.butyl-carbonyl compared to carbomethoxy (**Table 5-2**). However, **14r** can never reach the bathochromicity of **1r**, even at angles near 0° (**Figure 5-5**A). These results indicate that the steric hindrance of *tert*.butyl-carbonyl explains, partly at least, the hypsochromicity of **14r**.

Table 5-2. Computed chemical descriptors (in eV) of electron-withdrawing auxochromes (EWA) in relation with the chromic shifts they induce experimentally in phenoxazinone/phenoxazine pairs.

EWA	HOMO	LUMO	H-L gap	ω^+
		bathochromic shifts		
Acetyl	-7.64	-0.59	7.06	1.01
γ-oxo-butenyl	-7.56	-1.59	5.97	2.05
		hypsochromic shifts		
Carbomethoxy	-8.59	0.01	8.60	0.72
Cyano	-10.61	0.32	10.93	0.74
*tert.*butyl-carbonyl	-7.42	-0.57	6.85	0.98

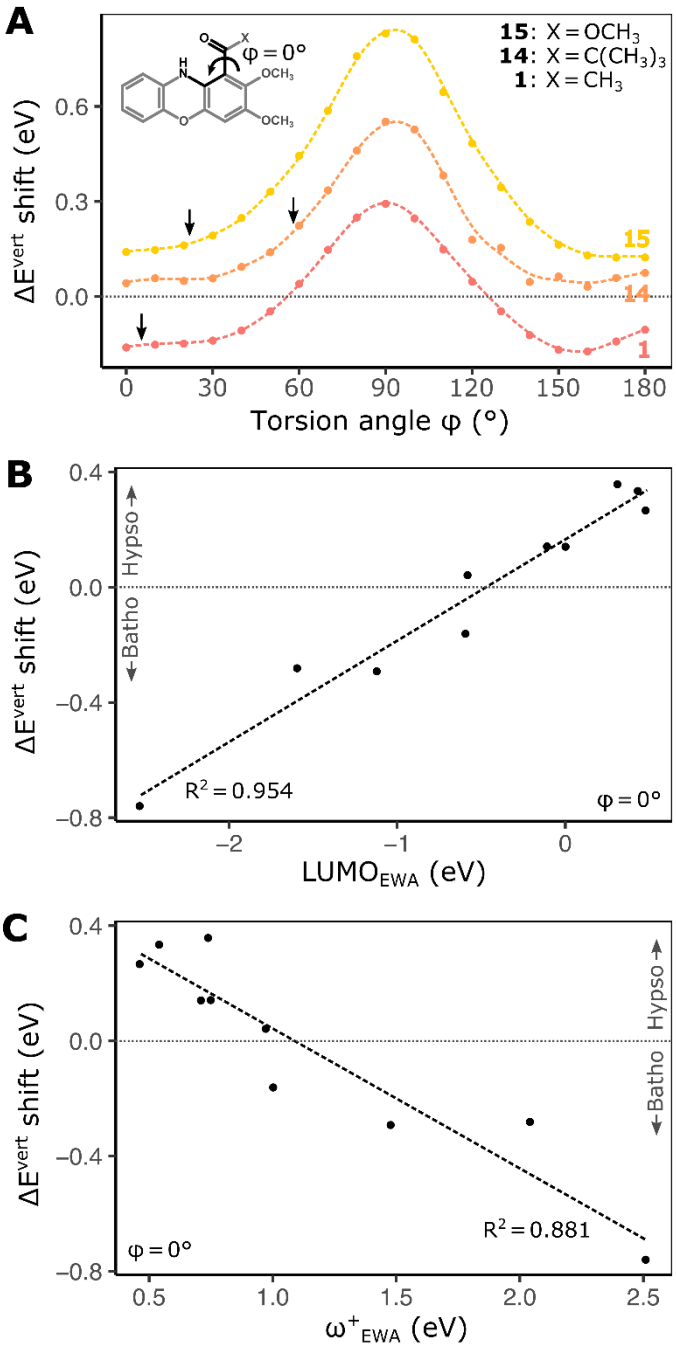

Figure 5-5. Comparison of computed chromic shifts (ΔE^{vert} shift) of phenoxazinone/phenoxazine pairs with geometric (A) and electronic (B-C) properties of electron-withdrawing auxochromes (EWA) in position 1.

Batho, bathochromy. Hypso, hypsochromy. Arrow, angle at the optimized geometry.

Next, we considered model systems obtained by functionalization of the 2-hydroxy-phenoxazin-3-one/2,3-dimethoxy-phenoxazine pairs with EWA with either stabilized (nitro) or destabilized (carboxamide) LUMOs (**Table S5-1** and **Figure 5-5**B-C). All substituents

were placed in position 1 and forced to lie within ring C plane after geometrical optimization to avoid torsion of molecular orbitals due to steric hindrance. The results show that LUMO energies of substituents explain 95 % of the variation in chromic shifts upon reduction (**Figure 5-5**B). They also confirme that increasing the electro-accepting power of substituents in position 1 leads to more bathochromic phenoxazines (**Figure 5-5**B-C and **Table S5-1**).

Application to Ommochromes and Other Phenoxazinone Dyes

Chromic shifts of two other important pairs of natural and technological relevance were next considered, namely xanthommatin/dihydroxanthommatin (bathochromic invertebrate pigments) and resorufin/dihydroresorufin (hypsochromic biotechnological dyes; see Figure 6 and **Table S5-2**).

The 8-substituted-oxo-pyrido[3,2-*a*]phenoxazin-3-one xanthommatin presents HOMO (-6.89 eV) and LUMO (-3.35 eV) energies very close to the mean HOMO and LUMO energies of the phenoxazinones investigated above (compare **Figure 5-6** with **Table 5-1** and **Figure S5-9**). The corresponding reduced 8-substituted-oxo-pyrido[3,2-*a*]-3-hydroxy-phenoxazine dihydroxanthommatin possesses not only a highly stabilized LUMO (-2.02 eV), but also a relatively stabilized LUMO+1 (-1.59 eV). Overall, the molecular orbitals of xanthommatin and dihydroxanthommatin resemble those of the phenoxazinones and phenoxazines described above both qualitatively and quantitatively (**Figure 5-6** and **Figure S5-9**), which indicates that the effect of EWA on the reduced state should also control their chromic shifts. The substituent in position 8 if ommochromes is closely related to acetyl, while the oxo-pyrido ring attached on positions 1 and 2 resembles γ-oxo-butenyl. The two corresponding carbonyl functions lie within ring A and C planes, respectively. All these characteristics predicted a bathochromic shift upon reduction. Accordingly, the molecular orbital gaps of dihydroxanthommatin are 3.21 eV (HOMO-LUMO) and 3.64 eV (HOMO-L+1), thus they lie within, and even beyond, the range of bathochromic transitions already investigated in this study (**Table 5-1**). In addition, dihydroxanthommatin hardness is the lowest we computed (**Table S5-2** and **Table 5-1**). Excited state computations consistently predict two bathochromically shifted electronic transitions, which involve a HOMO-LUMO and a HOMO-L+1 transitions, respectively (**Table S5-2**). Both transitions are characterized by a significant ICT (**Table S5-1** and **Figure 5-6**). The first excited state (S1) is less intense than the second (S2) and their ΔE^{vert} bracket the experimental value ($\Delta E_{S1}{}^{vert}$ = 2.25 eV <

ΔE^{exp} = 2.58 eV < $\Delta E_{S2}{}^{vert}$ = 2.69 eV), which corresponds to the maximum of a broad absorption peak (Linzen, 1974).

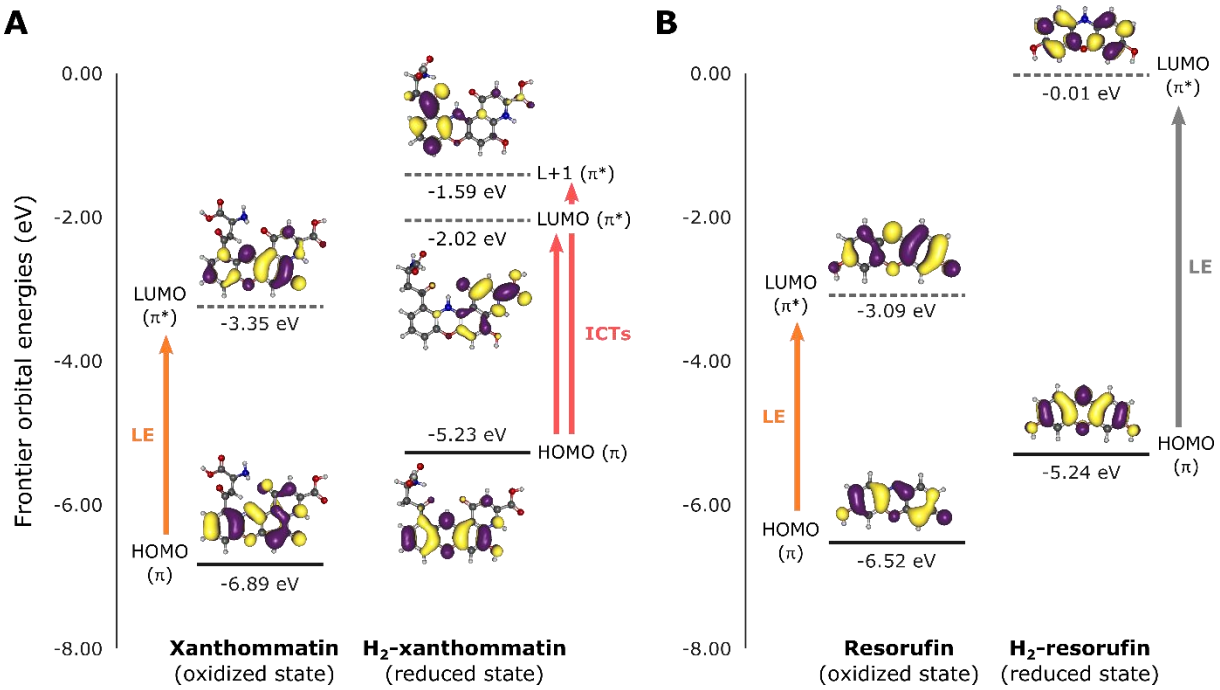

Figure 5-6. Orbital diagrams of the bathochromic ommochrome pair xanthommatin/dihydroxanthommatin and the hypsochromic pair resorufin/dihydroresorufin.
ICTs, intramolecular charge-transfers; LE, local excitation.

On the contrary, the resorufin/dihydroresorufin pair presents all the characteristics associated to hypsochromic shifts: the absence of EWA, a small HOMO-LUMO gap in the oxidized state, a highly destabilized LUMO and high chemical hardness (**Figure 5-6** and **Table S5-2**). Accordingly, TD-M05 calculations predict a highly hypsochromic shift upon reduction (1.05 eV; **Table S5-2**). To the best of our knowledge, the exact experimental absorbance of dihydroresorufin has never been reported in the literature, but resorufin is known to lose its color upon reduction (Song *et al.*, 2014), which is in agreement with our calculations.

Discussion

The above reported results clearly show that the model originally proposed by Schäfer and Geyer to explain the experimentally observed chromic shifts in substituted phenoxazinone/phenoxazine pairs, which correlates bathochromic shifts to an increase in resonance structures (Schäfer & Geyer, 1972), is unable to explain qualitatively why 1-acetyl-

phenoxazines are bathochromic and why the closely-related 1-carbomethoxy-phenoxazines are hypsochromic. Our analysis, based on modern descriptors of aromaticity, invalidates the general applicability of this model, showing that there is no clear correlation between descriptors of aromaticity and bond conjugation with color changes upon reduction. On the other hand, it appears that bathochromic and hypsochromic shifts correlate well with electronic properties of reduced forms, in particular with all descriptors containing information on the strength and nature of the EWA present in the molecule, such as LUMO energy, electro-accepting power and EA.

On this basis, to explain the color-changing behavior of substituted phenoxazinones upon reduction, we propose the following structure-property model. (**Figure 5-7**). The bright excited state of phenoxazinones (i.e. oxidized forms) that is responsible for the yellow-orange color of this chromophore is of Locally Excited (LE) character stemming from a π-π* transition. This transition is not particularity affected by EWA in position 1, explaining why excitation energies of substituted phenoxazinones do not vary significantly as a function of the EWA. Therefore, the energy of this LE state in phenoxazinones defines a common reference for bathochromy and hypsochromy of substituted phenoxazines (**Figure 5-7**B). The 3-hydroxy-phenoxazine chromophore (i.e the reduced form of the pair) is on the other hand characterized by a bright excited state displaying a partial intramolecular CT (ICT) character (**Figure 5-7**A). When 3-hydroxy-phenoxazine is substituted in position 1 with a EWA, the EWA LUMO hybridizes with the phenoxazine UMOs and stabilizes them, thus lowering the energy of ICT. The strength of stabilization depends primarily on two factors (**Figure 5-7**A): (1) an electronic one that is the energy of EWA LUMO and (2) a structural one that is the magnitude of the dihedral angle formed by the EWA with the corresponding phenoxazine ring ruling its conjugation.

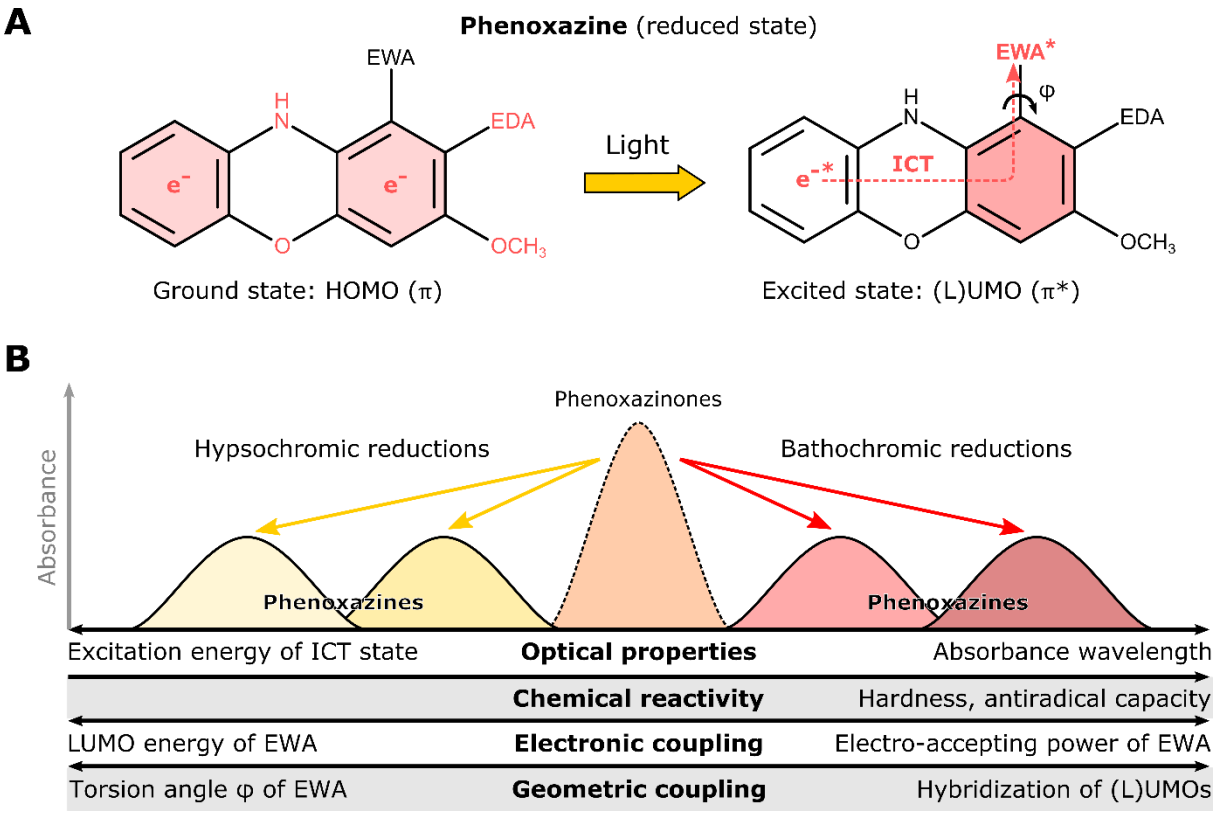

Figure 5-7. Model of the effect of geometric and electronic couplings on chromic shifts and chemical behaviors of phenoxazinone/phenoxazine pairs upon reduction.
EWA, electron-withdrawing auxochrome. EDA, electron-donating auxochrome. ICT, intramolecular charge-transfer. $e^{-(*)}$, (excited) electron.

First, EWAs with high (low) electro-accepting powers stabilize (destabilize) the corresponding substituted phenoxazine UMOs, which decreases (increases) their excitation energies and leads to bathochromic (hypsochromic) shifts upon reduction (**Figure 5-7**B). This translates into ICT associated to lower (higher) energies, hence into red (yellow)-shifted colors (**Figure 5-7**B). This mechanism explains why acetyl and carbomethoxy induced bathochromic and hypsochromic shifts, respectively.

Second, from a structural viewpoint, when a substituent in position 1 is coplanar with the phenoxazine ring, the (L)UMOs are fully conjugated and thus highly stabilized. Structural decoupling decreases this effect (**Figure 5-7**B) explaining why sterically hindered EWA, despite having a high electro-accepting power can indeed induce hypsochromic shifts, as in the case of the *tert*.butyl-carbonyl. The same applies for the methylated phenoxazine nitrogen that induced a hypsochromic shift because of steric hindrance with the acetyl in position 1, as already proposed by Schäfer and Geyer (Schäfer & Geyer, 1972). Overall, we propose that

electronic and geometric interactions of EWA with the phenoxazine UMOs produce a wide range of ICT energies, which ultimately leads to a continuous hypso-to-bathochromic scale (**Figure 5-7**B).

Note that this model can be refined in several ways. For example, we could take into account the effect of electron-donating auxochromes (EDA) on the phenoxazine HOMO. This would explain why HOMO-LUMO gaps, rather than LUMO alone, better predicted chromic shifts in the complete set of investigated compounds (in which EDA in position 2 varies). We could also add the effect of EWA in other positions than 1. From the investigated compounds, it appears that EWA at position 5, 6, 7 and 8 have an effect on the phenoxazinone LUMO too, which (slightly) modifies the threshold for bathochromy. Most interestingly, EWA in position 8 could interact with the EWA in position 1 either synergistically (both EWA are similar and stabilize the same ICT, see **8r**), additively (different bathochromic EWA stabilize two different ICT, see dihydroxanthommatin) or antagonistically (hypsochromic and bathochromic EWA lead to ICT not stabilized enough, see **9r**). Note that for pair **9** TD-M05 calculations could not predict the correct color-changing behavior upon reduction. This indicates that other parameters not modelled in this study, such as direct solvent interactions (Barone *et al.*, 2014), could also finely tune the color-changing effect of reduction.

Of note, the structure-to-property relation found here has also implication for the reactivity of these compounds. Indeed, HOMO-LUMO gap and LUMO energy are known to be directly related to hardness and electron affinity, respectively, which define some aspects of the chemical reactivity of a compound (Pearson, 1992). Our calculations showed that those two chemical parameters were highly correlated with the direction of chromic shift. We conclude that the softer and the more electrophilic a phenoxazine is, the more bathochromic and antiradical it becomes.

Conclusions

In this study, we unraveled the electronic mechanisms behind the atypical bathochromic (i.e. red shift) reduction of ommochrome pigments in invertebrates, particularly at play in the ecologically important nuptial coloration of dragonflies (Futahashi *et al.*, 2012). We established the relation between the nature and strength of electron-withdrawing auxochromes (EWA) that rules the magnitude of the phenoxazine intramolecular charge-

transfer and the observed chromic shift. Other parameters, such as the angle formed by EWA with the attached phenoxazine ring, tune the direction of the chromic shift upon reduction.

From a technological viewpoint, crafting phenoxazines with new EWAs that allow a wider range of chromic shifts than currently available (Kumar *et al.*, 2018) might foster the field of ommochrome-based electro-chromic devices. The influence of EWA conjugation on chromic shifts suggests that these devices could be made even more flexible by dynamically altering the torsion angle of EWAs, for example through tunable interactions with the coated surface.

From a biological viewpoint, it is well established that optical properties and chemical behaviors are both important functions of pigments (Needham, 1974; McGraw, 2005; Gandía-Herrero, Escribano, & García-Carmona, 2016; Ostrovsky & Dontsov, 2019). By linking together those two functions through EWA properties, our study suggests that invertebrates may have favored bathochromic ommochromes because of both their better capacity to protect cells against reactive species in the reduced state, as previously suggested (Romero & Martínez, 2015), and their tunable red shift, which we discuss in two biological situations. First, the occurrence of a decarboxylated form of xanthommatin can be explained by its decarboxylated EWA producing a less bathochromic reduced state. It could therefore allow a wider range of colorations than with xanthommatin alone, as seen in cephalopods (Williams *et al.*, 2016). Second, it has long been known that absorbance spectra of ommochromes are red-shifted in insects eyes compared to *in vitro* (Langer, 1967, 1975; Höglund *et al.*, 1970). We propose that properties of the matrix in which ommochromes are deposited and that alter their absorbance, such as proteins (Langer, 1967; Williams *et al.*, 2019b) and metals (White & Michaud, 1980; Liao *et al.*, 2011), do so by modulating the electrophilicity and the conjugation of ommochrome EWAs, leading ultimately to their bathochromic behaviors uniquely observed *in vivo*.

In conclusion, our study reinforces the idea that the unique electronic properties of ommochromes make them a powerful technological and biological framework to tune rapidly and efficiently color-changing materials.

Acknowledgments

We are grateful to Alistar Ottochian, Michele Turelli and Bernardino Tirri for their technical support. F.F. thanks the ENS de Lyon for financial support. I.C. gratefully acknowledges support from the European Research Council (ERC) for funding under the European Union's Horizon 2020 research and innovation program (grant agreement No 648558, STRIGES CoG grant). This works formed part of the doctoral dissertation of F.F. under the supervision of J.C.

Supplemental Information

Supplemental Text

Basis Set and Functional Benchmarks

The efficiency of different basis-sets were compared considering the 2-amino-7-methoxy-phenoxazin-3-one molecule as test case, since X-ray structural data are available (Buckley, Charalambous, & Henrick, 1982). Only distances between non-hydrogen atoms were considered. In agreement with previous studies on other organic compounds (Jacquemin *et al.,* 2011), we found that a split-valence triple-zeta basis-set including two sets of polarization functions provides a mean absolute and a standard deviation down to 0.0115 Å and 0.0071 Å, respectively (**Figure S5-1**). These results are not significantly improved by adding more polarization and diffuse functions. Therefore the B3LYP-D3(BJ)/6-311G(d,p) level of theory was used for all structural optimizations.

To select the basis set to be used for TDDFT calculations, we considered different basis-sets to compute the ΔE^{vert} of the 2-amino-7-hydroxy-phenoxazin-3-one molecule using the B3LYP functional and we monitored the convergence of computed ΔE^{vert}. These calculations showed that the addition of one set of diffuse and polarization functions has the highest effect (**Figure S5-2**), in agreement with previous studies (Jacquemin *et al.*, 2011; Escudero *et al.*, 2015). Indeed, at 6-31+G(d) level, the computed ΔE^{vert} already converged to nearly 100 % of the value computed using the largest basis set considered –and feasible for a routine study of all compounds, namely the 6-311+G(2d,2p) (**Figure S5-2**). The 6-31+G(d) basis-set was therefore retained for computing excited states properties (i.e. absorption spectra) of all compounds.

To select the best functional for TDDFT modelling, a series of common meta-GGA, hybrid and range-separated hybrid functionals were benchmarked against experimental values, considering both excitation energies and chromic shifts. Specifically, BMK (Boese & Martin, 2004), M05 (Zhao *et al.*, 2005), M05-2X (Zhao, Schultz, & Truhlar, 2006), M06-HF (Zhao & Truhlar, 2006), τHCTHhyb (Boese & Handy, 2002), TPSSh (Staroverov *et al.*, 2003), PBE0 (Adamo & Barone, 1999), B3LYP (Becke, 1993), M11 (Peverati & Truhlar,

2011), LC-ωHPBE (Henderson *et al.*, 2009), CAM-B3LYP (Yanai, Tew, & Handy, 2004) and ωB97X-D (Chai & Head-Gordon, 2008) functionals were tested.

Computation of Descriptors

Dihedral angles, bond lengths and harmonic oscillator model of aromaticity for heterocycle electron delocalization (HOMHED) were computed at CPCM-B3LYP-D3(BJ)/6-311G(d,p) level using the Gabedit program.

Restricted Hartree-Fock energies (E), highest occupied molecular orbitals (HOMO), lowest unoccupied molecular orbitals (LUMO), HOMO-LUMO gaps and ground state (GS) dipole moments were obtained by single-point (SP) calculations at CPCM-M05/6-31+G(d)//CPCM-B3LYP-D3(BJ)/6-311G(d,p) level.

ΔE^{vert}, oscillator strengths, weight of single determinants, transition dipole moments, excited state (ES) dipole moments and unrelaxed charge transfer distances (D_{CT}) (Le Bahers *et al.*, 2011) were computed at NonEq-CPCM-TD-M05/6-31+G(d)//CPCM-B3LYP-D3(BJ)/6-311G(d,p) level.

Nucleus-independent chemical shifts (NICS) were computed at the center of each ring (NICS(0)) at CPCM-GIAO-M05/6-31+G(d)//CPCM-B3LYP-D3(BJ)/6-311G(d,p) level, using the gauge-including atomic orbital (GIAO) method (Chen *et al.*, 2005).

Unrestricted energies of radical cations (E^+) and anions (E^-) were computed by SP calculations at CPCM-M05/6-31+G(d)//CPCM-B3LYP-D3(BJ)/6-311G(d,p) level. The following equations were used to obtain the associated chemical parameters (Jacquemin & Adamo, 2015).

(1) Ionization energy: $\mathrm{IE} = E^+ - E$

(2) Electron affinity: $\mathrm{EA} = E - E^-$

(3) Chemical hardness: $\eta = \mathrm{IE} - \mathrm{EA}$

(4) Electro-accepting power: $\omega^+ = \frac{(\mathrm{IE}+3\mathrm{EA})^2}{16(\mathrm{IE}-\mathrm{EA})}$

Exceptions in the Phenoxazinone/Phenoxazine Series

The phenoxazinone/phenoxazine series experimentally investigated by Schäfer and Geyer (Schäfer & Geyer, 1972) presents pairs with particular chemical functionalizations that affect their optical properties beyond the mere chromic reduction effect.

First, pairs **11** and **12** possess an extra aromatic group conjugated to the phenoxazinone/phenoxazine chromophore in position 2 (**Figure 5-1**, main text). Such chemical group greatly modifies electron densities in ground and excited states. Thus, they are expected to behave differently from other pairs and thus will not provide meaningful information about the general mechanisms of bathochromic reductions in ommochromes.

Second, the pair **9** has repeatedly failed to be correctly modelled by our TDDFT approach. Thus, the parameters computed for this pair may not be reliable; they are therefore not included in this study.

Calculation of the HOMHED index

Geometric-based indices derived from the harmonic oscillator model for aromaticity (HOMA) provide a quantitative view of electron delocalization for aromatic π-bond systems (Szatylowicz, Stasyuk, & Krygowski, 2016). For heteroaromatic compounds, such as phenoxazinones and phenoxazines, the harmonic oscillator model of heterocyclic electron delocalization (HOMHED) allows a better description of π- and *n*-electron delocalizations in both cyclic and acyclic structures. This index was parametrized using experimental data from a wide range of reference compounds with various heteroatomic bonds (Frizzo & Martins, 2012). HOMHED of *n* alternating bonds is calculated using the following equation and parameters:

$$\mathrm{HOMHED} = 1 - \frac{1}{n} * \left(\sum_i \alpha_i * \sum_j \left(R_{i,\mathrm{opt}} - R_{i,j} \right) \right)$$

α_{CC} = 78.6

α_{CN} = 87.4

α_{CO} = 77.2

$R_{CC,opt}$ = 1.387 Å

$R_{CN,opt}$ = 1.339 Å

$R_{CO,opt}$ = 1.282 Å

For each type of bonds (i = CC, CN, CO, etc.), HOMHED compares the bond lengths ($R_{i,j}$) of an actual compound (here at the optimized geometry) to the optimal bond lengths ($R_{i,opt}$) of a fully aromatic system. Each bond type is normalized with a different α_i factor to yield HOMHED = 1 for pure aromatic compounds, 0 for non-aromatic ones and < 0 for aromatic ones. In this study, we used the HOMHED index in two ways (**Figure 5-2**A-B in the main text and **Figure S5-7** in this file): to assess aromaticity of ring C (cHOMHED, six cyclic bonds) and to quantify electron delocalization in the vicinity of the substituent in position 1 (sHOMHED, six acyclic bonds). The latter was chosen because it should directly relate to variation in resonance of phenoxazines upon substitution. According to Schäfer and Geyer model (Schäfer & Geyer, 1972), bathochromic phenoxazines are expected to have an increased resonance, and thus higher sHOMHED than hypsochromic phenoxazines.

E_{XC} Functional Benchmark results

TDDFT calculations are extremely sensitive to quality of the exchange-correlation functional used (Laurent & Jacquemin, 2013). To the best of our knowledge, a benchmark of functionals to compute $E^{vert\text{-}abs}$ of various phenoxazinones and phenoxazines is not available (but see other studies that performed TDDFT computations on ommochromes (Romero & Martínez, 2015; Williams *et al.*, 2019b). Therefore, we tested several hybrid, meta-GGA and range-separated hybrid (RSH) functionals by comparing computed $E^{vert\text{-}abs}$ with experimental

maximum excitation energies (ΔE^{exp}) for the series of phenoxazinones and phenoxazines taken from (Schäfer & Geyer, 1972). Only three functionals (M05, BMK and CAM-B3LYP) provided MAE for excitation energies below the expected accuracy of TDDFT methods in predicted vertical excitations [0.2 eV (Jacquemin & Adamo, 2015)] for both phenoxazinones and phenoxazines, while three others performed slightly worse for phenoxazines (M05-2X, ωB97X-D and PBE0; **Figure S5-3**). In particular, M05 provided good correlation to experimental values (**Figure S5-4**). The correlation is lower for phenoxazinones because experimental are typically within a ±0.2 eV range. The comparison between calculated chromic shifts (ΔE_{red}^{vert} - ΔE_{ox}^{vert}) and experimental chromic shifts (ΔE_{red}^{exp} - ΔE_{ox}^{exp}) gave similar trends, with BMK and M05 being the best functionals, closely followed by M05-2X, CAM-B3LYP, ωB97X-D and PBE0 (**Figure S5-5**). However, M05 outperformed BMK by displaying better linear correlation between predicted and experimental values and by predicting correctly 15 (vs 12) chromic shifts over 18 (**Figure S5-6**). Overall, M05 functional results as the most reliable functional for predicting the chromic reduction of phenoxazinones to phenoxazines.

Description of the phenoxazine chromophore

Knowing that EWA were the main hypsochromic/bathochromic drivers, we investigated which electronic properties of the phenoxazine chromophore they could affect most. The main molecular orbitals of 2-hydroxy-phenoxazin-3-one and 2,3-dimethoxy-phenoxazine are depicted in **Figure S5-11**. TD-M05 calculations of these chromophores are also shown. Clearly, molecular orbitals and excitation energies of 2-hydroxy-phenoxazin-3-one were very similar to those of substituted phenoxazine-3-ones (compare **Figure S5-9** and **Figure S5-11**), again showing that EWA did not affect significantly the oxidized state. The same conclusion applied to the reduced state HOMO. The biggest difference between the parent phenoxazine chromophore and its EWA-substituted forms lied in the energies and the ranking of unoccupied orbitals (**Figure S5-9** and **Figure S5-11**). The first excited transition of 2,3-dimethoxyphenoxazine had a localized $\pi\pi^*$ character and a low oscillator strength (**Figure S5-11**). The two following excited transitions S2 and S3 fell further in the UV region but their oscillator strengths were higher and they presented a partial CT character toward ring A and C (**Figure S5-11**), respectively, reminiscent of those observed for EWA-substituted phenoxazines (**Figure S5-9**). The chromic shifts associated to transitions S2 and S3 were

computed at 1.09 and 1.19 eV, respectively, which corresponded to the far hypsochromic range (**Table 5-1**).

Supplemental Figures

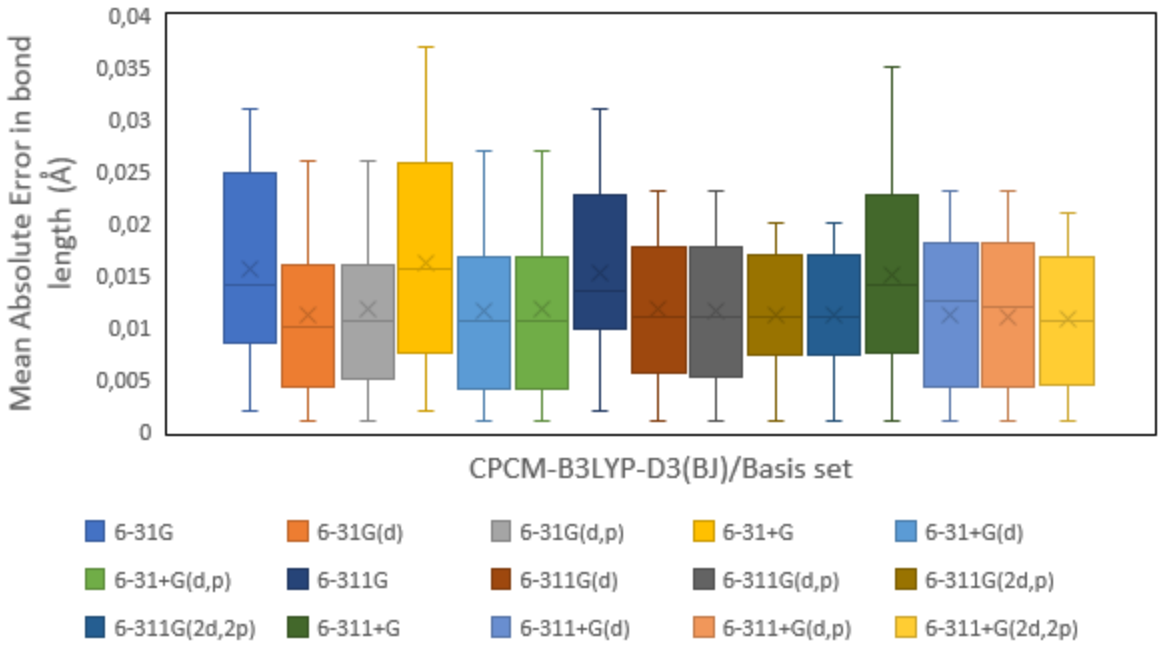

Figure S5-1. Mean absolute errors in computed B3LYP bond lengths of 2-amino-7-methoxy-phenoxazine-3-one as a function of the basis set used.
Experimental crystallographic data have been considered as reference.

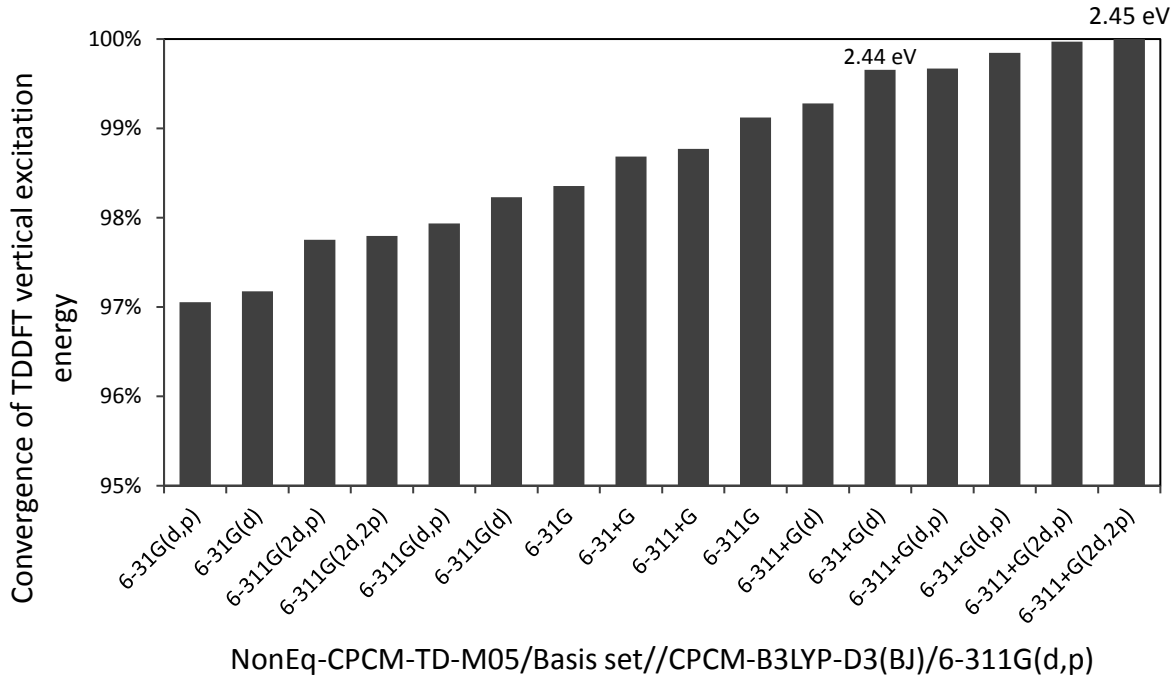

Figure S5-2. Basis-set dependence of the first vertical excitation energy computed for the 2-amino-7-methoxy-phenoxazine-3-one molecule.
M05-computed vertical excitation energies at the 6-311+G(2d,2p) level have been considered as reference.

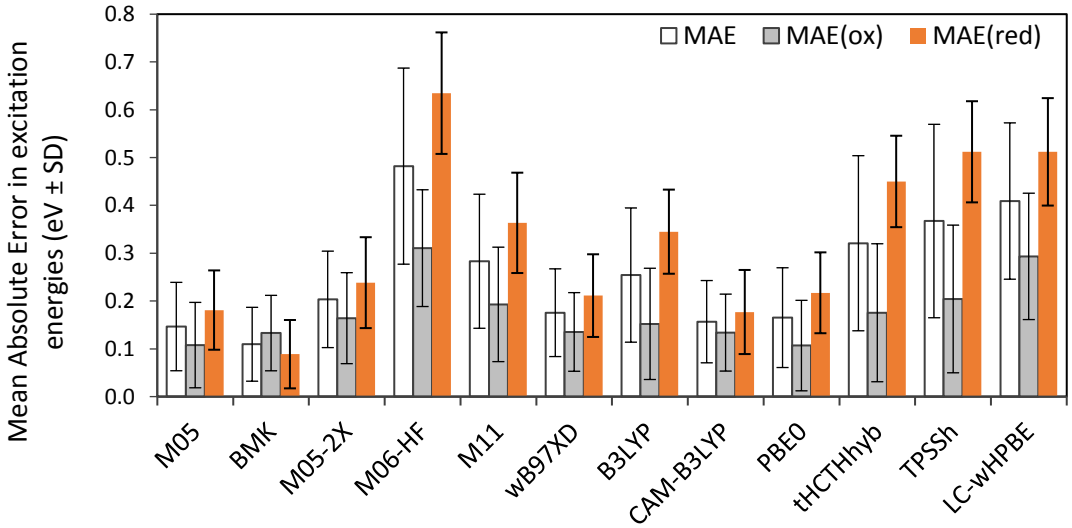

Figure S5-3. Mean absolute errors (MAE) in computed vertical excitation energies of phenoxazinones and phenoxazines for a series of functionals.
Experimental maximum excitation energies have been considered as a reference. MAE(ox), MAE of phenoxazinones only. MAE(red), MAE of phenoxazines only.

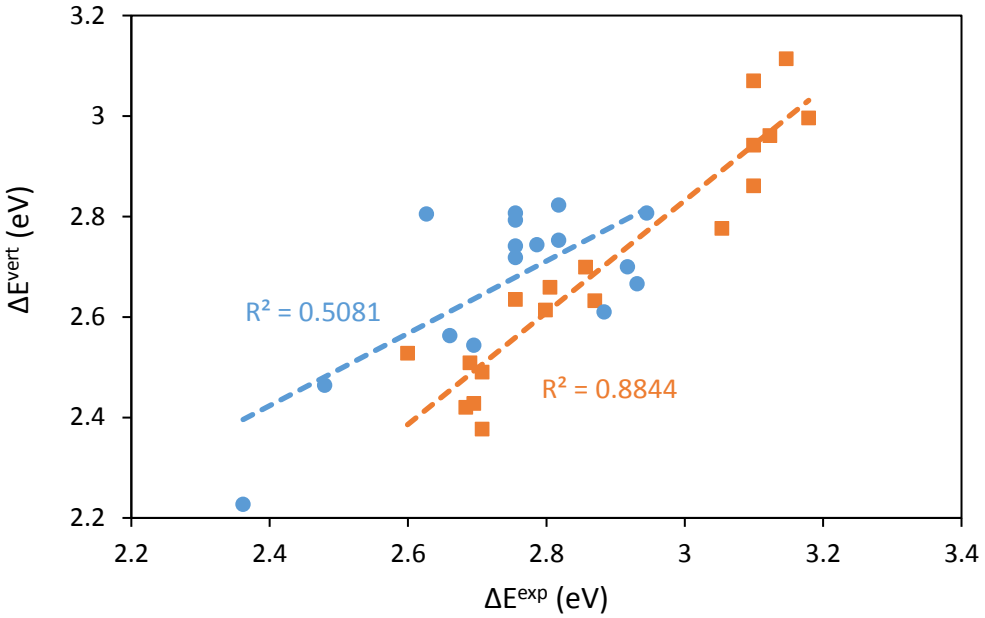

Figure S5-4. Comparison of M05-computed vertical excitation energies (ΔE^{vert}) with experimental maximum excitation energies (ΔE^{exp}).
Dots, phenoxazinones (oxidized state). Squares, phenoxazines (reduced state).

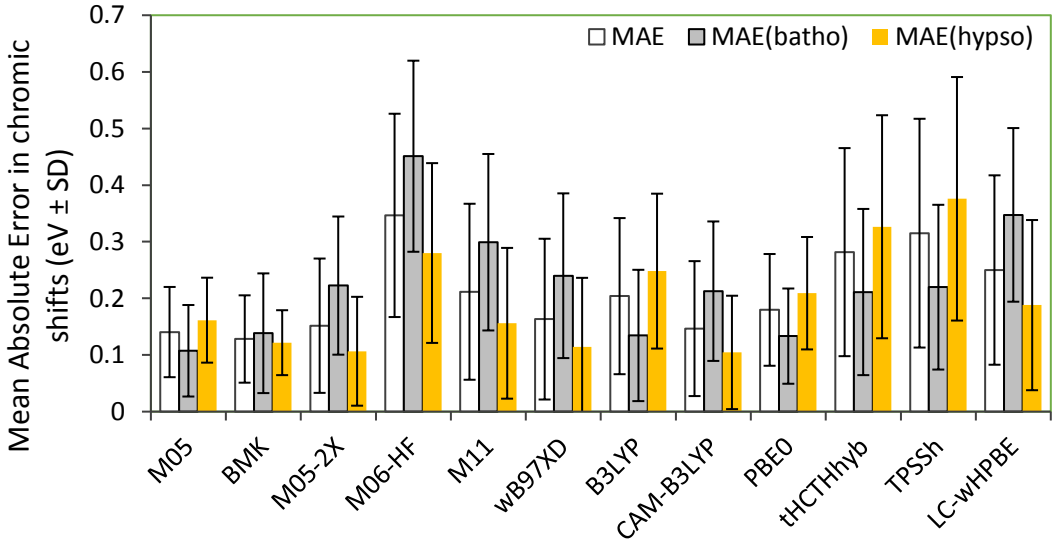

Figure S5-5. Mean absolute error (MAE) in computed vertical chromic shifts of phenoxazinones/phenoxazines pairs for a series of functionals.
Experimental chromic shifts have been considered as a reference. MAE(batho), MAE of experimentally bathochromic pairs only. MAE(hypso), MAE of experimentally hypsochromic pairs only.

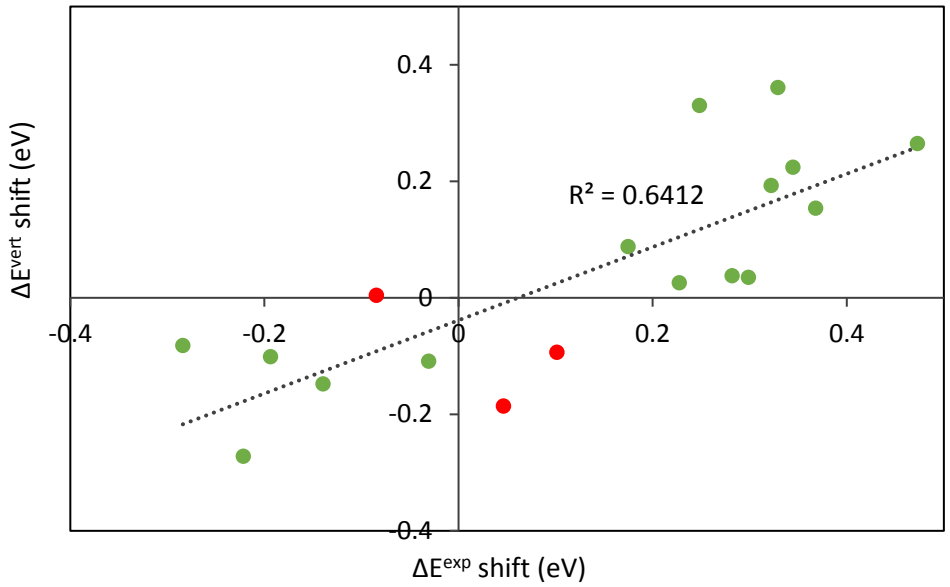

Figure S5-6. Comparison of M05-computed chromic shifts (ΔE^{vert} shift) with experimental shifts (ΔE^{exp} shift) of phenoxazinone/phenoxazine pairs.
Red dots, pairs of phenoxazinone/phenoxazine for which theoretical chromic shifts do not match experimental ones.

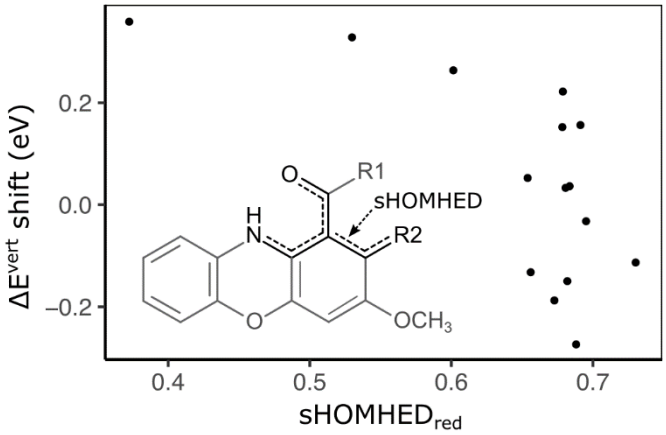

Figure S5-7. Comparison of computed chromic shifts (ΔE^{vert} shift) of phenoxazinone/phenoxazine pairs with the sHOMHED values of corresponding reduced phenoxazines (red).

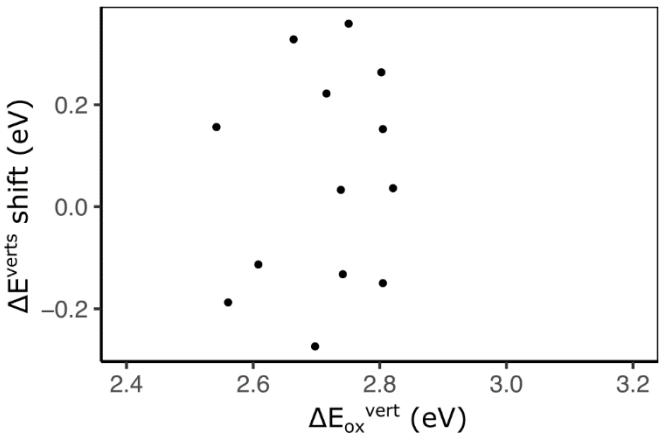

Figure S5-8. Comparison of computed chromic shifts (ΔE^{vert} shift) of phenoxazinone/phenoxazine pairs with the vertical excitation energies of corresponding oxidized phenoxazinones (ΔE_{ox}^{vert}).

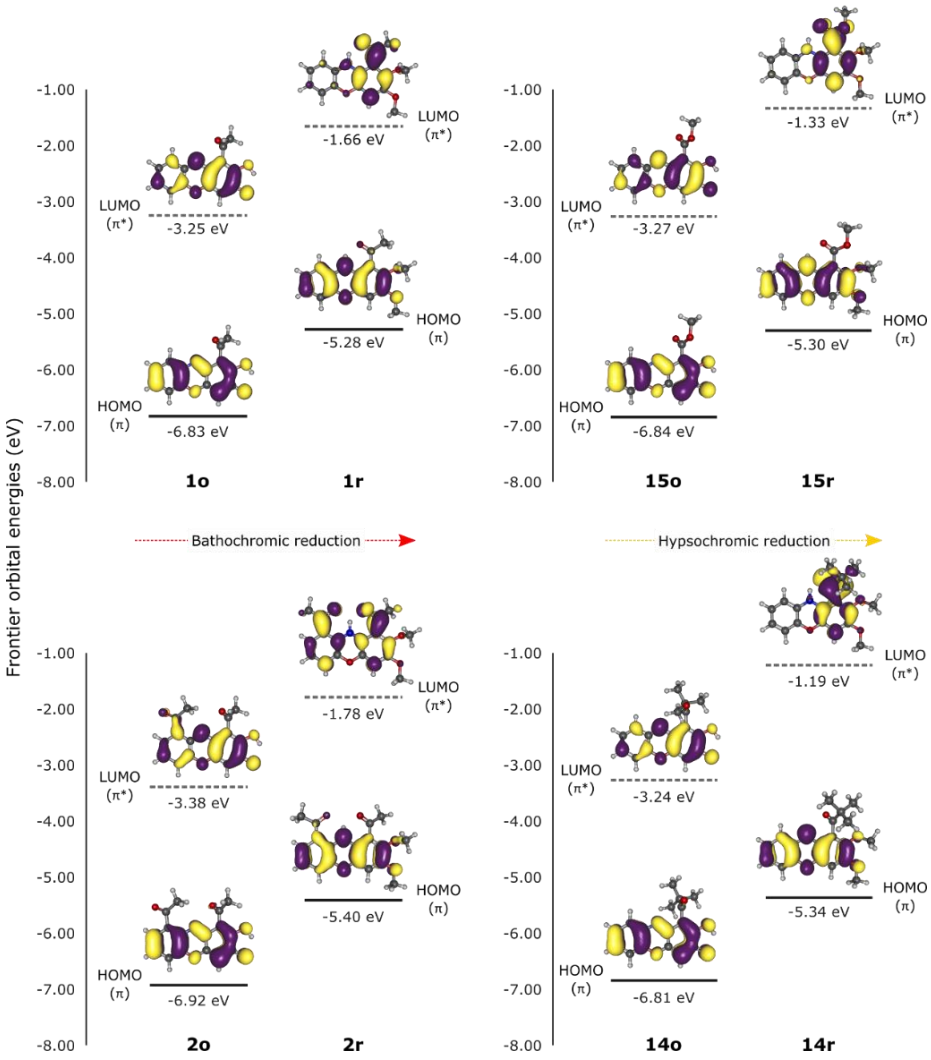

Figure S5-9. Frontier orbital diagrams of two bathochromic phenoxazinone/phenoxazine pairs (1 and 2) and two hypsochromic ones (15 and 14).

In each orbital diagram, phenoxazinone (oxidized state, Xo) and phenoxazine (reduced state, Xr) are depicted on the left and on the right, respectively.

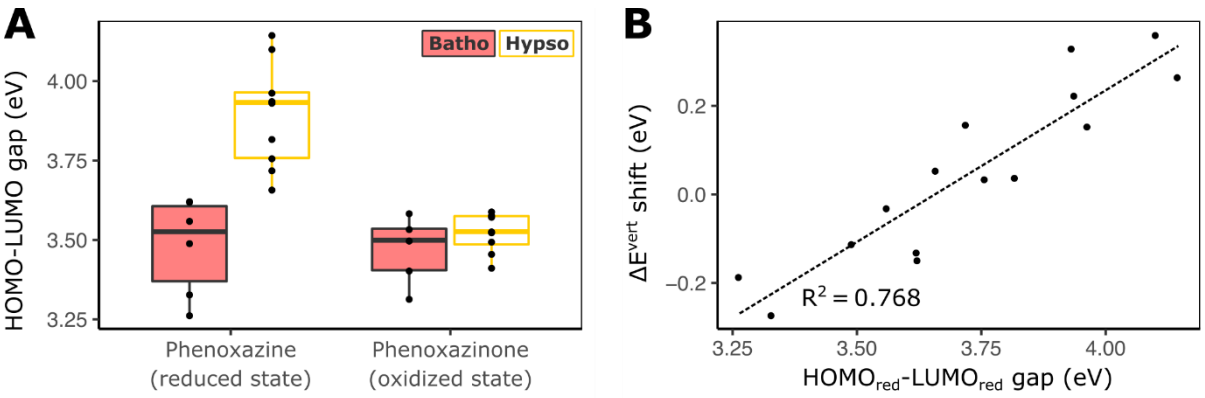

Figure S5-10. Comparison of computed chromic shifts (ΔE^{vert} shift) with HOMO-LUMO gaps of phenoxazinone/phenoxazine pairs.

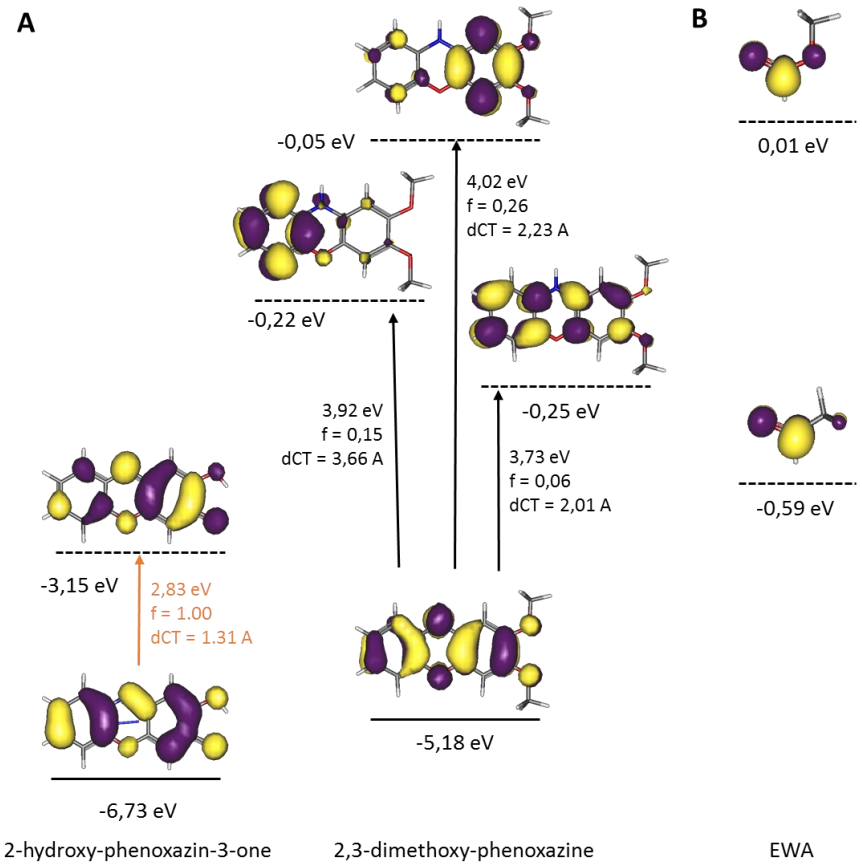

Figure S5-11. Molecular orbital diagrams of unsubstituted 2-hydro-phenoxazine-3-one, 2,3-dimethoxy-phenoxazine and of two electron-withdrawing auxochromes (EWA).

A) Oxidized and reduced states are depicted on the left and on the right, respectively. Arrows indicate excited state transitions from HOMO to (L)UMOs. **B**) LUMOs of acetyl and carbomethoxy auxochromes are depicted at the bottom and at the top, respectively. Hybridization of these LUMOs is maximized with the L+2 orbital of 2,3-dimethoxy-phenoxazine.

Supplemental Tables

Table S5-1. Electronic parameters of electron-withdrawing auxochromes in relation with the chromic shifts they induce theoretically.

Electron-withdrawing auxochrome (EWA) in position 1[a]	**HOMO (eV)**	**LUMO (eV)**	**HOMO-LUMO gap (eV)**	**Electro-accepting power ω^+ (eV)**	**Chromic shift in 1-EWA-2,3-dimethoxyphenoxazine (eV)**
EWA associated to bathochromic shifts					
Nitro	-9.52	-2.52	6.99	2.51	-0.76
Gamma-oxo-butenyl	-7.56	-1.59	5.97	2.05	-0.28
Formyl	-7.86	-1.11	6.74	1.48	-0.29
Acetyl	-7.64	-0.59	7.06	1.01	-0.15
EWA associated to hypsochromic shifts					
tert.butyl-carbonyl	-7.42	-0.57	6.85	0.98	0.07
Carboxyl	-8.76	-0.10	8.66	0.75	0.14
Cyano	-10.61	0.32	10.93	0.74	0.36
Carbomethoxy	-8.59	-0.01	8.60	0.72	0.15
N-methyl-carboxamide	-7.76	0.44	8.20	0.57	0.34
Carboxamide	-7.93	0.49	8.42	0.47	0.27

[a] Dihedral angles between EWA and phenoxazines were set to 0°.

Table S5-2. Computed electronic and structural parameters of oxidized xanthommatin and resorufin and their respective reduced forms.

	Xanthommatin		**Resorufin**	
	Oxidized form	Reduced form	Oxidized form	Reduced form
ΔE^{exp} (eV)	2,81	2,58	2,58	> 3,10
ΔE^{vert} (eV)	2,75	2,25 (S1) 2,69 (S2)	2,63	3,68
HOMO energy (eV)	-6,89	-5,23	-6,52	-5,24
LUMO energy (eV)	-3,35	-2,02 (S1) -1,59 (S2: L+1)	-3,09	-0,01
HOMO-LUMO gap (eV)	3,54	3,21 (S1) 3,64 (S2: HOMO-L+1)	3,43	5,23
Oscillator strength	0,77	0,10 (S1) 0,35 (S2)	0,88	0,03
Transition dipole moment (D)	11,47	1,85 (S1) 5,35 (S2)	13,71	0,31
Chemical hardness η (eV)	N.C.	2,39	N.C.	4,23
Dipole moment of GS (D)	6,68	8,13	8,70	0,77
Dipole moment of ES (D)	2,62	18,22	11,38	0,74
NICS(0) of ring C (ppm)	-0,99	9,35	-0,63	8,48
cHOMHED of ring C	0,63	0,98	0,69	0,99
D_{CT} (Å)	0,92	4,80 (S1) 2,76 (S2)	1,82	0,74

S1, first excited state. S2, second excited state.

N.C., not computed.

Computed Data

See Supplemental File in (Figon *et al.*, 2020).

Optimized Structures

See Supplemental File in (Figon *et al.*, 2020).

5.3 Conclusion

Dans cette étude, les comportements optiques d'une série de modèles d'ommochromes présentant expérimentalement des changements de couleur hypsochromiques et bathochromiques ont été modélisés. En étudiant les effets des substituants et leur nature, il a pu être déterminé que l'état réduit des ommochromes était principalement affecté par l'électrophilicité des substituants en position 1 et 8, alors que l'état oxydé restait inchangé. Nous en avons déduit que le changement de couleur bathochromique des ommochromes était dû à la capacité de l'état réduit à réarranger ses électrons excités en les déplaçant vers l'auxochrome en position 1 ou 8. Cette facilité (en termes énergétiques) à réarranger ses électrons en absorbant la lumière est corrélée avec la capacité à accepter de nouveaux électrons, et donc au comportement antiradicalaire. En réponse au *point 1* du **chapitre 3** (p. 115), ces résultats suggèrent que la plasticité des ommochromes en termes de changement de couleur, tant *in vivo* que dans les technologies biomimétiques, proviendrait de la manipulation des couplages électroniques et géométriques entre les auxochromes et le chromophore réduit. En parallèle et pour répondre au *point 4* du **chapitre 3** (p. 116), le fait que les invertébrés produisent des ommochromes qui permettent un changement de couleur bathochromique relativement prononcé indiquerait que ces mêmes ommochromes auraient pu être sélectionnés pour leurs relativement bonnes capacités antiradicalaires. Il reste cependant à déterminer si un tel effet est possible et significatif *in vivo*.

D'un point de vue méthodologique, un certain nombre de points pourraient être améliorés dans de futures études. D'une part, l'obtention de spectres UV-Vis expérimentaux d'autres ommochromes (tels que ceux décrits dans le **chapitre 4**) dans leurs états oxydés et réduits permettrait de tester notre modèle sur des molécules plus complexes et proches des ommochromes biologiques. On pourrait alors procéder à des investigations sur l'effet bathochromique de deux auxochromes en position 1 et 8 avec des électrophilicités différentes. D'autre part, certaines approximations faites dans notre approche de modélisation pourraient être revues pour coller au mieux à la réalité du processus d'absorption en solution. Par exemple, la prise en compte explicite des molécules d'eau et de leurs liaisons hydrogènes pourrait influencer le pouvoir électrophile des auxochromes et donc expliquer pour partie les différences obtenues entre les énergies d'excitation prédites et expérimentales. Parallèlement, le choix a été fait de calculer les longueurs d'onde d'absorbance à partir de l'énergie verticale

d'excitation, qui correspond à la transition entre l'état de base à géométrie optimale vers l'état excité sans relaxation géométrique (donc à la même géométrie ; approximation verticale). Or, le véritable processus d'absorption implique une modification de la géométrie à l'état excité (approximation adiabatique), ainsi qu'un couplage entre l'absorption UV-Vis et les modes vibratoires atomiques (effet vibronique). En d'autres termes, les atomes d'une molécule ne sont pas figés et leurs multiples déplacements influencent l'énergie lumineuse absorbée par la molécule. Cette approximation adiabatique et vibronique permet d'améliorer la précision des calculs, de modéliser les bandes d'absorption plutôt que des raies d'absorption, ainsi que de résoudre certains des cas les plus complexes pour lesquels l'approximation verticale ne fonctionne pas du tout, quelle que soit la fonctionnelle. Cependant, cette approximation nécessite des temps de calcul beaucoup plus longs et ne sont en pratique pas toujours possibles. En particulier, les géométries à l'état de base et à l'état excité doivent se chevaucher un maximum pour permettre de résoudre certains couplages. Des tests sur les modèles d'ommochromes ont ainsi montré que les fonctions carbonyles attachées aux cycles phénoxazinones présentent des degrés de liberté géométrique trop fort ; la géométrie optimale à l'état excité devient trop différente de celle à l'état de base. Ainsi, nous n'avons pour l'instant pas réussi à appliquer le modèle adiabatique avec effets vibroniques aux ommochromes car les calculs de couplage vibronique ne convergent pas. D'autres tests et développements sont donc nécessaires pour modéliser les caractéristiques optiques des ommochromes afin de s'approcher au mieux de la réalité biologique.

Chapitre 6 – Les organites pigmentés apparentés aux endolysosomes à l'origine des changements de couleur des araignées crabes

Pigment cells have much in common and, while they are functionally and morphologically distinct from one another, they are rather closely related.

Joseph T. Bagnara *et al*. (1979), *Science*

6.0 Sommaire

CHAPITRE 6 – LES ORGANITES PIGMENTES APPARENTES AUX ENDOLYSOSOMES A L'ORIGINE DES CHANGEMENTS DE COULEUR DES ARAIGNEES CRABES 217

6.0 SOMMAIRE 218
6.1 OBJECTIFS ET METHODOLOGIES 219
6.2 TRAVAIL EXPÉRIMENTAL 220
Abstract *220*
Introduction *221*
Materials and Methods *224*
Specimen Sampling 224
Reagents and Solutions 224
Integument Fixation and Embedding 224
Transmission Electron Microscopy 225
Electron Tomography 225
Synchrotron X-Ray Fluorescence 226
Scanning Transmission Electron Microscopy 227
Correlative Synchrotron X-Ray Fluorescence and Scanning Transmission Electron Microscopy 227
Image Analysis and Quantification 227
Statistical Analysis 228
Results *228*
High-Pressure Freezing and Freeze Substitution Preserve Cells of Crab Spiders in an Unprecedented Manner 228
Pigment Organelles Possess Ultrastructural and Chemical Endolysosomal Features 229
Morphology and Metal Identity of Pigment Organelles Vary with Coloration 233
Formation and Degradation of Pigment Organelles in Relation to Secretory and Endolysosomal Systems. 237
Discussion *242*
Simultaneous Anabolism and Catabolism of Pigment ELROs within the Same Cell 242
The Endolysosomal System Provides a Universal Platform for Pigmentation 244
The Endolysosomal System is Fully Functionalized for Reversible Color Changes 245
Conclusion 247
Acknowledgment *247*
Supplemental Information *248*
6.3 CONCLUSION 254

6.1 Objectifs et méthodologies

Jusqu'à présent, je me suis intéressé aux pigments en eux-mêmes, c'est-à-dire à leur structure chimique, à leur biosynthèse et à la façon dont ils interagissent avec la lumière (**chapitres 3 et 4**). Nous avons vu dans les **chapitres 1 et 2** que les pigments ne sont pas les seuls acteurs du changement de couleur morphologique car ils sont généralement déposés dans une matrice à l'intérieur d'organites membranaires spécialisés. C'est l'ensemble des événements qui mènent à la formation des organites pigmentés, à leur développement, à leur sécrétion, et parfois à leur destruction, qui produit *in fine* une partie des changements de couleur morphologique. En particulier, chez l'araignée crabe *Misumena vatia* (la thomise variable), un processus intracellulaire permettrait de former et de recycler en permanence des organites pigmentés. Ce cycle de vie dynamique aboutirait *in fine* à l'alternance de formes jaunes et blanches chez cette espèce, chez d'autres araignées crabes et même chez des insectes. L'étude de ce cycle de vie intracellulaire pourrait de plus renseigner sur le catabolisme d'autres systèmes pigmentés s'il s'avérait que les organites pigmentés des araignées crabes étaient apparentés aux lysosomes, comme le sont les mélanosomes et les ptérinosomes [famille des LROs récemment renommée ELROs ; (Delevoye, Marks, & Raposo, 2019)].

L'objectif de ce chapitre est d'étudier, à l'échelle subcellulaire, les organites pigmentés d'araignées crabes blanches et jaunes. Par rapport aux études précédentes, j'emploie des techniques permettant (i) de préserver les structures cellulaires dans un état quasi-natif (cryofixation par *High-Pressure Freezing* et *Freeze Substitution*), (ii) de visualiser l'ultrastructure des organites pigmentés en trois dimensions (tomographie électronique) et (iii) d'analyser la composition en métaux de ces organites (fluorescence des rayons X issus du rayonnement Synchrotron). En l'absence de marqueurs moléculaires chez les araignées crabes, contrairement aux organismes modèles, seules ces techniques permettent d'identifier des marqueurs de ELROs comme les vésicules intraluminales, les tubulations membranaires ou encore l'accumulation de calcium et de zinc.

6.2 Travail expérimental

The within-cell life cycle of endolysosome-related pigment organelles leads to reversible color changes in crab spiders

Abstract

Reversible color change is a fascinating ability within the animal kingdom. Pigment-based mechanisms enabling morphological color changes are widespread in vertebrates and invertebrates. Yet, how pigment cells accommodate both formation and degradation of pigments for reversibility is not understood in most cases. Here, we studied color-changing crab spiders in which alternating yellowing and bleaching phases occur through pigment organelles in integument cells. We performed multimodal 2D/3D electron microscopy imaging techniques, Synchrotron X-ray fluorescence and their correlative combination, on high-pressure frozen and freeze-substituted integuments. We found ultrastructural and chemical evidence that pigment organelles are endolysosome-related organelles (ELRO), a family of specialized organelles comprising vertebrate melanosomes. Our results suggest that yellowing of crab spiders arises from the formation of intraluminal fibrils and the deposition of metals within pigment ELROs, which likely originate from secretory/endocytic pathways. Bleaching appears to proceed via the lysosomal degradation of pigment and the removal of metals from pigment organelles, concomitantly to various heterotypic fusion events leading to degradative and recycling states. Some of these intracellular processes mirror melanogenesis and the biogenesis of other pigment ELROs, which identifies the endolysosomal system as a universal platform for pigmentation. Moreover, the unique within-cell life cycle of pigment organelles in this invertebrate provides a window to the enigmatic catabolism and recycling of pigment ELROs. Overall, crab spiders offer a striking example of how the endolysosomal system of pigment cells has been fully functionalized, from anabolism to catabolism and recycling, to allow reversible morphological color changes.

Introduction

Color change is the fascinating ability of an organism to adapt its body coloration depending on its environment and physiology (Figon & Casas, 2018). Color changes are referred to as morphological when they result from dynamical modifications of pigment metabolism (Umbers *et al.*, 2014). Their biological functions range from aggressive mimicry in spiders (Théry & Casas, 2009) and seasonal camouflage in birds (Zimova *et al.*, 2018) to photoprotection in human (Jablonski & Chaplin, 2017). In all these cases, reversible color changes result from cyclic anabolic pigmentation phases, followed by catabolic bleaching phases. Therefore, understanding morphological color changes requires to unravel the cellular mechanisms of both anabolic and catabolic phases, as well as how they relate to each other to allow reversibility.

Pigmentation phases usually rely on the biogenesis of specialized membrane-bound organelles in which pigments are synthesized and stored. Pigment organelles of mammals (melanosomes), fishes (melanosomes, pterinosomes and iridosomes) and insects (ommochromasomes, pterinosomes, uric acid granules and flavin granules) are all members of the endolysosome-related organelle (ELRO) family (Delevoye *et al.*, 2019). ELROs mainly derive their membrane and content from the endolysosomal system (Bowman *et al.*, 2019), which forms a complex and active network of membrane-bound compartments deriving from endocytic and secretory (i.e. post-Golgi) pathways (Klumperman & Raposo, 2014). Detailed investigations of the intracellular processes and trafficking leading to the biogenesis of pigment ELROs have been largely performed on mammalian melanosomes. They showed that melanocytes divert ultrastructural components of the endolysosomal system to progressively mature melanosomes in which melanin polymerizes before being transferred to keratinocytes (Raposo & Marks, 2007). However, apart from melanosomes, there is a lack of ultrastructural investigations on how the endolysosomal architecture regulates other pigment systems. Yet, investigating how the endolysosomal system participates in accommodating the anabolism of various pigments can help unravelling the commonalities and differences in pigmentation phases during color changes.

Compared to pigmentation phases, bleaching phases and their intracellular processes remain even more mysterious. While bleaching can simply results from the death of

pigmented cells, such as during peeling (Candi, Schmidt, & Melino, 2005), it is compatible with pigment cells remaining alive too (Figon & Casas, 2019). This phenomenon questions how pigment cells accommodate both the production and the removal of pigment organelles, as well as whether there are recycling pathways that connect the two phases. In melanosomal systems, the occurrence of degradation as a common physiological process required for the life cycle of melanosomes is still highly debated (Schraermeyer, 1993; Borovanský & Elleder, 2003; Ho & Ganesan, 2011; Bowman & Marks, 2018). Most degradative compartments containing melanin are autophagic and occur in pathological contexts, such as in melanoma and vitiligo (Borovanský & Elleder, 2003). Physiological occurrence of melanosomal degradation within melanocytes has been attributed to either the lysosomal character of melanosomes or to their fusion with *bona fide* lysosomes, the classical lytic organelles of the late endolysosomal pathway (Borovanský & Elleder, 2003). Overall, evidence for physiological degradations of pigment ELROs remains scarce, probably because of a lack of studies focusing on biological systems in which pigments are actively produced and removed within the same cell.

Color-changing crab spiders are sit-and-wait predators of pollinators, which can dynamically match the flower color on which they sit, presumably for aggressive crypsis (Théry & Casas, 2002; Brechbühl *et al.*, 2010; Anderson & Dodson, 2015). They do so by reversibly changing their body coloration between white and yellow via the metabolism of yellow pigments in integument cells (Llandres *et al.*, 2013). During yellowing (i.e. anabolic phase), pigments are deposited within specialized intracellular organelles (Insausti & Casas, 2008). During bleaching, pigment organelles are thought to undergo an autocatalytic process and to recycle their membrane for another cycle of yellowing (Insausti & Casas, 2009). However, ultrastructural evidence for this recycling process is scarce and we do not fully apprehend how both anabolism and catabolism of pigments organelles of crab spiders fit within intracellular trafficking pathways (Figon & Casas, 2019). Testing the hypothesis that these pigment organelles are members of the ELRO family may help positioning them into the endolysosomal system, which in return might provide insights into the roles of the endolysosomal system in both pigmentation and bleaching phases.

Pigment ELROs have been classically defined by their dependence to specific proteins involved in various genetic diseases in humans, such as Hermansky-Pudlak and Griscelli

syndromes (Marks *et al.*, 2013; Delevoye *et al.*, 2019). However, such genetic dependences cannot be tested in spiders because they are barely genetically tractable. Therefore, other markers of endolysosomal origin should be sought for. ELROs often bear ultrastructural signatures of their endolysosomal origin, such as endosomal/Golgi connections, intraluminal vesicles (ILVs), fibrils and membrane tubulations (Klumperman & Raposo, 2014). Those labile signatures are best retained by high-pressure freezing (HPF), which avoids artifacts produced by chemical fixatives (Hurbain *et al.*, 2017). For example, approaches combining 2D electron microscopy (EM) and 3D electron tomography (ET) with HPF successfully revealed the ultrastructural origin of ELROs like melanosomes (Hurbain *et al.*, 2008) and Weibel-Palade bodies (Zenner *et al.*, 2007; Valentijn *et al.*, 2008). We therefore applied these approaches to color-changing crab spiders to investigate the putative relationships between pigment organelles and the endolysosomal system.

ELROs have recently emerged as important regulators of metals by storing and releasing them in a dynamic manner (Blaby-Haas & Merchant, 2014). Pigment ELROs are especially implicated because they accumulate zinc, calcium and other metallic ions (White & Michaud, 1980; Ukhanov, 1991; Gorniak *et al.*, 2014; Takamiya *et al.*, 2016). Under the hypothesis that pigment organelles of crab spiders are ELROs, we expect them to be major sites of metallic accumulation in pigment cells. Given the sub-micrometric size of pigment organelles (Insausti & Casas, 2008), detection of metals in their lumen can only be tackled by the most sensitive and spatially resolved imaging methods (McRae *et al.*, 2009). Synchrotron X-ray fluorescence (SXRF) is the state-of-the-art chemical imaging technique to map multiple trace elements down to a few tens of nanometers in biological samples (Gorniak *et al.*, 2014; Decelle *et al.*, 2019, 2020). Thanks to the optical design of the Nanoscopium beamline of the Synchrotron SOLEIL, hierarchical length-scale SXRF allows to screen millimetric samples and to target multiple sub-micrometric sites of metallic deposition rapidly, i.e. without moving the sample or using another beamline (Somogyi *et al.*, 2015). Besides, since SXRF is a non-destructive technique, correlative SXRF and EM are feasible approaches to unambiguously associate metals with subcellular compartments (Kashiv *et al.*, 2016; Decelle *et al.*, 2020, 2020). Therefore, we used the combination of HPF with EM, ET and SXRF as a multimodal imaging toolbox to investigate the intracellular origin of pigment organelles in color-changing crab spiders.

In this study, we visualized the fine 2D/3D ultrastructure of pigment organelles and we mapped their metal profile at various metabolic stages in white and yellow crab spiders. We classified pigment ELROs into two anabolic types and four catabolic types based on their ultrastructure. We found that pigment organelles, particularly anabolic stages, harbored key labile features, such as fibril-bearing ILVs, membrane tubulations and metals, which relate them to ELROs. We also reported evidence that endosomal and/or secretory compartments could be involved in the biogenesis of anabolic types. Finally, we visualized the 3D architecture of catabolic types and we investigated their relationships with lytic compartments of the endolysosomal system, providing new structural information on how pigment organelles are processed and recycled within the endolysosomal pathway during bleaching.

Materials and Methods

Specimen Sampling

Misumena vatia (Clerck, 1757) crab spiders were collected in fields around the city of Tours, France, during summers 2018 and 2019. White and yellow individuals were sampled on plants harboring white and yellow flowers, respectively. They were kept individually in plastic vials no more than a week before dissection and fixation to avoid pigmentation loss.

Reagents and Solutions

Glucose, Fetal Bovine Serum (FBS), magnesium chloride, sodium chloride and potassium chloride were purchased from Sigma-Aldrich. Uranyl acetate, lead citrate, Durcupan ACM, anhydrous acetone and osmium tetroxide were purchased from EMS.

Integument Fixation and Embedding

Crab spiders were sacrificed and fixed one at a time. For each individual, a few mm^2 piece of integument was dissected from the opistosoma in Ringer's solution (86 mM NaCl, 5.4 mM KCl and 3 mM $MgCl_2$) supplemented with 2.2 % glucose for isotonicity. The integument piece was rinsed in 100 % FBS and placed in a 200 µm carrier filled with 100 % FBS serving as cryoprotectant. High-pressure freezing (HPF) was performed with HPM100 (Leica Microsystems) or HPM Live µ (CryoCapCell). Frozen integuments were transferred from liquid nitrogen to anhydrous acetone containing 2 % H_2O/1 % OsO_4 pre-cooled at -90 °C.

Freeze substitution (FS) was performed with AFS or AFS2 (Leica Microsystems) using the following FS schedule: -90 °C for 1 h, +4°C/h for 15 h and -30 °C for 5 h. Integuments were then placed at 4 °C for 1 h and at room temperature for 1 h.

Freeze-substituted integuments were rinsed three times in anhydrous acetone and incubated overnight in 50 % anhydrous acetone/50 % Durcupan ACM (11.3 g epoxy resin, 10 g 964 hardener, 0.5 g dibutyl phthalate and 0.2 g 964 accelerator). Acetone was evaporated by warming at 40 °C for 1 h. Integuments were infiltrated with 100 % Durcupan ACM for 5 h at room temperature. The 100 % Durcupan ACM was renewed and integuments were polymerized at 60 °C for at least 48 h.

Transmission Electron Microscopy

Ultra-thin sections (70 nm) were cut with ultramicrotome UCT (Leica Microsystems) using Ultra 35° diamond knife (DIATOME). Sections were picked on carbon/formvar coated grids and further processed for staining. Sections were contrasted at room temperature with aqueous 2 % uranyl acetate for 10 min in darkness and then with Reynolds 4 % lead citrate for 1 min in CO_2-free conditions. Stained sections were imaged at 80 kV with transmission electron microscope Tecnai Spirit (Thermo Fischer Scientific) equipped with QUEMESA CCD Camera (EMSIS) controlled by iTEM software (EMSIS).

Electron Tomography

Thin sections (300 nm) were cut with ultramicrotome UCT (Leica Microsystems) using histo Jumbo diamond knife (DIATOME). Sections were picked on carbon/formvar coated finder grids and further processed for gold labelling and staining. Random labeling was performed on both section sides with gold nanoparticles PAG 15 nm (EMS) before staining as described in the previous section. Single-tilt series with an angular range of -60° to +60° with 1° increment were imaged at 200 kV using transmission electron microscope Tecnai G2 (Thermo Fischer Scientific) equipped with TemCam-F416 4k CMOS camera (TVIPS) controlled by EM-Tools software (TVIPS). Alignment of projection images and tomogram computing (resolution-weighted back projection) were performed with Etomo in IMOD software (Mastronarde & Held, 2017) using PAG 15 nm as artificial fiducial markers. Manual

contouring and three-dimensional reconstructions were performed with 3dmod in IMOD software (Kremer, Mastronarde, & McIntosh, 1996).

Synchrotron X-Ray Fluorescence

Semi-thin sections (500 nm) were cut with microtome RM2265 (Leica Microsystems) using histo Jumbo diamond knife (DIATOME). Sections were deposited at the surface of distilled water drops lying on silicon nitride membranes (membrane size: 1 mm x 1 mm, membrane thickness: 1 µm, frame size: 5 mm x 5 mm, frame thickness 200 µm; Silson). Membranes were quickly dried for a few seconds at 60 °C on a hot plate. Frames were glued on plastic washers by polish nail to mount them on holders for Synchrotron X-ray fluorescence (SXRF).

Hierarchical length-scale SXRF imaging was performed at the Nanoscopium beamline of Synchrotron SOLEIL at Gif-sur-Yvette, France. Multi-elemental maps were acquired by fast continuous raster-scanning using the FLYSCAN scheme (Medjoubi *et al.*, 2013) with spatial resolutions from 2 µm x 2 µm per pixel down to 50 nm x 50 nm per pixel. Full X-ray spectra (fluorescence and scattering) were recorded for each pixel using two silicon drift detectors (KETEK) placed at ±120° to the beam direction (Somogyi *et al.*, 2015) and with exposure times from 300 ms to 10 ms per pixel. A 9.7 keV photon beam energy at the double-crystal monochromator (DCM; CINEL) was used to excite all native elements from Al to Zn without exciting Os, which was added as a fixative during FS. The latter was specifically excited for morphological information by changing, on the fly, the DCM beam energy to 10.3 keV.

When the same region was scanned sequentially at 9.7 and 10.3 keV, some misalignments between the two maps could occur due to imperfect motor positions at the nanoscale. Endogenous elements and osmium maps were thus aligned back using DaVis software (LaVision). The following parameters were used: "fill-up empty spaces", "smoothing 2x at 3 px x 3 px" and "deformation with vector field". Zinc signal was retained as marker for alignment because it presented similar features to osmium both in nuclei and cuticles, which allowed for a meaningful map correlation. During alignment, zinc maps were left unchanged while osmium maps were locally and non-linearly deformed by pixel extrapolation and smoothing processes.

Scanning Transmission Electron Microscopy

Frames analyzed by SXRF were removed from plastic washers by carefully dissolving nail polish using acetone. A custom sample holder was crafted to accommodate frame sizes. Sections were not further stained by uranyl acetate and lead citrate, only osmium provided electron contrast to allow a direct comparison with SXRF maps. Electron micrographs were taken using scanning transmission electron microscopy mode at 200 kV with field emission gun JEM-2200FS (JEOL) equipped with bright-field STEM detector controlled by Recorder software (JEOL).

Correlative Synchrotron X-Ray Fluorescence and Scanning Transmission Electron Microscopy

Images of the same integument regions were sequentially acquired by SXRF and then by STEM. Correlative imaging was performed using eC-CLEM plugin (Paul-Gilloteaux *et al.*, 2017) in Icy software (de Chaumont *et al.*, 2012). STEM images and osmium (or zinc) maps were set as target and transformed images, respectively. Non-rigid registration was done using natural fiducials markers, such as cuticle edges, nuclei and sample defects, which were easily and unambiguously observed in osmium/zinc maps and STEM micrographs.

Image Analysis and Quantification

The different stages of pigment organelles observable in TEM images were manually contoured in several cells per individual. To calculate the proportions of pigment organelle types, three yellow and three white spiders captured the same day and cryofixed at the same time were used as biological replicates. Proportions were reported as the mean ± standard deviation of the three spiders per color. Morphometric data (maximum Feret diameter as a proxy of size and elongation ratio as a proxy of ellipticity) were automatically computed using Icy software and were reported as the mean ± standard deviation of 666 and 779 organelles observed in the three white and the tree yellow spiders, respectively.

For endogenous element quantifications, backgrounds of SXRF maps were removed by subtracting to each pixel the average pixel value within a rectangular region comprising only resin using Fiji software (Schindelin *et al.*, 2012). Structures positive for osmium were manually selected in deformed Os maps using round ROIs of 4 px (diameter of 800 nm) in

Icy software. ROIs were copy-pasted onto native metal maps. Mean pixel values within ROIs were calculated and extracted using Icy software.

Statistical Analysis

All statistical analyses were performed using R software (R Core Team, 2017). Principal component analyses and hierarchical clustering were done using FactoMineR library. Statistical differences between SXRF populations were tested first by non-parametric Kruskal-Wallis tests and then by pairwise Wilcoxon tests. Only p-values below 0.05 were considered as statistically significant.

Results

High-Pressure Freezing and Freeze Substitution Preserve Cells of Crab Spiders in an Unprecedented Manner

Previous studies that investigated ultrastructural aspects of color changes in crab spiders used conventional electron microscopy (EM), meaning that tissues were chemically fixed (Insausti & Casas, 2008, 2009). Conventional EM offered important insights into color changes at the subcellular level by visualizing the complex anabolic and catabolic maturation of pigment organelles during reversible color changes. However, this technique is not suited to investigate labile features, such as membrane protrusions, endosomal structures and metal distribution, which requires fixation close to the native state. In the last years, high-pressure freezing coupled to freeze substitution (HPF-FS) has proven to be a method of choice for meeting such requirements in relatively thick samples (Zenner *et al.*, 2007; Hurbain *et al.*, 2008; Sosinsky *et al.*, 2008; Hurbain & Sachse, 2011; Kashiv *et al.*, 2016; Ripoll *et al.*, 2018).

EM of crab spider integuments fixed by HPF-FS delivered unprecedented ultrastructural details (**Figure S6-1**). We could observe, among others, well-defined Golgi stacks and endosomes (featuring intraluminal vesicles and fibrils, as well as membrane invaginations and tubulations), coated cytoplasmic vesicles, microtubules, as well as lipid droplets delimited by a lipid monolayer in close association with endoplasmic reticulum (ER; **Figure S6-1**). Therefore, HPF-FS was used for the rest of this study in order to investigate the fine ultrastructure and the elemental composition of color-changing crab spiders.

Pigment Organelles Possess Ultrastructural and Chemical Endolysosomal Features

Pigment organelles of various animals belong to the vast family of endlysosome-related organelles (ELROs). It has been hypothesized that pigment organelles of crab spiders were ELROs too, although they might originate from endoplasmic reticulum as well (Insausti & Casas, 2008, 2009; Figon & Casas, 2019). In the absence of molecular and genetic tools, fine ultrastructural and chemical features are the best evidence for elucidating the pigment organelle lineage.

HPF-FS successfully preserved limiting membranes of pigmented organelles at various maturation stages (**Figure 6-1**A and subsequent figures), showing the typical ~8-nm-thick bilayer structure (**Figure 6-1**A, inset) (Robertson, 1960). As previously described (Insausti & Casas, 2008, 2009), morphologies and pigmented status of pigment organelles were diverse, but all forms presented from time to time intraluminal vesicles (**Figure 6-1**B-D and **Figure S6-2**A-C) and tubulating membranes (**Figure 6-1**E-G and **Figure S6-2**D). Intraluminal vesicles (ILVs) were clearly membrane-bound (**Figure 6-1**B, inset) and some were attached, or at least closely associated, to the limiting membrane (**Figure 6-1**B and D, insets). One particular feature of these ILVs was the presence of a fibrillary material attached to their luminal face (**Figure 6-1**B-C). Electron tomography (ET) revealed that those fibrils possessed a sheet-like structure in three dimensions, which was indeed expanding from the ILV surface into the pigment organelle lumen (**Figure 6-1**D, inset), similar to endosomes and early stages of melanosomes (Hurbain *et al.*, 2008). Tubules in continuity with pigment organelle membranes were also observed protruding into the cytoplasm (**Figure 6-1**E-G). Their lumen was usually denser than that of pigment organelles (**Figure 6-1**E), indicating that they were carrying substantial amounts of materials either from or toward pigment organelles. ET revealed a tubule whose end was not connected to any other organelles and with a very narrow connection to the pigment organelle (**Figure 6-1**F-G). These characteristics suggest that tubules emerged from pigment organelle membranes, elongated and then underwent fission at their neck to be released in the cytoplasm, similar to recycling melanosomal tubules (Dennis *et al.*, 2016; Ripoll *et al.*, 2018). However, in the absence of dynamic evidence, we cannot rule out that these tubules came from the cytoplasm and fused with pigment organelles to deliver their content, again similarly to melanosomes receiving tubular endosomal carriers (Ripoll *et al.*, 2018).

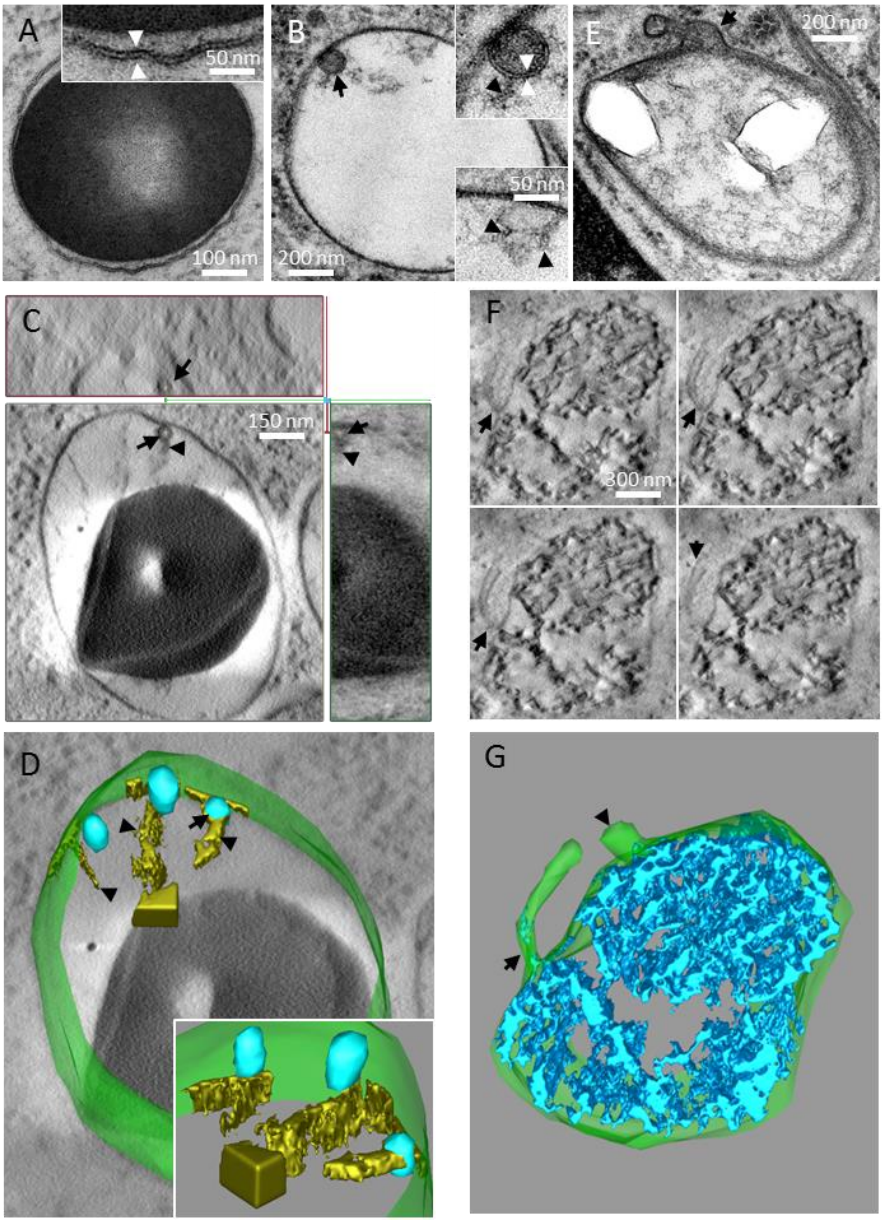

Figure 6-1. High-pressure freezing reveals labile ultrastructural features that relate pigment organelles of crab spiders to endolysosome-related organelles.
(A) Limiting membrane of a pigment organelle. Inset, double-leaflet structure (white arrowheads) of the limiting membrane. (B) An early stage pigment organelle containing an intraluminal vesicle (ILV, black arrow). Top inset, double-leaflet structure (white arrowheads) of the ILV membrane bearing fibrils (black arrowhead). Bottom inset, similar fibrils are attached to the limiting membrane. (C) Electron tomogram slices showing a fibril-bearing (black arrowhead) ILV (black arrow) attached to the limiting membrane of a pigment organelle. Top panel, XZ plane. Middle panel, XY plane. Right panel, YZ plane. (D) Three-dimensional reconstruction of the pigment organelle depicted in C showing its limiting membrane (green), ILVs (blue, black arrow) and fibrils (gold, black arrowhead). Inset, zoom on the isosurfacing of fibrils, showing their sheet-like structure attached to membranes. (E) A membrane tubulation (black arrow) in continuity with the limiting membrane of an early stage pigment organelles. (F) Electron tomogram slices in the Z direction of a pigment organelle bearing a membrane tubulation (black arrow). (G) Three-dimensional reconstruction of the pigment organelle depicted in F showing the continuity between its limiting membrane and two tubules (arrow and arrowhead).

We then investigated whether metal accumulation was also a feature of crab spider pigment organelles. To that purpose, we performed Synchrotron X-ray fluorescence (SXRF) experiments on semi-thin sections of integuments fixed by HPF-FS. We expected metals, if any, to be distributed locally and at low concentrations. To gain structural information during the SXRF mapping, we took advantage of the presence of exogenously applied osmium (used as fixative during HPF-FS) to delineate structures at different scales, such as cuticle and cell layers (**Figure 6-2**A), pigment cells (**Figure 6-2**B) and organelles (cytosolic Os-positive structures; **Figure 6-2**C-E). The mapping of native metals revealed that those Os-positive structures differentially accumulated zinc (Zn), calcium (Ca) and, in rare occasions, cobalt (Co; **Figure 6-2**D, inset and **Figure S6-3**). The absence of these metals in regions stained by Os (e.g. the endocuticle; **Figure 6-2**F) implied that these metals were not artifacts of the fixation process, but rather of biological significance. To clearly demonstrate that the Os-positive structures were pigment organelles, we imaged the same regions by scanning transmission electron microscopy (STEM), which can visualize the ultrastructure of micrometric samples (Sousa & Leapman, 2012). This correlative SXRF and STEM approach showed that Os-positive structures corresponded to the dense intraluminal material of pigment organelles (**Figure 6-2**E). SXRF mapping at a resolution of 50 nm/px even recapitulated the heterogeneous intraluminal organization of some pigment organelles (**Figure 6-2**E, arrow). Finally, by combining this correlative approach with the maps of native metals, we unambiguously showed that pigments organelles were the main cytosolic sites of metal deposition in pigment cells (**Figure 6-2**F).

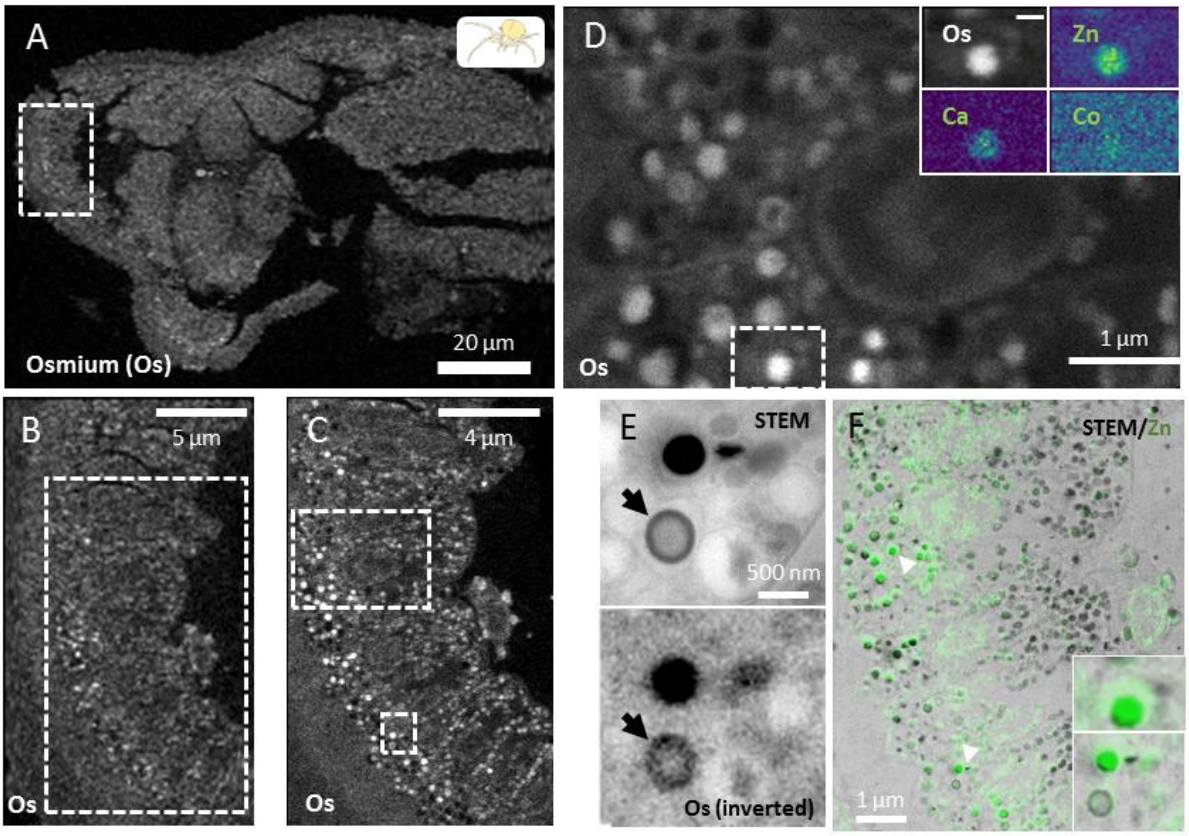

Figure 6-2. Correlative Synchrotron X-ray fluorescence and scanning transmission electron microscopy reveals metal accumulation in pigment organelles.
(A-D) Hierarchical length-scale Synchrotron X-ray (SXRF) fluorescence of osmium enables the structural mapping of high-pressure frozen integuments from tissues down to subcellular organelles. (A) Resolution, 2 µm/px. Integration time, 10 ms. (B) Zoom on the region depicted in A. Resolution, 500 nm/px. Integration time, 20 ms. (C) Zoom on the region depicted in B. Resolution, 100 um/px. Integration time, 20 ms. (D) Zoom of the upper region depicted in C. Resolution, 50 um/px. Integration time, 20 ms. Inset, osmium and three native metals (zinc, calcium and cobalt) colocalize to punctate structures in the region depicted in D. Resolution, 50 um/px. Integration times, 20 ms (osmium) and 300 ms (native metals). (E) Scanning transmission electron microscopy (STEM) and SXRF of osmium in the lower region depicted in C showing that Os-positive punctate structures are pigment organelles (arrow). (F) Correlative SXRF and STEM of zinc of the whole region depicted in C showing that pigment organelles are the main sites of metal accumulation. SXRF resolution before correlation, 200 nm/px.

Overall, the nano-imaging investigation of integuments preserved in a near-native state demonstrated that pigment organelles of crab spiders possessed key labile features, namely intraluminal vesicles, membrane tubulations and various metals. These characteristics are shared by other well-documented pigment systems, such as vertebrate melanosomes (D'Alba & Shawkey, 2019) and insect ommochromasomes (Figon & Casas, 2019). They thus relate pigment organelles of crab spiders to ELROs (Delevoye *et al.*, 2019).

Morphology and Metal Identity of Pigment Organelles Vary with Coloration

Pigment organelles are the intracellular actors of color changes in crab spiders. Their ultrastructural and chemical dynamics are thus likely to be linked to pigmentation status. Therefore, we investigated by TEM and correlative XRF-STEM the different populations of pigment organelles that were observed in white and yellow integuments.

As previously described (Insausti & Casas, 2008, 2009), yellow crab spiders differed from white individuals by the density and the organization of intraluminal materials within pigment organelles (**Figure 6-3**A-B). White integuments revealed homogeneous profiles in which only the amount of intraluminal materials varied among pigment organelles (**Figure 6-3**A, C). On contrary, pigment organelles of yellow integuments were more diverse, showing heterogeneous intraluminal structures (**Figure 6-3**B). Based on these observations, we classified pigment organelles into six morphological types (**Figure 6-3**C). The a-type possesses a diffuse fibrillary material (**Figure 6-3**D, a), with various stages of density (**Figure 6-3**C). The b-type is fully packed with dense materials (**Figure 6-3**D, b), indicating it is highly pigmented. The c-type is usually a deformed organelle characterized by several cores of dense materials forming clusters (**Figure 6-3**D, c). The d-type possesses a core of dense material with a more diffuse material at the periphery (**Figure 6-3**D, d). The e-type shows a reversed pattern with a dense crown of material at the limiting membrane and an electron-lucent center (**Figure 6-3**D, e). Finally, the f-type is characterized by a well-developed network of fibrils resembling a ball of wool (**Figure 6-3**D, f). Note that b-, d- and e-type-like structures were observed among the cores of c-types (**Figure S6-4**). Morphometric analyses indicated that all pigment organelles were roundish (mean ellipticity of 1.27), except c-types that were more elongated (ellipticity value of 1.5 and diameter of 0.90 µm; **Table 6-1**). a-types represented the vast majority of pigment organelles in white integuments (97 %) compared to yellow ones (11 %), which possessed predominantly b- and e-types (41 % and 25 %, respectively; **Table 6-1**). c- to f-types were absent from white integuments (**Table 6-1**). These results support that a-types are early (unpigmented) stages of pigment organelles, while b- to f-types are responsible for the yellow coloration.

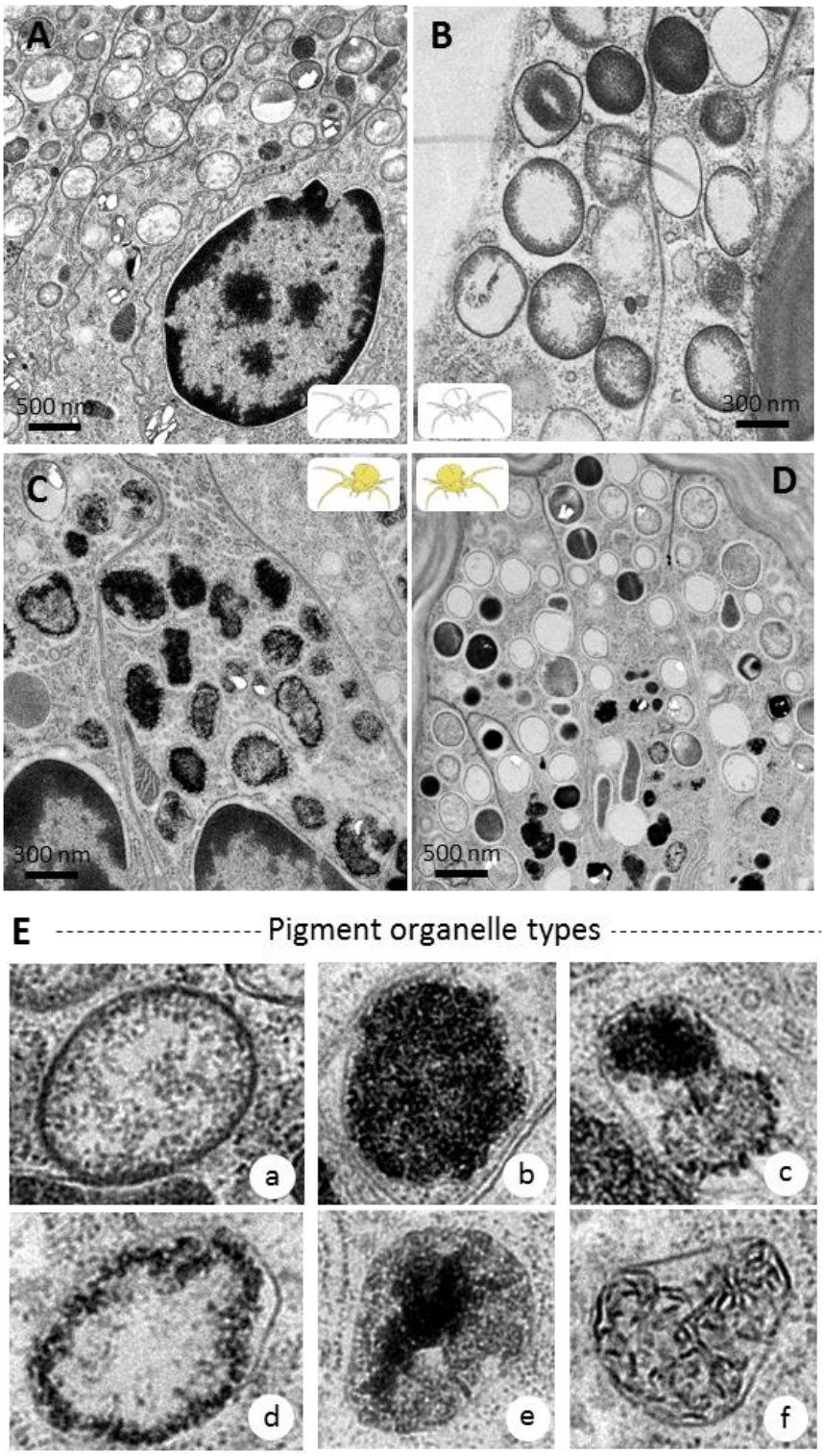

Figure 6-3. Ultrastructural diversity and typology of pigment organelles.
(A) Early stages of pigment organelles in a white crab spider. (B) Pigment organelles at different stages of filling in a white spider. (C) Pigment organelles only observed in a yellow crab spider. (D) Variety of pigment organelles observed in yellow spiders. (E) Pigment organelles are categorized into six types labelled a to f according to the organization and the aspect of their luminal content.

Table 6-1. Characteristics of pigment organelle types in relation to coloration.

Pigment organelle type	a	b	c	d	e	f
Proportion (mean ± SD)	97 ± 4 % (W[a]) 11 ± 9 % (Y[b])	3 ± 4 % 41 ± 26 %	N.D. 11 ± 2 %	N.D. 4 ± 3 %	N.D. 25 ± 11 %	N.D. 8 ± 7 %
Size[c] (µm)	0,73 (W) 0,80 (Y)	0,60 0,75	N.D 0,90	N.D 0,74	N.D 0,73	N.D. 0,71
Ellipticity[d]	1,30 (W) 1,33 (Y)	1,23 1,27	N.D. 1,50	N.D. 1,25	N.D. 1,26	N.D. 1,28

[a] Total of 666 pigment organelles in N = 3 white spiders
[b] Total of 779 pigment organelles in N = 3 yellow spiders
[c] Maximum Feret diameter
[d] Elongation ratio

We next investigated whether the morphological diversity of pigment organelles we described was associated to a variation in metals. First, we compared the distribution of metals in white and yellow integuments using Os as a structural marker of pigment organelles (**Figure 6-4**A and B). Both types of integuments showed high densities of pigment organelles (Os-positive structures) but yellow ones harbored higher amounts of Os (**Figure 6-4**B), in agreement with the presence of more pigmented organelles in these tissues. While native metals (Zn, Ca and Co) were found in similar concentrations within nuclei of both white and yellow integuments (**Figure 6-4**A and B), only pigment organelles of yellow tissues accumulated significant amounts of Ca and Co (**Figure 6-4**B). Zn was seemingly present in some pigment organelles of white integuments, albeit in fewer amounts than in yellow tissues. These results suggest that metals are preferentially associated with yellow coloration. We then investigated whether there was a relationship between Os and the presence of metals in yellow integuments. In **Figure 6-4**C, each dot represents a single Os-positive pigment organelle from the region depicted in **Figure 6-4**B. The multivariate analysis by principal component analysis of the main metals detected by SXRF led to the description of three populations after hierarchical clustering. The first population was characterized by low concentrations of metals, including Os, indicating that the less pigmented organelles (based on Os signal) accumulated less metals. Second and third populations were mostly similar in terms of pigmentation but differed in their concentrations of native metals. Zn, Co and Ca were 1.40, 1.67 and 1.80 times more concentrated, respectively, in population 3 than in population 2 (**Figure 6-4**C). We then asked whether this heterogeneity in metal distribution

was related to morphological diversity. A correlative XRF-STEM experiment was performed to categorize each Os-positive structure within one of the pigment organelle types described in **Figure 6-4**D. **Figure 6-4**E shows that Os signal recapitulates the pattern of intraluminal density in pigment organelles as population 1 was enriched in a-, d- and e-types. Populations 2 and 3 did not segregate to distinct morphological types, they were rather enriched in b- and c-types, as well as in organelles that were intermediate between a- and b-types. Nonetheless, population 1 was clearly underrepresented in fully pigmented b-types (**Figure 6-4**E), which further supports a link between pigmentation status and metals.

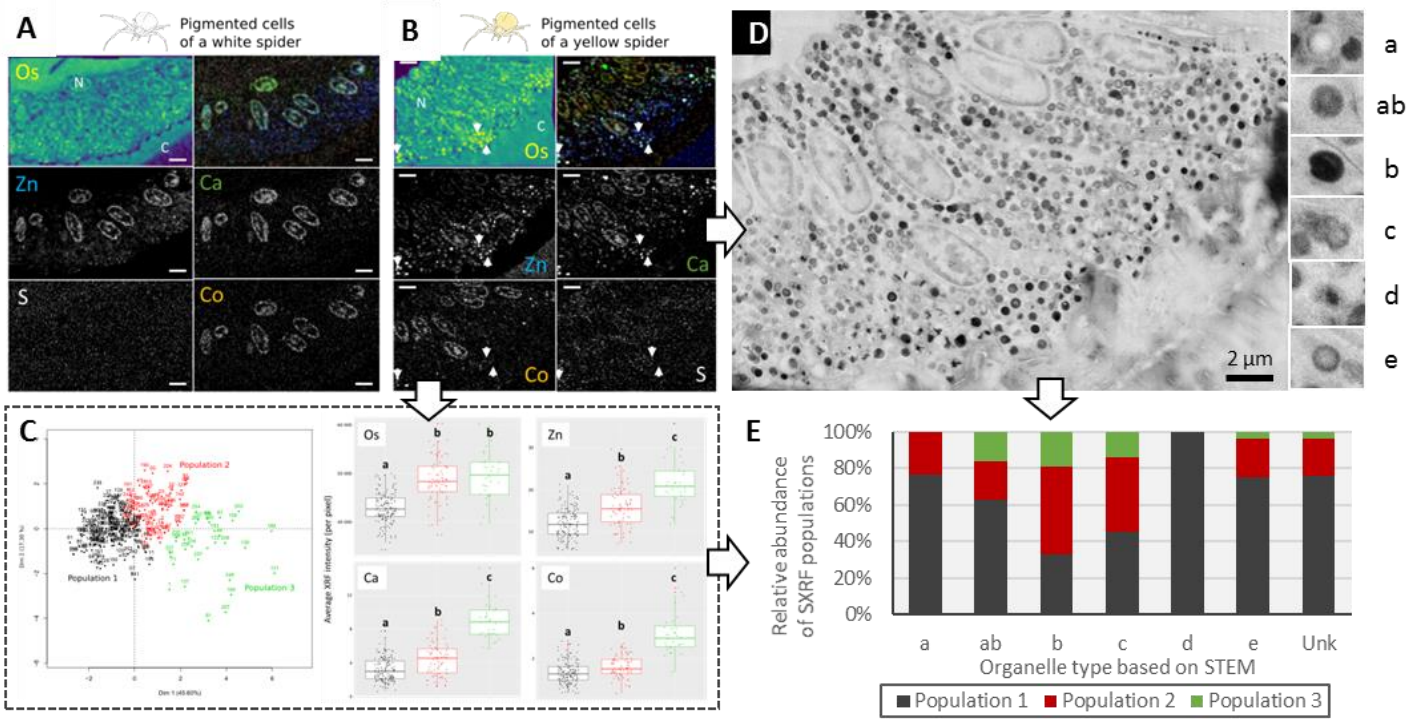

Figure 6-4. Pigment organelles differentially accumulate metals according to coloration and maturation stages.

(A-B) Synchrotron X-ray fluorescence (XRF) mapping of osmium (Os) and native zinc (Zn), calcium (Ca), cobalt (Co) and sulfur (S) in white (A) and yellow (B) integuments. Top right panels, merging of Zn, Ca, Co and S signals. C, cuticle. N, nucleus. Scale: 2 µm. (C) Principal component analysis and hierarchical clustering of Os-positive organelles spotted in B based on their average content in Zn, Ca, Co, S and Ni. Statistical significant differences are indicated by different letters (P-value < 0.05). (D) Scanning transmission electron micrograph (STEM) of the region depicted in B. Right insets, examples of pigment organelle types as seen in STEM. An ab-type was considered because the 500-nm thickness made the distinction between maturing a-types and early b-types difficult. (E) Relative abundance of SXRF populations observed in C according to organelle types based on correlative SXRF-STEM of the region shown in B and D. Unk, unknown organelles whose ultrastructure by STEM was too ambiguous to be classified.

Formation and Degradation of Pigment Organelles in Relation to Secretory and Endolysosomal Systems.

We next investigated the intracellular processes underlying pigment organelle biogenesis, maturation and degradation. Since pigment organelles likely are ELROs, we hypothesized that endolysosomal and secretory systems (i.e. Golgi and post-Golgi compartments) were the main actors of these processes. Therefore, we looked for ultrastructural evidence of an association between Golgi apparatus, endosomes, late endosomes and lysosomes with pigment ELROs.

Despite the careful investigation of several crab spiders, we never observed Golgi apparatus with the typical stacked morphology in pigment cells, contrary to other cell-types (**Figure S6-1**). However, we spotted on several occasions elongated, swollen and superimposed tubulo-saccular complexes that were in the close vicinity of a-type pigment organelles (**Figure 6-5**A). Those complexes were mainly found in the perinuclear region and sometimes in association with centrioles (**Figure S6-5**), both of which are spatial landmarks of Golgi apparatus. Furthermore, these complexes where mainly associated to endosomes, microtubules, as well as free tubules and vesicles, indicating that they were markedly active regions (**Figure 6-5**A-C). Strikingly, swollen cisternae of these complexes resembled the most electron-lucent a-types (**Figure 6-5**B and C), suggesting that pigment organelles could originate from these budding structures. We next performed three-dimensional analyses by ET to further unravel the unique morphology of these complexes and their relationships with other compartments. **Figure 6-5**D reveals that tubulo-saccular complexes were composed of distinct side-by-side compartments, each being a highly complex network of membranes forming tubules, saccules and elongated structures (**Figure 6-5**D, inset). Free vesicles were typically observed in between these compartments (**Figure 6-5**D and E). Two budding profiles observed in **Figure 6-5**D indicate that tubulo-saccular complexes may be one source of the high density in free vesicles. The presence of an endosome with typical ILVs and an attached tubule (**Figure 6-5**D) indicates that endosomal compartments could also generate some of the tubular and vesicular carriers observed in this region. Moreover, **Figure 6-5**D shows that tubulo-saccular complexes are surrounded by a-type pigment organelles with different densities of intraluminal fibrils, which suggests that a-types matured in this part of the cell. Multiple vesicles could be seen in the vicinity of a-types, particularly at the interface with tubulo-saccular complexes (**Figure 6-5**D). Strikingly, the swollen compartment from the

tubulo-saccular complex harboring an attached vesicle contained elongated fibrils that emanated from the luminal face of the limiting membrane (**Figure 6-5**E), which is reminiscent of fibrils in a-types. This observation further supports that pigment organelles originate from tubulo-saccular complexes.

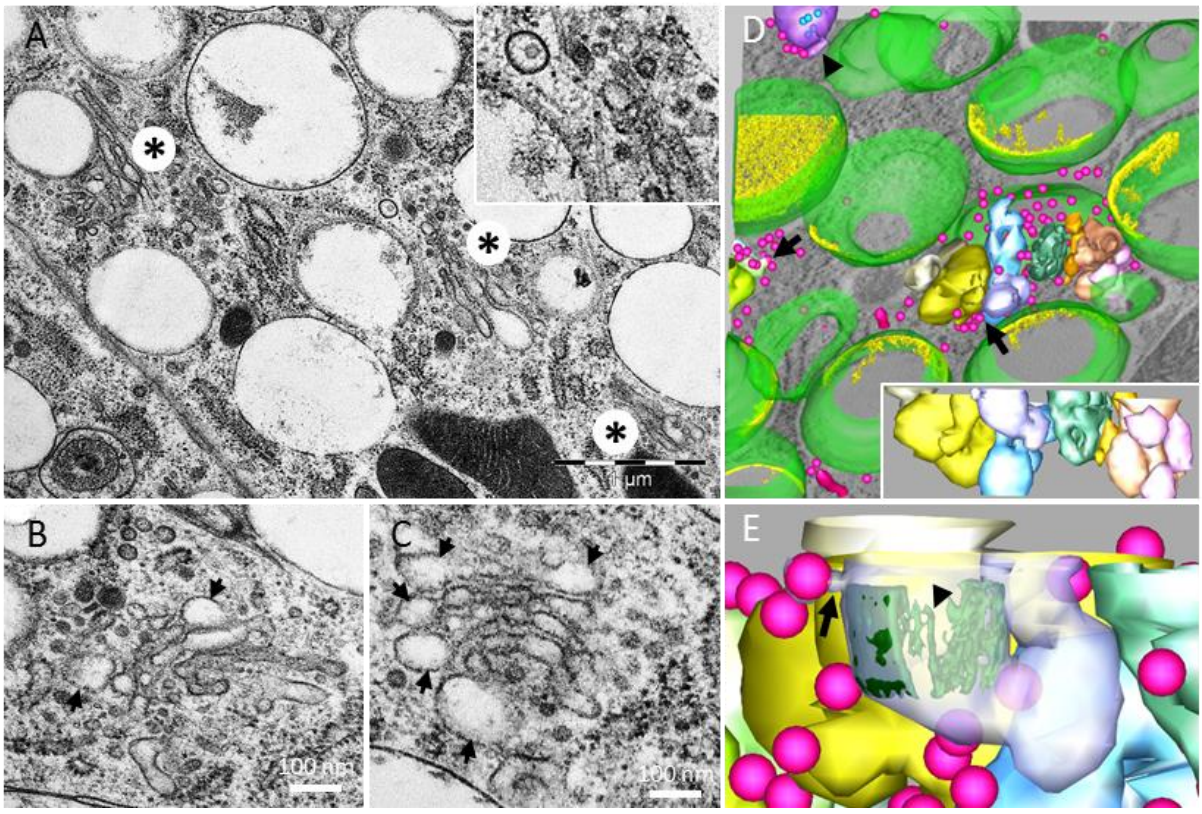

Figure 6-5. Maturing a-type pigment organelles are associated to tubulo-saccular regions, which are associated to endosomes and enriched in vesicular and tubular carriers.
(A-E) Tubulo-saccular complexes (asterisks) are in the close vicinity of a-type pigment organelles. Inset of A, zoom on an endosome, uncoated vesicles, coated vesicles and microtubules. (B-C) Tubulo-saccular complexes showing swollen structures (arrows), numerous free vesicles and sometimes superimposed structures. (D) Three-dimensional reconstruction of a tubulo-saccular region showing a-type pigment organelles (green membrane and yellow intraluminal material), vesicles and tubules (magenta), endosome (purple membrane and blue intraluminal vesicles) and tubulo-saccular complexes comprised of side-by-side compartments (different colors). Part of a second tubulo-saccular complex is seen on the left, surrounded by vesicles. Inset, View of the tubulo-saccular complex in z-dimension showing the network of membranes and swollen compartments. Arrows, budding vesicles from tubulo-saccular complexes. Arrowhead, tubule emanating from the endosome. (E) Details of one compartment from the main tubulo-vesicular complex showing the constricted neck of a budding vesicle (arrow) and intraluminal materials (green) forming fibril-like structures (arrowhead) attached to the luminal membrane.

The rather limited size of swollen compartments in tubulo-saccular complexes questions how a-types acquire sizes up to a micrometer and sometimes even more (see **Figure**

6-5A). Two mechanisms could be invoked: numerous fusion events with vesicular and tubular carriers, and homotypic fusion events between smaller a-types. The many vesicles and microtubules in tubulo-saccular regions (**Figure 6-5**) are clues to the first mechanism. However, we reason that if it were the main mechanism to bring membrane to a-types, we should have observed many more vesicles attached to the limiting membrane of a-types given their large size. On contrary, homotypic fusion events between a-types were more readily observed (**Figure 6-6**), indicating that these events were more frequent and thus predominant. However, we cannot exclude that those observations corresponded to fission rather than fusion events. We reason that fission events of such big organelles would constrain their morphology, leading to their deformation near fission sites. Considering the relatively undisturbed aspect of limiting membranes, especially the absence of a constricted neck (**Figure 6-6**), fusion events seem more likely. Finally, microtubules were often spotted in the very close vicinity of fusion sites (**Figure 6-6**C), which indicates that this process was driven by cytoskeleton in a dynamic manner. Taken together, these results suggest that a-type pigment organelles likely grow via dynamic processes, including homotypic fusion events, as well as fusion with vesicular and tubular carriers.

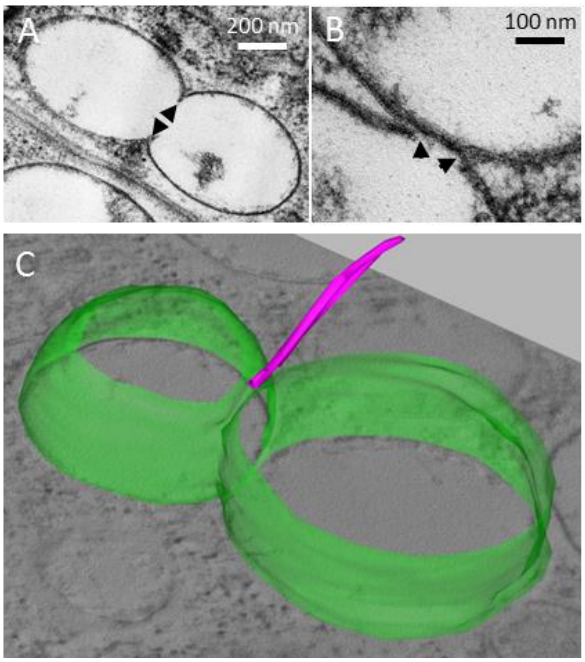

Figure 6-6. Evidence of homotypic fusion events between a-type pigment organelles in white spiders.
(A-B) Continuity of limiting membranes (arrowheads) suggest homotypic fusion events between a-type pigment organelles. (C) Three-dimensional reconstruction of fused a-type pigment organelles (green membrane) showing a microtubule (magenta) closely-associated to the fusion site.

Finally, we were interested in how b- to f-types were related to each other, hypothesizing that they represented successive stages in the processing and degradation of pigment organelles. We therefore investigated yellow integuments using 2D and 3D EM looking for ultrastructural markers of relatedness and degradation. **Figure 6-7**A-E show that intraluminal materials of e- and f-types are similar to each other, forming a core of dense material that extends in three dimensions and that connects the limiting membrane via proteinaceous tubular structures forming pillars (**Figure 6-7**A and C, inset). The three pigment organelles shown in **Figure 6-7**B-E mostly differ by the amount of holes in their cores. It suggests that f-types, whose fibrils are intertwined sheets, represent the latest stages of centrifugal degradation (from panels B to E in **Figure 6-7**), in which only a backbone of sheets remains while most of the intraluminal material on it is gone. We next investigated cluster-like c-type pigment organelles. First, we observed in several instances endosomes, multivesicular bodies and lysosome-like organelles in the vicinity of c- to f-types (**Figure 6-7**F). The numerous associated tubules, vesicles and microtubules (**Figure 6-7**F, inset) indicate that these organelles, of the late endolysosomal pathway, were highly active. **Figure 6-7**H shows a typical c-type cluster of five pigment organelles enclosed within a single limiting membrane, which could have resulted from heterotypic fusion events between different pigment organelle types, such as those observed in **Figure 6-7**G. Here, we observe a clear fusion event between two b- and e-types with continuous limiting membranes but with their respective lumens that have not mixed together yet (**Figure 6-7**G). Furthermore, a membrane extension seems to connect the middle e-type with another b-type (**Figure 6-7**G), which indicates another probable fusion event. Strikingly, the lumen density of the e-type resembles that of lysosome-like organelles (**Figure 6-7**G and H), suggesting that this organelle may have already fused with a lysosome (see **Figure S6-6** for examples of pigment materials within lysosomal compartments). The three-dimensional reconstruction of a c-type reveals that poles of materials are indeed mostly independent of each other (i.e. there is no extent mixing of their contents, which are in different stages of degradation; **Figure 6-7**I), apart from some bridging regions where pillar-like structures connect to each other (**Figure 6-7**I, inset). This is reminiscent of the membrane-connecting structures observed in **Figure 6-7**B, suggesting that these bridges are structural vestiges of organelles before their fusion. Altogether, these results support the idea that c-types are single-membrane-bound clusters

formed by heterotypic fusion events between pigment organelles, and possibly with lysosomes too.

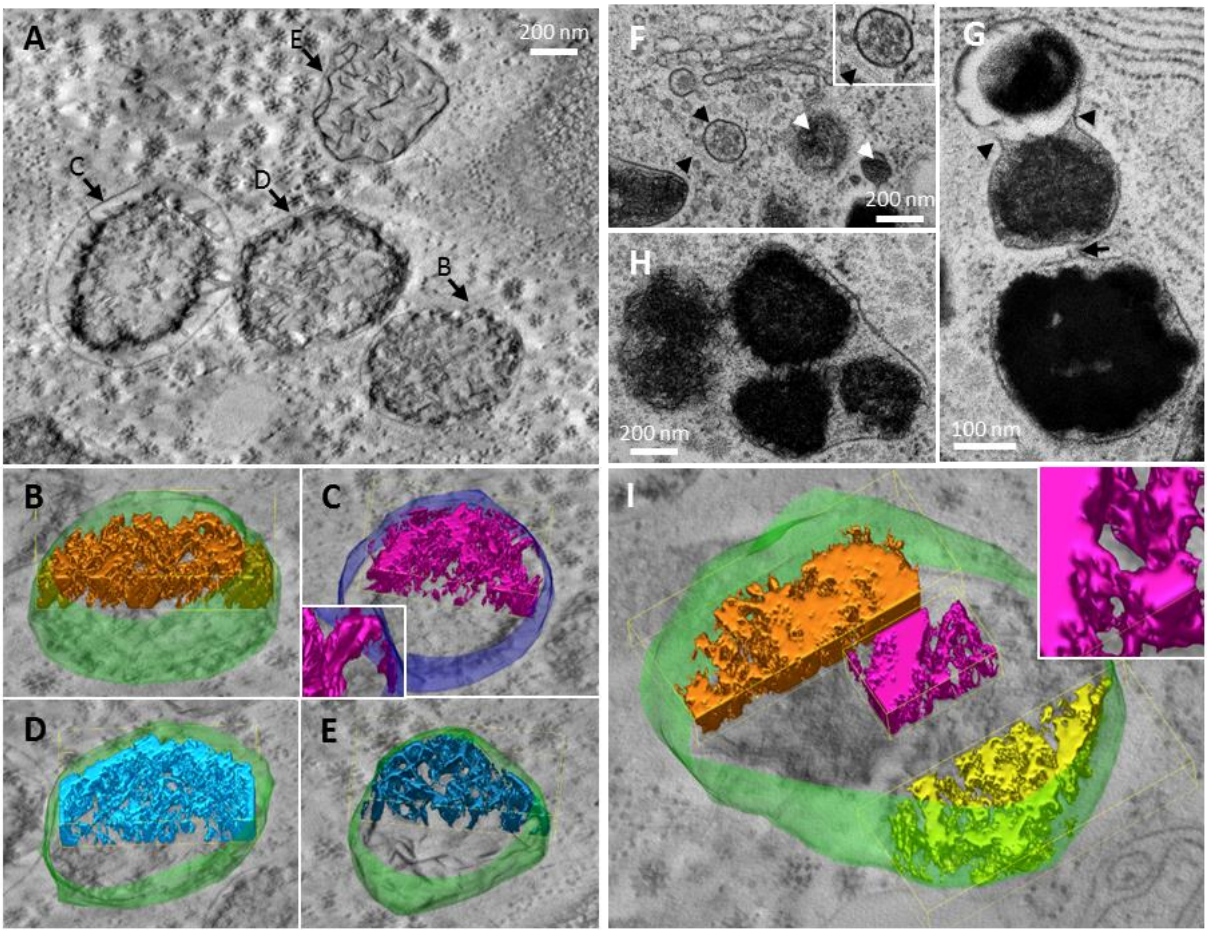

Figure 6-7. Evidence of intraluminal degradation and clustering of pigment organelles in yellow spiders.
(A-E) Electron tomography of e- and f-types pigment organelles. (A) Electron tomogram slice in the XY plane. (B-E) Three-dimensional reconstructions of the limiting membrane (green or blue) and the luminal content (isosurface rendering, multicolor) of pigment organelles depicted in A. Inset of C, zoom showing a pillar-like structure linking the luminal content to the limiting membrane. (F) A multivesicular body (black arrow, inset), two lysosomes (white arrows) and microtubules (arrowhead, inset) in proximity of late stages pigment organelles. (G) Continuity (arrowheads) and close-vicinity (arrow) of limiting membranes suggest heterotypic fusion events between different types of pigment organelles. (H-I) Single-membrane cluster of pigment organelles (i.e. c-type pigment organelle). (I) Three-dimensional reconstruction of a cluster containing two types (orange and yellow) of pigment organelle contents with some connection sites (inset, magenta).

Discussion

Simultaneous Anabolism and Catabolism of Pigment ELROs within the Same Cell

Previous studies on chemically fixed crab spiders proposed that reversible color changes originated from cyclic metabolism of pigments and from turnover of pigment organelle membranes, leading to various anabolic, catabolic and recycled stages of pigment organelles (Insausti & Casas, 2008, 2009). Our morphological typology of near-native state pigment organelles overlaps with that of chemically fixed cells and extends it thanks to fine labile ultrastructures preserved by HPF-FS. Particularly, we described intraluminal vesicles, fibrils and metals, membrane tubulations, and homotypic/heterotypic fusion events, which collectively show that pigment organelles are ELROs. These results also provide new insight into their anabolism, catabolism and recycling that we now discuss.

Anabolic stages (maturing a-types and fully pigmented b-types) were proposed to form via organelle precursors originating from either ER (Insausti & Casas, 2008) or Golgi vesicles (Insausti & Casas, 2009). Our study does not provide any evidence that ER is directly involved in this process. We rather observed on multiple occasions a-types in the vicinity of active tubulo-saccular regions comprising endosomal compartments, microtubules, vesicles and tubules. Furthermore, intraluminal fibrils similar to those of a-types were observed in tubulo-saccular compartments. Altogether, these observations indicate that pigment organelles originate from these tubulo-saccular complexes in the perinuclear area. It is unclear whether these organelles are modified Golgi apparatus (stacked structure, numerous free vesicles) or endosomal compartments (tubular membranes, intraluminal fibrils). Indeed, both are known to be morphologically plastic (Mironov *et al.*, 2017; Hoffman *et al.*, 2020) and to be directly involved in ELRO assembly (Bowman *et al.*, 2019). Cytochemical experiments that could distinguish endosomal from Golgi compartments based on their enzymatic activities may clarify whether pigment organelles mainly originate from the secretory or the endocytic system.

New catabolic stages of pigment organelles were observed in yellow integuments preserved by HPF-FS, namely c-types (clusters of pigment cores), d-types (degraded content at the periphery), e-types (degraded content at the center) and f-types (intertwined sheet-like content). We suggest they represent sequential degradative stages of fully pigmented b-types

based on the following 2D/3D ultrastructural evidence. First, some pigmented ELROs have an intermediate morphology between b- and d/e-types, namely a highly dense but slightly disorganized content. Second, their dense content appears to be mainly degraded in a centrifuge manner, leaving intertwined sheet-like scaffolds that are reminiscent of growing sheet-like fibrils in maturing a-types. Third, contact sites between degraded contents and limiting membranes are reminiscent of nucleation points from which fibrils grew in a-types. Finally, catabolic stages contain the same metals than b-types, albeit at lower concentrations. Based on these results, we propose the following catabolic pathway: b-types are degraded into d-/e-types and then into f-types, while clustering into c-types occurs by heterotypic fusions in between all these stages. This fusion process might be facilitated by the accumulation of Ca in pigment ELROs, since Ca^{2+} is known to activate fusion of endolysosomal organelles (Pryor *et al.*, 2000). To test this metabolic sequence of pigment ELROs, dynamical studies are warranted, such as tracking the proportion of each pigment ELRO types in crab spiders at different yellowing and bleaching stages.

Recycling pigment organelles back by autophagy for another cycle of yellowing after the complete catabolism of their content has been also proposed (Insausti & Casas, 2009). However, this hypothesis is not supported by our observations because the electron-lucent vacuoles associated to ER whorls and previously hypothesized to be recycled pigment organelles (Insausti & Casas, 2009) are actually lipid droplets. Yet, alternative recycling pathways of the endolysosomal system might still be at play. Indeed, endolysosomal organelles, including pigment ELROs like melanosomes, are known to recycle their content and membrane via tubulations (Yu *et al.*, 2010; Dennis *et al.*, 2016; Bissig *et al.*, 2017; Ripoll *et al.*, 2018). We observed tubulations of a c-type, which indicates that materials are actively recycled from catabolic stages during bleaching. Particularly, since metals are less concentrated in d- to f-types than in b-types, it is conceivable that tubules recycle metals for another turn of yellowing, hence bridging catabolism to anabolism of ELROs.

Overall, our results support the idea that color changes are based on highly-dynamic intracellular processes, which involve the continuous remodeling of both pigment organelle contents and membranes within the same cell. The presence of all pigment organelle types in yellow spiders indicates that their anabolism and catabolism proceed simultaneously within the same cell, highlighting the great metabolic turnover of pigment cells (Insausti & Casas,

2009). The numerous glycogen rosettes, mitochondria and lipid droplets observed in our electron micrographs and tomograms may provide the fuel for such a metabolic activity. We did not find any evidence of endocytosis or exocytosis at the plasma membrane, nor of any typical Golgi apparatus in pigment cells (contrary to other cell types); however, we observed multiple endolysosomal organelles, tubulo-saccular complexes and a vast majority of pigment ELROs. We therefore propose that secretory and endolysosomal systems are highly specialized in pigment cells and primarily functionalized for pigmentation.

The Endolysosomal System Provides a Universal Platform for Pigmentation

ELROs are not only characterized by common features related to their endolysosomal origin, but also by their morphological and functional diversity (Delevoye *et al.*, 2019). These variations on a common "ELRO theme" are based on commonalities in ELRO assembly and on the unique plasticity of the endolysosomal system (Bowman *et al.*, 2019). ELROs comprise a growing list of pigment organelles in distantly-related animals, including mammalian melanosomes (Orlow, 1995), fish pterinosomes (Navarro *et al.*, 2008), insect ommochromasomes and pterinosomes (Lloyd *et al.*, 1998), lepidopteran riboflavin and uric acid granules (Zhang *et al.*, 2017a, 2018a), and now pigment organelles of crab spiders (this study). How both commonalities and plasticity of the endolysosomal system, which we discuss in turn, affect these various pigment systems has broad implications for understanding animal coloration.

We observed that pigment ELROs of crab spiders possess several ultrastructural and metal features common to mammalian melanosomes, including intraluminal vesicles, sheet-like fibrils attached to limiting membranes, and accumulation of zinc and calcium (Shibata, Prota, & Mishima, 1993; Hurbain *et al.*, 2008; Gorniak *et al.*, 2014). Intraluminal vesicles and metals have also been variably described in pheomelanosomes (Stanka, 1974; Jimbow *et al.*, 1979), fish pterinosomes (Blanchard *et al.*, 1991), insect pterinosomes (Shoup, 1966), while various metals are found within insect ommochromasomes (White & Michaud, 1980; Gribakin *et al.*, 1987). These results collectively suggest that endolysosomal precursors of pigment ELROs possess conserved ultrastructural and metal components that may be required for the pigmentation process *per se*, independently of the pigment involved.

ELROs are also characterized by their various morphologies, in association with the different biological contexts in which they are produced (Delevoye *et al.*, 2019). This is especially true for pigment ELROs that produce different types of pigment. For example, eumelanosomes containing black eumelanin are characterized by an oblong shape, which is due to the unidirectional elongation of amyloidogenic fibrils attached to ILVs that act as nucleation points (Hurbain *et al.*, 2008). On contrary, pheomelanosomes containing yellow/red pheomelanin are round, which is due to the formation of an amorphous matrix around ILVs (Jimbow *et al.*, 1979). Here, we found that the roundish form of pigment ELROs in crab spiders is associated to ILVs that remain close to the limiting membrane and to a fibrillation process occurring in all directions from the limiting membrane toward the organelle center. This internal morphology leads to a more disorganized matrix than in eumelanosomes, and therefore round organelles. Furthermore, we frequently observed maturing a-types free of any ILV, which could be explained by back fusions of ILVs with the limiting membrane during pigmentation. This dynamic internal morphology may allow fibrils to nucleate from the lumenal face of the limiting membrane. The structural differences between pigment ELROs therefore suggest that plasticity is an important characteristic of endolysosomal systems to accommodate anabolism of various pigments in distantly-related species.

Overall, the importance of both commonalities and plasticity in the architecture of the endolysosomal system suggests that it can act as a universal platform for pigmentation in various contexts.

The Endolysosomal System is Fully Functionalized for Reversible Color Changes

How cells handle degradation of pigment organelles is a key question to understand the bleaching process of color changes in animals. Pigments can be removed either by the cell death of pigment cells (Stubenhaus *et al.*, 2016) or by the intracellular processing of pigment organelles while maintaining pigment cells alive (Insausti & Casas, 2009). Intracellular removal of pigments is classically mediated by three non-exclusive canonical mechanisms, namely secretion, lysosomal activity and autophagy. We already ruled out the possibility that pigment ELROs are catabolized and recycled by autophagy. Similarly, we never observed pigment organelles in the extracellular space nor their fusion with the plasma membrane,

precluding thus their secretion. This leaves lysosomal activity as the remaining possible mechanisms for intracellular removal of pigments. In the case of melanosomes, lytic activities were proposed to occur in two ways (Borovanský & Elleder, 2003). First, the fusion of melanosomes with *bona fide* lysosomes delivers lysosomal hydrolases and other lytic enzymes within melanosomes. Second, the lytic enzymes that are intrinsically associated with melanosomes because of their lysosomal character get activated. In the following, we discuss the body of evidence from our study that could support the occurrence of these two mechanisms during bleaching in crab spiders.

First, we observed in several occasions catabolic ELROs with a dense granular lumen resembling that of multivesicular bodies and lysosomes, as well as catabolic ELROs fused with lysosomes. These results therefore show that lysosome can deliver their lytic content to pigment ELROs. The ELRO identity of pigment organelles might facilitate their direct fusion with lysosomes by harboring endolysosomal fusing machineries (Luzio, Gray, & Bright, 2010). Second, we note that catabolic d-, e- and f-types have nearly the same size as fully pigmented b-types. Catabolic types also do not always show a lysosome-like granular lumen. These results indicate that catabolic ELROs can be formed without extensive addition of lysosomal membrane, which supports the hypothesis that pigment ELROs possess an autocatalytic activity (Insausti & Casas, 2009). Because pigment organelles are ELROs, such a lysosomal autocatalytic activity could stem from their endolysosomal character, similar to melanosomes. Furthermore, clustering of pigment ELROs into c-types raises the interesting possibility that this autocatalytic activity may serve to degrade other pigment ELROs. This process would hence mimic the effect of lysosomal fusion by delivering the lytic material of catabolically-active ELROs to unaltered ones.

Overall, our study provides evidence that pigment cells bleach via the *in situ* non-autophagic degradation of pigment ELROs, which involves lytic and recycling functions of the endolysosomal system. Hence, we propose that, in the context of morphological color changes, the endolysosomal system is adapted and fully functionalized not only to produce and store pigments, but also to catabolize them.

Conclusion

Color-changing crab spiders offer a striking example of how pigment cells accommodate the entire life cycle of pigment ELROs. Pigment cells seem indeed to have adapted their ubiquitous endolysosomal system to support the biogenesis of pigment ELROs, their degradation and their recycling. While biogenesis of pigment ELROs seems largely conserved across distantly-related species, and yet plastic, further studies are warranted to unravel the commonalities and specificities of their catabolism in color-changing organisms. Indeed, investigating in more details the overlooked catabolism of ELROs has potential physiological relevance, not only for color-changing crab spiders but also for the maintenance of light screening in the human eye (Schraermeyer, 1993; Borovanský & Elleder, 2003).

Acknowledgment

We thank Teresita Insausti for her help with the resin embedding protocol of crab spiders. We are particularly indebted to Graça Raposo for hosting F.F. in her team. We thank Cédric Delevoye for insightful discussion and Maryse Romao for technical assistance. We are grateful to Ilse Hurbain and Xavier Heiligenstein for their help in performing HPF-FS, EM and correlative imaging. We thank Sylvain Trépout for his help in performing STEM. We would like to acknowledge the Cell and Tissue Imaging Platform – PICT-IBiSA (member of France–Bioimaging – ANR-10-INBS-04) of UMR144 and US43-UMS2016 of Institut Curie for help with electron microscopy. We acknowledge SOLEIL for provision of synchrotron radiation facilities and we would like to thank Andrea Somogyi and Kadda Medjoubi for discussions and their help in operating the Nanoscopium beamline (projects 20180104 and 20190205).

Supplemental Information

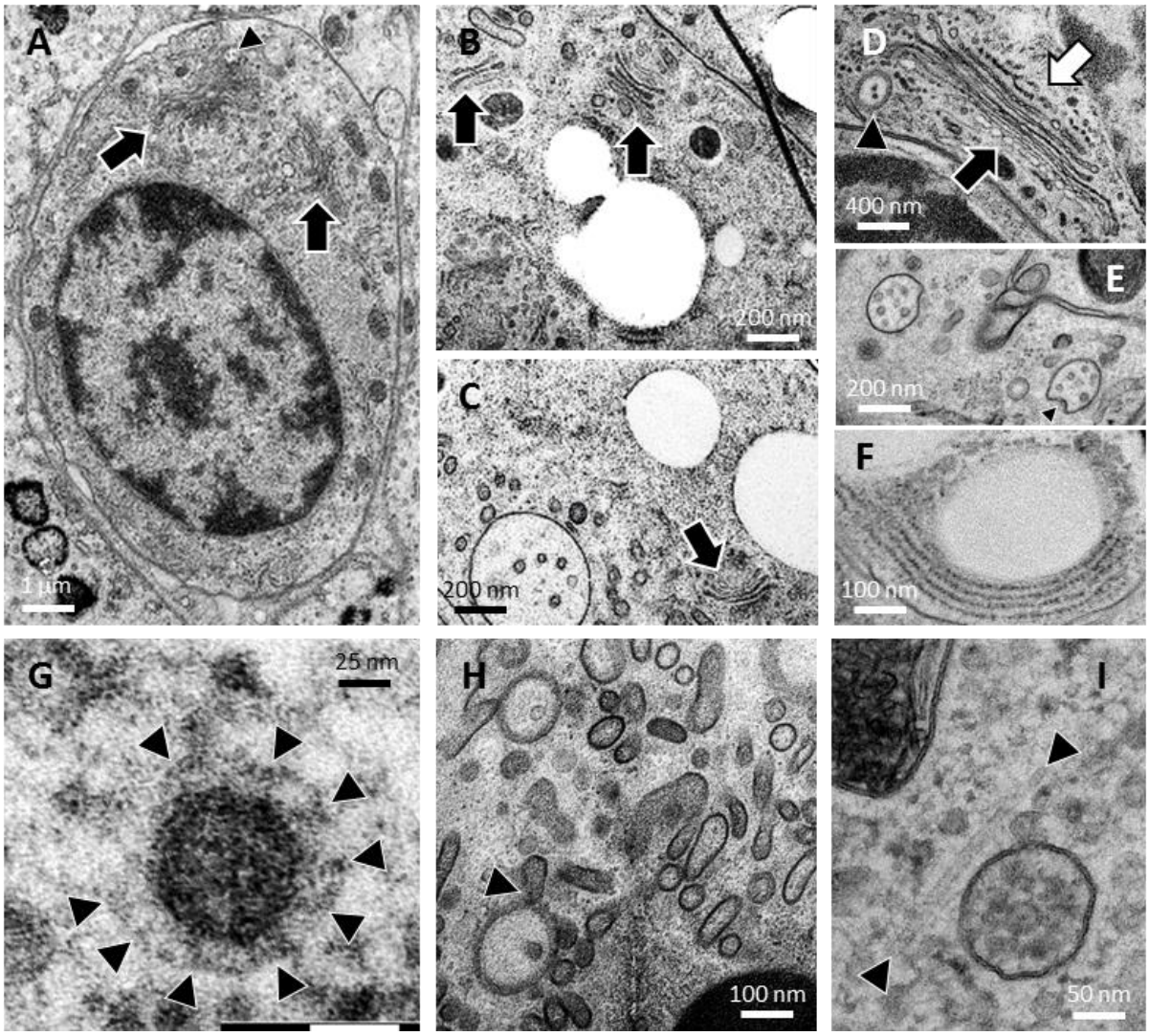

Figure S6-1. Ultrastructure of crab spider cells preserved by high-pressure freezing and freeze substitution.

(A) A non-pigment cell showing well-preserved nucleus, mitochondria, Golgi apparatus with clear stacked structures and budding profiles (arrows) and a closely associated endosome (arrowhead). (B-C) Multiple Golgi apparatus (arrows) with neat stacked structures within a non-pigment cell. (D) A stacked and budding Golgi apparatus showing distinct cis- (white arrow) and trans- (black arrow) sides in a non-pigment cell. An endosome harboring intraluminal vesicles (arrowhead) is closely associated. (E) Two endosomal compartments with multiple intraluminal vesicles (ILVs) and fibrils. The limiting membrane of one of these endosomal compartments is budding inward (arrowhead), likely forming a new ILV. (F) A lipid droplet closely associated to endoplasmic reticulum. (G) A cytosolic vesicle displaying a coat of proteins (arrowhead) resembling clathrin. (H) Endosomes and tubules within a non-pigment cell. An endosome display a tabulating membrane (arrowhead). (I) A microtubule (arrowheads pointing to its ends) closely associated to cytosolic vesicles and to a budding multivesicular body.

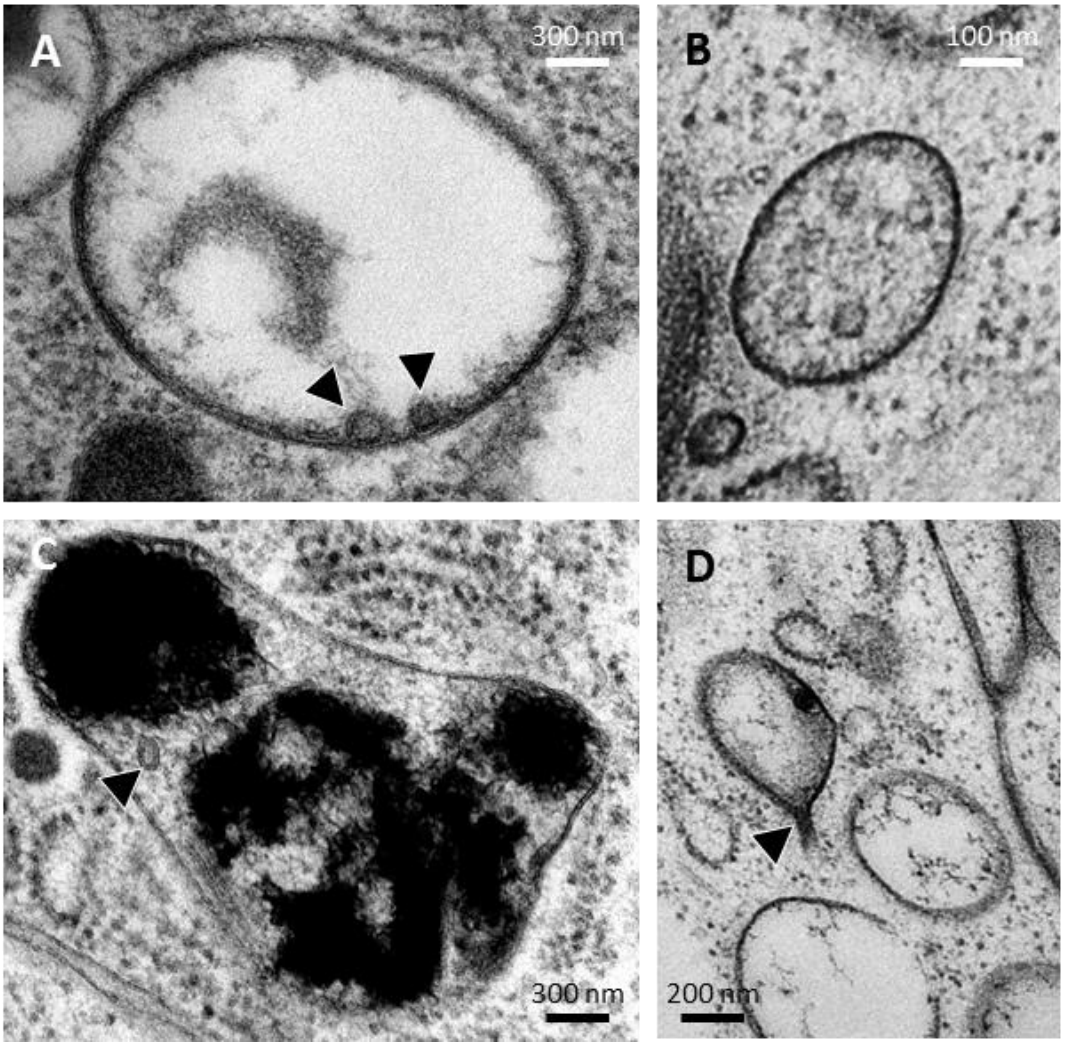

Figure S6-2. Intraluminal vesicles and membrane tubulations of pigment organelles.
(A) Two intaluminal vesicles (arrowheads) closely associated to the limiting membrane of an early a-type pigment organelle. (B) Intraluminal vesicles and fibrils in a multivesicular body resembling a maturating a-type pigment organelle. (C) A intraluminal vesicle (arrowhead) within a c-type cluster of pigment organelles. (D) Tubulation of the limiting membrane (arrowhead pointing toward the tubule neck) of an early a-type pigment organelle.

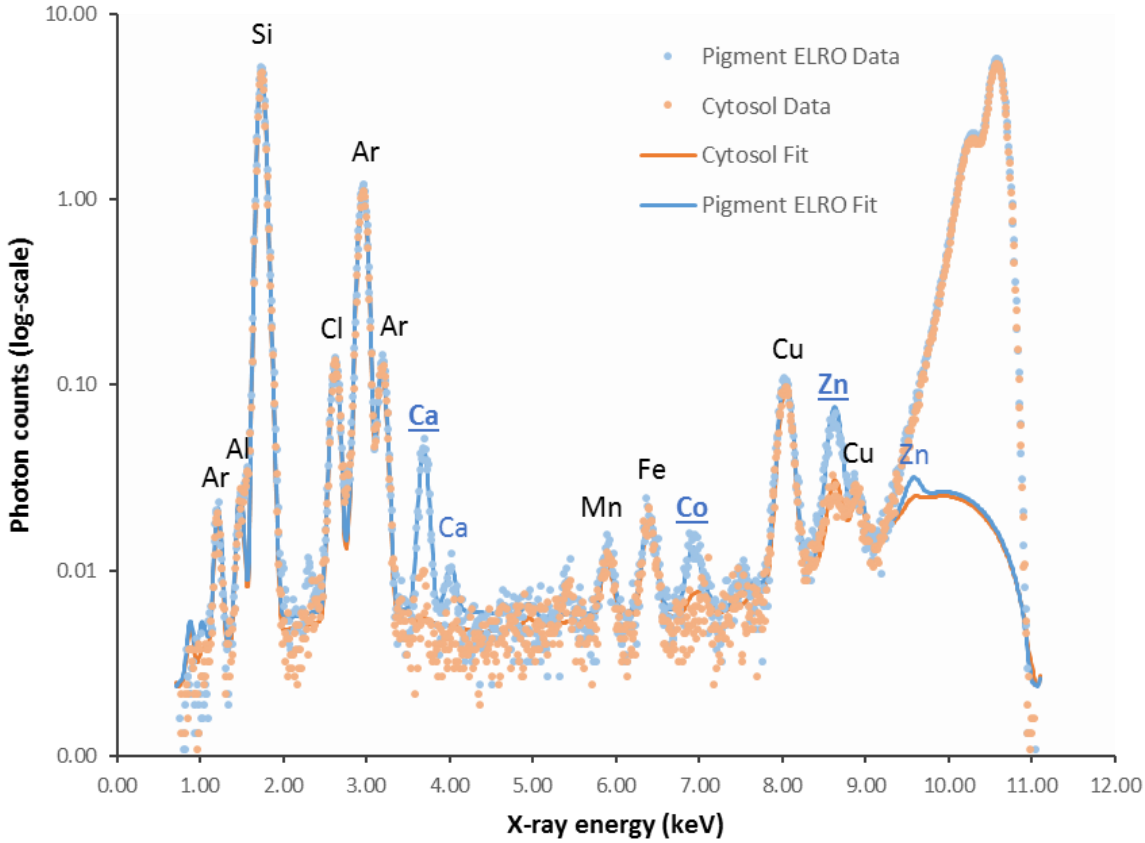

Figure S6-3. Recorded Synchrotron X-ray spectra of two intracellular regions within the same cell.
X-ray fluorescence of native metals were obtained by exciting the area shown in the inset of **Figure 6-2**, which contains a single pigment organelle surrounded by cytosol, at 9.7 keV (DCM). Recorded data are displayed as dots. Main fluorescence peaks (K-lines) of elements between Al and Zn are shown as continuous lines. X-ray energies above 9.7 keV are dominated by scattered X-rays. Elements indicated in blue fonts (Ca, Co and Zn) are those with higher fluorescence in the pigment organelle than in the cytosol. The peaks of underlined elements are those used for metal mappings in this study.

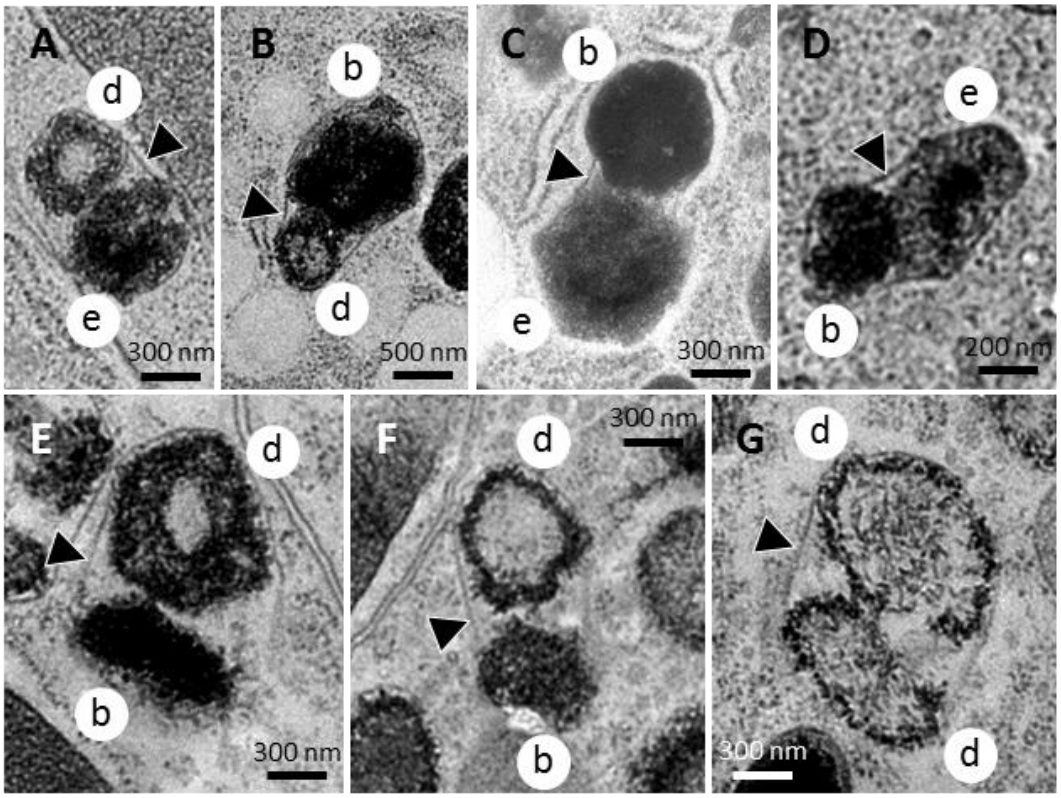

Figure S6-4. Various pigment organelle types observed within c-type clusters.
(A-G) The various types of pigment organelles recognizable within c-type clusters are indicated by their respective letters. All c-types possess a single limiting membrane (arrowheads).

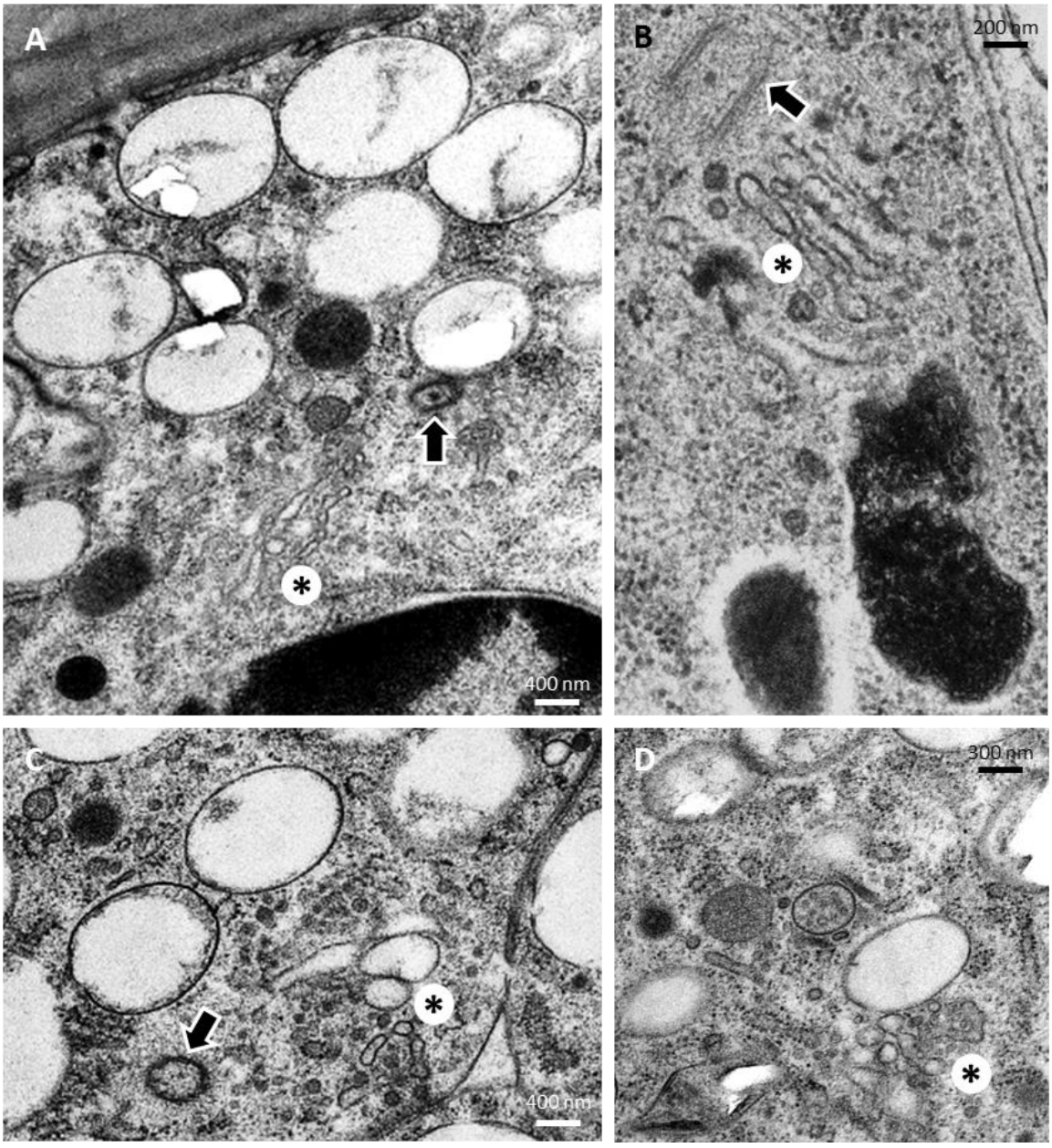

Figure S6-5. Examples of tubulo-saccular complexes in pigment cells of crab spiders.
(A-C) Centrioles (arrows) can be observed in regions where tubulo-saccular complexes (asterisk) are situated. (D) Another example of a tubulo-saccular complex closely associated to an early a-type pigment organelle, endosomal compartments, vesicles and tubules.

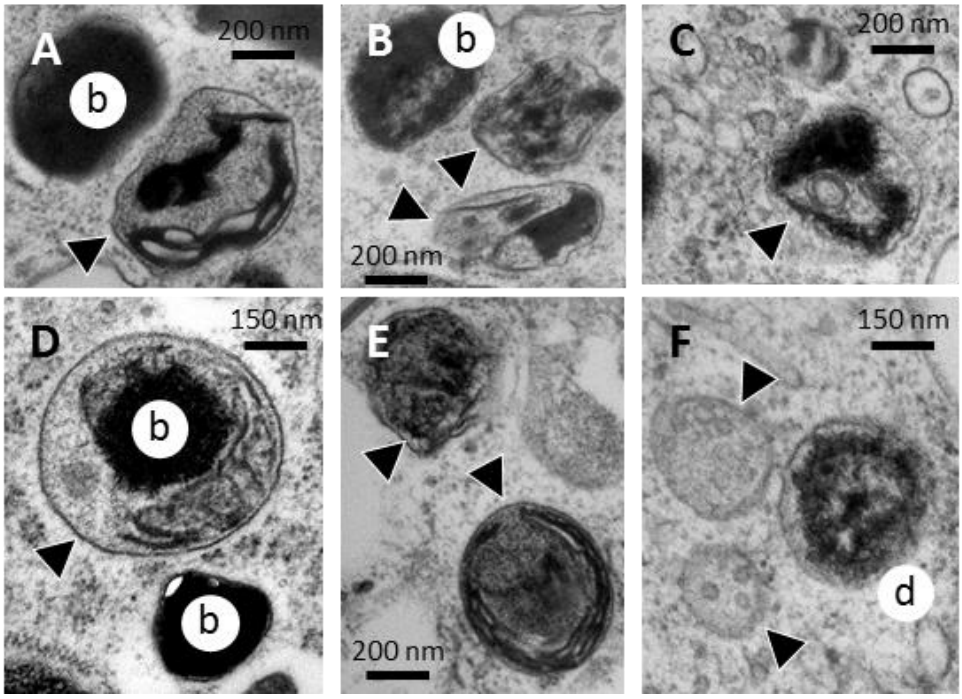

Figure S6-6. Ultrastructural evidence of lysosomal degradation of pigment organelles.
(A-E) Lysosomal compartments (arrowheads) displaying a single limiting-membrane, dense lumens, heterogeneous and aggregated materials, as well as cores of b-type pigment organelles are observed, sometimes in the close vicinity of free pigment organelles. (F) Two multivesicular bodies (arrowheads) with dense granular lumens resembling late endosomes are closely associated to a d-type pigment organelle.

6.3 Conclusion

Dans cette étude, le changement de couleur de l'araignée crabe *Misumena vatia* a été étudié à l'échelle subcellulaire. Pour préserver les cellules et les organites dans un état quasi-natif, la cryofixation par HPF-FS a été utilisée. La combinaison et la corrélation de différentes modalités d'imagerie ont permis d'affilier les organites pigmentés des araignées crabes aux ELROs, répondant ainsi au *point 6* du **chapitre 3** (p. 117). La description des différents stades de maturation des ELROs pigmentés des araignées crabes, ainsi que la visualisation en trois dimensions de leur architecture, indiquent que leur cycle de vie est un processus complexe. Celui-ci sembler démarrer au niveau de régions tubulo-sacculaires et continuer avec des fusions homotypiques menant à l'élargissement des ELROs. En parallèle, la pigmentation semble se développer au sein des organites via la formation de fibrilles démarrant depuis la membrane limitante, ainsi que celle des vésicules intraluminales. L'anabolisme se termine par le remplissage complet du lumen, donnant cet aspect très dense aux ELROs pigmentés. Lors du catabolisme, un ensemble d'étapes mènent à la dégradation du contenu intraluminal. Des événements de fusion hétérotypique entre stades de dégradation, mais aussi avec les lysosomes, pourraient expliquer la dépigmentation des ELROs. Un recyclage membranaire via la tubulation de la membrane limitante des ELROs cataboliques pourrait permettre de récupérer du matériel membranaire et intraluminal. Ainsi, ces données étayent l'hypothèse du cycle de vie intracellulaire de ELROs pigmentés (*point 9* du **chapitre 3**, p. 118) comme moyen de réaliser des changements de couleur morphologique réversibles à l'échelle cellulaire. Cependant, ces résultats ne semblent pas indiquer que des processus autophagiques soient à l'œuvre pour dégrader spécifiquement le contenu des organites pigmentés et recycler leur membrane limitante dans son entièreté. Les systèmes endolysosomaux et sécrétoires (post-Golgi) seraient les principales sources de membrane pour la (re)formation des ELROs pigmentés. Des expériences complémentaires sont requises pour valider la séquence de maturation anabolique et catabolique proposée. En particulier, un suivi temporel des populations d'ELROs pigmentés chez des araignées en cours de jaunissement et de blanchiment apporterait des informations supplémentaires sur la filiation entre les différents types d'ELROs pigmentés. En théorie, il devrait aussi être possible d'injecter des traceurs des voies endolysosomales [ex. transferrine ; (Raposo *et al.*, 2001)] aux araignées crabes et de révéler leurs *patterns* d'accumulation intracellulaire en microscopie électronique. En pratique,

cela demande de pouvoir manipuler expérimentalement les araignées crabes et leur coloration, ce qui est une tâche ardue. De plus, il faudrait que le traceur présent dans l'hémolympe soit endocyté par les cellules tégumentaires pigmentés, phénomène qui n'est pas connu.

De manière innatendue, une accumulation de cobalt dans les cellules pigmentées, et plus particulièrement dans les ELROs les plus pigmentés, a été observée. Or, le cobalt est un métal rare géologiquement et biologiquement parlant. On remarque dans ces expériences qu'aussi bien les araignées blanches que jaunes accumulent du cobalt dans leurs noyaux, indiquant qu'il n'y avait probablement pas de différences d'approvisionnement en cobalt. Cela pose donc la question de la raison de son accumulation dans les ELROs pigmentés chez les araignées jaunes. Je propose deux explications. Premièrement, le cobalt pourrait être, comme de nombreux métaux (zinc, cuivre, etc.), nécessaire à la formation et à la stabilisation des pigments en tant que cofacteur enzymatique. On pourrait alors supposer une translocation active du cobalt vers les ELROs en cours de maturation pour favoriser le jaunissement. Deuxièmement, le cobalt pourrait agir comme un métal de transition toxique, par exemple en déplaçant le zinc ou le fer sans avoir leurs effets biologiques. Les cellules auraient alors comme moyen de défense la séquestration du cobalt dans les ELROs, en particulier les plus pigmentés puisque les pigments sont généralement des chélateurs d'ions métalliques. Des approches expérimentales sont nécessaires pour répondre à ces questions. En particulier, il serait envisageable d'apporter du cobalt, ou tout autre métal lourd, à des araignées de différentes couleurs et de voir si cela impacte leur survie ou encore leur capacité à changer de couleur. Le suivi de ces métaux serait réalisé par fluorescence des rayons X au Synchrotron, selon le protocole mis en place dans ce chapitre.

Chapitre 7 – Discussion générale : la biologie intégrative des ommochromes

No single hypothesis can explain the coloration of living things. Nonetheless, we need not conclude that coloration is arbitrary, nor that the many hypotheses are unrelated.

Edward H. Burtt, Jr. (1974), *BioSciences*

7.0 Sommaire

CHAPITRE 7 – DISCUSSION GENERALE : LA BIOLOGIE INTEGRATIVE DES OMMOCHROMES 257

7.0 SOMMAIRE 258

7.1 INTRODUCTION 259

7.2 LE ROLE CLE DES OMMOCHROMES EN TANT QUE PIGMENTS CHANGEANT DE COULEUR 260

Les bases physico-chimiques des changements de couleur dus aux pigments 260

La plasticité à plusieurs échelles des ommochromes les rend efficaces comme pigments changeant de couleur 263

Au-delà des changements de couleur chez les invertébrés : le potentiel des ommochromes pour le biomimétisme 265

7.3 LES FONCTIONS BIOCHIMIQUES ET PHYSIOLOGIQUES DES OMMOCHROMES EN-DEHORS DE L'ASPECT VISUEL 266

Les ommochromes peuvent-ils agir en tant que transporteurs d'électrons ? Ce que nous apprennent les phénazines bactériennes 267

Les propriétés antiradicalaires et proradicalaires des ommochromes 269

Les propriétés détoxifiantes des ommochromes 271

Les propriétés photoprotectrices et phototoxiques des ommochromes 273

La thermorégulation 275

Conclusion sur les multiples rôles biologiques des ommochromes et de leurs changements de couleur .. 276

7.4 DES CONTEXTES ECOLOGIQUES DE L'UTILISATION DES OMMOCHROMES 276

L'écophysiologie du polyphénisme de phase des criquets 277

L'écophysiologie de la couleur nuptiale des libellules et des demoiselles 278

L'écophysiologie des changements de couleurs chez les araignées crabes 279

7.5 LES OMMOCHROMES DANS LE CONTEXTE D'UNE ORIGINE COMMUNE DES ORGANITES PIGMENTES 282

7.6 CONCLUSION : « LE CARACTERE MULTI-TEXTURE » DE LA COULEUR 285

7.1 Introduction

Dans ces travaux, j'ai étudié les mécanismes des changements de couleur morphologiques chez les invertébrés. Je me suis particulièrement intéressé aux différentes échelles biologiques auxquelles se produisent les changements de couleur, depuis les molécules jusqu'aux organites pigmentés. Dans le **Chapitre 2** (Figon & Casas, 2018), j'ai présenté une revue intégrative des acteurs physiologiques, cellulaires et moléculaires des changements de couleur. Les fonctions biologiques des changements de couleur qui ne font pas forcément intervenir l'effet visuel ont été discutés. Dans le **Chapitre 3** (Figon & Casas, 2019), j'ai présenté une synthèse sur la biochimie et la biologie cellulaire des ommochromes, une famille de pigments restreinte aux invertébrés. Ensemble, ces deux chapitres ont pointé les nouvelles pistes et les questions clés à partir desquelles mon travail expérimental a été construit. Dans le **Chapitre 4** (Figon *et al.*, In press), la spectrométrie de masse en tandem couplée à la chromatographie liquide a été utilisée pour identifier la position centrale de la xanthommatine non cyclisée dans la voie de biosynthèse des ommochromes. Cet intermédiaire labile permet de relier la structure des ommatines, de couleur jaune à rouge, aux ommines violettes, qui sont notamment impliquées dans les changements de couleur des céphalopodes. Dans le **Chapitre 5**, le comportement bathochromique atypique des ommochromes lorsqu'ils sont réduits a été modélisé en utilisant la chimie quantique. Il s'est avéré que les propriétés optiques et les capacités antiradicalaires des ommochromes sont en fait deux facettes de la même pièce, c'est-à-dire les propriétés électroniques de l'état réduit. Dans le **Chapitre 6**, les changements de couleur morphologiques des araignées crabes ont été étudiées à l'échelle subcellulaire en utilisant différentes modalités d'imagerie, dont la fluorescence des rayons X Synchrotron (SXRF) et la tomographie électronique (ET), sur des téguments fixés par congélation à haute pression (HPF). Des marqueurs ultrastructuraux et chimiques (métaux) de l'apparentement des organites pigmentés des araignées crabes aux organites associés aux endolysosomes ont pu être mis en évidence. Cela a aussi révélé la complexité des étapes ultrastructurales qui mènent à la biogenèse, pendant le jaunissement, et à la dégradation/recyclage pendant le blanchiment des araignées crabes.

Dans ce **Chapitre 7**, je discute de la portée de ces résultats en termes de compréhension de la biologie intégrative des changements de couleur morphologiques. Premièrement, je rassemble les preuves que les ommochromes sont particulièrement à même

de produire ces changements de couleur, ce qui pourrait expliquer leur évolution chez les invertébrés. Deuxièmement, je mets en évidence les fonctions alternatives des ommochromes, en-dehors de l'aspect visuel, et je discute des potentiels mécanismes qui leurs sont associés en me basant sur ces résultats. Troisièmement, j'argumente sur le fait qu'une approche écophysiologique est nécessaire pour révéler la complexité des changements de couleur en revisitant trois exemples classiques de contextes écologiques du changement de couleur. Enfin, j'aborde les implications évolutives des résultats de cette thèse en lien avec les cellules et les organites pigmentés des animaux.

7.2 Le rôle clé des ommochromes en tant que pigments changeant de couleur

Les ommochromes sont une des rares familles de pigments à être restreintes à un groupe précis d'animaux (c'est-à-dire les invertébrés) alors que les mélanines, les ptérines, les purines, les caroténoïdes, les porphyrines et les quinones sont présentes chez quasiment tous les grands groupes d'animaux (Needham, 1974). L'absence d'ommochromes chez les vertébrés est toujours inexpliquée bien que tous les animaux possèdent la même voie des kynurénines (Linzen, 1974) et qu'ils produisent tous des enzymes capables de dimériser des *ortho*-aminophénoles (Eggert *et al.*, 1995). Néanmoins, l'usage répandu des ommochromes chez l'ensemble des invertébrés comme pigments des yeux et des téguments indique qu'ils possèdent des fonctions biologiques importantes.

Les changements de couleur sont le résultat d'une interaction dynamique entre la lumière et la matière (**Chapitre 1** et **Chapitre 2**). La dualité onde–corpuscule de la lumière produit deux types principaux de changements de couleur, ceux basés sur la diffusion (ex. le bleu Tyndall) et ceux basés sur l'absorption (ex. les couleurs chimiques). Dans ces travaux, je me suis intéressé aux changements de couleur morphologiques qui reposent principalement sur des mécanismes d'absorption. Cependant, par souci d'exhaustivité, je mentionne aussi dans ce qui suit des cas où les pigments sont impliqués dans la diffusion de la lumière.

Les bases physico-chimiques des changements de couleur dus aux pigments

D'un point de vue théorique, un pigment peut changer de couleur (processus autrement appelé « chromisme ») en modifiant n'importe lequel des paramètres qui contrôlent

la façon dont il interagit avec la lumière (**Table 7-1**). En pratique, tous ces paramètres ne sont pas équivalents ou n'ont pas été démontrés dans un contexte biologique. Par exemple, le pH des cellules et de leurs compartiments ne peut être ni trop acide ni trop basique, ce qui limite donc la portée de l'acidochromisme *in vivo*. Il faut aussi noter que la couleur provient souvent de la combinaison entre un pigment et une structure photonique, telles que des cristaux réflecteurs situés en-dessous des pigments, sur laquelle un organisme peut aussi jouer pour changer sa couleur (Shawkey & D'Alba, 2017; Williams *et al.*, 2019b). En somme, la physique et la chimie des changements de couleur impliquent des mécanismes morphologiques très divers. Dans la suite, je discute en quoi les ommochromes sont particulièrement efficaces dans le changement de couleur en reliant leurs propriétés aux différents types de chromisme (**Table 7-1**). Cette approche pourrait apporter des indications sur les raisons de leur succès et de leur évolution chez les invertébrés.

Table 7-1. Paramètres influençant l'interaction entre la lumière et la matière et qui interviennent potentiellement dans le changement de couleur des pigments

Paramètre	**Interaction lumière–matière**	**Principal effet sur la couleur**	**Exemple biologique chez les animaux**
Taille des particules pigmentées	Diffusion	Les plus petites particules diffusent les plus petites longueurs d'onde	Nanosphères de ptérines chez certaines demoiselles (Henze *et al.*, 2019)
Distribution des particules pigmentées	Diffusion	Les structures ordonnées peuvent provoquer des interférences lumineuses	Nanosphères de ptérines chez les demoiselles (Henze *et al.*, 2019)
Concentration (concentratochromisme)	Absorption	Modifie principalement la saturation et parfois la teinte (ex. des pigments jaunes très concentrés peuvent apparaître oranges)	Jaunissement et blanchiment des araignées crabes [**Chapitre 6** ; (Insausti & Casas, 2008; Llandres *et al.*, 2013)]
pH (acidochromisme)	Absorption	Modifie la teinte (dépend du pigment)	Aucun
Etat redox (électrochromisme)	Absorption	La réduction blanchit généralement le pigment, sauf pour les ommochromes (bathochromie)	Coloration nuptiale de certaines libellules (Futahashi *et al.*, 2012)
Solvant (solvatochromisme) et la matrice	Absorption	Modifie la teinte en agissant sur la polarité du milieu (dépend du pigment)	Yeux composés (Linzen, 1974)
Agrégation des pigments (agrégachromisme)	Absorption	Modifie la teinte en fonction de l'interaction entre les monomères de pigment	Aucun
Fonctionnalisation chimique	Absorption	Modifie la teinte en fonction du groupement	Diversité de couleurs entre les chromatophores de céphalopodes (Williams *et al.*, 2016) Vieillissement des chromatophores de céphalopodes ? [**Chapitre 4** ; (Figon *et al.*, In press)]
Complexation avec des métaux (metallochromisme)	Absorption	Modifie la teinte en fonction du métal et du pigment	Les yeux composés ? (White & Michaud, 1980)
Tautomères (position des hydrogènes)	Absorption	Modifie la teinte par un changement de la délocalisation électronique (dépend du pigment)	Tautomérisation de la métarhodopsine (Matthews *et al.*, 1963)
Conformères (souvent du photochromisme)	Absorption	Modifie la teinte par un changement de la délocalisation électronique (dépend du pigment)	Photoisomérisation du rétinal dans la rhodopsine et la métarhodopsine (Matthews *et al.*, 1963)

La plasticité à plusieurs échelles des ommochromes les rend efficaces comme pigments changeant de couleur

Dans ce qui suit, j'avance des arguments sur le fait que les capacités plastiques et multi-échelles de changement de couleur des ommochromes, comparés à d'autres pigments, pourraient être une des raisons de leur succès.

L'étude de chimie quantique du **Chapitre 5** montre que les ommochromes possèdent à l'état réduit des propriétés électroniques uniques qui contrôlent leur réduction bathochromique (exemple d'électrochromisme). En particulier, les couplages électroniques d'auxochromes accepteurs d'électrons (EWA) à l'état réduit, mais pas à l'état oxydé, diminuent les énergies d'excitation et donc permettent l'absorption de grandes longueurs d'onde. Sans ces EWA, qui proviennent de la chaîne d'acide aminé de la 3-hydroxykynurénine, les transitions bathochromiques lors de la réduction ne seraient pas possibles ; les ommochromes seraient alors blanchis lors de la réduction, comme la grande majorité des pigments (Needham, 1974). De plus, le niveau de couplage géométrique de l'EWA ajuste l'effet bathochromique (exemple de chromisme basé sur les conformères). Cela suggère que les changements de couleur peuvent varier *in vivo* à travers les interactions entre l'EWA et la matrice dans laquelle les ommochromes sont déposés, en particulier les protéines et les métaux avec qui ils se lient (exemple de chromisme basé sur la complexation). L'étude biochimique de la voie des ommochromes du **Chapitre 4** (Figon *et al.*, In press) suggère que la xanthommatine non cyclisée pourrait être le chaînon structural manquant entre les ommochromes de différentes couleurs, c'est-à-dire les ommatines et les ommines. De la même façon que le dépôt d'eumélanines et de phéomélanines est dynamique (Ito & Wakamatsu, 2008), l'approvisionnement dynamique des précurseurs d'ommines pourrait mener aux changements de couleur des chromatophores de céphalopodes au cours de leur vie, sans qu'il y ait besoin de reprogrammer entièrement le métabolisme cellulaire (exemple de chromisme basé sur la fonctionnalisation chimique). Enfin, l'étude de la biologie cellulaire des araignées crabes du **Chapitre 6** a révélé que le développement intracellulaire des organites pigmentés associés aux endolysosomes (ELROs) menait à divers stades anaboliques et cataboliques. Ces stades différaient en particulier par leurs structures et leur densité intraluminales, les organites pigmentés les plus denses étant aussi les plus colorés et ceux avec le plus de métaux. De plus, les ELROs pigmentés sont connus pour être capables de faire

varier leur pH entre l'acide et le neutre au cours de leur maturation (Zhou *et al.*, 2018). Ainsi, les changements de couleur des araignées crabes reposeraient en premier lieu sur la production/dégradation des pigments (exemple de concentratochromisme), et en second lieu sur la complexation avec des protéines/métaux (exemple de chromisme basé sur la complexation), voire sur le pH (exemple d'acidochromisme). Concernant ces deux derniers types de chromismes, une étude plus approfondie de la composition intraluminale des ELROs pigmentés est nécessaire afin de s'assurer de leurs potentielles implications.

En somme, ces travaux révèlent que les ommochromes sont des pigments plastiques dont la coloration est ajustable grâce à divers mécanismes qui altèrent soit leurs états électroniques, soit leur structure chimique, soit leur développement intracellulaire. Cependant, les changements de couleur ne sont pas l'apanage des ommochromes ; les mélanines et les ptérines sont aussi impliquées dans les changements de couleur morphologiques (Umbers *et al.*, 2014; Figon & Casas, 2018). Je propose donc l'hypothèse suivante : la principale différence entre les ommochromes et les autres pigments est que les ommochromes sont capables de réagir plus rapidement aux variations de leur environnement cellulaire, se rapprochant ainsi des changements de couleur physiologiques. En effet, les ommochromes sont les seuls pigments pour lesquels un électrochromisme a été démontré *in vivo* ; et d'un point de vue chimique, les réactions redox sont rapides et relativement faciles à réaliser à l'intérieur d'une cellule. Au contraire, passer de la biosynthèse d'eumélanines à celle de phéomélanines ou produire de nouvelles ptérines prend potentiellement plus de temps ou plus d'énergie parce que ce sont des réactions métaboliques plus coûteuses qu'une « simple » altération de l'état redox local. De plus, la relative petite taille des ommochromes (en tant que dimères) comparée aux mélanines hautement polymérisées pourrait faciliter leur dégradation. Enfin, dans le contexte du filtrage de la lumière dans les yeux composés, qui est l'une des fonctions des ommochromes la mieux connue et la plus répandue, la possibilité d'ajuster de manière dynamique les longueurs d'onde absorbées par les ommochromes pourrait avoir facilité l'évolution de la variété de photorécepteurs connus à ce jour (Stavenga, Wehling, & Belušič, 2017). L'ajustement par le couplage de l'EWA pourrait donc avoir eu une fonction clé pour favoriser ces pigments dans les yeux des insectes. À ma connaissance, de telles propriétés n'ont jamais été démontrées ni discutées chez d'autres pigments de l'œil, que ce soit les mélanines ou les ptérines.

Au-delà des changements de couleur chez les invertébrés : le potentiel des ommochromes pour le biomimétisme

La couleur des animaux est depuis longtemps une source d'inspiration pour les scientifiques, les ingénieurs et les artistes (Caro *et al.*, 2017a). L'exemple phare est celui d'Abbott H. Thayer qui a étudié le camouflage chez les animaux (Thayer & Thayer, 1909), avec des applications dans les arts et l'armée (Diamond & Bond, 2013). Plus récemment, des peintures pouvant changer de couleur (pigments photoniques) ont été conçues pour imiter la fascinante palette de couleurs iridescentes des céphalopodes, des coléoptères et des papillons (Schenk, 2015; Clough *et al.*, 2019; Cai *et al.*, 2019). En comparaison, le biomimétisme des changements de couleur morphologiques est moins développé malgré les nombreuses propriétés de changement de couleur des pigments chimiques. La principale raison est probablement que de tels changements de couleur reposent avant tout sur des associations complexes entre les pigments et leur matrice, ce qui est difficilement reproductible avec des matériaux synthétiques, ou encore sur le pH et la solvatation qui ne sont généralement pas compatibles avec la plupart des contextes, tels que la peinture, les appareils électroniques, etc. Cependant, les ommochromes apportent une autre façon d'ajuster les couleurs chimiques à travers les réactions redox, qui peuvent se dérouler dans tous les environnements (solides, liquides et gazeux) et par d'autres moyens que les réactions chimiques, en particulier par un courant électrique. Ainsi, l'électrochromisme de la xanthommatine a été mis à profit pour concevoir un appareil électrochromique dont la couleur peut varier en fonction de la tension électrique qui lui est appliquée (Kumar *et al.*, 2018). En couplant une couche de xanthommatine avec une surface bleue, les auteurs ont pu obtenir une palette de couleurs dynamiques (Kumar *et al.*, 2018). Cependant, il reste encore des défis à relever avec cette technologie. Tout d'abord, la palette de couleurs obtenues est principalement située dans l'espace du jaune-rouge à cause de l'utilisation d'une surface bleu foncé dont la couleur n'est pas ajustable à cause des limitations intrinsèques de la xanthommatine. Deuxièmement, une perte de contraste est observée au cours du temps et des utilisations. Enfin, les vitesses de changement de couleur restent de l'ordre de quelques secondes. Alors que les deux dernières limitations sont principalement liées à l'utilisation d'électrolytes en phase liquide (Kumar *et al.*, 2018), les travaux de cette thèse pourraient apporter des solutions partielles à la première difficulté, et donc permettre d'obtenir une plus large palette de couleurs dépendantes de l'état redox.

La première stratégie consisterait à utiliser des couches indépendantes avec différents ommochromes afin d'imiter la coloration dynamique des céphalopodes. Des couches de xanthommatine oxydée/réduite produiraient les teintes jaunes à rouges. Des couches d'ommines, dont la couleur dépend aussi de l'état redox (Needham, 1974), absorberaient à des longueurs d'onde plus élevées afin d'obtenir des changements de couleur dans le bleu. La combinaison de ces différentes couches augmenterait ainsi l'étendue des couleurs accessibles « simplement » en ajustant deux tensions électriques indépendantes. La deuxième stratégie serait de concevoir des phénoxazinones substituées avec une variété d'EWA et d'EDA, telles que la série de Schäfer et Geyer (Schäfer & Geyer, 1972). Combiner ses différentes formes substituées produirait une gamme de couleurs différentes, tant à l'état oxydé (EDA) qu'à l'état réduit (EWA), un peu comme la teinte des chromatophores de céphalopodes qui est en corrélation avec le ratio de xanthommatine par rapport à sa forme décarboxylée (Williams *et al.*, 2016). De plus, le fait que de tels substituants agissent aussi sur le potentiel de réduction de composés apparentés aux phénoxazines [voir plus bas l'exemple des phénazines ; (Wang & Newman, 2008] implique que la réduction/oxydation des différentes phénoxazines substituées pourrait se produire à différentes tensions électriques. Cela permettrait de réaliser des changements de couleur séquentiels de chaque phénoxazine et donc d'obtenir des combinaisons de couleur ajustables. Enfin, le lien entre le changement de couleur et la coplanarité des substituants avec le chromophore phénoxazine suggère qu'il y a encore bien d'autres moyens pour ajuster finement le changement de couleur des ommochromes. En somme, l'utilisation des ommochromes dans le domaine du biomimétisme de couleur est encore dans ses balbutiements ; il faut davantage d'études numériques et expérimentales pour connaître leurs potentiels avantages et limites.

7.3 Les fonctions biochimiques et physiologiques des ommochromes en-dehors de l'aspect visuel

Mise à part la coloration, les pigments ont de multiples fonctions liées à leurs propriétés physiques, chimiques et biosynthétiques. Ces fonctions vont de l'homéostasie redox à la photoprotection et à la thermorégulation en passant par l'immunité [**Chapitre 1** ; (Needham, 1974; Hill & McGraw, 2006)]. Cependant, les pigments peuvent aussi être délétères, comme le montre la maladie humaine appelée porphyrie aigüe dans laquelle les porphyrines produisent des espèces réactives dangereuses qui altèrent certains organes (del C.

Batlle, 1993). Dans la suite, je discute, à partir des résultats de cette thèse, ces fonctions indirectement liées à la couleur des ommochromes.

Les ommochromes peuvent-ils agir en tant que transporteurs d'électrons ? Ce que nous apprennent les phénazines bactériennes

Bien que le comportement optique des ommochromes lors de leur réduction soit unique dans le règne animal, ils partagent cette bathochromie avec certaines phénazines qui sont des pigments bactériens (Price-Whelan, Dietrich, & Newman, 2006; Wang & Newman, 2008). De manière assez remarquable, le chromophore des phénazines, basé sur deux cycles carbonés joints par deux atomes d'azote, est très semblable aux phénoxazinones (**Figure 7-1**A). Les phénazines sont donc très proches des ommochromes en termes de structure, suggérant que le chromophore des phénazines possède les mêmes propriétés électroniques que les phénoxazinones. Les fonctions biologiques des phénazines sont multiples, depuis le transport d'électrons permettant le métabolisme en conditions anoxiques jusqu'au *quorum sensing* (Price-Whelan *et al.*, 2006; Glasser, Saunders, & Newman, 2017). Dans la suite, je fais la comparaison entre les ommochromes et les phénazines, ce qui pourrait apporter des indices sur certaines fonctions négligées des ommochromes, ainsi que sur les propriétés électroniques qui sous-tendent le transfert d'électrons chez les phénazines.

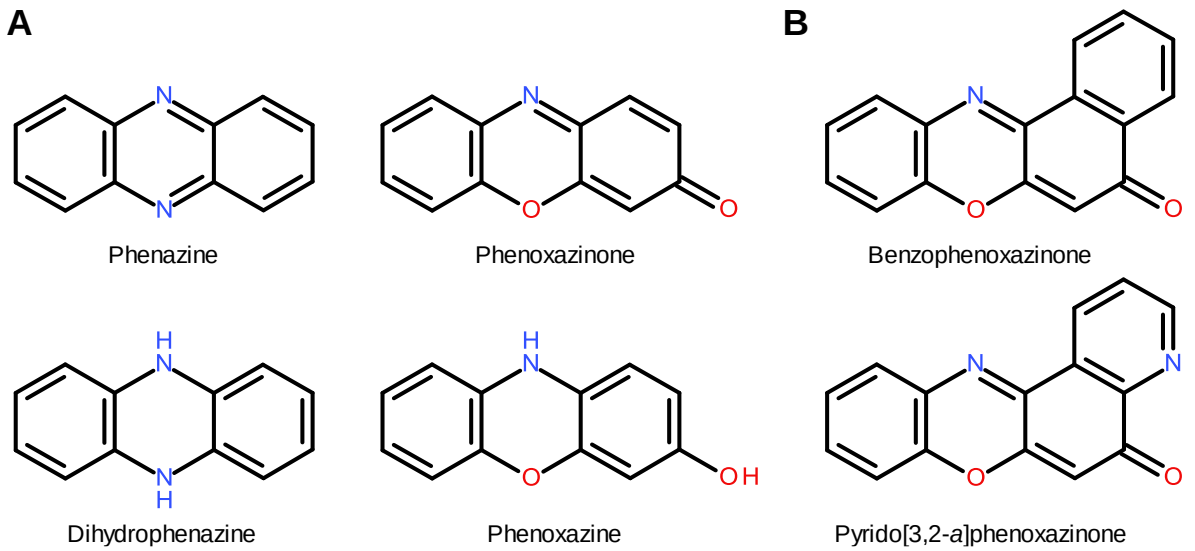

Figure 7-1. Formules chimiques des phénazines et des phénoxazinones.
A) Formes oxydés (haut) et réduites (bas). B) Deux modèles tétracycliques de la xanthommatine.

Les propriétés de changement de couleur des phénazines dépendent directement de leur structure moléculaire, à l'instar des ommochromes (Wang & Newman, 2008). Les phénazines avec des auxochromes donneurs d'électrons (EDA) sont hypsochromiques (ex. la pyocyanine et la 1-hydroxyphénazine), alors que celles avec des auxochromes accepteurs d'électrons (EWA) sont bathochromiques (ex. la phénazine-1-carboxylate et la phénazine-1-carboxamide). Les résultats du **Chapitre 5** et des modélisations quantiques préliminaires des phénazines (**Table 7-2**) indiquent que les transitions chromiques des phénazines sont contrôlées par les mêmes couplages à l'état réduit que les ommochromes, c'est-à-dire que les EWA favorisent la bathochromie alors que les EDA favorisent l'hypsochromie. De plus, les EWA sont connues pour augmenter le potentiel de réduction des phénazines oxydées en réduisant la densité électronique sur les cycles, ce qui a pour effet d'augmenter leur capacité à accepter de nouveaux électrons (Chen *et al.*, 2013). Cet effet est probablement proportionnel à la force électro-acceptrice des EWA. On peut donc faire la prédiction que les phénazines les plus bathochromiques sont aussi celles qui possèdent les potentiels de réduction les plus élevés. Cependant, il faut bien noter qu'il n'existe pas « meilleur composé redox », et ce parce que la capacité d'un système à céder/recevoir des électrons est toujours dépendante du système qui reçoit/cède ces mêmes électrons. Par exemple, la pyocyanine réagit bien avec l'oxygène, alors que la phénazine-1-carboxylate est plus réactive avec l'oxyde de fer (III). Ainsi, les hauts potentiels de réduction des phénazines bathochromiques, et donc des ommochromes, devront toujours être remis dans leur contexte physiologique. Néanmoins, ces résultats sur les phénazines indiquent bien que les substituants chimiques permettent de faire le lien entre l'activité redox et le comportement optique, ce qui est aussi envisageable pour les ommochromes. Cette comparaison entre phénazines et ommochromes suggère donc que ces derniers pourraient fonctionner comme transporteurs d'électrons dans des environnements cellulaires où le taux d'oxygène est faible, comme l'illustre le changement de couleur basé sur les ommochromes des œufs du ver marin *Urechis caupo* lorsqu'ils sont placés dans différentes conditions en oxygène (Horowitz & Baumberger, 1941; Rothschild & Tyler, 1958; Linzen, 1959).

Table 7-2. Calculs quantiques de l'électrochromisme de deux phénazines ayant des substituants différents.

Phénazine	Type de substituent	Etat redox	Excitation verticale*
1-Hydroxyphénazine	Auxochrome donneur d'électron	Oxydé	2.70 eV / 459 nm
		Réduit	3.84 eV / 323 nm hypsochromique
Acide phénazine-1-carboxylique	Auxochrome accepteur d'électron	Oxydé	3.00 eV / 414 nm
		Réduit	2.67 eV / 464 nm bathochromique

* Les calculs ont été réalisés avec la TDDFT selon la méthodologie du **Chapitre 5**.

Les propriétés antiradicalaires et proradicalaires des ommochromes

La question des propriétés anti- et proradicalaires d'un composé est généralement complexe. Tout d'abord, un radical, qui est un composé chimique possédant des électrons célibataires, peut être détruit soit par un gain d'électron (on parle d'activité antioxydante *stricto sensu*), soit par une perte d'électron [on parle d'activité antiréductrice ; (Martínez *et al.*, 2008)]. Deuxièmement, n'importe quel composé antiradicalaire peut devenir proradicalaire. La principale raison à cela est que ces propriétés dépendent de multiples paramètres autres que la nature même du composé, telles que sa concentration (les antiradicaux très concentrés ont tendance à s'autooxyder), la présence d'autres composés redox (ex. les métaux), la compartimentation, la lumière (photoactivation), etc. Enfin, la biogénèse des pigments utilise des réactions d'oxydation qui elles-mêmes peuvent produire des radicaux, comme l'illustre la voie des kynurénines menant aux ommochromes (Bolognese *et al.*, 1990; Ishii *et al.*, 1992; Zhuravlev *et al.*, 2016). Ce n'est donc qu'une fois qu'on connaît ces paramètres en milieu physiologique qu'on peut inférer le caractère anti- ou proradicalaire d'un métabolite (Carr & Frei, 1999). Dans ce qui suit, je continue la discussion de la réactivité chimique abordée dans le **Chapitre 3** (Figon & Casas, 2019) et le **Chapitre 5**, en insistant sur le fait que les ommochromes possèdent aussi cette potentielle double activité anti- et prodicalaire.

L'activité antiradicalaire des ommochromes a déjà été suggérée il y a plus de cinquante ans (Nishikimi, Yamada, & Yagi, 1978). Cette activité est maintenant bien

documentée par des études *in silico* (Romero & Martínez, 2015; Zhuravlev *et al.*, 2016), *in vitro* (Martin *et al.*, 2019; Ushakova *et al.*, 2019; Chan-Higuera *et al.*, 2019) et *in vivo* (Ostrovsky, Sakina, & Dontsov, 1987; Fedorovich & Ostrovsky, 1999; Insausti *et al.*, 2013). Les résultats du **Chapitre 5** révèlent que les états réduits les plus bathochromiques sont aussi ceux qui possèdent l'affinité électronique la plus haute, suggérant qu'ils peuvent encore être réduits. Ainsi, les phénoxazines « rouges » pourraient agir comme antiréducteurs en arrachant des électrons aux radicaux. De plus, puisque les phénoxazines peuvent revenir à l'état oxydé (phénoxazinone) en perdant des électrons, ils peuvent aussi agir comme antioxydants. En somme, les ommochromes réduits pourraient avoir une fonction versatile en prévenant les dommages à la fois oxydatifs et réducteurs des radicaux. Enfin, il faut noter qu'un antiradical n'est efficace à l'échelle de l'organisme que s'il peut être facilement mobilisé, transporté et utilisé par n'importe quel tissu. C'est d'ailleurs une des raisons pour laquelle les caroténoïdes sont considérés comme étant de meilleurs antiradicaux que les mélanines (Hill & McGraw, 2006), ces derniers étant des polymères insolubles qui ne peuvent être échangés qu'entre cellules voisines. Les ommochromes se caractérisent par leur très faible solubilité dans les solvants aqueux, mises à part l'ommatine D et la rhodommatine qui sont des formes conjuguées de la dihydroxanthommatine avec des groupements sulfate et glucose, respectivement (Linzen, 1974). Ces deux ommochromes sont d'ailleurs généralement retrouvés dans l'hémolymphe des insectes, en particulier des chenilles (Linzen, 1974). Cela soulève l'intéressante possibilité que ces formes hydrosolubles d'ommochromes pourraient servir d'antiradicaux mobiles pour protéger d'autres tissus que seulement les yeux et le tégument.

L'utilisation des phénoxazinones comme agents antitumoraux et antibactériens a très largement été étudiée depuis la découverte de l'actinomycine D en 1940 (Waksman & Woodruff, 1940), à peu près en même temps que la description des premiers ommochromes (Becker, 1939). L'actinomycine D est formé d'une aminophénazinone substituée, ce qui lui donne sa couleur rouge vif, conjuguée avec deux pentapeptides cycliques. La voie de biosynthèse des actinomycines est très semblable à celle des ommochromes puisque tous deux dérivent du tryptophane à travers la voie des kynurénines et la dimérisation d'*ortho*-aminophénols [**Chapitre 4** ; (Figon *et al.*, In press; Hollstein, 1974; Le Roes-Hill *et al.*, 2009)]. De la même façon que l'actinomycine D présente une activité biologique, les benzophénoxazinones et les pyrido[3,2-*a*]phénoxazinones non-substituées (**Figure 7-1**B), qui

ressemblent aux ommochromes, ont une activité antiproliférative *in vivo* (Bolognese *et al.*, 2002b, 2002a). Un mécanisme envisagé pour expliquer cette activité chez l'actinomycine D est qu'elle se réduit relativement facilement en acceptant un nouvel électron et donc qu'elle produit des dommages radicalaires (Bolognese *et al.*, 2002a). Puisque cette propriété est basée sur la capacité à accepter de nouveaux électrons, les composés les plus actifs devraient être ceux avec la plus forte électrophilicité. En conséquence, les pyrido[3,2-*a*]phénoxazinones substituées avec un groupe nitro sont parmi les composés les plus actifs (Bolognese *et al.*, 2002a). De tels résultats sont en accord avec les calculs du **Chapitre 5** montrant que la force électro-acceptrice de l'EWA nitro diminue fortement l'écart entre l'HOMO et la LUMO en réduisant le niveau de la LUMO, et donc en augmentant l'affinité électronique. Que les ommochromes, qui sont des phénoxazines bathochromiques, puissent provoquer des dommages oxydatifs parce qu'ils ont une affinité électronique relativement élevée (**Chapitre 5**) reste encore au stade d'hypothèse. De nouvelles études devraient aborder cette question en testant tout d'abord si la dihydroxanthommatine peut être encore plus réduite dans des conditions proches de celles physiologiques.

En conclusion, un faisceau d'indices suggère que les ommochromes et leurs états redox réversibles pourraient avoir des activités pro- et antiradicalaires, du moins en théorie. La transition bathochromique des ommochromes pourrait être une propriété clé puisqu'elle serait liée à la capacité de l'état réduit à se réduire encore plus ; cet état réduit pourrait donc agir en même temps comme composé de défense (proradical) et antioxydant/antiréducteur (antiradical). Il est maintenant nécessaire d'obtenir plus d'informations sur les conditions dans lesquelles les ommochromes sont déposés car elles pourraient grandement influencer les coûts et les bénéfices de ces pigments dans la gestion des stress oxydants et radicalaires.

Les propriétés détoxifiantes des ommochromes

Les ommochromes ont depuis longtemps été considérés comme les produits finaux du catabolisme du tryptophane, empêchant l'accumulation de cet acide aminé toxique pour les insectes, en particulier pendant la mue durant laquelle la protéolyse est abondante (Linzen, 1974). Cette propriété détoxifiante pourrait expliquer pourquoi les ommochromes s'accumulent dans les voies digestives de nombreux insectes, ainsi que dans le méconium de

plusieurs papillons (le méconium étant la première substance excrétée par l'imago à son émergence).

De la même façon que les mélanines sont connues pour lier les métaux, les ommochromes ont démontré une capacité à détoxifier les métaux, tels que le fer qui est impliqué dans la peroxydation des lipides et les réactions Fenton (Ostrovsky *et al.*, 1987). Dans cette thèse, j'ai montré que les organismes qui produisent des ommochromes accumulent aussi des métaux, comme on a pu l'observer chez les araignées crabes (**Chapitre 6**) ou encore dans les ommochromasomes purifiés de mouches domestiques (**Figure 7-2**). Il a été proposé que la fonction acide carboxylique du cycle pyridine de la pirénoxine, une pyrido[3,2-*a*]phénoxazinone très semblable à la xanthommatine, avait une fonction centrale dans la complexation du calcium (Liao *et al.*, 2011) ; ceci indiquerait alors que la xanthommatine décarboxylée serait moins efficace que la xanthommatine pour séquestrer des métaux potentiellement dangereux. Une telle différence de fonction pourrait alors expliquer pourquoi la xanthommatine décarboxylée est moins abondante que la xanthommatine *in vivo* [**Chapitre 4** ; (Figon *et al.*, In press)].

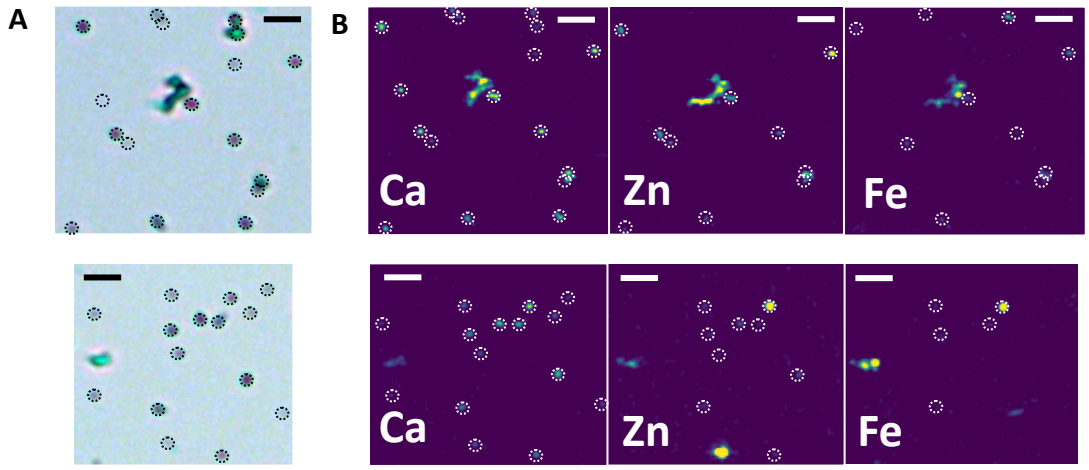

Figure 7-2. Composition chimique des ommochromasomes purifiés à partir des yeux de mouches domestiques.
Les ommochromasomes ont été purifiés d'après le protocole du **Chapitre 4** et analysés par fluorescence des rayons X Synchrotron (SXRF) comme décrit dans le **Chapitre 6**. **A**) Microscopie optique. Cercles en pointillé, ommochromasomes isolés. **B**) Signaux SXRF des métaux endogènes à partir des mêmes champs que ceux montrés en (A). Cercles en pointillé, ommochromasomes observables en (A) qui sont positifs pour le métal considéré. Barres d'échelle, 5 µm. Temps d'acquisition : 300 ms/px, résolution spatiale : 200 nm/px.

Les propriétés photoprotectrices et phototoxiques des ommochromes

Une des autres fonctions bien connues des pigments est leur capacité à protéger les cellules contre les rayonnements lumineux dangereux. La photoprotection repose sur deux mécanismes. D'un côté, les pigments peuvent filtrer les rayonnements UV avant qu'ils ne dégradent l'ADN et les autres composants cellulaires. De l'autre, les pigments ont aussi la capacité de désactiver les radicaux qui ont été produits en amont par les rayonnements UV (ce qu'on appelle la photooxydation). Ce dernier phénomène est très semblable à l'activité antiradicalaire discutée ci-dessus, je n'y reviendrai donc pas ici. Dans la suite, je m'intéresse aux interactions entre la lumière et les ommochromes qui peuvent se traduire soit par des effets bénéfiques (photoprotection), soit par des effets délétères (photoxicité) pour la cellule.

Les formes oxydées et réduites des ommochromes diffèrent non seulement par leur couleur (c'est-à-dire par leur absorption dans le domaine du visible), mais aussi par leur capacité à absorber les UV. Ainsi, le spectre d'absorbance de la dihydroxanthommatine se caractérise par un épaulement dans la région des UV-B (entre 290 et 320 nm) et un large pic centré sur 380 nm dans le domaine des UV-A (entre 320 et 400 nm). Au contraire, le spectre d'absorbance de la xanthommatine présente un pic dans le domaine des UV-C (qui sont généralement déjà largement absorbés par la couche d'ozone) et un pic intense centré autour de 440 nm dans le visible. On peut donc s'attendre à ce que l'état réduit des ommochromes soit plus efficace pour filtrer les rayonnements UV effectivement dangereux que l'état oxydé, alors que ce dernier serait plus à même de filtrer les rayonnements violets capables d'activer d'autres pigments photosensibles (discutés plus bas). La capacité réversible de changement de couleur des ommochromes pourrait alors permettre de filtrer de manière dynamique à la fois les UV et les longueurs d'onde du visible les plus énergétiques grâce à un système pigmentaire unique mais versatile. Dans tous les cas, la présence de pigments, quel que soit leur état redox, devrait fournir une protection contre les UV, ce qui est illustré par l'araignée crabe *Thomisus spectabilis* qui présente un phénotype blanc non-pigmenté qui peut dans certains cas refléter les UV alors que le phénotype jaune pigmenté absorbe toujours les UV (Gawryszewski *et al.*, 2015).

Malgré le fait que les pigments peuvent fournir une photoprotection, ils sont potentiellement phototoxiques car les états photoexcités ont la capacité de revenir à l'état fondamental en réagissant avec d'autres molécules (Björn & Huovinen, 2008). Par exemple,

les porphyrines libres de la peau sont particulièrement dangereuses pour l'organisme car leur état photoexcité mène à la formation d'espèces réactives (activité proradicalaire photodépendante), qui sont impliquées dans les maladies du métabolisme héminique, telles que la porphyrie chez les humains (del C. Batlle, 1993). La phototoxicité survient selon trois mécanismes principaux (Björn & Huovinen, 2008). Premièrement, les molécules photoexcitées peuvent réagir et se conjuguer avec d'autres composants cellulaires (ex. la photodimérisation des résidus de thymine de l'ADN). Deuxièmement, elles peuvent transférer des électrons ou des protons à d'autres molécules et ainsi produire des radicaux. Troisièmement, les molécules photoexcitées dans le cadre de la photosensibilité peuvent passer de l'état de singlet (^{1}S*) à l'état de triplet (^{3}S*), qui est un état excité rare mais à longue durée de vie. Ce triplet peut, entre autres, réagir avec l'état de triplet de l'oxygène moléculaire ($^3O_2$) et produire soit l'oxygène moléculaire à l'état de singlet ($^1O_2$), soit l'anion radicalaire superoxyde ($O_2^{\bullet-}$), qui sont toutes deux des espèces très réactives. À ma connaissance, que les ommochromes puissent agir comme des phototoxines n'est pas connu. Cependant, les études photochimiques menées par Bolognese *et al*, ainsi que les résultats de cette thèse, suggèrent que les ommochromes sont des composés labiles *in vitro*, particulièrement en présence de lumière [**Chapitre 4** ; (Figon *et al.*, In press; Bolognese *et al.*, 1988c, 1988d; Bolognese & Liberatore, 1988)]. Ainsi, la photoréduction, la photoaddition et la photo-ouverture du cycle phénoxazinone se produisent spontanément en solution, ce qui indique que les états excités des ommochromes sont réactifs. Ils pourraient donc aussi réagir avec des composants cellulaires *in vivo*. En parallèle, les kynurénines sont connues pour réticuler les protéines de la lentille de l'œil durant la formation de la cataracte via leur chaîne d'acide aminé (Korlimbinis & Truscott, 2006; Sherin *et al.*, 2010). Puisque les ommochromes possèdent la même chaîne d'acide aminé, il y a un risque qu'ils puissent aussi se conjuguer avec des protéines lors de leur photoexcitation et donc qu'ils altèrent leurs fonctions. Pour finir, l'état de triplet des ommochromes n'a jamais été étudié, il est donc difficile de savoir s'ils pourraient agir comme photosensibilisateurs. Cependant, les métabolites de la voie des kynurénines, par exemple l'acide xanthurénique, peuvent passer de ^{1}S* à ^{3}S* (Yanshole *et al.*, 2010; Zelentsova *et al.*, 2013) et donc produire du $O_2^{\bullet-}$ (Roberts *et al.*, 2000). Ces résultats suggèrent alors que le cœur pyrido[3,2-*a*]phénoxazinone, qui est structurellement très semblable à l'acide xanthurénique, pourrait se comporter de la même manière lors de sa photoexcitation. Une étude récente sur les planaires (ou vers plats) a d'ailleurs révélé que les

biogenèses des ommochromes et des porphyrines étaient intimement liées (Stubenhaus *et al.*, 2016). On ne sait pas à ce stade si les ommochromes protègent ou favorisent la phototoxicité des porphyrines dans ce modèle planairien de la porphyrie aigüe, mais des études complémentaires devraient améliorer notre compréhension du rôle de la pigmentation à base d'ommochromes dans la photoprotection et la phototoxicité.

La thermorégulation

En plus de la photoprotection, l'autre potentielle fonction des ommochromes qui dépend de la lumière mais n'intervient pas dans les effets visuels est la thermorégulation. En absorbant l'énergie des photons, les pigments réchauffent leur environnement (Stuart-Fox, Newton, & Clusella-Trullas, 2017), ce qui explique pourquoi les surfaces sombres sont généralement plus chaudes que les surfaces froides. Cette capacité à capturer la lumière a été décrite, entre autres, pour les mélanines des champignons (Pinkert & Zeuss, 2018; Krah *et al.*, 2019), les pigments de levures (Cordero *et al.*, 2018), les mélanines et les papiliochromes de papillons (Wasserthal, 1975; Berthier, 2005), ainsi que pour les mélanines et les ptérines des hyménoptères (Plotkin *et al.*, 2010). Il n'y a donc pas de raison de penser que les ommochromes ne possèdent pas les mêmes capacités de thermorégulation, bien qu'on manque de preuves expérimentales claires. Pourtant, il existe plusieurs exemples de couleurs sombres basées sur les ommochromes chez les insectes qui sont déclenchées par des faibles températures (Linzen, 1974; Daniels *et al.*, 2014), ce qui souligne l'importance des changements de couleur dus aux ommochromes lorsque les conditions climatiques sont changeantes.

La thermorégulation dépend non seulement de l'absorption des longueurs d'onde dans l'UV et le visible, mais aussi, et peut-être de manière plus marquée, de l'absorption/réflexion des infrarouges [IR ; (Stuart-Fox *et al.*, 2017; Medina *et al.*, 2018; Munro *et al.*, 2019; Krishna *et al.*, 2020; Tsai *et al.*, 2020)]. On ignore à l'heure actuelle si les changements de couleur des ommochromes altèrent aussi leur absorption dans le domaine des IR, mais il faudrait s'y intéresser pour pouvoir décrire les interactions entre les ommochromes et la lumière de la manière la plus complète possible. L'absorption dans le domaine des IR repose principalement sur les déplacements atomiques (vibrations, etc.), qui peuvent être modélisés numériquement. Ainsi, la chimie quantique pourrait par exemple donner des informations sur

de potentielles différences d'absorption par la xanthommatine et la dihydroxanthommatine dans le domaine des IR.

Conclusion sur les multiples rôles biologiques des ommochromes et de leurs changements de couleur

Pour conclure les **Sections 7.2** et **7.3**, il apparaît que les ommochromes forment un système pigmentaire versatile, dont les capacités de changement de couleur à plusieurs échelles ont pu participer à leur large utilisation chez les invertébrés. L'implication des ommochromes et des ommochromasomes dans les **changements de couleur physiologiques** des céphalopodes et les **changements de couleur morphologiques** de divers insectes et araignées est maintenant bien établie, avec les effets qu'on leur connaît sur (1) **la communication visuelle**. De plus en plus de preuves indirectes suggèrent que les états redox des ommochromes fourniraient (2) **un système tampon plastique pour lutter contre les stress oxydatifs et radicalaires**, tout du moins en théorie. Des expériences supplémentaires sont nécessaires pour tester cette fonction *in vivo*. La comparaison des ommochromes avec les pigments des bactéries (phénazines) et des champignons (actinomycines) indique que les ommochromes pourraient avoir un rôle de (3) **transporteur d'électrons** ou bien de (4) **composés de défense**. La production d'ommochromes pourrait aussi permettre de (5) **détoxifier certains métabolites et métaux**. Enfin, la mise en place d'une pigmentation basée sur les ommochromes, ainsi que l'effet de l'état redox sur leur absorption lumineuse, pourrait être à la base de leur utilisation comme (6) **photoprotecteurs** et (7) **thermorégulateurs**. Enfin, le plus important est que l'ensemble de ces fonctions soit basée sur le **lien structure–propriété** des ommochromes, que ce soit à l'échelle moléculaire (configuration électronique) ou cellulaire (ommochromasomes).

Dorénavant, il faut comprendre en quelle mesure ces fonctions ont une réalité biologique. Seulement, leurs interactions risquent de complexifier l'écologie des changements de couleur, ce qui nécessite une approche intégrative de cette plasticité phénotypique.

7.4 Des contextes écologiques de l'utilisation des ommochromes

L'écophysiologie, aussi appelée écologie physiologique, physiologie écologique ou encore physiologie environnementale, est le domaine scientifique qui rassemble la

physiologie et l'écologie de traits phénotypiques afin de comprendre leur évolution dans des cadres écologiques bien définis (Tracy *et al.*, 1982; Nentwig, 2013). Ce domaine fait donc appel par définition à de nombreuses disciplines qui intègrent les mécanismes des échelles les plus petites (les cellules et les molécules, dont leurs états électroniques) jusqu'aux plus grandes (les organismes et les espèces). Dans la suite, je m'intéresse à trois exemples de changements de couleur morphologiques qui reposent sur les ommochromes et qui ont été étudiés à différentes échelles (Figon & Casas, 2018). J'aborde ainsi (i) le polyphénisme de phase des criquets (Pener & Simpson, 2009; Tanaka *et al.*, 2016), (ii) la couleur nuptiale des libellules (Futahashi, 2016) et (iii) le changement de couleur des araignées crabes (Morse, 2007; Théry & Casas, 2009). Je discute alors la possibilité que d'autres fonctions du changement de couleur, en dehors de leurs effets visuels, pourraient expliquer au moins en partie l'écologie de ces espèces.

L'écophysiologie du polyphénisme de phase des criquets

Le polyphénisme de phase des criquets se traduit par des changements comportementaux et morphologiques lorsqu'ils s'agrègent (Pener & Simpson, 2009; Ayali, 2019). Dans la phase solitaire, les criquets sont principalement verts et ne représentent pas de danger pour l'agriculture. Par contre, dans la phase grégaire, les criquets deviennent foncés et bien plus voraces ; ils peuvent alors provoquer d'importants dommages dans les plantations (Cullen *et al.*, 2017). Les changements de couleur associés à ce polyphénisme de phases sont à l'origine de transformations dans la manière dont les criquets interagissent avec leur environnement. On pense ainsi que dans la phase solitaire, les criquets adoptent une coloration cryptique (homochromie) pour se cacher de leurs prédateurs. À l'inverse, la couleur de la phase grégaire est supposée signaler leur toxicité (aposématisme) qui est acquise par une transition vers une nourriture composée de plus de plantes toxiques (Pener & Simpson, 2009; Tanaka *et al.*, 2016). De plus, les couleurs grégaires se répandent dans les populations, comme le démontre le fait que les stimuli visuels foncés et dynamiques induisent le polyphénisme de phase chez des individus solitaires qui normalement évitent leurs congénères (Tanaka *et al.*, 2016).

D'autres paramètres environnementaux, dont l'humidité et la température, complexifient ce phénomène de polyphénisme de phase (Pener & Simpson, 2009; Tanaka *et*

al., 2016; Ayali, 2019). Leurs effets ajoutent en particulier un autre niveau de variation de couleur aux phases solitaires et grégaires, allant du jaune au beige et au marron. Ainsi, les hautes (basses) températures font diminuer (augmenter) les couleurs foncées dans la phase grégaire ; ce qui a mené certains chercheurs à vouloir modifier notre conception de l'écologie du polyphénisme de phase (Tanaka *et al.*, 2016). Puisque l'effet de la température et de l'humidité rappelle la loi de Gloger, qui postule que les animaux sont plus foncés dans les régions froides (Delhey, 2019), il est possible que le potentiel effet thermorégulateur des ommochromes joue un rôle dans le polyphénisme de phase. De plus, l'augmentation de l'activité métabolique (à travers une transition en termes de nourriture, de locomotion aérienne, etc.) associée au polyphénisme de phase (Pener & Simpson, 2009) pourrait déclencher la production des ommochromes comme détoxifiants ou tampons redox. En somme, avant de pouvoir tirer des conclusions sur la valeur adaptative du polyphénisme de phase des criquets en termes d'effets visuels, il est nécessaire de réaliser des études sur les potentiels rôles physiologiques que pourraient jouer les ommochromes lors des changements de couleur associés.

L'écophysiologie de la couleur nuptiale des libellules et des demoiselles

La couleur nuptiale des libellules (ex. des genres *Sympetrum* et *Crocothemis*) et des demoiselles (ex. des genres *Xanthagrion* et *Pyrrhomosa*) se traduit par un fort dimorphisme sexuel. Ce changement de couleur morphologique est supposé servir de signal pour que les femelles sachent quels mâles sont matures et prêts à copuler (Futahashi *et al.*, 2012). Il pourrait aussi servir de signal visuel pour que les mâles puissent reconnaître le sexe de leurs congénères, ce qui amène parfois à des couples mâle-mâle dans les cas où l'un des deux possède une couleur semblable à celle des femelles (Futahashi, 2017). Récemment, la transition bathochromique liée à la maturité sexuelle des demoiselles rouge-et-bleu (*X. erythroneurum*) a été associée à une augmentation du taux de succès reproducteur en conditions contrôlées (dans des cages) et dans la nature (Khan & Herberstein, 2019). Cependant, cette étude n'a pas pu séparer les effets de possibles facteurs de confusions, telle que la production de phéromones au moment de la maturité sexuelle. Il n'y a donc pour l'instant aucune preuve que le principal facteur contrôlant les comportements reproducteurs soit la couleur nuptiale.

En l'absence de preuves expérimentales claires allant dans le sens d'une fonction de signalisation de la couleur nuptiale, il faut toujours considérer les autres fonctions potentielles associées aux changements de couleur des ommochromes. Il a ainsi été proposé que la couleur rouge des mâles libellules matures fournissait une photoprotection pendant les périodes de patrouille de leurs territoires ensoleillés (Futahashi, 2016), une hypothèse qui est en accord avec la différence d'absorption entre la xanthommatine (jaune) et la dihydroxanthommatine (rouge). La maturité sexuelle pourrait aussi imposer une activité métabolique plus élevée (par exemple induite par des comportements de défense du territoire et d'harcèlement des femelles), ce qui augmenterait potentiellement le stress oxydant. La dihydroxanthommatine pourrait alors servir de tampon pour atténuer la production d'espèces réactives dépendantes de l'oxygène pendant ces périodes très actives.

Enfin, il faut aussi considérer que les fonctions biochimiques et de signalisation des ommochromes sont intimement liées. Par exemple, l'accumulation de caroténoïdes, qui sont bien connus pour leurs pouvoirs antioxydants chez les oiseaux, permet aux femelles de repérer les mâles avec les meilleures qualités. Ainsi, de manière similaire, les mâles libellules pourraient afficher de manière honnête leur bonne santé en réduisant leur stock de xanthommatine en dihydroxanthommatine ; les mâles les plus rouges seraient de fait ceux avec les meilleures capacités antiradicalaires. En somme, l'importance adaptative et les fonctions biologiques de la couleur nuptiale des libellules et des demoiselles, si elles existent, nécessitent plus d'études attentives aux effets pléiotropes des ommochromes.

L'écophysiologie des changements de couleurs chez les araignées crabes

Les araignées crabes sont des prédateurs écologiquement importants de la strate herbacée (Morse, 2007). Elles font plus particulièrement partie d'interactions tritrophiques avec les insectes et les plantes. De plus en plus d'indices pointent l'influence des araignées crabes sur la pollinisation, aussi bien du côté des fleurs que des pollinisateurs (Heiling, Herberstein, & Chittka, 2003; Dukas & Morse, 2003, 2005; Romero & Vasconcellos-Neto, 2004; Robertson & Maguire, 2005; Llandres *et al.*, 2011; Huey & Nieh, 2017; Knauer, Bakhtiari, & Schiestl, 2018). Bien que les fonctions biologiques du changement de couleur des araignées crabes fassent toujours l'objet de recherches actives, certains résultats indiquent qu'elles jouent un rôle dans la structuration des interactions entre araignées, insectes et

plantes, comme illustré par trois espèces d'araignées crabes. L'araignée crabe européenne *Thomisus onustus* est ainsi capable de réduire son contraste chromatique dans le système visuel de ses proies, ce qui signifie que ses changements de couleur du jaune vers le blanc, et vice-versa, lui permet de se fondre dans la couleur de la fleur sur laquelle elle chasse ; une stratégie qui s'appelle le mimétisme agressif (Théry & Casas, 2002; Théry *et al.,* 2004). Cette stratégie pourrait avoir fait évoluer les interactions proies-prédateurs vers des systèmes toujours plus efficaces de camouflage, chez le prédateur, et de détection, chez la proie. En plus des classiques couleurs blanches et jaunes, l'araignée crabe australienne *Thomisus spectabilis* présente une troisième « couleur » qui reflète les UV et trompe les pollinisateurs (Herberstein & Gawryszewski, 2013; Gawryszewski *et al.,* 2015). Cet effet d'attraction des pollinisateurs par les araignées crabes pourrait potentiellement influencer la pollinisation et donc l'évolution de la couleur des fleurs. Cependant, l'effet de tromperie par les araignées crabes dépend aussi d'autres paramètres, tels que l'espèce d'abeille en question (Llandres *et al.*, 2011), ainsi que la taille et le comportement de l'araignée (Llandres & Rodríguez-Gironés, 2011). Chez l'autre principale espèce d'araignée crabe européenne, *Misumena vatia*, il a été montré de manière répétée que la couleur du corps n'a pas d'incidence positive sur les taux de capture de proies (Brechbühl *et al.*, 2010; Brechbühl, Casas, & Bacher, 2011). En accord avec ces résultats, le camouflage parfait (c'est-à-dire l'incapacité totale pour une proie de détecter l'araignée) interviendrait aléatoirement dans la nature et ne serait donc pas le résultat d'une adaptation locale à la couleur des fleurs (Defrize *et al.*, 2010). Tous ces résultats sont à mettre en lien avec le fait que le système visuel des insectes peut identifier *M. vatia* à courte distance même dans des cas où nous, humains, avec notre système visuel très différent aurions affirmé que l'araignée était parfaitement camouflée. En somme, le mimétisme agressif ne permet pas d'expliquer l'ensemble des changements de couleur chez toutes les espèces d'araignées crabes, ce qui suggère que d'autres fonctions biologiques sont possibles.

La capacité des araignées à changer de couleur a été attribuée à de multiples reprises à la voie des ommochromes (Seligy, 1972; Insausti & Casas, 2008; Riou & Christidès, 2010; Llandres *et al.*, 2013) ; la nature exacte des pigments jaunes n'est pourtant toujours pas connue (obs. pers.). Néanmoins, la présence indéniable de 3-hydroxykynurénine chez les araignées jaunes par rapport aux blanches indique que le jaunissement est lié au métabolisme du tryptophane à travers la voie des kynurénines (Llandres *et al.*, 2013). De plus, quel que soit

le pigment, les organites pigmentés accumulent des métaux dans la forme jaune, dont certains sont potentiellement dangereux comme le cobalt (**Chapitre 6**). Ces résultats suggèrent collectivement que la pigmentation des araignées crabes pourrait permettre de détoxifier soit des composés endogènes (le tryptophane), soit exogènes (le cobalt et autres métaux lourds). Il a aussi été souligné que les coûts physiologiques de la réversibilité des changements de couleur morphologiques n'ont jamais été évalués malgré leur importance dans le maintien d'une telle plasticité (**Chapitre 2**). Le cycle de vie unique des organites pigmentés des araignées crabes pourrait offrir un moyen de réduire les coûts anaboliques de la pigmentation en recyclant une partie des organites pigmentés via des processus autocatalytiques, lysosomaux et de recyclage membranaires (tubules ; **Chapitre 6**). En parallèle, le fait que les araignées crabes produisent un nombre significatif d'organites pigmentés immatures, qui pourraient contenir les métabolites précoces de la voie des kynurénines (Insausti & Casas, 2008), suggère que ces organites jouent un rôle autre que la pigmentation. En effet, la couleur blanche est seulement due à une couche de cristaux de guanines réflecteurs située sous le tégument, et ne nécessite pas les organites pigmentés immatures (Gawryszewski *et al.*, 2015). Or, les kynurénines absorbent les UV-A (autour de 360-370 nm) et se retrouveraient dans les organites pigmentés immatures (kynurénine) et matures (3-hydroxykynurénine et ses dérivés). Les organites pigmentés, quelle que soit la couleur finale, pourraient donc jouer un rôle en-dehors de la couleur en assurant une photoprotection contre les UV. De plus, la compartimentation dans des organites pourrait protéger le reste de la cellule des potentiels effets proradicalaire et phototoxiques des kynurénines.

En somme, les araignées crabes offrent un exemple intrigant où les multiples fonctions des changements de couleurs associés aux ommochromes et à leurs précurseurs pourraient expliquer les stratégies variées adoptées par trois espèces distinctes. Ainsi, pour chaque espèce la fonction prédominante serait différente, bien que toutes aient probablement pu contribuer à l'écologie du changement de couleur à un moment ou à un autre.

7.5 Les ommochromes dans le contexte d'une origine commune des organites pigmentés

Dans un article fondateur, Joseph T. Bagnara et ses collègues ont suggéré que toutes les cellules pigmentées des vertébrés dérivaient d'une cellule souche commune (Bagnara *et al.*, 1979). Les multiples observations de cellules et d'organites pigmentés mosaïques (Bagnara, 1972) menèrent les auteurs à prédire qu'il y avait un unique système subcellulaire qui produisait et stockait les pigments chez tous les vertébrés (Bagnara *et al.*, 1979). Ils postulèrent donc que tous les organites pigmentés devaient dériver d'un même organite primordial (Bagnara *et al.*, 1979). Dans ce qui suit, j'évoque la façon dont la recherche sur les cellules pigmentées a largement validé et étendu ces hypothèses depuis 40 ans. Je discute aussi des résultats de cette thèse en les mettant en lien avec le cadre évolutif de Bagnara *et al.*, contribuant ainsi à une meilleure compréhension des systèmes pigmentés chez les animaux.

Bagnara *et al.* suggérèrent que le réticulum endoplasmique (ER), en association avec des vésicules dérivées du Golgi, représentait l'organite pigmenté primordial (Bagnara *et al.*, 1979). On sait maintenant que les organites pigmentés des vertébrés, mais aussi des insectes, font partie de la famille des organites apparentés aux endolysosomes [ELRO, **Chapitre 3** ; (Figon & Casas, 2019; Delevoye *et al.*, 2019)]. Les ELROs, dont les fonctions ne sont pas restreintes à la pigmentation, obtiennent leur membrane principalement des compartiments endosomaux et post-Golgi (Bowman *et al.*, 2019). Ainsi, l'endosome, qui reçoit aussi de la membrane et du contenu cellulaire de la part du Golgi, représenterait très vraisemblablement l'organite pigmenté primordial. En accord avec cela, il y a des preuves de l'apparentement entre les organites pigmentés des araignées crabes et ELROs, suggérant que leur formation est associée à des complexes tubulo-sacculaires issus soit des endosomes, soit du Golgi (**Chapitre 6**). Ces résultats étendent donc le modèle du lignage endolysosomal aux organites pigmentés des araignées, ce qui conforte d'autant plus l'idée que les ELROs ont une fonction conservée dans la pigmentation des animaux. Enfin, à partir des résultats du **Chapitre 6** et de l'étude des autres ELROs pigmentés, je fais l'hypothèse que le système endolysosomal possède des caractéristiques clés qui ont favorisé son évolution en tant que support de la pigmentation (**Table 7-3**).

Table 7-3. Le lien structure–propriété des organites apparentés aux endolysosomes (ELROs) et ses fonctions dans la pigmentation

Propriété	**Ultrastructure et composants des ELROs**	**Lien possible avec la pigmentation**
Centre du trafic intracellulaire	Machineries de fusion avec les vésicules et les tubules [ex. t-SNARE STX3; (Yatsu *et al.*, 2013)] Transporteurs de métabolites [ex. white; (Mackenzie *et al.*, 2000)]	Rassembler au même endroit les précurseurs de pigments, les enzymes, chromogéniques, etc.
Identité d'organite	Marqueurs spécifiques de population et de maturation [ex. Rab7; (Kawakami *et al.*, 2008)]	Contrôle des stades de pigmentation (Raposo & Marks, 2007)
Compartimentation	Membrane limitante (ex. ELROs pigmentés des araignées crabes, **Chapitre 6**) Vésicules intraluminales [ILVs ; **Chapitre 6** et (Hurbain *et al.*, 2008)]	Compartimentation du métabolisme Protection de la cellule contre de potentielles réactions dangereuses Point de nucléation pour les éléments de support à la pigmentation (ex. fibres amyloïdes sur les ILVs)
Mobilité	Protéines moteur [ex. kinésine-2 et dynéine ; (De Rossi *et al.*, 2015)] Cytosquelette [microtubule ; (De Rossi *et al.*, 2015) et **Chapitre 6**]	Changement de couleur physiologique Sécrétion
Homéostasie des métaux	Accumulation de métaux [ex. Ca^{2+} et Zn^{2+} ; (White & Michaud, 1980; Gorniak *et al.*, 2014) et **Chapitre 6**] Transporteurs de métaux [ex. TPC2 ; (Bellono *et al.*, 2014; Ambrosio *et al.*, 2016)]	Biosynthèse des pigments (ex. enzymes contenant des métaux) Pigments comme chélateurs de métaux
Recyclage	Tubulation membranaire [(Ripoll *et al.*, 2018) et **Chapitre 6**]	Changement de couleur morphologique
Dégradation	Environnement lytique [ex. pH acide et hydrolases lysosomales ; (Borovanský & Elleder, 2003)] Fusions avec des lysosomes (**Chapitre 6**)	Blanchiment dans le changement de couleur
Sécrétion	Arrimage à la membrane et autres composants de l'exocytose [ex. Rab27a; (Booth, Seabra, & Hume, 2012)]	Transfert à d'autres types cellulaires (ex. kératinocytes)

Il est maintenant bien établi que les cellules pigmentées des chordés, c'est-à-dire les vertébrés et les tuniciers (ex. la cione), partagent une origine dans le neurectoderme, quel que soit le pigment qu'elles produisent (York & McCauley, 2020). À ma connaissance, le lignage des cellules pigmentées chez les invertébrés protostomiens, dont les insectes, les araignées et les céphalopodes, n'est pas connue. Des études sur le destin cellulaire dans les ommatidies de drosophile ont montré que le positionnement, mais pas le lignage, déterminait la différenciation en cellules pigmentées (Lawrence & Green, 1979). Ces résultats laissent à penser que la pigmentation est d'une certaine manière plus plastique chez les insectes que chez les chordés. Une telle plasticité pourrait avoir permis la cooptation des voies pigmentaires de l'œil par d'autres parties du corps (Vargas-Lowman *et al.*, 2019). Enfin, on ne sait pas encore si les cellules pigmentées des planaires (vers plats apparentés aux arthropodes) dérivent (1) du neurectoderme ou (2) de l'endoderme [issues donc du tube digestif ; (Lindsay-Mosher & Pearson, 2019)]. Dans le premier scénario évolutif, tous les animaux bilatériens posséderaient des cellules pigmentées dérivant de l'ectoderme. Or, les cellules pigmentées des vertébrés dérivent principalement des cellules des crêtes neurales, une population très plastique de cellules migratrices (York & McCauley, 2020). Les invertébrés, dont les tuniciers, les céphalochordés et les protostomiens, possèdent aussi des neuroblastes migrateurs, qu'on appelle neuroblastes du bord latéral, qui auraient certaines homologies avec les cellules des crêtes neurales (Zhao, Chen, & Liu, 2019). Cela soulève l'hypothèse intéressante que toutes les cellules pigmentées des animaux partagent une origine commune vieille de plus de 500 millions d'années ; ce qui expliquerait aussi pourquoi les pigments se retrouvent dans le système nerveux des mammifères [sous forme de neuromélanine ; (Youdim, Ben-Shachar, & Riederer, 1994)] et des insectes [sous forme d'ommochromes ; (Sawada *et al.*, 2000)]. À l'inverse, dans le second scénario évolutif, les cellules pigmentées auraient évolué au moins deux fois indépendamment chez les animaux bilatériens, c'est-à-dire une fois depuis l'endoderme chez les protostomiens et une fois depuis l'ectoderme chez les deutérostomiens. Ce scénario expliquerait lui pourquoi les ommochromes et les granules jaunes de flavine se retrouvent dans la voie digestive des insectes et des araignées (Linzen, 1974; Needham, 1974). En tout cas, quel que soit le scénario évolutif, le système endolysosomal a certainement joué un rôle central en fournissant une plateforme plastique et ubiquitaire, permettant le métabolisme de divers pigments dans des contextes biologiques très variés.

7.6 Conclusion : « Le caractère multi-texturé » de la couleur

Dans l'introduction de cette thèse (**Chapitre 1**), j'ai donné un rapide aperçu de l'historique de la façon dont les biologistes ont interprété la valeur adaptative des couleurs depuis le milieu du 19e siècle. À partir de la fin du 20e siècle, il apparaît très clairement que l'effet visuel des pigments ne permettait pas d'expliquer la palette de couleurs observables chez les animaux ; les propriétés biochimiques des pigments devaient aussi être prises en compte. Pour reprendre les propos de l'historienne des sciences Sharon Kingsland, « le caractère multi-texturé du problème de la couleur au début du [20e] siècle[14] » s'applique non seulement à l'histoire de la science de la couleur, mais aussi à la biologie de la couleur.

Qu'en est-il de la situation actuelle ? La biologie de la couleur chez les animaux est sans aucun doute un domaine de recherche majeur et très actif. De récent essais et revues ont souligné la nécessité de réaliser des études intégratives et multidisciplinaires pour mieux comprendre la complexité de la couleur des animaux (Caro *et al.*, 2017b; Cuthill *et al.*, 2017). Cependant, on peut regretter qu'aucun (bio)chimiste, photobiologiste ou biologiste cellulaire n'ait été inclus dans ces programmes. Une absence particulièrement flagrante lorsqu'on observe que les seules fonctions mentionnées de la couleur, en-dehors de l'aspect visuel, sont la thermorégulation et le filtrage des UV (Caro *et al.*, 2017b; Cuthill *et al.*, 2017). Bien qu'on ne puisse pas nier l'impact majeur de la fonction visuelle des couleurs, cette thèse et l'ensemble des références qu'elle contient plaident pour une approche réellement intégrative de la biologie de la couleur.

[14] Traduit de (Kingsland, 1978, p. 223) : « the multitextured character of the coloration problem at the turn of the century »

Bibliographie

ADAMO, C. & BARONE, V. (1999) Toward reliable density functional methods without adjustable parameters: The PBE0 model. *The Journal of Chemical Physics* **110**, 6158–6170.

ADAMO, C. & BARONE, V. (2000) A TDDFT study of the electronic spectrum of s-tetrazine in the gas-phase and in aqueous solution. *Chemical Physics Letters* **330**, 152–160.

ALLOUCHE, A.-R. (2011) Gabedit-A graphical user interface for computational chemistry softwares. *Journal of Computational Chemistry* **32**, 174–182.

AMARAL, M., LEVY, C., HEYES, D.J., LAFITE, P., OUTEIRO, T.F., GIORGINI, F., LEYS, D. & SCRUTTON, N.S. (2013) Structural basis of kynurenine 3-monooxygenase inhibition. *Nature* **496**, 382–385.

AMBROSIO, A.L., BOYLE, J.A., ARADI, A.E., CHRISTIAN, K.A. & DI PIETRO, S.M. (2016) TPC2 controls pigmentation by regulating melanosome pH and size. *Proceedings of the National Academy of Sciences* **113**, 5622–5627.

ANDERSON, A.G. & DODSON, G.N. (2015) Colour change ability and its effect on prey capture success in female *Misumenoides formosipes* crab spiders: Colour change and foraging in a crab spider. *Ecological Entomology* **40**, 106–113.

ANSTEY, M.L., ROGERS, S.M., OTT, S.R., BURROWS, M. & SIMPSON, S.J. (2009) Serotonin Mediates Behavioral Gregarization Underlying Swarm Formation in Desert Locusts. *Science* **323**, 627–630.

ARCHETTI, M., DÖRING, T.F., HAGEN, S.B., HUGHES, N.M., LEATHER, S.R., LEE, D.W., LEV-YADUN, S., MANETAS, Y., OUGHAM, H.J. & SCHABERG, P.G. (2009) Unravelling the evolution of autumn colours: an interdisciplinary approach. *Trends in ecology & evolution* **24**, 166–173.

AUERSWALD, L., FREIER, U., LOPATA, A. & MEYER, B. (2008) Physiological and morphological colour change in Antarctic krill, Euphausia superba: a field study in the Lazarev Sea. *Journal of Experimental Biology* **211**, 3850–3858.

AVILA, F., FRIGUET, B. & SILVA, E. (2015) Photosensitizing Activity of Endogenous Eye Lens Chromophores: An Attempt to Unravel Their Contributions to Photo-Aging and Cataract Disease. *Photochemistry and Photobiology* **91**, 767–779.

AYALI, A. (2019) The puzzle of locust density-dependent phase polyphenism. *Current Opinion in Insect Science* **35**, 41–47.

BAGNARA, J. (1972) Interrelationships of melanophores, iridophores and xanthophores. In *Pigmentation: Its Genesis and Biological Control* (ed V. RILEY), pp. 171–180. Appleton-Century-Crofts, New-York.

BAGNARA, J., MATSUMOTO, J., FERRIS, W., FROST, S., TURNER, W., TCHEN, T. & TAYLOR, J. (1979) Common origin of pigment cells. *Science* **203**, 410–415.

BARBIER-BRYGOO, H., JOYARD, J., PUGIN, A. & RANJEVA, R. (1997) Intracellular compartmentation and plant cell signalling. *Trends in plant science* **2**, 214–222.

BARONE, V., BICZYSKO, M., BORKOWSKA-PANEK, M. & BLOINO, J. (2014) A Multifrequency Virtual Spectrometer for Complex Bio-Organic Systems: Vibronic and Environmental Effects on the UV/Vis Spectrum of Chlorophyll *a*. *ChemPhysChem* **15**, 3355–3364.

BATES, H.W. (1862) XXXII. Contributions to an Insect Fauna of the Amazon Valley. Lepidoptera: Heliconidae. *Transactions of the Linnean Society of London* **23**, 495–566.

BEADLE, G.W. & EPHRUSSI, B. (1936) The differentiation of eye pigments in Drosophila as studied by transplantation. *Genetics* **21**, 225.

BECKE, A. (1993) Density-functional thermochemistry. III. The role of exact exchange. *The Journal of Chemical Physics* **98**, 5648.

BECKE, A.D. & JOHNSON, E.R. (2007) Exchange-hole dipole moment and the dispersion interaction revisited. *The Journal of Chemical Physics* **127**, 154108.

BECKER, E. (1939) Uber die Natur des Augenpigments von Ephestia kuhniella und seinen Vergleich mit den Augenpigmenten anderer Insekten. *Biologisches Zentralblatt* **59**, 597–627.

BECKER, E. (1942) Über Eigenschaften, Verbreitung und die Genetisch-Entwicklungsphysiologische Bedeutung der Pigmente der Ommatin- und Ommingruppe (Ommochrome) bei den Arthropoden. *Zeitschrift für Induktive Abstammungs- und Vererbungslehre* **80**, 157–204.

BEDDARD, F.E. (1892) *Animal coloration; an account of the principal facts and theories relating to the colours and markings of animals.* S. Sonnenschein & co., London.

BELLAMY, D. (1958) The structure and metabolic properties of tissue preparations from Schistocerca gregaria (desert locust). *Biochemical Journal* **70**, 580–589.

BELLONO, N.W., ESCOBAR, I.E., LEFKOVITH, A.J., MARKS, M.S. & OANCEA, E. (2014) An intracellular anion channel critical for pigmentation. *eLife* **3**.

BENHRA, N., LALLET, S., COTTON, M., LE BRAS, S., DUSSERT, A. & LE BORGNE, R. (2011) AP-1 Controls the Trafficking of Notch and Sanpodo toward E-Cadherin Junctions in Sensory Organ Precursors. *Current Biology* **21**, 87–95.

BERTHIER, S. (2005) Thermoregulation and spectral selectivity of the tropical butterfly Prepona meander: a remarkable example of temperature auto-regulation. *Applied Physics A* **80**, 1397–1400.

BISSIG, C., HURBAIN, I., RAPOSO, G. & VAN NIEL, G. (2017) PIKfyve activity regulates reformation of terminal storage lysosomes from endolysosomes. *Traffic* **18**, 747–757.

BJÖRN, L.O. (ed) (2015) *Photobiology*. Springer New York, New York, NY.

BJÖRN, L.O. & HUOVINEN, P. (2008) Phototoxicity. In *Photobiology* pp. 479–502. Springer.

BLABY-HAAS, C.E. & MERCHANT, S.S. (2014) Lysosome-related Organelles as Mediators of Metal Homeostasis. *Journal of Biological Chemistry* **289**, 28129–28136.

BLANCHARD, P.D., ANGUS, R.A., MORRISON, R.L., FROST-MASON, S.K. & SHEETZ, J.H. (1991) Pigments and Ultrastructures of Pigment Cells in Xanthic Sailfin Mollies (Poecilia latipinna). *Pigment Cell Research* **4**, 240–246.

BOESE, A.D. & HANDY, N.C. (2002) New exchange-correlation density functionals: The role of the kinetic-energy density. *The Journal of Chemical Physics* **116**, 9559–9569.

BOESE, A.D. & MARTIN, J.M.L. (2004) Development of density functionals for thermochemical kinetics. *The Journal of Chemical Physics* **121**, 3405–3416.

BOLOGNESE, A., BONOMO, R.P., CHILLEMI, R. & SCIUTO, S. (1990) Oxidation of 3-hydroxykynurenine. An EPR investigation. *Journal of Heterocyclic Chemistry* **27**, 2207–2208.

BOLOGNESE, A., CORREALE, G., MANFRA, M., LAVECCHIA, A., MAZZONI, O., NOVELLINO, E., BARONE, V., LA COLLA, P. & LODDO, R. (2002a) Antitumor Agents. 2. Synthesis, Structure−Activity Relationships, and Biological Evaluation of Substituted 5 *H* -Pyridophenoxazin-5-ones with Potent Antiproliferative Activity. *Journal of Medicinal Chemistry* **45**, 5217–5223.

BOLOGNESE, A., CORREALE, G., MANFRA, M., LAVECCHIA, A., MAZZONI, O., NOVELLINO, E., BARONE, V., PANI, A., TRAMONTANO, E., LA COLLA, P., MURGIONI, C., SERRA, I., SETZU, G. & LODDO, R. (2002b) Antitumor Agents. 1. Synthesis, Biological Evaluation, and Molecular Modeling of 5 *H* -Pyrido[3,2- *a*]phenoxazin-5-one, a Compound with Potent Antiproliferative Activity. *Journal of Medicinal Chemistry* **45**, 5205–5216.

BOLOGNESE, A. & LIBERATORE, R. (1988) Photochemistry of ommochrome pigments. *Journal of Heterocyclic Chemistry* **25**, 1243–1246.

BOLOGNESE, A., LIBERATORE, R., PISCITELLI, C. & SCHERILLO, G. (1988a) A Light-Sensitive Yellow Ommochrome Pigment From the House Fly. *Pigment Cell Research* **1**, 375–378.

BOLOGNESE, A., LIBERATORE, R., RIENTE, G. & SCHERILLO, G. (1988b) Oxidation of 3-hydroxykynurenine. A reexamination. *Journal of Heterocyclic Chemistry* **25**, 1247–1250.

BOLOGNESE, A., LIBERATORE, R. & SCHERILLO, G. (1988c) Photochemistry of ommochromes and related compounds. *Journal of Heterocyclic Chemistry* **25**, 979–983.

BOLOGNESE, A., LIBERATORE, R. & SCHERILLO, G. (1988d) Photochemistry of ommochromes and related compounds. Part II. *Journal of Heterocyclic Chemistry* **25**, 1251–1254.

BOLOGNESE, A. & SCHERILLO, G. (1974) Occurrence and characterization of a labile xanthommatin precursor in some invertebrates. *Experientia* **30**, 225–226.

BOOTH, A.E.G., SEABRA, M.C. & HUME, A.N. (2012) Rab27a and melanosomes: a model to investigate the membrane targeting of Rabs. *Biochemical Society Transactions* **40**, 1383–1388.

BORN, M. & OPPENHEIMER, R. (1927) Zur Quantentheorie der Molekeln. *Annalen der Physik* **389**, 457–484.

BOROVANSKÝ, J. & ELLEDER, M. (2003) Melanosome degradation: fact or fiction. *Pigment Cell Research* **16**, 280–286.

BOROVANSKÝ, J. & RILEY, P.A. (2011) *Melanins and Melanosomes: Biosynthesis, Structure, Physiological and Pathological Functions*. John Wiley & Sons, Weinheim.

BOUTHIER, A. & LHONORÉ, J. (1984) Developmental changes in the amount of pigments, inorganic material and uric acid in Locusta migratoria cinerascens Fabr. (Orthoptera, Acrididae) epidermis, during the last larval instar and the imaginal life. *Journal of Comparative Physiology B* **154**, 549–560.

BOWMAN, S.L., BI-KARCHIN, J., LE, L. & MARKS, M.S. (2019) The road to lysosome-related organelles: Insights from Hermansky-Pudlak syndrome and other rare diseases. *Traffic* **20**, 404–435.

BOWMAN, S.L. & MARKS, M.S. (2018) Shining a Light on Black Holes in Keratinocytes. *Journal of Investigative Dermatology* **138**, 486–489.

BOYD, R.K., BASIC, C. & BETHEM, R.A. (2008) *Trace Quantitative Analysis by Mass Spectrometry*. John Wiley & Sons, Ltd, Chichester, UK.

BOZZOLA, J.J. & RUSSELL, L.D. (1999) *Electron microscopy: principles and techniques for biologists*2nd ed. Jones and Bartlett, Sudbury, Mass.

BRECHBÜHL, R., CASAS, J. & BACHER, S. (2010) Ineffective crypsis in a crab spider: a prey community perspective. *Proceedings of the Royal Society B: Biological Sciences* **277**, 739–746.

BRECHBÜHL, R., CASAS, J. & BACHER, S. (2011) Diet choice of a predator in the wild: overabundance of prey and missed opportunities along the prey capture sequence. *Ecosphere* **2**, art133.

BRITTON, G. (1983) *The biochemistry of natural pigments*. Cambridge University Press, New York.

BRITTON, G., LIAAEN-JENSEN, S. & PFANDER, H. (eds) (1995) *Carotenoids*. Birkhäuser Verlag, Basel ; Boston.

BUCKLEY, R.G., CHARALAMBOUS, J. & HENRICK, K. (1982) 2-Amino-7-methoxy-3 *H* -phenoxazin-3-one. *Acta Crystallographica Section B Structural Crystallography and Crystal Chemistry* **38**, 289–291.

BURGESS, J., JAUREGUI, M., TAN, J., ROLLINS, J., LALLET, S., LEVENTIS, P.A., BOULIANNE, G.L., CHANG, H.C., LE BORGNE, R., KRAMER, H. & BRILL, J.A. (2011) AP-1 and clathrin are essential for secretory granule biogenesis in Drosophila. *Molecular Biology of the Cell* **22**, 2094–2105.

BUROVINA, I.V., GRIBAKIN, F.G., PETROSYAN, A.M., PIVOVAROVA, N.B., POGORELOV, A.G. & POLYANOVSKY, A.D. (1978) Ultrastructural localization of potassium and calcium in an insect ommatidium as demonstrated by X-ray microanalysis. *Journal of Comparative Physiology A* **127**, 245–253.

BURTT, E.H. (1981) The Adaptiveness of Animal Colors. *BioScience* **31**, 723–729.

BUTENANDT, A. (1957) Über Ommochrome, eine Klasse natürlicher Phenoxazon-Farbstoffe. *Angewandte Chemie* **69**, 16–23.

BUTENANDT, A., BIEKERT, E., KOGA, N. & TRAUB, P. (1960) Über Ommochrome, XXI. Konstitution und Synthese des Ommatins D. *Hoppe-Seyler´s Zeitschrift für physiologische Chemie* **321**, 258–275.

BUTENANDT, A., BIEKERT, E., KÜBLER, H., LINZEN, B. & TRAUB, P. (1963) Über Ommochrome, XXII. Konstitution und Synthese des Rhodommatins. *Hoppe-Seyler´s Zeitschrift für physiologische Chemie* **334**, 71–83.

BUTENANDT, A. & SCHÄFER, W. (1962) Ommochromes. In *Recent Progress in the Chemistry of Natural and Synthetic Colouring Matters and Related Fields* pp. 13–33. Academic Press, New York, NY.

BUTENANDT, A., SCHIEDT, U. & BIEKERT, E. (1954) Über Ommochrome, III. Mitteilung: Synthese des Xanthommatins. *Justus Liebigs Annalen der Chemie* **588**, 106–116.

BUTENANDT, A., WEIDEL, W. & BECKER, E. (1940) Kynurenin als Augenpigmentbildung auslösendes Agens bei Insekten. *Die Naturwissenschaften* **28**, 63–64.

DU BUY, H.G., SHOWACRE, J.L. & HESSELBACH, M.L. (1963) Enzymic and other similarities of melanoma granules and mitochondria. *Annals of the New York Academy of Sciences* **100**, 569–583.

BYBEE, S.M., YUAN, F., RAMSTETTER, M.D., LLORENTE-BOUSQUETS, J., REED, R.D., OSORIO, D. & BRISCOE, A.D. (2012) UV Photoreceptors and UV-Yellow Wing Pigments in *Heliconius* Butterflies Allow a Color Signal to Serve both Mimicry and Intraspecific Communication. *The American Naturalist* **179**, 38–51.

DEL C. BATLLE, A.M. (1993) Porphyrins, porphyrias, cancer and photodynamic therapy — a model for carcinogenesis. *Journal of Photochemistry and Photobiology B: Biology* **20**, 5–22.

CADENA, V., RANKIN, K., SMITH, K.R., ENDLER, J.A. & STUART-FOX, D. (2017) Temperature-induced colour change varies seasonally in bearded dragon lizards. *Biological Journal of the Linnean Society*.

CAI, T., HAN, K., YANG, P., ZHU, Z., JIANG, M., HUANG, Y. & XIE, C. (2019) Reconstruction of Dynamic and Reversible Color Change using Reflectin Protein. *Scientific Reports* **9**.

CANDI, E., SCHMIDT, R. & MELINO, G. (2005) The cornified envelope: a model of cell death in the skin. *Nature Reviews Molecular Cell Biology* **6**, 328–340.

CAPECE, L., LEWIS-BALLESTER, A., BATABYAL, D., DI RUSSO, N., YEH, S.-R., ESTRIN, D.A. & MARTI, M.A. (2010) The first step of the dioxygenation reaction carried out by tryptophan dioxygenase and indoleamine 2,3-dioxygenase as revealed by quantum mechanical/molecular mechanical studies. *JBIC Journal of Biological Inorganic Chemistry* **15**, 811–823.

CARO, T. (2017) Wallace on Coloration: Contemporary Perspective and Unresolved Insights. *Trends in Ecology & Evolution* **32**, 23–30.

CARO, T., STODDARD, M.C. & STUART-FOX, D. (2017a) Animal coloration research: why it matters. *Philosophical Transactions of the Royal Society B: Biological Sciences* **372**, 20160333.

CARO, T., STODDARD, M.C. & STUART-FOX, D. (2017b) Animal coloration: production, perception, function and application. *Philosophical Transactions of the Royal Society B: Biological Sciences* **372**, 20170047.

CARR, A. & FREI, B. (1999) Does vitamin C act as a pro-oxidant under physiological conditions? *The FASEB Journal* **13**, 1007–1024.

CASIDA, M.E. (1995) Time-Dependent Density Functional Response Theory for Molecules. In *Recent Advances in Computational Chemistry* pp. 155–192. WORLD SCIENTIFIC.

CASIDA, M.E. (2009) Time-dependent density-functional theory for molecules and molecular solids. *Journal of Molecular Structure: THEOCHEM* **914**, 3–18.

CASPARI, E. (1949) Physiological action of eye color mutants in the moths Ephestia kühniella and Ptychopoda seriata. *The Quarterly review of biology* **24**, 185–199.

CHAI, J.-D. & HEAD-GORDON, M. (2008) Long-range corrected hybrid density functionals with damped atom–atom dispersion corrections. *Physical Chemistry Chemical Physics* **10**, 6615.

CHANDLER, D.E. (1984) Comparison of quick-frozen and chemically fixed sea-urchin eggs: structural evidence that cortical granule exocytosis is preceded by a local increase in membrane mobility. *Journal of Cell Science* **72**, 23–36.

CHAN-HIGUERA, J.E., SANTACRUZ-ORTEGA, H. DEL C., CARBONELL-BARRACHINA, Á.A., BURGOS-HERNÁNDEZ, A., ROBLES-SÁNCHEZ, R.M., CRUZ-RAMÍREZ, S.G. & EZQUERRA-BRAUER, J.M. (2019) Xanthommatin is Behind the Antioxidant Activity of the Skin of Dosidicus gigas. *Molecules* **24**, 3420.

CHAUHAN, P., HANSSON, B., KRAAIJEVELD, K., DE KNIJFF, P., SVENSSON, E.I. & WELLENREUTHER, M. (2014) De novo transcriptome of Ischnura elegans provides insights into sensory biology, colour and vision genes. *BMC Genomics* **15**, 808.

DE CHAUMONT, F., DALLONGEVILLE, S., CHENOUARD, N., HERVÉ, N., POP, S., PROVOOST, T., MEAS-YEDID, V., PANKAJAKSHAN, P., LECOMTE, T., LE MONTAGNER, Y., LAGACHE, T., DUFOUR, A. & OLIVO-MARIN, J.-C. (2012) Icy: an open bioimage informatics platform for extended reproducible research. *Nature Methods* **9**, 690–696.

CHEESEMAN, J.R., TRUCKS, G.W., KEITH, T.A. & FRISCH, M.J. (1996) A comparison of models for calculating nuclear magnetic resonance shielding tensors. *The Journal of Chemical Physics* **104**, 5497–5509.

CHELI, V.T., DANIELS, R.W., GODOY, R., HOYLE, D.J., KANDACHAR, V., STARCEVIC, M., MARTINEZ-AGOSTO, J.A., POOLE, S., DIANTONIO, A., LLOYD, V.K., CHANG, H.C., KRANTZ, D.E. & DELL'ANGELICA, E.C. (2010) Genetic modifiers of abnormal organelle biogenesis in a Drosophila model of BLOC-1 deficiency. *Human Molecular Genetics* **19**, 861–878.

CHEN, J.-J., CHEN, W., HE, H., LI, D.-B., LI, W.-W., XIONG, L. & YU, H.-Q. (2013) Manipulation of Microbial Extracellular Electron Transfer by Changing Molecular Structure of Phenazine-Type Redox Mediators. *Environmental Science & Technology* **47**, 1033–1039.

CHEN, Z., WANNERE, C.S., CORMINBOEUF, C. & PUCHTA, R. (2005) Nucleus-Independent Chemical Shifts (NICS) as an Aromaticity Criterion. *Chemical Reviews* **105**, 3842–3888.

CIOFINI, I. & ADAMO, C. (2007) Accurate Evaluation of Valence and Low-Lying Rydberg States with Standard Time-Dependent Density Functional Theory. *The Journal of Physical Chemistry A* **111**, 5549–5556.

CLOUGH, J.M., GUIMARD, E., RIVET, C., SPRAKEL, J. & KODGER, T.E. (2019) Photonic Paints: Structural Pigments Combined with Water-Based Polymeric Film-Formers for Structurally Colored Coatings. *Advanced Optical Materials*, 1900218.

COLÍN-GONZÁLEZ, A.L., MALDONADO, P.D. & SANTAMARÍA, A. (2013) 3-Hydroxykynurenine: An intriguing molecule exerting dual actions in the Central Nervous System. *NeuroToxicology* **34**, 189–204.

CÖLLN, K., HEDEMANN, R. & OJIJO, E. (1981) A method for the isolation of ommochrome-containing granules from insect eyes. *Experientia* **37**, 44–46.

CONNAHS, H., RHEN, T. & SIMMONS, R.B. (2016) Transcriptome analysis of the painted lady butterfly, Vanessa cardui during wing color pattern development. *BMC Genomics* **17**, 270.

CORDERO, R.J.B., ROBERT, V., CARDINALI, G., ARINZE, E.S., THON, S.M. & CASADEVALL, A. (2018) Impact of Yeast Pigmentation on Heat Capture and Latitudinal Distribution. *Current Biology* **28**, 2657-2664.e3.

CORNEL, A.J., Q. BENEDICT, M., SALAZAR RAFFERTY, C., HOWELLS, A.J. & COLLINS, FRANK.H. (1997) Transient expression of the Drosophila melanogaster cinnabar gene rescues eye color in the white eye (WE) strain of Aedes aegypti. *Insect Biochemistry and Molecular Biology* **27**, 993–997.

COSSI, M., REGA, N., SCALMANI, G. & BARONE, V. (2003) Energies, structures, and electronic properties of molecules in solution with the C-PCM solvation model. *Journal of Computational Chemistry* **24**, 669–681.

CRESCENZI, O., CORREALE, G., BOLOGNESE, A., PISCOPO, V., PARRILLI, M. & BARONE, V. (2004) Observed and calculated ^{1}H- and ^{13}C-NMR chemical shifts of substituted 5H-pyrido[3,2-a]- and 5H-pyrido[2,3-a]phenoxazin-5-ones and of some 3H-phenoxazin-3-one derivatives. *Org. Biomol. Chem.* **2**, 1577–1581.

CRONIN, T.W. (2014) *Visual ecology*. Princeton University Press, Princeton.

CROUCHER, P.J., BREWER, M.S., WINCHELL, C.J., OXFORD, G.S. & GILLESPIE, R.G. (2013) De novo characterization of the gene-rich transcriptomes of two color-polymorphic spiders, Theridion grallator and T. californicum (Araneae: Theridiidae), with special reference to pigment genes. *BMC Genomics* **14**, 862.

CULLEN, D.A., CEASE, A.J., LATCHININSKY, A.V., AYALI, A., BERRY, K., BUHL, J., DE KEYSER, R., FOQUET, B., HADRICH, J.C., MATHESON, T., OTT, S.R., POOT-PECH, M.A., ROBINSON, B.E., SMITH, J.M., SONG, H., ET AL. (2017) From Molecules to Management: Mechanisms and Consequences of Locust Phase Polyphenism. In *Advances in Insect Physiology* pp. 167–285. Elsevier.

CUTHILL, I.C., ALLEN, W.L., ARBUCKLE, K., CASPERS, B., CHAPLIN, G., HAUBER, M.E., HILL, G.E., JABLONSKI, N.G., JIGGINS, C.D., KELBER, A., MAPPES, J., MARSHALL, J., MERRILL, R., OSORIO, D., PRUM, R., ET AL. (2017) The biology of color. *Science* **357**, eaan0221.

D'ALBA, L. & SHAWKEY, M.D. (2019) Melanosomes: Biogenesis, Properties, and Evolution of an Ancient Organelle. *Physiological Reviews* **99**, 1–19.

DANIELE, T., HURBAIN, I., VAGO, R., CASARI, G., RAPOSO, G., TACCHETTI, C. & SCHIAFFINO, M.V. (2014) Mitochondria and Melanosomes Establish Physical Contacts Modulated by Mfn2 and Involved in Organelle Biogenesis. *Current Biology* **24**, 393–403.

DANIELS, E.V., MURAD, R., MORTAZAVI, A. & REED, R.D. (2014) Extensive transcriptional response associated with seasonal plasticity of butterfly wing patterns. *Molecular Ecology* **23**, 6123–6134.

DANIELS, E.V. & REED, R.D. (2012) Xanthurenic acid is a pigment in Junonia coenia butterfly wings. *Biochemical Systematics and Ecology* **44**, 161–163.

DE PROFT, F. & GEERLINGS, P. (2001) Conceptual and Computational DFT in the Study of Aromaticity. *Chemical Reviews* **101**, 1451–1464.

DE ROSSI, M.C., DE ROSSI, M.E., SUED, M., RODRÍGUEZ, D., BRUNO, L. & LEVI, V. (2015) Asymmetries in kinesin-2 and cytoplasmic dynein contributions to melanosome transport. *FEBS Letters* **589**, 2763–2768.

DE VIJLDER, T., VALKENBORG, D., LEMIÈRE, F., ROMIJN, E.P., LAUKENS, K. & CUYCKENS, F. (2017) A tutorial in small molecule identification via electrospray ionization-mass spectrometry: The practical art of structural elucidation. *Mass Spectrometry Reviews*.

DECELLE, J., STRYHANYUK, H., GALLET, B., VERONESI, G., SCHMIDT, M., BALZANO, S., MARRO, S., UWIZEYE, C., JOUNEAU, P.-H., LUPETTE, J., JOUHET, J., MARÉCHAL, E., SCHWAB, Y., SCHIEBER, N.L., TUCOULOU, R., ET AL. (2019) Algal Remodeling in a Ubiquitous Planktonic Photosymbiosis. *Current Biology* **29**, 968-978.e4.

DECELLE, J., VERONESI, G., GALLET, B., STRYHANYUK, H., BENETTONI, P., SCHMIDT, M., TUCOULOU, R., PASSARELLI, M., BOHIC, S., CLODE, P. & MUSAT, N. (2020) Subcellular Chemical Imaging: New Avenues in Cell Biology. *Trends in Cell Biology*, S0962892419302211.

DEFRIZE, J., THERY, M. & CASAS, J. (2010) Background colour matching by a crab spider in the field: a community sensory ecology perspective. *Journal of Experimental Biology* **213**, 1425–1435.

DELEVOYE, C., HEILIGENSTEIN, X., RIPOLL, L., GILLES-MARSENS, F., DENNIS, M.K., LINARES, R.A., DERMAN, L., GOKHALE, A., MOREL, E., FAUNDEZ, V., MARKS, M.S. & RAPOSO, G. (2016) BLOC-1 Brings Together the Actin and Microtubule Cytoskeletons to Generate Recycling Endosomes. *Current Biology* **26**, 1–13.

DELEVOYE, C., MARKS, M.S. & RAPOSO, G. (2019) Lysosome-related organelles as functional adaptations of the endolysosomal system. *Current Opinion in Cell Biology* **59**, 147–158.

DELHEY, K. (2019) A review of Gloger's rule, an ecogeographical rule of colour: definitions, interpretations and evidence. *Biological Reviews*.

DEMARTINI, D.G., IZUMI, M., WEAVER, A.T., PANDOLFI, E. & MORSE, D.E. (2015) Structures, Organization, and Function of Reflectin Proteins in Dynamically Tunable Reflective Cells. *Journal of Biological Chemistry* **290**, 15238–15249.

DEMARTINI, D.G., KROGSTAD, D.V. & MORSE, D.E. (2013) Membrane invaginations facilitate reversible water flux driving tunable iridescence in a dynamic biophotonic system. *Proceedings of the National Academy of Sciences* **110**, 2552–2556.

DENNIS, M.K., DELEVOYE, C., ACOSTA-RUIZ, A., HURBAIN, I., ROMAO, M., HESKETH, G.G., GOFF, P.S., SVIDERSKAYA, E.V., BENNETT, D.C., LUZIO, J.P., GALLI, T., OWEN, D.J., RAPOSO, G. & MARKS, M.S. (2016) BLOC-1 and BLOC-3 regulate VAMP7 cycling to and from melanosomes via distinct tubular transport carriers. *The Journal of Cell Biology* **214**, 293–308.

DERAVI, L.F., MAGYAR, A.P., SHEEHY, S.P., BELL, G.R.R., MATHGER, L.M., SENFT, S.L., WARDILL, T.J., LANE, W.S., KUZIRIAN, A.M., HANLON, R.T., HU, E.L. & PARKER, K.K. (2014) The structure-function relationships of a natural nanoscale photonic device in cuttlefish chromatophores. *Journal of The Royal Society Interface* **11**, 20130942–20130942.

DI TOMMASO, S., BOUSQUET, D., MOULIN, D., BALTENNECK, F., RIVA, P., DAVID, H., FADLI, A., GOMAR, J., CIOFINI, I. & ADAMO, C. (2017) Theoretical approaches for predicting the color of rigid dyes in solution. *Journal of Computational Chemistry* **38**, 998–1004.

DIAMOND, J. & BOND, A.B. (2013) *Concealing coloration in animals*. The Belknap Press of Harvard University Press, Cambridge, Massachusetts.

DIBONA, C.W., WILLIAMS, T.L., DINNEEN, S.R., JONES LABADIE, S.F. & DERAVI, L.F. (2016) A Method for Extracting Pigments from Squid *Doryteuthis pealeii*. *Journal of Visualized Experiments*.

DINNEEN, S.R., OSGOOD, R.M., GREENSLADE, M.E. & DERAVI, L.F. (2016) Color Richness in Cephalopod Chromatophores Originating from High Refractive Index Biomolecules. *The Journal of Physical Chemistry Letters*, 313–317.

DOBRY, A.S. & FISHER, D.E. (2018) The Biology of Pigmentation. In *Melanoma* (eds D.E. FISHER & B.C. BASTIAN), pp. 1–30. Springer New York, New York, NY.

DUARTE, R.C., FLORES, A.A.V. & STEVENS, M. (2017) Camouflage through colour change: mechanisms, adaptive value and ecological significance. *Philosophical Transactions of the Royal Society B: Biological Sciences* **372**, 20160342.

DUKAS, R. & MORSE, D.H. (2003) Crab spiders affect flower visitation by bees. *Oikos* **101**, 157–163.

DUKAS, R. & MORSE, D.H. (2005) Crab spiders show mixed effects on flower-visiting bees and no effect on plant fitness components. *Écoscience* **12**, 244–247.

DUNN, W.B., ERBAN, A., WEBER, R.J.M., CREEK, D.J., BROWN, M., BREITLING, R., HANKEMEIER, T., GOODACRE, R., NEUMANN, S., KOPKA, J. & VIANT, M.R. (2013) Mass appeal: metabolite identification in mass spectrometry-focused untargeted metabolomics. *Metabolomics* **9**, 44–66.

DUSTMANN, J.H. (1987) Eye-Colour Mutants of the Honeybee. *Bee World* **68**, 124–128.

EGGERT, C., TEMP, U., DEAN, J.F. & ERIKSSON, K.-E.L. (1995) Laccase-mediated formation of the phenoxazinone derivative, cinnabarinic acid. *FEBS letters* **376**, 202–206.

ELOFSSON, R. & HALLBERG, E. (1973) Correlation of ultrastructure and chemical composition of crustacean chromatophore pigment. *Journal of ultrastructure research* **44**, 421–429.

ENDLER, J.A. & MAPPES, J. (2017) The current and future state of animal coloration research. *Philosophical Transactions of the Royal Society B: Biological Sciences* **372**, 20160352.

ESCUDERO, D., LAURENT, A.D. & JACQUEMIN, D. (2015) Time-Dependent Density Functional Theory: A Tool to Explore Excited States. In *Handbook of Computational Chemistry* (ed J. LESZCZYNSKI), pp. 1–35. Springer Netherlands, Dordrecht.

EVANS, A.B., ACOSTA, M.L. & BOLSTAD, K.S. (2015) Retinal Development and Ommin Pigment in the Cranchiid Squid Teuthowenia pellucida (Cephalopoda: Oegopsida). *PLOS ONE* **10**, e0123453.

EVANS, J.M., DAY, J.P., CABRERO, P., DOW, J.A.T. & DAVIES, S.-A. (2008) A new role for a classical gene: White transports cyclic GMP. *Journal of Experimental Biology* **211**, 890–899.

EWART, G.D., CANNELL, D., COX, G.B. & HOWELLS, A.J. (1994) Mutational analysis of the traffic ATPase (ABC) transporters involved in uptake of eye pigment precursors in Drosophila melanogaster. Implications for structure-function relationships. *Journal of Biological Chemistry* **269**, 10370–10377.

FAHRENBACH, W.H. (1969) The morphology of the eyes of Limulus. II. Ommatidia of the compound eye. *Zeitschrift Fur Zellforschung Und Mikroskopische Anatomie (Vienna, Austria: 1948)* **93**, 451–483.

FALCÓN-PÉREZ, J.M., ROMERO-CALDERÓN, R., BROOKS, E.S., KRANTZ, D.E. & DELL'ANGELICA, E.C. (2007) The Drosophila Pigmentation Gene pink (p) Encodes a Homologue of Human Hermansky-Pudlak Syndrome 5 (HPS5). *Traffic* **8**, 154–168.

FARMER, L.A., HAIDASZ, E.A., GRIESSER, M. & PRATT, D.A. (2017) Phenoxazine: A Privileged Scaffold for Radical-Trapping Antioxidants. *The Journal of Organic Chemistry*.

FEDOROVICH, A.D.-I. & OSTROVSKY, M.L.-M. (1999) Comparative study of spectral and antioxidant properties of pigments from the eyes of two Mysis relicta (Crustacea, Mysidaceal populations, with different light damage resistance. *J Comp Physiol B* **169**, 157–164.

FERGUSON, L.C. & JIGGINS, C.D. (2009) Shared and divergent expression domains on mimetic *Heliconius* wings. *Evolution & Development* **11**, 498–512.

FERRÉ, N., FILATOV, M. & HUIX-ROTLLANT, M. (eds) (2016) *Density-functional methods for excited states*. Springer, Cham.

FIGON, F. & CASAS, J. (2018) Morphological and Physiological Colour Changes in the Animal Kingdom. In *eLS* (ed JOHN WILEY & SONS LTD), pp. 1–11. John Wiley & Sons, Ltd, Chichester, UK.

FIGON, F. & CASAS, J. (2019) Ommochromes in invertebrates: biochemistry and cell biology. *Biological Reviews* **94**, 156–183.

FIGON, F., CASAS, J., CIOFINI, I. & ADAMO, C. (2020) Electronic Couplings in the Reduced State Lie at the Origin of Color Changes of Ommochromes. preprint, ChemRxiv.

FIGON, F. & LORIN, T. (2019) La coloration des Animaux : éléments de physique et de chimie. *Planet-Vie*. https://planet-vie.ens.fr/thematiques/cellules-et-molecules/biophysique/la-coloration-des-animaux-elements-de-physique-et-de [accessed 25 May 2020].

FIGON, F., MUNSCH, T., CROIX, C., VIAUD-MASSUARD, M.-C., LANOUE, A. & CASAS, J. (In press) Uncyclized xanthommatin is a key ommochrome intermediate in invertebrate coloration. *Insect Biochemistry and Molecular Biology*.

FOX, D.L. (1944) Biochromes. *Science* **100**, 470–471.

FOX, D.L. (1976) *Animal biochromes and structural colours: physical, chemical, distributional & physiological features of coloured bodies in the animal world*2d ed. University of California Press, Berkeley.

FRISCH, M.J., TRUCKS, G.W., SCHLEGEL, H.B., SCUSERIA, G.E., ROBB, M.A., CHEESEMAN, J.R., SCALMANI, G., BARONE, V., PETERSSON, G.A., NAKATSUJI, H., LI, X., CARICATO, M., MARENICH, A.V., BLOINO, J., JANESKO, B.G., ET AL. (2016) *Gaussian 16 Rev. C.01*. Wallingford, CT.

FRIZZO, C.P. & MARTINS, M.A.P. (2012) Aromaticity in heterocycles: new HOMA index parametrization. *Structural Chemistry* **23**, 375–380.

FUGE, H. (1967) Die Pigmentbildung im Auge von Drosophila melanogaster und ihre Beeinflussung durch den white +-Locus. *Zeitschrift für Zellforschung und Mikroskopische Anatomie* **83**, 468–507.

FUJII, T., DAIMON, T., UCHINO, K., BANNO, Y., KATSUMA, S., SEZUTSU, H., TAMURA, T. & SHIMADA, T. (2010) Transgenic analysis of the BmBLOS2 gene that governs the translucency of the larval integument of the silkworm, Bombyx mori. *Insect Molecular Biology* **19**, 659–667.

FUJIKAWA, K., SATOH, A.K., KAWAMURA, S. & OZAKI, K. (2002) Molecular and Functional Characterization of a Unique Rab Protein, RABRP1, Containing the WDIAGQE Sequence in a GTPase Motif. *Zoological Science* **19**, 981–993.

FUJIWARA, H. & NISHIKAWA, H. (2016) Functional analysis of genes involved in color pattern formation in Lepidoptera. *Current Opinion in Insect Science* **17**, 16–23.

FUTAHASHI, R. (2016) Color vision and color formation in dragonflies. *Current Opinion in Insect Science* **17**, 32–39.

FUTAHASHI, R. (2017) Molecular Mechanisms Underlying Color Vision and Color Formation in Dragonflies. In *Diversity and Evolution of Butterfly Wing Patterns* (eds T. SEKIMURA & H.F. NIJHOUT), pp. 303–320. Springer Singapore, Singapore.

FUTAHASHI, R., KURITA, R., MANO, H. & FUKATSU, T. (2012) Redox alters yellow dragonflies into red. *Proceedings of the National Academy of Sciences* **109**, 12626–12631.

FUZEAU-BRAESCH, S. (1985) Colour changes. In *Comprehensive insect physiology, biochemistry and pharmacology* (eds G.A. KERKUT & L.I. GILBERT), p. Pergamon Press, Oxford.

GANDÍA-HERRERO, F., ESCRIBANO, J. & GARCÍA-CARMONA, F. (2016) Biological Activities of Plant Pigments Betalains. *Critical Reviews in Food Science and Nutrition* **56**, 937–945.

GAO, J., YAO, L., XIA, T., LIAO, X., ZHU, D. & XIANG, Y. (2018) Biochemistry and structural studies of kynurenine 3-monooxygenase reveal allosteric inhibition by Ro 61-8048. *The FASEB Journal* **32**, 2036–2045.

GAWRYSZEWSKI, F.M., BIRCH, D., KEMP, D.J. & HERBERSTEIN, M.E. (2015) Dissecting the variation of a visual trait: the proximate basis of UV-Visible reflectance in crab spiders (Thomisidae). *Functional Ecology* **29**, 44–54.

GÁZQUEZ, J.L., CEDILLO, A. & VELA, A. (2007) Electrodonating and Electroaccepting Powers. *The Journal of Physical Chemistry A* **111**, 1966–1970.

GHOSHAL, A., DEMARTINI, D.G., ECK, E. & MORSE, D.E. (2013) Optical parameters of the tunable Bragg reflectors in squid. *Journal of The Royal Society Interface* **10**, 20130386–20130386.

GILES, G.I., COLLINS, C.A., STONE, T.W. & JACOB, C. (2003) Electrochemical and in vitro evaluation of the redox-properties of kynurenine species. *Biochemical and Biophysical Research Communications* **300**, 719–724.

GLASSER, N.R., SAUNDERS, S.H. & NEWMAN, D.K. (2017) The Colorful World of Extracellular Electron Shuttles. *Annual Review of Microbiology* **71**, 731–751.

GO, Y.-M. & JONES, D.P. (2008) Redox compartmentalization in eukaryotic cells. *Biochimica et Biophysica Acta (BBA) - General Subjects* **1780**, 1273–1290.

GORNIAK, T., HARASZTI, T., SUHONEN, H., YANG, Y., HEDBERG-BUENZ, A., KOEHN, D., HEINE, R., GRUNZE, M., ROSENHAHN, A. & ANDERSON, M.G. (2014) Support and challenges to the melanosomal casing model based on nanoscale distribution of metals within iris melanosomes detected by X-ray fluorescence analysis. *Pigment Cell & Melanoma Research* **27**, 831–834.

GRAMATES, L.S., MARYGOLD, S.J., SANTOS, G. DOS, URBANO, J.-M., ANTONAZZO, G., MATTHEWS, B.B., REY, A.J., TABONE, C.J., CROSBY, M.A., EMMERT, D.B., FALLS, K., GOODMAN, J.L., HU, Y., PONTING, L., SCHROEDER, A.J., ET AL. (2017) FlyBase at 25: looking to the future. *Nucleic Acids Research* **45**, D663–D671.

GRANT, P., MAGA, T., LOSHAKOV, A., SINGHAL, R., WALI, A., NWANKWO, J., BARON, K. & JOHNSON, D. (2016) An Eye on Trafficking Genes: Identification of Four Eye Color Mutations in Drosophila. *G3 Genes|Genomes|Genetics*.

GRIBAKIN, F.G., BUROVINA, I.V., CHESNOKOVA, Y.G., NATOCHIN, Y.V., SHAKMATOVA, Y.I., UKHANOV, K.Y. & WOYKE, E. (1987) Reduced magnesium content in non-pigmented eyes of the honey bee (Apis mellifera L.). *Comparative Biochemistry and Physiology Part A: Physiology* **86**, 689–692.

GRIMME, S., EHRLICH, S. & GOERIGK, L. (2011) Effect of the damping function in dispersion corrected density functional theory. *Journal of Computational Chemistry* **32**, 1456–1465.

GRUBBS, N., HAAS, S., BEEMAN, R.W. & LORENZEN, M.D. (2015) The ABCs of Eye Color in Tribolium castaneum: Orthologs of the Drosophila white, scarlet, and brown Genes. *Genetics* **199**, 749–759.

GUAN, Z., CAI, T., LIU, Z., DOU, Y., HU, X., ZHANG, P., SUN, X., LI, H., KUANG, Y., ZHAI, Q., RUAN, H., LI, X., LI, Z., ZHU, Q., MAI, J., ET AL. (2017) Origin of the Reflectin Gene and Hierarchical Assembly of Its Protein. *Current Biology*.

GUIJAS, C., MONTENEGRO-BURKE, J.R., DOMINGO-ALMENARA, X., PALERMO, A., WARTH, B., HERMANN, G., KOELLENSPERGER, G., HUAN, T., URITBOONTHAI, W., AISPORNA, A.E., WOLAN, D.W., SPILKER, M.E., BENTON, H.P. & SIUZDAK, G. (2018) METLIN: A Technology Platform for Identifying Knowns and Unknowns. *Analytical Chemistry* **90**, 3156–3164.

HAN, Q., BEERNTSEN, B.T. & LI, J. (2007) The tryptophan oxidation pathway in mosquitoes with emphasis on xanthurenic acid biosynthesis. *Journal of Insect Physiology* **53**, 254–263.

HAN, Q., ROBINSON, H. & LI, J. (2012) Biochemical identification and crystal structure of kynurenine formamidase from *Drosophila melanogaster*. *Biochemical Journal* **446**, 253–260.

HANLON, R.T., CHIAO, C.-C., MATHGER, L.M., BARBOSA, A., BURESCH, K.C. & CHUBB, C. (2009) Cephalopod dynamic camouflage: bridging the continuum between background matching and disruptive coloration. *Philosophical Transactions of the Royal Society B: Biological Sciences* **364**, 429–437.

HARANO, T. & CHINO, H. (1971) A new diaphorase from Bombyx silkworm eggs—Cytochrome c reductase activity mediated with xanthommatin. *Archives of Biochemistry and Biophysics* **146**, 467–476.

HARRIS, D.A., KIM, K., NAKAHARA, K., VÁSQUEZ-DOORMAN, C. & CARTHEW, R.W. (2011) Cargo sorting to lysosome-related organelles regulates siRNA-mediated gene silencing. *The Journal of Cell Biology* **194**, 77–87.

HAWES, P., NETHERTON, C.L., MUELLER, M., WILEMAN, T. & MONAGHAN, P. (2007) Rapid freeze-substitution preserves membranes in high-pressure frozen tissue culture cells. *Journal of microscopy* **226**, 182–189.

HAYWA, D.O. (2002) *Quantum Mechanics for Chemists*. Royal Society of Chemistry, Cambridge.

HE, X., LINDSAY-MOSHER, N., LI, Y., MOLINARO, A.M., PELLETTIERI, J. & PEARSON, B.J. (2017) FOX and ETS family transcription factors regulate the pigment cell lineage in planarians. *Development*, dev.156349.

HEARL, W.G. & BRUCE JACOBSON, K. (1984) Eye pigment granules of Drosophila melanogaster. *Insect Biochemistry* **14**, 329–335.

HEILING, A.M., HERBERSTEIN, M.E. & CHITTKA, L. (2003) Pollinator attraction: Crab-spiders manipulate flower signals. *Nature* **421**, 334–334.

HEILING, S., KHANAL, S., BARSCH, A., ZUREK, G., BALDWIN, I.T. & GAQUEREL, E. (2016) Using the knowns to discover the unknowns: MS-based dereplication uncovers structural diversity in 17-hydroxygeranyllinalool diterpene glycoside production in the Solanaceae. *The Plant Journal* **85**, 561–577.

HENDERSON, T.M., IZMAYLOV, A.F., SCALMANI, G. & SCUSERIA, G.E. (2009) Can short-range hybrids describe long-range-dependent properties? *The Journal of Chemical Physics* **131**, 044108.

HENZE, M.J., LIND, O., WILTS, B.D. & KELBER, A. (2019) Pterin-pigmented nanospheres create the colours of the polymorphic damselfly *Ischnura elegans*. *Journal of The Royal Society Interface* **16**, 20180785.

HERBERSTEIN, M.E. & GAWRYSZEWSKI, F.M. (2013) UV and Camouflage in Crab Spiders (Thomisidae). In *Spider Ecophysiology* (ed W. NENTWIG), pp. 349–359. Springer Berlin Heidelberg, Berlin, Heidelberg.

HILL, G.E. & MCGRAW, K.J. (eds) (2006) *Bird coloration*. Harvard University Press, Cambridge, Mass.

HO, H. & GANESAN, A.K. (2011) The pleiotropic roles of autophagy regulators in melanogenesis: Autophagy and melanogenesis. *Pigment Cell & Melanoma Research* **24**, 595–604.

HOFFMAN, D.P., SHTENGEL, G., XU, C.S., CAMPBELL, K.R., FREEMAN, M., WANG, L., MILKIE, D.E., PASOLLI, H.A., IYER, N., BOGOVIC, J.A., STABLEY, D.R., SHIRINIFARD, A., PANG, S., PEALE, D., SCHAEFER, K., ET AL. (2020) Correlative three-dimensional super-resolution and block-face electron microscopy of whole vitreously frozen cells. *Science* **367**, eaaz5357.

HOFFMANN, K.H. (1984) Color and Color Changes. In *Environmental Physiology and Biochemistry of Insects* (ed K.H. HOFFMANN), pp. 206–224. Springer Berlin Heidelberg, Berlin, Heidelberg.

HÖGLUND, G., LANGER, H., STRUWE, G. & THORELL, B. (1970) Spectral absorption by screening pigment granules in the compound eyes of a moth and a wasp. *Zeitschrift für Vergleichende Physiologie* **67**, 238–242.

HOHENBERG, P. & KOHN, W. (1964) Inhomogeneous Electron Gas. *Physical Review* **136**, B864–B871.

HOLL, A. (1987) Coloration and chromes. In *Ecophysiology of spiders* (ed W. NENTWIG), pp. 16–25. Springer, Berlin, Heidelberg.

HOLL, A. & RÜDIGER, W. (1975) Micromatabilin, a new biliverdin conjugate in the spider, Micromata rosea (Sparassidae). *Journal of Comparative Physiology B* **98**, 189–191.

HOLLSTEIN, U. (1974) Actinomycin. Chemistry and mechanism of action. *Chemical Reviews* **74**, 625–652.

HONG, L. & SIMON, J.D. (2007) Current Understanding of the Binding Sites, Capacity, Affinity, and Biological Significance of Metals in Melanin. *The Journal of Physical Chemistry B* **111**, 7938–7947.

HORI, M. & RIDDIFORD, L.M. (1981) Isolation of ommochromes and 3-hydroxykynurenine from the tobacco hornworm, Manduca sexta. *Insect Biochemistry* **11**, 507–513.

HOROWITZ, N.H. & BAUMBERGER, J.P. (1941) Studies on the respiratory pigment of Urechis eggs. *Journal of Biological Chemistry* **141**, 407–415.

HOWELLS, A.J., SUMMERS, K.M. & RYALL, R.L. (1977) Developmental patterns of 3-hydroxykynurenine accumulation in white and various other eye color mutants of Drosophila melanogaster. *Biochemical Genetics* **15**, 1049–1059.

HUANG, W., GONG, Z., LI, J. & DING, J. (2013) Crystal structure of Drosophila melanogaster tryptophan 2,3-dioxygenase reveals insights into substrate recognition and catalytic mechanism. *Journal of Structural Biology* **181**, 291–299.

HUEY, S. & NIEH, J.C. (2017) Foraging at a safe distance: crab spider effects on pollinators. *Ecological Entomology* **42**, 469–476.

HUME, A.N. & SEABRA, M.C. (2011) Melanosomes on the move: a model to understand organelle dynamics. *Biochemical Society Transactions* **39**, 1191–1196.

HURBAIN, I., GEERTS, W.J., BOUDIER, T., MARCO, S., VERKLEIJ, A.J., MARKS, M.S. & RAPOSO, G. (2008) Electron tomography of early melanosomes: implications for melanogenesis and the generation of fibrillar amyloid sheets. *Proceedings of the National Academy of Sciences*, pnas–0803488105.

HURBAIN, I., ROMAO, M., BERGAM, P., HEILIGENSTEIN, X. & RAPOSO, G. (2017) Analyzing Lysosome-Related Organelles by Electron Microscopy. In *Lysosomes* (eds K. ÖLLINGER & H. APPELQVIST), pp. 43–71. Springer New York, New York, NY.

HURBAIN, I. & SACHSE, M. (2011) The future is cold: cryo-preparation methods for transmission electron microscopy of cells. *Biology of the Cell* **103**, 405–420.

INSAUSTI, T.C. & CASAS, J. (2008) The functional morphology of color changing in a spider: development of ommochrome pigment granules. *Journal of Experimental Biology* **211**, 780–789.

INSAUSTI, T.C. & CASAS, J. (2009) Turnover of pigment granules: Cyclic catabolism and anabolism of ommochromes within epidermal cells. *Tissue and Cell* **41**, 421–429.

INSAUSTI, T.C., LE GALL, M. & LAZZARI, C.R. (2013) Oxidative stress, photodamage and the role of screening pigments in insect eyes. *Journal of Experimental Biology* **216**, 3200–3207.

ISHII, T., IWAHASHI, H., SUGATA, R. & KIDO, R. (1992) Formation of hydroxanthommatin-derived radical in the oxidation of 3-hydroxykynurenine. *Archives of biochemistry and biophysics* **294**, 616–622.

ITO, K., KATSUMA, S., YAMAMOTO, K., KADONO-OKUDA, K., MITA, K. & SHIMADA, T. (2009) A 25bp-long insertional mutation in the BmVarp gene causes the waxy translucent skin of the silkworm, Bombyx mori. *Insect Biochemistry and Molecular Biology* **39**, 287–293.

ITO, K., KIDOKORO, K., KATSUMA, S., SHIMADA, T., YAMAMOTO, K., MITA, K., KADONO-OKUDA, K. & BELL, J. (2012) Positional cloning of a gene responsible for the *cts* mutation of the silkworm, *Bombyx mori*. *Genome* **55**, 493–504.

ITO, S. & WAKAMATSU, K. (2008) Chemistry of Mixed Melanogenesis—Pivotal Roles of Dopaquinone. *Photochemistry and Photobiology* **84**, 582–592.

IWAHASHI, H. & ISHII, T. (1997) Detection of the oxidative products of 3-hydroxykynurenine using high-performance liquid chromatography–electrochemical detection–ultraviolet absorption detection–electron spin resonance spectrometry and high-performance liquid chromatography–electrochemical detection–ultraviolet absorption detection–mass spectrometry. *Journal of Chromatography A* **773**, 23–31.

JABLONSKI, N.G. & CHAPLIN, G. (2017) The colours of humanity: the evolution of pigmentation in the human lineage. *Philosophical Transactions of the Royal Society B: Biological Sciences* **372**, 20160349.

JACQUEMIN, D. & ADAMO, C. (2015) Computational Molecular Electronic Spectroscopy with TD-DFT. In *Density-Functional Methods for Excited States* (eds N. FERRÉ, M. FILATOV & M. HUIX-ROTLLANT), pp. 347–375. Springer International Publishing, Cham.

JACQUEMIN, D., PERPÈTE, E.A., CIOFINI, I. & ADAMO, C. (2009a) Accurate Simulation of Optical Properties in Dyes. *Accounts of Chemical Research* **42**, 326–334.

JACQUEMIN, D., PREAT, J., PERPÈTE, E.A., VERCAUTEREN, D.P., ANDRÉ, J.-M., CIOFINI, I. & ADAMO, C. (2011) Absorption spectra of azobenzenes simulated with time-dependent density functional theory. *International Journal of Quantum Chemistry* **111**, 4224–4240.

JACQUEMIN, D., WATHELET, V., PERPÈTE, E.A. & ADAMO, C. (2009b) Extensive TD-DFT Benchmark: Singlet-Excited States of Organic Molecules. *Journal of Chemical Theory and Computation* **5**, 2420–2435.

JENSEN, F. (2017) *Introduction to computational chemistry*Third edition. John Wiley & Sons, Chichester, UK ; Hoboken, NJ.

JIMBOW, K., OIKAWA, O., SUGIYAMA, S. & TAKEUCHI, T. (1979) Comparison of Eumelanogenesis and Pheomelanogenesis in Retinal and Follicular Melanocytes; Role of Vesculo-globular Bodies in Melanosome Differentiation. *Journal of Investigative Dermatology* **73**, 278–284.

JOHNSEN, S. (2012) *The optics of life: a biologist's guide to light in nature*. Princeton University Press, Princeton, NJ.

KAMETAKA, S., KAMETAKA, A., YONEKURA, S., HARUTA, M., TAKENOSHITA, S., GOTO, S. & WAGURI, S. (2012) AP-1 clathrin adaptor and CG8538/Aftiphilin are involved in Notch signaling during eye development in Drosophila melanogaster. *Journal of Cell Science* **125**, 634–648.

KASHIV, Y., AUSTIN, J.R., LAI, B., ROSE, V., VOGT, S. & EL-MUAYED, M. (2016) Imaging trace element distributions in single organelles and subcellular features. *Scientific Reports* **6**.

KAWAKAMI, A., SAKANE, F., IMAI, S., YASUDA, S., KAI, M., KANOH, H., JIN, H.-Y., HIROSAKI, K., YAMASHITA, T., FISHER, D.E. & JIMBOW, K. (2008) Rab7 Regulates Maturation of Melanosomal Matrix Protein gp100/Pmel17/Silv. *Journal of Investigative Dermatology* **128**, 143–150.

KAXIRAS, E., TSOLAKIDIS, A., ZONIOS, G. & MENG, S. (2006) Structural Model of Eumelanin. *Physical Review Letters* **97**, 218102.

KAYSER, H. (1985) Pigments. In *Biochemistry* (eds G.A. KERKUT & L.I. GILBERT), pp. 367–415. Elsevier, Pergamon, Amsterdam.

KHAN, M.K. & HERBERSTEIN, M.E. (2019) Ontogenetic colour change signals sexual maturity in a non-territorial damselfly. *Ethology*, eth.12959.

KHAN, S.A., REICHELT, M. & HECKEL, D.G. (2017) Functional analysis of the ABCs of eye color in Helicoverpa armigera with CRISPR/Cas9-induced mutations. *Scientific Reports* **7**, 40025.

KIKKAWA, H. (1953) Biochemical Genetics of Bombyx mori (Silkworm). In *Advances in Genetics* (ed M. DEMEREC), pp. 107–140. Elsevier, Berlin, Heidelberg, New York and Tokyo.

KINGSLAND, S. (1978) Abbott thayer and the protective coloration debate. *Journal of the History of Biology* **11**, 223–244.

KITSON, T.M. (1998) The Oxidative Addition Reaction between Compounds of Resorufin (7-Hydroxy-3H-phenoxazin-3-one) and 2-Mercaptoethanol. *Bioorganic Chemistry* **26**, 63–73.

KLUMPERMAN, J. & RAPOSO, G. (2014) The Complex Ultrastructure of the Endolysosomal System. *Cold Spring Harbor Perspectives in Biology* **6**, a016857–a016857.

KNAUER, A.C., BAKHTIARI, M. & SCHIESTL, F.P. (2018) Crab spiders impact floral-signal evolution indirectly through removal of florivores. *Nature Communications* **9**.

KOCH, P.B., BEHNECKE, B. & FFRENCH-CONSTANT, R.H. (2000) The molecular basis of melanism and mimicry in a swallowtail butterfly. *Current Biology* **10**, 591–594.

KOHN, W., BECKE, A.D. & PARR, R.G. (1996) Density functional theory of electronic structure. *The Journal of Physical Chemistry* **100**, 12974–12980.

KOHN, W. & SHAM, L.J. (1965) Self-Consistent Equations Including Exchange and Correlation Effects. *Physical Review* **140**, A1133–A1138.

KOLB, G. (1977) The structure of the eye of Pieris brassicae L. (Lepidoptera). *Zoomorphologie* **87**, 123–146.

KÖNIG, C. & NEUGEBAUER, J. (2012) Quantum Chemical Description of Absorption Properties and Excited-State Processes in Photosynthetic Systems. *ChemPhysChem* **13**, 386–425.

KORLIMBINIS, A. & TRUSCOTT, R.J.W. (2006) Identification of 3-Hydroxykynurenine Bound to Proteins in the Human Lens. A Possible Role in Age-Related Nuclear Cataract †. *Biochemistry* **45**, 1950–1960.

KRAH, F.-S., BÜNTGEN, U., SCHAEFER, H., MÜLLER, J., ANDREW, C., BODDY, L., DIEZ, J., EGLI, S., FRECKLETON, R., GANGE, A.C., HALVORSEN, R., HEEGAARD, E., HEIDEROTH, A., HEIBL, C., HEILMANN-CLAUSEN, J., ET AL. (2019) European mushroom assemblages are darker in cold climates. *Nature Communications* **10**, 2890.

KREMER, J.R., MASTRONARDE, D.N. & MCINTOSH, J.R. (1996) Computer Visualization of Three-Dimensional Image Data Using IMOD. *Journal of Structural Biology* **116**, 71–76.

KRETZSCHMAR, D., POECK, B., ROTH, H., ERNST, R., KELLER, A., PORSCH, M., STRAUSS, R. & PFLUGFELDER, G.O. (2000) Defective Pigment Granule Biogenesis and Aberrant Behavior Caused by Mutations in the Drosophila AP-3β Adaptin Gene ruby. *Genetics* **155**, 213–223.

KRISHNA, A., NIE, X., WARREN, A.D., LLORENTE-BOUSQUETS, J.E., BRISCOE, A.D. & LEE, J. (2020) Infrared optical and thermal properties of microstructures in butterfly wings. *Proceedings of the National Academy of Sciences* **117**, 1566–1572.

KUMAR, A., WILLIAMS, T.L., MARTIN, C.A., FIGUEROA-NAVEDO, A.M. & DERAVI, L.F. (2018) Xanthommatin-Based Electrochromic Displays Inspired by Nature. *ACS Applied Materials & Interfaces*.

LANGER, H. (1967) Über die Pigmentgranula im Facettenauge von Calliphora erythrocephala. *Zeitschrift für vergleichende Physiologie* **55**, 354–377.

LANGER, H. (1975) Properties and functions of screening pigments in insect eyes. In *Photoreceptor optics* pp. 429–455. Springer, Berlin, Heidelberg.

LAURENT, A.D. & JACQUEMIN, D. (2013) TD-DFT benchmarks: A review. *International Journal of Quantum Chemistry* **113**, 2019–2039.

LAWRENCE, P.A. & GREEN, S.M. (1979) Cell lineage in the developing retina of Drosophila. *Developmental Biology* **71**, 142–152.

LE BAHERS, T., ADAMO, C. & CIOFINI, I. (2011) A Qualitative Index of Spatial Extent in Charge-Transfer Excitations. *Journal of Chemical Theory and Computation* **7**, 2498–2506.

LE ROES-HILL, M., GOODWIN, C. & BURTON, S. (2009) Phenoxazinone synthase: what's in a name? *Trends in Biotechnology* **27**, 248–258.

LHONORE, D., ANGLO, A. & MARCAILLOU, C. (1973) Données histophysiologiques sur le développement post-embryonnaire d'un insecte Trichoptère (Phryganea varia Fab.). *Annales de Limnologie* **9**, 157–176.

LI, C. & MEINERTZHAGEN, I.A. (1997) The effects of 20-hydroxyecdysone on the differentiation in vitro of cells from the eye imaginal disc from Drosophila melanogaster. *Invertebrate neuroscience: IN* **3**, 57–69.

LI, J., BEERNTSEN, B.T. & JAMES, A.A. (1999) Oxidation of 3-hydroxykynurenine to produce xanthommatin for eye pigmentation: a major branch pathway of tryptophan catabolism during pupal development in the yellow fever mosquito, Aedes aegypti. *Insect biochemistry and molecular biology* **29**, 329–338.

LI, J. & LI, G. (1997) Transamination of 3-hydroxykynurenine to produce xanthurenic acid: a major branch pathway of tryptophan metabolism in the mosquito, Aedes aegypti, during larval development. *Insect biochemistry and molecular biology* **27**, 859–867.

LI, P., CUI, Y., SONG, C. & ZHANG, H. (2017) A systematic study of phenoxazine-based organic sensitizers for solar cells. *Dyes and Pigments* **137**, 12–23.

LIAO, J.-H., CHEN, C.-S., HU, C.-C., CHEN, W.-T., WANG, S.-P., LIN, I.-L., HUANG, Y.-H., TSAI, M.-H., WU, T.-H., HUANG, F.-Y. & WU, S.-H. (2011) Ditopic Complexation of Selenite Anions or Calcium Cations by Pirenoxine: An Implication for Anti-Cataractogenesis. *Inorganic Chemistry* **50**, 365–377.

LIGON, R.A. & MCCARTNEY, K.L. (2016) Biochemical regulation of pigment motility in vertebrate chromatophores: a review of physiological color change mechanisms. *Current Zoology* **62**, 237–252.

LINDSAY-MOSHER, N. & PEARSON, B.J. (2019) The true colours of the flatworm: Mechanisms of pigment biosynthesis and pigment cell lineage development in planarians. *Seminars in Cell & Developmental Biology* **87**, 37–44.

LINZEN, B. (1959) Über Ommochrome, XV. Über die Identifizierung des „Urechochroms“ als Xanthommatin. *Hoppe-Seyler´s Zeitschrift für physiologische Chemie* **314**, 12–14.

LINZEN, B. (1974) The Tryptophan → Ommochrome Pathway in Insects. In *Advances in Insect Physiology* (eds J.E. TREHERNE, M.J. BERRIDGE & V.B. WIGGLESWORTH), pp. 117–246. Elsevier, Academic Press.

LINZEN, B. & BÜCKMANN, D. (1961) Biochemische und histologische Untersuchungen zur Umfärbung der Raupe von Cerura vinula L. *Zeitschrift für Naturforschung B* **16**, 6–18.

LIU, S.-H., LUO, J., YANG, B.-J., WANG, A.-Y. & TANG, J. (2017) *karmoisin* and *cardinal* ortholog genes participate in the ommochrome synthesis of *Nilaparvata lugens* (Hemiptera: Delphacidae). *Insect Science*.

LLANDRES, A.L., FIGON, F., CHRISTIDÈS, J.-P., MANDON, N. & CASAS, J. (2013) Environmental and hormonal factors controlling reversible colour change in crab spiders. *Journal of Experimental Biology* **216**, 3886–3895.

LLANDRES, A.L., GAWRYSZEWSKI, F.M., HEILING, A.M. & HERBERSTEIN, M.E. (2011) The effect of colour variation in predators on the behaviour of pollinators: Australian crab spiders and native bees. *Ecological Entomology* **36**, 72–81.

LLANDRES, A.L. & RODRÍGUEZ-GIRONÉS, M.A. (2011) Spider Movement, UV Reflectance and Size, but Not Spider Crypsis, Affect the Response of Honeybees to Australian Crab Spiders. *PLoS ONE* **6**, e17136.

LLOYD, V., RAMASWAMI, M. & KRÄMER, H. (1998) Not just pretty eyes: Drosophila eye-colour mutations and lysosomal delivery. *Trends in cell biology* **8**, 257–259.

LLOYD, V.K., SINCLAIR, D.A., ALPERYN, M. & GRIGLIATTI, T.A. (2002) *Enhancer of garnet* /δAP-3 is a cryptic allele of the *white* gene and identifies the intracellular transport system for the white protein. *Genome* **45**, 296–312.

LLOYD, V.K., SINCLAIR, D.A., WENNBERG, R., WARNER, T.S., HONDA, B.M. & GRIGLIATTI, T.A. (1999) A genetic and molecular characterization of the *garnet* gene of *Drosophila melanogaster*. *Genome* **42**, 1183–1193.

LÓPEZ, S. & ALONSO, S. (2014) Evolution of Skin Pigmentation Differences in Humans. In *Encyclopedia of Life Sciences* (ed JOHN WILEY & SONS LTD), p. John Wiley & Sons, Ltd, Chichester, UK.

LORENZEN, M.D., BROWN, S.J., DENELL, R.E. & BEEMAN, R.W. (2002) Cloning and characterization of the Tribolium castaneum eye-color genes encoding tryptophan oxygenase and kynurenine 3-monooxygenase. *Genetics* **160**, 225–234.

LŐRINCZ, P., TAKÁTS, S., KÁRPÁTI, M. & JUHÁSZ, G. (2016) iFly: The eye of the fruit fly as a model to study autophagy and related trafficking pathways. *Experimental Eye Research* **144**, 90–98.

LUZIO, J.P., GRAY, S.R. & BRIGHT, N.A. (2010) Endosome–lysosome fusion. *Biochemical Society Transactions* **38**, 1413–1416.

LUZIO, J.P., HACKMANN, Y., DIECKMANN, N.M.G. & GRIFFITHS, G.M. (2014) The Biogenesis of Lysosomes and Lysosome-Related Organelles. *Cold Spring Harbor Perspectives in Biology* **6**, a016840–a016840.

MA, J., PLESKEN, H., TREISMAN, J.E., EDELMAN-NOVEMSKY, I. & REN, M. (2004) Lightoid and Claret: A rab GTPase and its putative guanine nucleotide exchange factor in biogenesis of Drosophila eye pigment granules. *Proceedings of the National Academy of Sciences* **101**, 11652–11657.

MACKENZIE, S.M., HOWELLS, A.J., COX, G.B. & EWART, G.D. (2000) Sub-cellular localisation of the white/scarlet ABC transporter to pigment granule membranes within the compound eye of Drosophila melanogaster. *Genetica* **108**, 239–252.

MANOUKAS, A.G. (1981) Effect of excess levels of individual amino acids upon survival, growth and pupal yield of *Dacus oleae* (Gmel.) larvae. *Journal of Applied Entomology* **91**, 309–315.

MAO, Y., HEAD-GORDON, M. & SHAO, Y. (2018) Unraveling substituent effects on frontier orbitals of conjugated molecules using an absolutely localized molecular orbital based analysis. *Chemical Science* **9**, 8598–8607.

MARKS, M.S., HEIJNEN, H.F. & RAPOSO, G. (2013) Lysosome-related organelles: unusual compartments become mainstream. *Current Opinion in Cell Biology* **25**, 495–505.

MARQUES, M., MAITRA, N.T., NOGUEIRA, F.M.S., GROSS, E.K.U. & RUBIO, A. (eds) (2012) *Fundamentals of time-dependent density functional theory*. Springer, Heidelberg.

MARQUES, M.A.L., LÓPEZ, X., VARSANO, D., CASTRO, A. & RUBIO, A. (2003) Time-Dependent Density-Functional Approach for Biological Chromophores: The Case of the Green Fluorescent Protein. *Physical Review Letters* **90**, 258101.

MARTEL, R.R. & LAW, J.H. (1991) Purification and properties of an ommochrome-binding protein from the hemolymph of the tobacco hornworm, Manduca sexta. *Journal of Biological Chemistry* **266**, 21392–21398.

MARTEL, R.R. & LAW, J.H. (1992) Hemolymph titers, chromophore association and immunological cross-reactivity of an ommochrome-binding protein from the hemolymph of the tobacco hornworm, Manduca sexta. *Insect Biochemistry and Molecular Biology* **22**, 561–569.

MARTIN, C.A., REZAEEYAZDI, M., COLOMBANI, T., DINNEEN, S.R., KUMAR, A., BENCHERIF, S.A. & DERAVI, L.F. (2019) A bioinspired, photostable UV-filter that protects mammalian cells against UV-induced cellular damage. *Chemical Communications*, 10.1039.C9CC06323D.

MARTIN, W. (2010) Evolutionary origins of metabolic compartmentalization in eukaryotes. *Philosophical Transactions of the Royal Society B: Biological Sciences* **365**, 847–855.

MARTÍNEZ, A., RODRÍGUEZ-GIRONÉS, M.A., BARBOSA, A. & COSTAS, M. (2008) Donator Acceptor Map for Carotenoids, Melatonin and Vitamins. *The Journal of Physical Chemistry A* **112**, 9037–9042.

MASTHAY, M.B. (1997) Color changes induced by pigment granule aggregation in chromatophores: a quantitative model based on Beer's Law. *Photochemistry and photobiology* **66**, 649–658.

MASTRONARDE, D.N. & HELD, S.R. (2017) Automated tilt series alignment and tomographic reconstruction in IMOD. *Journal of Structural Biology* **197**, 102–113.

MÄTHGER, L.M. (2003) Rapid colour changes in multilayer reflecting stripes in the paradise whiptail, Pentapodus paradiseus. *Journal of Experimental Biology* **206**, 3607–3613.

MÄTHGER, L.M., DENTON, E.J., MARSHALL, N.J. & HANLON, R.T. (2009) Mechanisms and behavioural functions of structural coloration in cephalopods. *Journal of The Royal Society Interface* **6**, S149–S163.

MÄTHGER, L.M. & HANLON, R.T. (2007) Malleable skin coloration in cephalopods: selective reflectance, transmission and absorbance of light by chromatophores and iridophores. *Cell and Tissue Research* **329**, 179–186.

MATTHEWS, R.G., HUBBARD, R., BROWN, P.K. & WALD, G. (1963) Tautomeric Forms of Metarhodopsin. *The Journal of General Physiology* **47**, 215–240.

MAYR, E. (1999) *Systematics and the origin of species, from the viewpoint of a zoologist*1st Harvard University Press pbk. ed. Harvard University Press, Cambridge, Mass.

MCGRAW, K.J. (2005) The antioxidant function of many animal pigments: are there consistent health benefits of sexually selected colourants? *Animal Behaviour* **69**, 757–764.

MCINTOSH, R., NICASTRO, D. & MASTRONARDE, D. (2005) New views of cells in 3D: an introduction to electron tomography. *Trends in Cell Biology* **15**, 43–51.

MCRAE, R., BAGCHI, P., SUMALEKSHMY, S. & FAHRNI, C.J. (2009) In Situ Imaging of Metals in Cells and Tissues. *Chemical Reviews* **109**, 4780–4827.

MEDINA, I., NEWTON, E., KEARNEY, M.R., MULDER, R.A., PORTER, W.P. & STUART-FOX, D. (2018) Reflection of near-infrared light confers thermal protection in birds. *Nature Communications* **9**.

MEDJOUBI, K., LECLERCQ, N., LANGLOIS, F., BUTEAU, A., LÉ, S., POIRIER, S., MERCÈRE, P., SFORNA, M.C., KEWISH, C.M. & SOMOGYI, A. (2013) Development of fast, simultaneous and multi-technique scanning hard X-ray microscopy at Synchrotron Soleil. *Journal of Synchrotron Radiation* **20**, 293–299.

MENG, Y., KATSUMA, S., MITA, K. & SHIMADA, T. (2009) Abnormal red body coloration of the silkworm, Bombyx mori, is caused by a mutation in a novel kynureninase. *Genes to Cells* **14**, 129–140.

MESSENGER, J.B. (2001) Cephalopod chromatophores: neurobiology and natural history. *Biological Reviews* **76**, 473–528.

MICHELS, H., SEINSTRA, R.I., UITDEHAAG, J.C.M., KOOPMAN, M., VAN FAASSEN, M., MARTINEAU, C.N., KEMA, I.P., BUIJSMAN, R. & NOLLEN, E.A.A. (2016) Identification of an evolutionary conserved structural loop that is required for the enzymatic and biological function of tryptophan 2,3-dioxygenase. *Scientific Reports* **6**, 39199.

MIRONOV, A.A., SESOROVA, I.S., SELIVERSTOVA, E.V. & BEZNOUSSENKO, G.V. (2017) Different Golgi ultrastructure across species and tissues: Implications under functional and pathological conditions, and an attempt at classification. *Tissue and Cell* **49**, 186–201.

MIROW, S. (1972) Skin color in the squids Loligo pealii and Loligo opalescens: I. Chromatophores. *Zeitschrift für Zellforschung und Mikroskopische Anatomie* **125**, 143–175.

MOORE, G.P. & SULLIVAN, D.T. (1978) Biochemical and genetic characterization of kynurenine formamidase from Drosophila melanogaster. *Biochemical Genetics* **16**, 619–634.

MORAN, N.A. & JARVIK, T. (2010) Lateral Transfer of Genes from Fungi Underlies Carotenoid Production in Aphids. *Science* **328**, 624–627.

MORGAN, T.H. (1910) Sex Limited Inheritance in Drosophila. *Science* **32**, 120–122.

MORSE, D.H. (2007) *Predator upon a flower: life history and fitness in a crab spider*. Harvard University Press, Cambridge, London.

VAN MOURIK, T., BÜHL, M. & GAIGEOT, M.-P. (2014) Density functional theory across chemistry, physics and biology. *Philosophical Transactions of the Royal Society A: Mathematical, Physical and Engineering Sciences* **372**, 20120488.

MÜLLER, F. (1879) Ituna and Thyridia: a remarkable case of mimicry in butterflies. *Proceedings of the Entomological Society of London*, 20–29.

MULLINS, C., HARTNELL, L.M. & BONIFACINO, J.S. (2000) Distinct requirements for the AP-3 adaptor complex in pigment granule and synaptic vesicle biogenesis in Drosophila melanogaster. *MGG - Molecular and General Genetics* **263**, 1003–1014.

MULLINS, C., HARTNELL, L.M., WASSARMAN, D.A. & BONIFACINO, J.S. (1999) Defective expression of the μ3 subunit of the AP-3 adaptor complex in the Drosophila pigmentation mutant carmine. *Molecular and General Genetics MGG* **262**, 401–412.

MUNDLE, S.O.C. & KLUGER, R. (2009) Decarboxylation via Addition of Water to a Carboxyl Group: Acid Catalysis of Pyrrole-2-Carboxylic Acid. *Journal of the American Chemical Society* **131**, 11674–11675.

MUNRO, J.T., MEDINA, I., WALKER, K., MOUSSALLI, A., KEARNEY, M.R., DYER, A.G., GARCIA, J., RANKIN, K.J. & STUART-FOX, D. (2019) Climate is a strong predictor of near-infrared reflectance but a poor predictor of colour in butterflies. *Proceedings of the Royal Society B: Biological Sciences* **286**, 20190234.

MURASE, D., HACHIYA, A., TAKANO, K., HICKS, R., VISSCHER, M.O., KITAHARA, T., HASE, T., TAKEMA, Y. & YOSHIMORI, T. (2013) Autophagy Has a Significant Role in Determining Skin Color by Regulating Melanosome Degradation in Keratinocytes. *Journal of Investigative Dermatology* **133**, 2416–2424.

MURK, J., POSTHUMA, G., KOSTER, A.J., GEUZE, H.J., VERKLEIJ, A.J., KLEIJMEER, M.J. & HUMBEL, B.M. (2003) Influence of aldehyde fixation on the morphology of endosomes and lysosomes: quantitative analysis and electron tomography. *Journal of microscopy* **212**, 81–90.

NADEAU, N.J. (2016) Genes controlling mimetic colour pattern variation in butterflies. *Current Opinion in Insect Science* **17**, 24–31.

NAKAZAWA, H., CHOU, F.E., ANDREWS, P.A. & BACHUR, N.R. (1981) Chemical reduction of actinomycin D and phenoxazone analog to free radicals. *The Journal of Organic Chemistry* **46**, 1493–1496.

NASSAU, K. (1987) The fifteen causes of color: The physics and chemistry of color. *Color Research & Application* **12**, 4–26.

NAVARRO, R.E., RAMOS-BALDERAS, J.L., GUERRERO, I., PELCASTRE, V. & MALDONADO, E. (2008) Pigment Dilution Mutants from Fish Models with Connection to Lysosome-Related Organelles and Vesicular Traffic Genes. *Zebrafish* **5**, 309–318.

NEEDHAM, A.E. (1974) *The significance of zoochromes*. Springer-Verlag, Berlin, Heidelberg, New York.

NENTWIG, W. (ed) (2013) *Spider Ecophysiology*. Springer Berlin Heidelberg, Berlin, Heidelberg.

NEWBIGIN, M.I. (1898) *Colour in nature; a study in biology*. John Murray, London.

NIJHOUT, H.F. (1997) Ommochrome pigmentation of the linea and rosa seasonal forms of Precis coenia (Lepidoptera: Nymphalidae). *Archives of insect biochemistry and physiology* **36**, 215–222.

NIJHOUT, H.F. (2010) Molecular and Physiological Basis of Colour Pattern Formation. In *Advances in Insect Physiology* (eds J. CASAS & S.J. SIMPSON), pp. 219–265. Elsevier, Academic Press.

NILSSON, D.-E. & KELBER, A. (2007) A functional analysis of compound eye evolution. *Arthropod Structure & Development* **36**, 373–385.

NISHIKAWA, H., IGA, M., YAMAGUCHI, J., SAITO, K., KATAOKA, H., SUZUKI, Y., SUGANO, S. & FUJIWARA, H. (2013) Molecular basis of wing coloration in a Batesian mimic butterfly, *Papilio polytes*. *Scientific Reports* **3**.

NISHIKIMI, M., YAMADA, H. & YAGI, K. (1978) Generation of superoxide anion with photoreduced phenoxazine derivative. *Photochemistry and Photobiology* **27**, 269–272.

NORMAN, M.D., FINN, J. & TREGENZA, T. (2001) Dynamic mimicry in an Indo-Malayan octopus. *Proceedings of the Royal Society B: Biological Sciences* **268**, 1755–1758.

OOI, C.E., MOREIRA, J.E., DELL'ANGELICA, E.C., POY, G., WASSARMAN, D.A. & BONIFACINO, J.S. (1997) Altered expression of a novel adaptin leads to defective pigment granule biogenesis in the Drosophila eye color mutant garnet. *The EMBO Journal* **16**, 4508–4518.

ORLOW, S.J. (1995) Melanosomes Are Specialized Members of the Lysosomal Lineage of Organelles. *Journal of Investigative Dermatology* **105**, 3–7.

OSANAI-FUTAHASHI, M., TATEMATSU, K., FUTAHASHI, R., NARUKAWA, J., TAKASU, Y., KAYUKAWA, T., SHINODA, T., ISHIGE, T., YAJIMA, S., TAMURA, T., YAMAMOTO, K. & SEZUTSU, H. (2016) Positional cloning of a Bombyx pink-eyed white egg locus reveals the major role of cardinal in ommochrome synthesis. *Heredity* **116**, 135–145.

OSANAI-FUTAHASHI, M., TATEMATSU, K. -I., YAMAMOTO, K., NARUKAWA, J., UCHINO, K., KAYUKAWA, T., SHINODA, T., BANNO, Y., TAMURA, T. & SEZUTSU, H. (2012) Identification of the Bombyx Red Egg Gene Reveals Involvement of a Novel Transporter Family Gene in Late Steps of the Insect Ommochrome Biosynthesis Pathway. *Journal of Biological Chemistry* **287**, 17706–17714.

OSTROVSKY, M.A. & DONTSOV, A.E. (2019) Vertebrate Eye Melanosomes and Invertebrate Eye Ommochromes as Antioxidant Cell Organelles: Part 2. *Biology Bulletin* **46**, 105–116.

OSTROVSKY, M.A., SAKINA, N.L. & DONTSOV, A.E. (1987) An antioxidative role of ocular screening pigments. *Vision Research* **27**, 893–899.

OXFORD, G.S. & GILLESPIE, R.G. (1998) Evolution and ecology of spider coloration. *Annual review of entomology* **43**, 619–643.

PANETTIERI, S., GJINAJ, E., JOHN, G. & LOHMAN, D.J. (2018) Different ommochrome pigment mixtures enable sexually dimorphic Batesian mimicry in disjunct populations of the common palmfly butterfly, *Elymnias hypermnestra*. *PLOS ONE* **13**, e0202465.

PARISI, G., CARFAGNA, M. & D'AMORA, D. (1976a) A proposed biosynthesis pathway of drosopterins in Drosophila melanogaster. *Journal of insect physiology* **22**, 415–423.

PARISI, G., CARFAGNA, M. & D'AMORA, D. (1976b) Biosynthesis of dihydroxanthommatin in Drosophila melanogaster: Possible involvement of xanthine dehydrogenase. *Insect Biochemistry* **6**, 567–570.

PARRILLI, M. & BOLOGNESE, A. (1992) 1H and 13C Chemical Shift Data of Some Ommochrome Models: Substituted Benzo[3,2-a]-5H-phenoxazin-5-one. *Heterocycles* **34**, 1829.

PATWARDHAN, A., BARDIN, S., MISEREY-LENKEI, S., LARUE, L., GOUD, B., RAPOSO, G. & DELEVOYE, C. (2017) Routing of the RAB6 secretory pathway towards the lysosome related organelle of melanocytes. *Nature Communications* **8**, 15835.

PAUL-GILLOTEAUX, P., HEILIGENSTEIN, X., BELLE, M., DOMART, M.-C., LARIJANI, B., COLLINSON, L., RAPOSO, G. & SALAMERO, J. (2017) eC-CLEM: flexible multidimensional registration software for correlative microscopies. *Nature methods* **14**, 102.

PEARSON, R.G. (1992) The electronic chemical potential and chemical hardness. *Journal of Molecular Structure: THEOCHEM* **255**, 261–270.

PENER, M.P. & SIMPSON, S.J. (2009) Locust Phase Polyphenism: An Update. In *Advances in Insect Physiology* pp. 1–272. Elsevier.

PERRELET, A., ORCI, L. & BAUMANN, F. (1971) Evidence for granulolysis in the retinula cells of a stomatopod crustacean, Squilla mantis. *The Journal of Cell Biology* **48**, 684–688.

PEVERATI, R. & TRUHLAR, D.G. (2011) Improving the Accuracy of Hybrid Meta-GGA Density Functionals by Range Separation. *The Journal of Physical Chemistry Letters* **2**, 2810–2817.

PHILLIPS, J.P. & FORREST, H.S. (1970) Terminal synthesis of xanthommatin in Drosophila melanogaster. II. Enzymatic formation of the phenoxazinone nucleus. *Biochemical Genetics* **4**, 489–498.

PHILLIPS, J.P., FORREST, H.S. & KULKARNI, A.D. (1973) Terminal synthesis of xanthommatin in Drosophila melanogaster. III. Mutational pleiotropy and pigment granule association of phenoxazinone synthetase. *Genetics* **73**, 45–56.

PINKERT, S. & ZEUSS, D. (2018) Thermal Biology: Melanin-Based Energy Harvesting across the Tree of Life. *Current Biology* **28**, R887–R889.

PLOTKIN, M., HOD, I., ZABAN, A., BODEN, S.A., BAGNALL, D.M., GALUSHKO, D. & BERGMAN, D.J. (2010) Solar energy harvesting in the epicuticle of the oriental hornet (Vespa orientalis). *Naturwissenschaften* **97**, 1067–1076.

POULTON, E.B. (1890) *The colours of animals, their meaning and use, especially considered in the case of insects*. D. Appleton and Company, New York.

PRICE-WHELAN, A., DIETRICH, L.E.P. & NEWMAN, D.K. (2006) Rethinking 'secondary' metabolism: physiological roles for phenazine antibiotics. *Nature Chemical Biology* **2**, 71–78.

PRUM, R.O., COLE, J.A. & TORRES, R.H. (2004) Blue integumentary structural colours in dragonflies (Odonata) are not produced by incoherent Tyndall scattering. *Journal of Experimental Biology* **207**, 3999–4009.

PRYOR, P.R., MULLOCK, B.M., BRIGHT, N.A., GRAY, S.R. & LUZIO, J.P. (2000) The Role of Intraorganellar Ca2+ in Late Endosome–Lysosome Heterotypic Fusion and in the Reformation of Lysosomes from Hybrid Organelles. *The Journal of Cell Biology* **149**, 10.

PUSHIE, M.J., PICKERING, I.J., KORBAS, M., HACKETT, M.J. & GEORGE, G.N. (2014) Elemental and Chemically Specific X-ray Fluorescence Imaging of Biological Systems. *Chemical Reviews* **114**, 8499–8541.

R CORE TEAM (2017) *R: A Language and Environment for Statistical Computing*. R Foundation for Statistical Computing, Vienna, Austria.

RAHMAN, M., HABERMAN, A., TRACY, C., RAY, S. & KRÄMER, H. (2012) *Drosophila mauve* Mutants Reveal a Role of LYST Homologs Late in the Maturation of Phagosomes and Autophagosomes: A *Drosophila* Model for Chediak-Higashi Syndrome. *Traffic* **13**, 1680–1692.

RAPOSO, G. & MARKS, M.S. (2007) Melanosomes — dark organelles enlighten endosomal membrane transport. *Nature Reviews Molecular Cell Biology* **8**, 786–797.

RAPOSO, G., TENZA, D., MURPHY, D.M., BERSON, J.F. & MARKS, M.S. (2001) Distinct Protein Sorting and Localization to Premelanosomes, Melanosomes, and Lysosomes in Pigmented Melanocytic Cells. *The Journal of Cell Biology* **152**, 809–824.

RASGON, J.L. & SCOTT, T.W. (2004) Crimson: a novel sex-linked eye color mutant of Culex pipiens L. (Diptera: Culicidae). *Journal of Medical Entomology* **41**, 385–391.

REAUME, A.G., KNECHT, D.A. & CHOVNICK, A. (1991) The rosy locus in Drosophila melanogaster: xanthine dehydrogenase and eye pigments. *Genetics* **129**, 1099–1109.

REED, R.D., MCMILLAN, W.O. & NAGY, L.M. (2008) Gene expression underlying adaptive variation in Heliconius wing patterns: non-modular regulation of overlapping cinnabar and vermilion prepatterns. *Proceedings of the Royal Society B: Biological Sciences* **275**, 37–46.

REED, R.D. & NAGY, L.M. (2005) Evolutionary redeployment of a biosynthetic module: expression of eye pigment genes vermilion, cinnabar, and white in butterfly wing development. *Evolution & development* **7**, 301–311.

REITER, S., HÜLSDUNK, P., WOO, T., LAUTERBACH, M.A., EBERLE, J.S., AKAY, L.A., LONGO, A., MEIER-CREDO, J., KRETSCHMER, F., LANGER, J.D., KASCHUBE, M. & LAURENT, G. (2018) Elucidating the control and development of skin patterning in cuttlefish. *Nature* **562**, 361–366.

RIDDIFORD, L.M. & AJAMI, A.M. (1971a) Purification and characterization of an ommochrome-protein from the eyes of saturniid moths. *Biochemistry* **10**, 1455–1460.

RIDDIFORD, L.M. & AJAMI, A.M. (1971b) Identification of an ommochrome in the eyes and nervous systems of saturniid moths. *Biochemistry* **10**, 1451–1455.

RIOU, M. & CHRISTIDÈS, J.-P. (2010) Cryptic Color Change in a Crab Spider (Misumena vatia): Identification and Quantification of Precursors and Ommochrome Pigments by HPLC. *Journal of Chemical Ecology* **36**, 412–423.

RIPOLL, L., HEILIGENSTEIN, X., HURBAIN, I., DOMINGUES, L., FIGON, F., PETERSEN, K.J., DENNIS, M.K., HOUDUSSE, A., MARKS, M.S., RAPOSO, G. & DELEVOYE, C. (2018) Myosin VI and branched actin filaments mediate membrane constriction and fission of melanosomal tubule carriers. *The Journal of Cell Biology* **217**, 2709–2726.

ROBERTS, J.E., WISHART, J.F., MARTINEZ, L. & CHIGNELL, C.F. (2000) Photochemical studies on xanthurenic acid. *Photochemistry and photobiology* **72**, 467–471.

ROBERTSON, I.C. & MAGUIRE, D.K. (2005) Crab spiders deter insect visitations to slickspot peppergrass flowers. *Oikos* **109**, 577–582.

ROBERTSON, J.D. (1960) A molecular theory of cell membrane structure. In *Verhandlungen Band II / Biologisch-Medizinischer Teil* (eds W. BARGMANN, D. PETERS & C. WOLPERS), pp. 159–171. Springer Berlin Heidelberg, Berlin, Heidelberg.

RODRIGUEZ-FERNANDEZ, I.A. & DELL'ANGELICA, E.C. (2015) Identification of Atg2 and ArfGAP1 as Candidate Genetic Modifiers of the Eye Pigmentation Phenotype of Adaptor Protein-3 (AP-3) Mutants in Drosophila melanogaster. *PLOS ONE* **10**.

ROMERO, G.Q. & VASCONCELLOS-NETO, J. (2004) Beneficial effects of flower-dwelling predators on their host plant. *Ecology* **85**, 446–457.

ROMERO, Y. & MARTÍNEZ, A. (2015) Antiradical capacity of ommochromes. *Journal of Molecular Modeling* **21**.

ROOSEVELT, T. (1911) Revealing and concealing coloration in birds and mammals. *Bulletin American Museum of Natural History* **30**, 119–231. New York: Published by order of the Trustees, American Museum of Natural History.

ROTHSCHILD, LORD & TYLER, A. (1958) The oxidative metabolism of eggs of Urechis caupo. *The Biological Bulletin* **115**, 136–146.

SANTORO, F. & JACQUEMIN, D. (2016) Going beyond the vertical approximation with time-dependent density functional theory. *Wiley Interdisciplinary Reviews: Computational Molecular Science* **6**, 460–486.

SANTORO, P. & PARISI, G. (1987) Biosynthesis of dihydroxanthommatin. *Insect Biochemistry* **17**, 635–638.

SAWADA, H. (1994) Biochemical studies on the pigment granules of insects : Accumulation and localization of ommochrome in epidermal cells of the silkworm, Bombyx mori. Tokyo Metropolitan University, Tokyo.

SAWADA, H., IINO, T. & TSUUÉ, M. (1997) Properties of ommochrome-binding proteins from the pigment granules in epidermal cells of the silkworm, Bombyx mori. *The Journal of Sericultural Science of Japan* **66**, 393–402.

SAWADA, H., NAKAGOSHI, M., MASE, K. & YAMAMOTO, T. (2000) Occurrence of ommochrome-containing pigment granules in the central nervous system of the silkworm, Bombyx mori. *Comparative Biochemistry and Physiology Part B: Biochemistry and Molecular Biology* **125**, 421–428.

SAWADA, H., NAKAGOSHI, M., YAMAMOTO, T., KATO, T., MASE, K., YAMAMOTO, T. & IZUMI, S. (2002) Purification and characterization of an ommin-binding protein from an acid-methanol extract of diapause eggs of the silkworm, Bombyx mori. *Journal of Insect Biotechnology and Sericology* **71**, 103–108.

SAWADA, H., TSUSUÉ, M., YAMAMOTO, T. & SAKURAI, S. (1990) Occurrence of xanthommatin containing pigment granules in the epidermal cells of the silkworm, Bombyx mori. *Insect Biochemistry* **20**, 785–792.

SAWADA, H., YAMAHAMA, Y., MASE, K., HIRAKAWA, H. & IINO, T. (2007) Molecular properties and tissue distribution of 30K proteins as ommin-binding proteins from diapause eggs of the silkworm, Bombyx mori. *Comparative Biochemistry and Physiology Part B: Biochemistry and Molecular Biology* **146**, 172–179.

SCHÄFER, W. & GEYER, I. (1972) Über das redoxverhalten der ommochrome UV/S-spektren von 3h-phenoxazinonen-(3) und phenoxazinen. *Tetrahedron* **28**, 5261–5279.

SCHENK, F. (2009) Nature's Fluctuating Colour Captured on Canvas? *International Journal of Design & Nature and Ecodynamics* **4**, 274–284.

SCHENK, F. (2015) Biomimetics, color, and the arts. In (eds A. LAKHTAKIA, M. KNEZ & R.J. MARTÍN-PALMA), p. 94290Z. San Diego, California, United States.

SCHINDELIN, J., ARGANDA-CARRERAS, I., FRISE, E., KAYNIG, V., LONGAIR, M., PIETZSCH, T., PREIBISCH, S., RUEDEN, C., SAALFELD, S., SCHMID, B., TINEVEZ, J.-Y., WHITE, D.J., HARTENSTEIN, V., ELICEIRI, K., TOMANCAK, P., ET AL. (2012) Fiji: an open-source platform for biological-image analysis. *Nature Methods* **9**, 676–682.

SCHRAERMEYER, U. (1993) Does Melanin Turnover Occur in the Eyes of Adult Vertebrates? *Pigment Cell Research* **6**, 193–204.

SCHRAERMEYER, U. & DOHMS, M. (1993) Atypical Granules in the Eyes of the White Mutant of Drosophila melanogaster Are Lysosome-Related Organelles. *Pigment cell research* **6**, 73–84.

SCHRAERMEYER, U., RACK, M. & STIEVE, H. (1993) Residual bodies resulting from photosensory membrane degradation are taken up by pigment cells in the eyes of the flyLucilia sp. *Cell & Tissue Research* **271**, 519–528.

SEIJI, M., FITZPATRICK, T.B., SIMPSON, R.T. & BIRBECK, M.S.C. (1963) Chemical Composition and Terminology Of Specialized Organelles (Melanosomes and Melanin Granules) in Mammalian Melanocytes. *Nature* **197**, 1082–1084.

SEKIMURA, T. & NIJHOUT, H.F. (2017) *Diversity and Evolution of Butterfly Wing Patterns: an Integrative Approach*. Springer Singapore Imprint : Springer, Singapore.

SELIGY, V.L. (1972) Ommochrome pigments of spiders. *Comparative Biochemistry and Physiology Part A: Physiology* **42**, 699–709.

SEVRIOUKOV, E.A., HE, J.-P., MOGHRABI, N., SUNIO, A. & KRÄMER, H. (1999) A Role for the deep orange and carnation Eye Color Genes in Lysosomal Delivery in Drosophila. *Molecular Cell* **4**, 479–486.

SHAH, R., MARGISON, K. & PRATT, D.A. (2017) The Potency of Diarylamine Radical-Trapping Antioxidants as Inhibitors of Ferroptosis Underscores the Role of Autoxidation in the Mechanism of Cell Death. *ACS Chemical Biology*.

SHAWKEY, M.D. & D'ALBA, L. (2017) Interactions between colour-producing mechanisms and their effects on the integumentary colour palette. *Philosophical Transactions of the Royal Society B: Biological Sciences* **372**, 20160536.

SHERIN, P.S., GRILJ, J., KOPYLOVA, L.V., YANSHOLE, V.V., TSENTALOVICH, Y.P. & VAUTHEY, E. (2010) Photophysics and Photochemistry of the UV Filter Kynurenine Covalently Attached to Amino Acids and to a Model Protein. *The Journal of Physical Chemistry B* **114**, 11909–11919.

SHESTOPAL, S.A., MAKUNIN, I.V., BELYAEVA, E.S., ASHBURNER, M. & ZHIMULEV, I.F. (1997) Molecular characterisation of the deep orange (dor) gene of Drosophila melanogaster. *Molecular and General Genetics MGG* **253**, 642–648.

SHIBATA, T., PROTA, G. & MISHIMA, Y. (1993) Non-Melanosomal Regulatory Factors in Melanogenesis. *Journal of Investigative Dermatology* **100**, S274–S280.

SHOUP, J.R. (1966) The development of pigment granules in the eyes of wild type and mutant Drosophila melanogaster. *The Journal of cell biology* **29**, 223–249.

SITARAM, A. & MARKS, M.S. (2012) Mechanisms of Protein Delivery to Melanosomes in Pigment Cells. *Physiology* **27**, 85–99.

SMITH, J.R., JAMIE, J.F. & GUILLEMIN, G.J. (2016) Kynurenine-3-monooxygenase: a review of structure, mechanism, and inhibitors. *Drug Discovery Today* **21**, 315–324.

SOLANO, F., JIMÉNEZ-CERVANTES, C., MARTÍNEZ-LIARTE, J.H., GARCÍA-BORRÓN, J.C., JARA, J.R. & LOZANO, J.A. (1996) Molecular mechanism for catalysis by a new zinc-enzyme, dopachrome tautomerase. *Biochemical Journal* **313**, 447–453.

SOMOGYI, A., MEDJOUBI, K., BARANTON, G., LE ROUX, V., RIBBENS, M., POLACK, F., PHILIPPOT, P. & SAMAMA, J.-P. (2015) Optical design and multi-length-scale scanning spectro-microscopy possibilities at the Nanoscopium beamline of Synchrotron Soleil. *Journal of Synchrotron Radiation* **22**, 1118–1129.

SONG, P., RUAN, M., SUN, X., ZHANG, Y. & XU, W. (2014) Theoretical Study of Resorufin Reduction Mechanism by $NaBH_4$. *The Journal of Physical Chemistry B* **118**, 10224–10231.

SOSINSKY, G.E., CRUM, J., JONES, Y.Z., LANMAN, J., SMARR, B., TERADA, M., MARTONE, M.E., DEERINCK, T.J., JOHNSON, J.E. & ELLISMAN, M.H. (2008) The combination of chemical fixation procedures with high pressure freezing and freeze substitution preserves highly labile tissue ultrastructure for electron tomography applications. *Journal of Structural Biology* **161**, 359–371.

SOUSA, A.A. & LEAPMAN, R.D. (2012) Development and application of STEM for the biological sciences. *Ultramicroscopy* **123**, 38–49.

STANKA, P. (1974) Ultrastructural study of pigment cells of human red hair. *Cell and Tissue Research* **150**.

STARK, W.S. & SAPP, R. (1988) Eye color pigment granules in wild-type and mutant Drosophila melanogaster. *Canadian journal of zoology* **66**, 1301–1308.

STAROVEROV, V.N., SCUSERIA, G.E., TAO, J. & PERDEW, J.P. (2003) Comparative assessment of a new nonempirical density functional: Molecules and hydrogen-bonded complexes. *The Journal of Chemical Physics* **119**, 12129–12137.

STAVENGA, D. (2002) Colour in the eyes of insects. *Journal of Comparative Physiology A: Sensory, Neural, and Behavioral Physiology* **188**, 337–348.

STAVENGA, D.G. (1989) Pigments in compound eyes. In *Facets of vision* (eds D.G. STAVENGA & R.C. HARDIE), pp. 152–172. Springer, Berlin, Heidelberg.

STAVENGA, D.G., LEERTOUWER, H.L. & WILTS, B.D. (2014) Coloration principles of nymphaline butterflies - thin films, melanin, ommochromes and wing scale stacking. *Journal of Experimental Biology* **217**, 2171–2180.

STAVENGA, D.G., WEHLING, M.F. & BELUŠIČ, G. (2017) Functional interplay of visual, sensitizing and screening pigments in the eyes of *Drosophila* and other red-eyed dipteran flies: Pigments of red-eyed flies. *The Journal of Physiology* **595**, 5481–5494.

STEVENS, M., RONG, C.P. & TODD, P.A. (2013) Colour change and camouflage in the horned ghost crab Ocypode ceratophthalmus. *Biological Journal of the Linnean Society* **109**, 257–270.

STEVENS, R., STEVENS, L. & PRICE, N. (1983) The stabilities of various thiol compounds used in protein purifications. *Biochemical Education* **11**, 70.

STUART-FOX, D. & MOUSSALLI, A. (2009) Camouflage, communication and thermoregulation: lessons from colour changing organisms. *Philosophical Transactions of the Royal Society B: Biological Sciences* **364**, 463–470.

STUART-FOX, D., NEWTON, E. & CLUSELLA-TRULLAS, S. (2017) Thermal consequences of colour and near-infrared reflectance. *Philosophical Transactions of the Royal Society B: Biological Sciences* **372**, 20160345.

STUBENHAUS, B.M., DUSTIN, J.P., NEVERETT, E.R., BEAUDRY, M.S., NADEAU, L.E., BURK-MCCOY, E., HE, X., PEARSON, B.J. & PELLETTIERI, J. (2016) Light-induced depigmentation in planarians models the pathophysiology of acute porphyrias. *eLife* **5**, e14175.

STUDER, D., HUMBEL, B.M. & CHIQUET, M. (2008) Electron microscopy of high pressure frozen samples: bridging the gap between cellular ultrastructure and atomic resolution. *Histochemistry and Cell Biology* **130**, 877–889.

SU, X., WELLEN, K.E. & RABINOWITZ, J.D. (2016) Metabolic control of methylation and acetylation. *Current Opinion in Chemical Biology* **30**, 52–60.

SUGUMARAN, M. & BAREK, H. (2016) Critical Analysis of the Melanogenic Pathway in Insects and Higher Animals. *International Journal of Molecular Sciences* **17**, 1753.

SULLIVAN, D.T., GRILLO, S.L. & KITOS, R.J. (1974) Subcellular localization of the first three enzymes of the ommochrome synthetic pathway in Drosophila melanogaster. *Journal of Experimental Zoology* **188**, 225–233.

SUMMERS, K.M., HOWELLS, A.J. & PYLIOTIS, N.A. (1982) Biology of Eye Pigmentation in Insects. In *Advances in Insect Physiology* (eds M.J. BERRIDGE, J.E. TREHERNE & V.B. WIGGLESWORTH), pp. 119–166. Elsevier, Academic Press.

SUMNER, F.B. (1937) Color and Pigmentation: Why They Should Interest Us as Biologists. *The Scientific Monthly* **44**, 350–352.

SUN, J., WU, W., LIU, C. & TONG, J. (2017a) Investigating the nanomechanical properties and reversible color change properties of the beetle *Dynastes tityus*. *Journal of Materials Science* **52**, 6150–6160.

SUN, Y., TIAN, L., WEN, J., ZHAO, J., ZHANG, W., XIE, C., ZHOU, M., QIU, X. & CHEN, D. (2017b) Morphologies of eumelanins from the ink of six cephalopods species measured by atomic force microscopy. *Journal of Ocean University of China* **16**, 461–467.

SUTHERLAND, R.L., MÄTHGER, L.M., HANLON, R.T., URBAS, A.M. & STONE, M.O. (2008) Cephalopod coloration model I Squid chromatophores and iridophores. *Journal of the Optical Society of America A* **25**, 588.

SUZUKI, T., OISO, N., GAUTAM, R., NOVAK, E.K., PANTHIER, J.-J., SUPRABHA, P.G., VIDA, T., SWANK, R.T. & SPRITZ, R.A. (2003) The mouse organellar biogenesis mutant buff results from a mutation in Vps33a, a homologue of yeast vps33 and Drosophila carnation. *Proceedings of the National Academy of Sciences* **100**, 1146–1150.

SZATYLOWICZ, H., STASYUK, O.A. & KRYGOWSKI, T.M. (2016) Calculating the Aromaticity of Heterocycles. In *Advances in Heterocyclic Chemistry* pp. 301–327. Elsevier.

TAKAMIYA, M., XU, F., SUHONEN, H., GOURAIN, V., YANG, L., HO, N.Y., HELFEN, L., SCHRÖCK, A., ETARD, C., GRABHER, C., RASTEGAR, S., SCHLUNCK, G., REINHARD, T., BAUMBACH, T. & STRÄHLE, U. (2016) Melanosomes in pigmented epithelia maintain eye lens transparency during zebrafish embryonic development. *Scientific Reports* **6**.

TAKEUCHI, K., SATOU, Y., YAMAMOTO, H. & SATOH, N. (2005) A Genome-Wide Survey of Genes for Enzymes Involved in Pigment Synthesis in an Ascidian, Ciona intestinalis. *Zoological Science* **22**, 723–734.

TANAKA, S., HARANO, K., NISHIDE, Y. & SUGAHARA, R. (2016) The mechanism controlling phenotypic plasticity of body color in the desert locust: some recent progress. *Current Opinion in Insect Science* **17**, 10–15.

TANAKA, Y. (1953) Genetics of the Silkworm, Bombyx mori. In *Advances in Genetics* (ed M. DEMEREC), pp. 239–317. Elsevier, Academic Press.

TATEMATSU, K., YAMAMOTO, K., UCHINO, K., NARUKAWA, J., IIZUKA, T., BANNO, Y., KATSUMA, S., SHIMADA, T., TAMURA, T., SEZUTSU, H. & DAIMON, T. (2011) Positional cloning of silkworm white egg 2 (w-2) locus shows functional conservation and diversification of ABC transporters for pigmentation in insects: Silkworm white egg 2 mutants. *Genes to Cells* **16**, 331–342.

TEYSSIER, J., SAENKO, S.V., VAN DER MAREL, D. & MILINKOVITCH, M.C. (2015) Photonic crystals cause active colour change in chameleons. *Nature Communications* **6**, 6368.

THAYER, A.H. & THAYER, G.H. (1909) *Concealing-coloration in the animal kingdom; an exposition of the laws of disguise through color and pattern: being a summary of Abbott H. Thayer's discoveries,*. The Macmillan Co., New York,.

THÉRY, M. & CASAS, J. (2002) Visual systems: predator and prey views of spider camouflage. *Nature* **415**, 133–133.

THÉRY, M. & CASAS, J. (2009) The multiple disguises of spiders: web colour and decorations, body colour and movement. *Philosophical Transactions of the Royal Society B: Biological Sciences* **364**, 471–480.

THÉRY, M., DEBUT, M., GOMEZ, D. & CASAS, J. (2004) Specific color sensitivities of prey and predator explain camouflage in different visual systems. *Behavioral Ecology* **16**, 25–29.

TOMODA, A., YONEYAMA, Y., YAMAGUCHI, T., SHIRAO, E. & KAWASAKI, K. (1990) Mechanism of Coloration of Human Lenses Induced by Near-Ultraviolet-Photo-Oxidized 3-Hydroxykynurenine (With 1 color plate). *Ophthalmic Research* **22**, 152–159.

TRACY, C.R., TURNER, J.S., BARTHOLOMEW, G.A., BENNETT, A., BILLINGS, W., CHABOT, B.F., GATES, D.M., HEINRICH, B., HUEY, R.B., JANZEN, D.H. & OTHERS (1982) What is physiological ecology? *Bulletin of the Ecological Society of America* **63**, 340–347. JSTOR.

TSAI, C.-C., CHILDERS, R.A., NAN SHI, N., REN, C., PELAEZ, J.N., BERNARD, G.D., PIERCE, N.E. & YU, N. (2020) Physical and behavioral adaptations to prevent overheating of the living wings of butterflies. *Nature Communications* **11**, 551.

TSENTALOVICH, Y.P., SNYTNIKOVA, O.A. & SAGDEEV, R.Z. (2008) Photochemical and thermal reactions of kynurenines. *Russian Chemical Reviews* **77**, 789–797.

UDA, H. (1932) On egg coloration of domestic silkworm. *Scientific papers dedicated to the tenth anniversary of the Miye College of Agriculture and Forestry*, 21–42.

UKHANOV, K.Y. (1991) Ommochrome pigment granules: A calcium reservoir in the dipteran eyes. *Comparative Biochemistry and Physiology Part A: Physiology* **98**, 9–16.

UMBERS, K.D.L., FABRICANT, S.A., GAWRYSZEWSKI, F.M., SEAGO, A.E. & HERBERSTEIN, M.E. (2014) Reversible colour change in Arthropoda. *Biological Reviews* **89**, 820–848.

UMEBACHI, Y. (1985) Papiliochrome, a New Pigment Group of Butterfly. *Zoological science* **2**, 163–174.

USHAKOVA, N., DONTSOV, A., SAKINA, N., BASTRAKOV, A. & OSTROVSKY, M. (2019) Antioxidative Properties of Melanins and Ommochromes from Black Soldier Fly Hermetia illucens. *Biomolecules* **9**, 408.

VALENTIJN, K.M., VALENTIJN, J.A., JANSEN, K.A. & KOSTER, A.J. (2008) A new look at Weibel–Palade body structure in endothelial cells using electron tomography. *Journal of Structural Biology* **161**, 447–458.

VAN DEN BRANDEN, C. & DECLEIR, W. (1976) A study of the chromotaphore pigments in the skin of the cephalopod Sepia officinalis. *Biologische Jaarb* **44**, 345–352.

VARGAS-LOWMAN, A., ARMISEN, D., FLORIANO, C.F.B., DA ROCHA SILVA CORDEIRO, I., VIALA, S., BOUCHET, M., BERNARD, M., LE BOUQUIN, A., SANTOS, M.E., BERLIOZ-BARBIER, A., SALVADOR, A., FIGUEIREDO MOREIRA, F.F., BONNETON, F. & KHILA, A. (2019) Cooption of the pteridine biosynthesis pathway underlies the diversification of embryonic colors in water striders. *Proceedings of the National Academy of Sciences*, 201908316.

VAZQUEZ, S., GARNER, B., SHEIL, M.M. & TRUSCOTT, R.J. (2000) Characterisation of the major autoxidation products of 3-hydroxykynurenine under physiological conditions. *Free radical research* **32**, 11–23.

VAZQUEZ, S., TRUSCOTT, R.J.W., O'HAIR, R.A.J., WEIMANN, A. & SHEIL, M.M. (2001) A study of kynurenine fragmentation using electrospray tandem mass spectrometry. *Journal of the American Society for Mass Spectrometry* **12**, 786–794.

VERON, J.E.N., O'FARRELL, A.F. & DIXON, B. (1974) The fine structure of odonata chromatophores. *Tissue and Cell* **6**, 613–626.

VOGLIARDI, S., BERTAZZO, A., COMAI, S., COSTA, C.V.L., ALLEGRI, G., SERAGLIA, R. & TRALDI, P. (2004) An investigation on the role of 3-hydroxykynurenine in pigment formation by matrix-assisted laser desorption/ionization mass spectrometry. *Rapid Communications in Mass Spectrometry* **18**, 1413–1420.

WACHMANN, E. (1969) Multivesikuläre und andere Einschlubkörper in den Retinulazellen der Sumpfgrille Pteronemobius heydeni (Fischer). *Zeitschrift für Zellforschung und Mikroskopische Anatomie* **99**, 263–276.

WAKSMAN, S.A. & WOODRUFF, H.B. (1940) Bacteriostatic and Bactericidal Substances Produced by a Soil Actinomyces. *Experimental Biology and Medicine* **45**, 609–614.

WALLACE, A.R. (1867) *Mimicry, and Other Protective Resemblances Among Animals*. Read Books Ltd.

WALLACE, A.R. (1877) The Colors of Animals and Plants. *The American Naturalist* **11**, 641–662.

WANG, L., KIUCHI, T., FUJII, T., DAIMON, T., LI, M., BANNO, Y., KATSUMA, S., SHIMADA, T. & BELL, J. (2013) Reduced expression of the *dysbindin*-like gene in the *Bombyx mori ov* mutant exhibiting mottled translucency of the larval skin. *Genome* **56**, 101–108.

WANG, P., QIU, Z., XIA, D., TANG, S., SHEN, X. & ZHAO, Q. (2017) Transcriptome analysis of the epidermis of the purple quail-like (q-lp) mutant of silkworm, Bombyx mori. *PLOS ONE* **12**, e0175994.

WANG, Y. & NEWMAN, D.K. (2008) Redox Reactions of Phenazine Antibiotics with Ferric (Hydr)oxides and Molecular Oxygen. *Environmental Science & Technology* **42**, 2380–2386.

WARNER, T.S., SINCLAIR, D., FITZPATRICK, K.A., SINGH, M., DEVLIN, R.H. & HONDA, B.M. (1998) The *light* gene of *Drosophila melanogaster* encodes a homologue of *VPS41* , a yeast gene involved in cellular-protein trafficking. *Genome* **41**, 236–243.

WASSERTHAL, L.T. (1975) The rôle of butterfly wings in regulation of body temperature. *Journal of Insect Physiology* **21**, 1921–1930.

WEISSBERG, A. & DAGAN, S. (2011) Interpretation of ESI(+)-MS-MS spectra—Towards the identification of "unknowns". *International Journal of Mass Spectrometry* **299**, 158–168.

WELLINGS, S.R. & SIEGEL, B.V. (1959) Role of Golgi apparatus in the formation of melanin granules in human malignant melanoma. *Journal of Ultrastructure Research* **3**, 147–154.

WHITE, R.H. & MICHAUD, N.A. (1980) Calcium is a component of ommochrome pigment granules in insect eyes. *Comparative Biochemistry and Physiology Part A: Physiology* **65**, 239–242.

WILLIAMS, T.L., DIBONA, C.W., DINNEEN, S.R., JONES LABADIE, S.F., CHU, F. & DERAVI, L.F. (2016) Contributions of Phenoxazone-Based Pigments to the Structure and Function of Nanostructured Granules in Squid Chromatophores. *Langmuir* **32**, 3754–3759.

WILLIAMS, T.L., LOPEZ, S.A. & DERAVI, L.F. (2019a) A Sustainable Route To Synthesize the Xanthommatin Biochrome via an Electro-catalyzed Oxidation of Tryptophan Metabolites. *ACS Sustainable Chemistry & Engineering*, acssuschemeng.9b01144.

WILLIAMS, T.L., SENFT, S.L., YEO, J., MARTÍN-MARTÍNEZ, F.J., KUZIRIAN, A.M., MARTIN, C.A., DIBONA, C.W., CHEN, C.-T., DINNEEN, S.R., NGUYEN, H.T., GOMES, C.M., ROSENTHAL, J.J.C., MACMANES, M.D., CHU, F., BUEHLER, M.J., ET AL. (2019b) Dynamic pigmentary and structural coloration within cephalopod chromatophore organs. *Nature Communications* **10**.

WITTKOPP, P.J. & BELDADE, P. (2009) Development and evolution of insect pigmentation: Genetic mechanisms and the potential consequences of pleiotropy. *Seminars in Cell & Developmental Biology* **20**, 65–71.

WUNDERLIN, J. & KROPF, C. (2013) Rapid Colour Change in Spiders. In *Spider Ecophysiology* (ed W. NENTWIG), pp. 361–370. Springer Berlin Heidelberg, Berlin, Heidelberg.

XUE, W.-H., XU, N., YUAN, X.-B., CHEN, H.-H., ZHANG, J.-L., FU, S.-J., ZHANG, C.-X. & XU, H.-J. (2017) CRISPR/Cas9-mediated knockout of two eye pigmentation genes in the brown planthopper, Nilaparvata lugens (Hemiptera: Delphacidae). *Insect Biochemistry and Molecular Biology*.

YAGO, M. (1989) Enzymic synthesis of papiliochrome II, a yellow pigment in the wings of papilionid butterflies. *Insect Biochemistry* **19**, 673–678.

YAMAGUCHI, Y. & HEARING, V.J. (2014) Melanocytes and Their Diseases. *Cold Spring Harbor Perspectives in Medicine* **4**, a017046–a017046.

YAMAMOTO, M., HOWELLS, A.J. & RYALL, R.L. (1976) The ommochrome biosynthetic pathway in Drosophila melanogaster: The head particulate phenoxazinone synthase and the developmental onset of xanthommatin synthesis. *Biochemical Genetics* **14**, 1077–1090.

YANAI, T., TEW, D.P. & HANDY, N.C. (2004) A new hybrid exchange–correlation functional using the Coulomb-attenuating method (CAM-B3LYP). *Chemical Physics Letters* **393**, 51–57.

YANSHOLE, V.V., SHERIN, P.S., GRITSAN, N.P., SNYTNIKOVA, O.A., MAMATYUK, V.I., GRILJ, J., VAUTHEY, E., SAGDEEV, R.Z. & TSENTALOVICH, Y.P. (2010) Photoinduced tautomeric transformations of xanthurenic acid. *Physical Chemistry Chemical Physics* **12**, 9502.

YATSU, A., OHBAYASHI, N., TAMURA, K. & FUKUDA, M. (2013) Syntaxin-3 Is Required for Melanosomal Localization of Tyrp1 in Melanocytes. *Journal of Investigative Dermatology* **133**, 2237–2246.

YEPIZ-PLASCENCIA, G.M., HO, C., MARTEL, R.R. & LAW, J.H. (1993) Molecular cloning and sequence of a novel ommochrome-binding protein cDNA from an insect, Manduca sexta. *Journal of Biological Chemistry* **268**, 2337–2340.

YORK, J.R. & MCCAULEY, D.W. (2020) The origin and evolution of vertebrate neural crest cells. *Open Biology* **10**, 190285.

YOUDIM, M.B., BEN-SHACHAR, D. & RIEDERER, P. (1994) The enigma of neuromelanin in Parkinson's disease substantia nigra. *Journal of Neural Transmission. Supplementum* **43**, 113–122.

YU, L., MCPHEE, C.K., ZHENG, L., MARDONES, G.A., RONG, Y., PENG, J., MI, N., ZHAO, Y., LIU, Z., WAN, F., HAILEY, D.W., OORSCHOT, V., KLUMPERMAN, J., BAEHRECKE, E.H. & LENARDO, M.J. (2010) Termination of autophagy and reformation of lysosomes regulated by mTOR. *Nature* **465**, 942–946.

ZANGWILL, A. & SOVEN, P. (1980) Density-functional approach to local-field effects in finite systems: Photoabsorption in the rare gases. *Physical Review A* **21**, 1561–1572.

ZELENTSOVA, E.A., SHERIN, P.S., SNYTNIKOVA, O.A., KAPTEIN, R., VAUTHEY, E. & TSENTALOVICH, Y.P. (2013) Photochemistry of aqueous solutions of kynurenic acid and kynurenine yellow. *Photochem. Photobiol. Sci.* **12**, 546–558.

ZENNER, H.L., COLLINSON, L.M., MICHAUX, G. & CUTLER, D.F. (2007) High-pressure freezing provides insights into Weibel-Palade body biogenesis. *Journal of Cell Science* **120**, 2117–2125.

ZHANG, H., KIUCHI, T., HIRAYAMA, C., BANNO, Y., KATSUMA, S. & SHIMADA, T. (2018a) A reexamination on the deficiency of riboflavin accumulation in Malpighian tubules in larval translucent mutants of the silkworm, Bombyx mori. *Genetica* **146**, 425–431.

ZHANG, H., KIUCHI, T., HIRAYAMA, C., KATSUMA, S. & SHIMADA, T. (2018b) Bombyx ortholog of the Drosophila eye color gene brown controls riboflavin transport in Malpighian tubules. *Insect Biochemistry and Molecular Biology* **92**, 65–72.

ZHANG, H., KIUCHI, T., WANG, L., KAWAMOTO, M., SUZUKI, Y., SUGANO, S., BANNO, Y., KATSUMA, S. & SHIMADA, T. (2017a) *Bm-muted*, orthologous to mouse *muted* and encoding a subunit of the BLOC-1 complex, is responsible for the *otm* translucent mutation of the silkworm *Bombyx mori*. *Gene* **629**, 92–100.

ZHANG, H., LIN, Y., SHEN, G., TAN, X., LEI, C., LONG, W., LIU, H., ZHANG, Y., XU, Y., WU, J., GU, J., XIA, Q. & ZHAO, P. (2017b) Pigmentary analysis of eggs of the silkworm Bombyx mori. *Journal of Insect Physiology* **101**, 142–150.

ZHANG, L., MAZO-VARGAS, A. & REED, R.D. (2017c) Single master regulatory gene coordinates the evolution and development of butterfly color and iridescence. *Proceedings of the National Academy of Sciences*, 201709058.

ZHANG, L. & REED, R.D. (2017) A Practical Guide to CRISPR/Cas9 Genome Editing in Lepidoptera. In *Diversity and Evolution of Butterfly Wing Patterns* (eds T. SEKIMURA & H.F. NIJHOUT), pp. 155–172. Springer Singapore, Singapore.

ZHAO, D., CHEN, S. & LIU, X. (2019) Lateral neural borders as precursors of peripheral nervous systems: A comparative view across bilaterians. *Development, Growth & Differentiation* **61**, 58–72.

ZHAO, Y., SCHULTZ, N.E. & TRUHLAR, D.G. (2005) Exchange-correlation functional with broad accuracy for metallic and nonmetallic compounds, kinetics, and noncovalent interactions. *The Journal of Chemical Physics* **123**, 161103.

ZHAO, Y., SCHULTZ, N.E. & TRUHLAR, D.G. (2006) Design of Density Functionals by Combining the Method of Constraint Satisfaction with Parametrization for Thermochemistry, Thermochemical Kinetics, and Noncovalent Interactions. *Journal of Chemical Theory and Computation* **2**, 364–382.

ZHAO, Y. & TRUHLAR, D.G. (2006) Density Functional for Spectroscopy: No Long-Range Self-Interaction Error, Good Performance for Rydberg and Charge-Transfer States, and Better Performance on Average than B3LYP for Ground States. *The Journal of Physical Chemistry A* **110**, 13126–13130.

ZHAO, Y., ZHANG, H., LI, Z., DUAN, J., JIANG, J., WANG, Y., ZHAN, S., AKINKUROLERE, R.O., XU, A., QIAN, H., MIAO, X., TAN, A. & HUANG, Y. (2012) A major facilitator superfamily protein participates in the reddish brown pigmentation in Bombyx mori. *Journal of Insect Physiology* **58**, 1397–1405.

ZHOU, B.-K., BOISSY, R.E., PIFKO-HIRST, S., MORAN, D.J. & ORLOW, S.J. (1993) Lysosome-Associated Membrane Protein-1 (LAMP-1) Is the Melanocyte Vesicular Membrane Glycoprotein Band II. *Journal of Investigative Dermatology* **100**, 110–114.

ZHOU, D., OTA, K., NARDIN, C., FELDMAN, M., WIDMAN, A., WIND, O., SIMON, A., REILLY, M., LEVIN, L.R., BUCK, J., WAKAMATSU, K., ITO, S. & ZIPPIN, J.H. (2018) Mammalian pigmentation is regulated by a distinct cAMP-dependent mechanism that controls melanosome pH. *Science Signaling* **11**, eaau7987.

ZHU, Y., ZHANG, J., LI, A., ZHANG, Y. & FAN, C. (2017) Synchrotron-based X-ray microscopy for sub-100 nm resolution cell imaging. *Current Opinion in Chemical Biology* **39**, 11–16.

ZHURAVLEV, A.V., VETROVOY, O.V. & SAVVATEEVA-POPOVA, E.V. (2018) Enzymatic and non-enzymatic pathways of kynurenines' dimerization: the molecular factors for oxidative stress development. *PLOS Computational Biology* **14**, e1006672.

ZHURAVLEV, A.V., ZAKHAROV, G.A., SHCHEGOLEV, B.F. & SAVVATEEVA-POPOVA, E.V. (2016) Antioxidant Properties of Kynurenines: Density Functional Theory Calculations. *PLOS Computational Biology* **12**, e1005213.

ZIEGLER, I. (1960) Zur Feinstruktur der Augengranula bei Drosophila Melanogaster. *Zeitschrift für Vererbungslehre* **91**, 206–209.

ZIEGLER, I. (1961) Genetic Aspects of Ommochrome and Pterin Pigments. In *Advances in Genetics* (eds E.W. CASPARI & J.M. THODAY), pp. 349–403. Elsevier, Academic Press.

ZIEGLER, I. & HARMSEN, R. (1970) The Biology of Pteridines in Insects. In *Advances in Insect Physiology* (eds J.W.L. BEAMENT, J.E. TREHERNE & V.B. WIGGLESWORTH), pp. 139–203. Elsevier, Academic Press.

ZIEGLER-GÜNDER, I. & JAENICKE, L. (1959) Zur Wirkungsweise des white-Allels bei Drosophila melanogaster. *Zeitschrift für Vererbungslehre* **90**, 53–61.

ZIMOVA, M., HACKLÄNDER, K., GOOD, J.M., MELO-FERREIRA, J., ALVES, P.C. & MILLS, L.S. (2018) Function and underlying mechanisms of seasonal colour moulting in mammals and birds: what keeps them changing in a warming world? *Biological Reviews*.

ZOLLINGER, H. (2003) *Color chemistry: syntheses, properties, and applications of organic dyes and pigments*, 3rd, rev. ed edition. Verlag Helvetica Chimica Acta; Wiley-VCH, Zürich: Weinheim

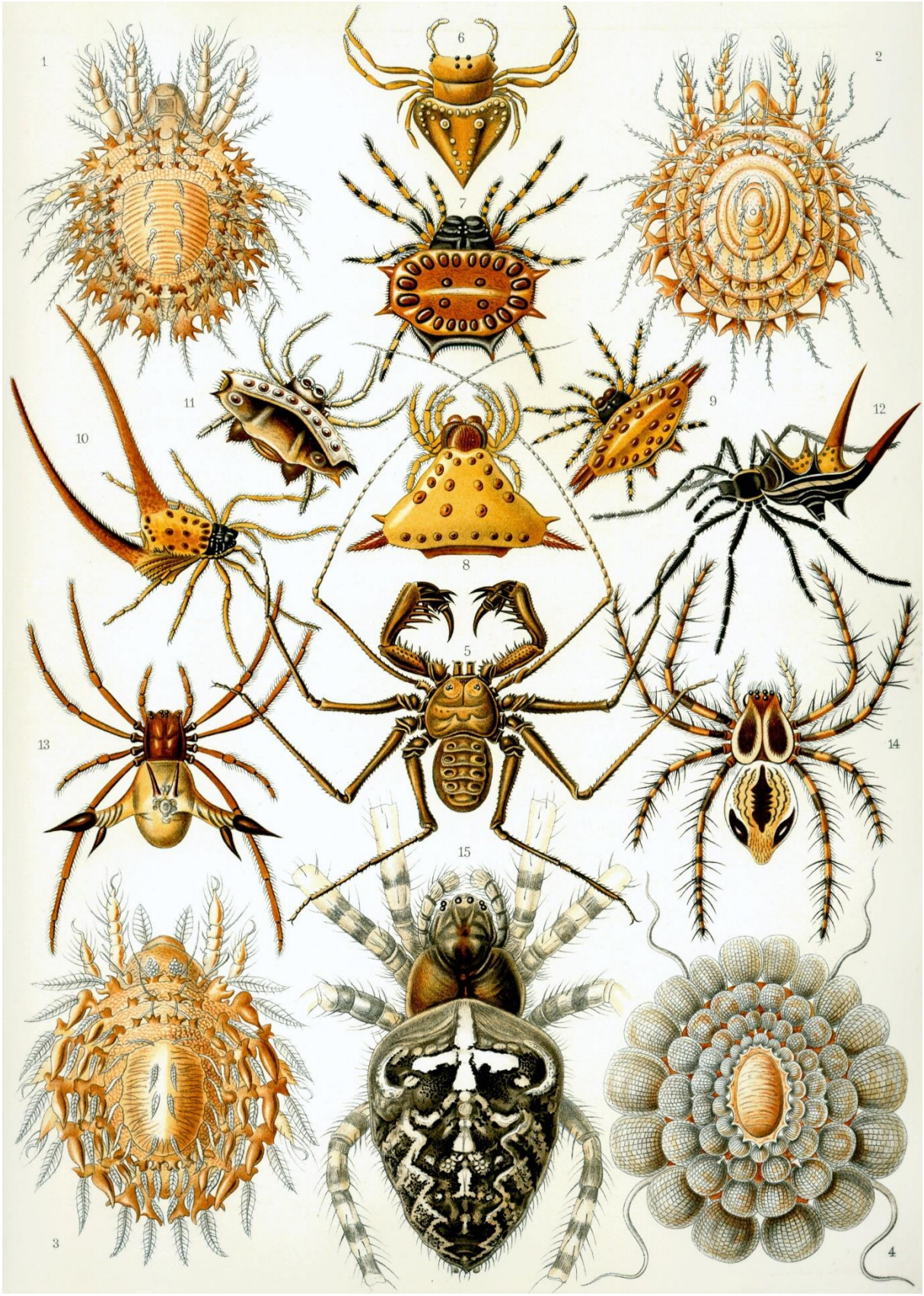

La diversité de formes et de couleurs chez les arachnides.
Lithographie d'Ernst Haeckel (1904), *Formes artistiques de la nature* (retouches : Wikimedia)

Florent FIGON

PHOTOBIOCHIMIE ET BIOLOGIE CELLULAIRE DES OMMOCHROMES : Implications dans le changement de couleur

Résumé

L'évolution de la capacité à changer de couleur chez les animaux est un sujet majeur. Son étude requiert une compréhension intégrée de l'importance biologique des couleurs. Dans ces travaux, j'explore la relation structure–fonction, en termes de changement de couleur, des pigments appelés ommochromes et de leurs organites. J'utilise pour cela la chimie analytique, la modélisation quantique et l'imagerie multimodale à l'échelle subcellulaire. Cette approche interdisciplinaire révèle que les bases photochimiques et intracellulaires des ommochromes déterminent, à la fois, leurs capacités à changer de couleur et leur réactivité chimique. Mes résultats renforcent l'idée que les changements de couleur des ommochromes sont une propriété multi-échelle qui a des effets sur des fonctions biologiques au-delà de la coloration, comme l'homéostasie redox et métallique.

Mots-clés : biologie cellulaire, changement de couleur, invertébré, ommochrome, photobiochimie, pigment

Résumé en anglais

The evolutionary reason why many animals display color changes remains a key question. Solving it requires an integrative understanding of the biological significance of colors. In this work, I investigate the structure–function relationship of color-changing ommochrome pigments and their organelles using analytical chemistry, quantum modelling and subcellular multimodal imaging. This interdisciplinary approach reveals that the photochemical and intracellular bases of ommochromes determine both their color-changing capacities and their chemical reactivity, among other pleiotropic functions. My results support the idea that color changes of ommochromes are a multiscale property that affects biologically relevant functions besides coloration, such as redox and metal homeostasis.

Keywords: cell biology, color change, invertebrate, ommochrome, photobiochemistry, pigment